VNiVERSiDAD
D SALAMANCA

Late Miocene astrochronology and basin evolution of the Atlantic side of the Betic Corridor linked to the Messinian Salinity Crisis

Bastiaan Cornelis Johannes van den Berg

Tesis Doctoral

Salamanca, 2016

VNiVERSiDAD
D SALAMANCA

Astrocronología y evolución de la sedimentación marina del margen Atlántico del Corredor Bético y su relación con la crisis de salinidad del Mesiniense

Memoria presentada por **Bastiaan Cornelis Johannes van den Berg** para optar al grado de **Doctor en Ciencias Geológicas** por la **Universidad de Salamanca**

Directores de la Tesis:

Dr. Francisco Javier Sierro Sánchez
Catedrático del Departamento de Geologia (Paleontología)
Facultad de Ciencias
Universidad de Salamanca

Dr. José Abel Flores Villarejo
Catedrático del Departamento de Geologia (Paleontología)
Facultad de Ciencias
Universidad de Salamanca

Salamanca, 2016

Dr. D. **Francisco Javier Sierro Sánchez** y Dr. D. **José Abel Flores Villarejo**, profesores del Área de Paleontología en el Departamento de Geología en la Facultad de Ciencias (Universidad de Salamanca)

CERTIFICAN QUE:

Bastiaan Cornelis Johannes van den Berg ha realizado en el Departamento de Geología en la Universidad de Salamanca y baja nuestra supervisión, el trabajo

"Astrocronología y evolución de la sedimentación marina del margen Atlántico del Corredor Bético y su relación con la crisis de salinidad del Mesiniense"

Y para que conste, firmamos el presente certificado en Salamanca, Abril de 2016

Los Directores:

Francisco Javier Sierro Sánchez José Abel Flores Villarejo

El doctorando:

Bastiaan Cornelis Johannes van den Berg

The research leading to this thesis has received funding from the People Programme (Marie Curie Actions) of the European Union's Seventh Framework Programme FP7/2007-2013/ under REA Grant Agreement No. 290201 MEDGATE, and from the Guadaltyc project (MINECO, CGL2012-30875). Funding from JCYL project SA263U14 is also acknowledged.

Venid hasta el borde les dijo

Tenemos miedo, podríamos caer

Venid hasta el borde les dijo, ellos fueron

Los empujó y… volaron

Guillaume Apollinaire

Table of Contents

Abstract

This thesis gives an overview in understanding the Late Miocene evolution of Mediterranean-Atlantic gateways in general and new results and insights for the Betic Corridor in particular. Betic Corridor research was done in two ways:

- By constructing a high-resolution age model for the Atlantic side of the corridor and linking changes in depositional environment to basin or corridor evolution and events in the Late Miocene Atlantic or Mediterranean region.
- By improving the chronostratigraphic framework of Late Miocene sediments in the western Betics and relating changes in depositional environment to corridor evolution.

During the Late Miocene, when the strait of Gibraltar probably did not exist yet, the Betic Corridor through southern Spain formed, together with the Rifian corridor through northern Morocco, the marine connection between the Atlantic Ocean and the Mediterranean Sea. Progressive restriction and finally closure of these marine gateways led to catastrophic changes in both Mediterranean sea-level and salinity. This event is known as the Messinian Salinity Crisis (MSC). Despite decades of research, the exact timing of closure, the geometry of the corridors, and the patterns of exchange through them still remain uncertain.

The first chapter of this thesis gives a comprehensive overview of the evolution of these Late Miocene gateways and the nature of Mediterranean-Atlantic exchange as deduced from published studies focussed both on the sediments preserved within the fossil corridors and inferences that can be derived from data in the adjacent basins. It also considers the possible impact of evolving exchange on both the Mediterranean and global climate and highlights the main enduring challenges for reconstructing past Mediterranean-Atlantic exchange.

The rest of this thesis focusses on the Atlantic side of the Betic Corridor. The eastern part of the Betic Corridor was divided in several sea branches, of which each closed separately in the late Tortonian due to sedimentary infill and tectonic uplift. However the timing of closure of the most western of these branches and probably the last existing, the Guadalhorce corridor, is still disputed. The western part of the Betic Corridor was formed by the Guadalquivir Basin. The entire water mass that passed through the branches mentioned above also passed through this basin, which opened to the Atlantic, so any change in the corridor geometry must have (indirectly) also influenced the water mass in this basin and hence the sedimentation. This basin is the missing link in Late Miocene Mediterranean-Atlantic gateway evolution research.

In Chapter 2 and 3 a high-resolution age model is constructed for the entire Messinian of the Guadalquivir Basin by tuning cyclical changes in elemental composition of the

sediments, visualized through XRF, to the astronomical target curves using magnetobiostratigraphic tie-points. Based on the age model the following observations were done and their regional or global relevance through possible linkage with Atlantic or Mediterranean events were considered.

- Two significant changes in sedimentation rate were found synchronously in both cores. One at 5.55 Ma coinciding with the onset of the final stage of MSC and a major deglaciation, and one at 5.33 Ma coinciding with the Miocene-Pliocene boundary and the reestablishment of fully marine conditions in the Mediterranean, terminating the MSC. This suggests that MSC events not only affected the Mediterranean Basin but probably also the Spanish Atlantic margin. The mechanism explaining these interbasinal correlations is unclear but some potential scenarios based on tectonics or changes in ocean currents are suggested.
- The benthic oxygen isotope record correlates well with the previously published Atlantic records of Ain el Beida, Loulja and ODP Site 982, suggesting the presence of North Atlantic Central Water and no direct influence of Mediterranean Outflow Water (MOW) on these sediments. However, an offset is recognized between the benthic oxygen isotope records of this margin and the Moroccan Atlantic margin for the late Messinian glacial period (5.9-5.5 Ma), concurrent with the first stages of the MSC. This might be the result of the decrease/cessation of the MOW in the Gibraltar Strait region.
- A gradual change in the nature of the typical fluctuations in geochemical composition of the sediments was recognized, which is associated with a gradual change in depositional environment from distal to proximal as the Guadalquivir Basin infilled. In the distal setting biogenic carbonate was diluted by cyclic influxes of detrital material; while in the proximal setting sedimentation is dominated by cyclic influxes of coarser grained terrestrial input.

In Chapter 4 the chronostratigraphic framework of the Ronda Basin and Antequera region, which are located adjacent to the Guadalhorce corridor, is improved. These key areas probably formed the northern part of that gateway and both indicate a shallowing upward sedimentary succession from marls to calcarenites. Biostratigraphic dating of the marls resulted in all cases in a late Tortonian age, older than 7.58 Ma. These observations suggest that the Guadalhorce corridor probably closed during the latest Tortonian-earliest Messinian. This is in line with results from the Arcos Basin and the late Tortonian closure of the Granada Basin, suggesting that the late Tortonian period of tectonic uplift in the eastern Betics, closing the eastern branches of the Betic Corridor, continued westward and also uplifted the western Betics. This resulted in a latest Tortonian-earliest Messinian closure of the Betic Corridor, well before the onset of the Messinian Salinity Crisis.

Resumen

Esta Tesis Doctoral brinda una visión general y plantea nuevas consideraciones para entender la evolución de los canales interoceánicos Atlántico-Mediterráneo durante el Mioceno tardío, se enfoca particularmente en la evolución del corredor Bético. La investigación se adelantó en dos etapas:

• Inicialmente, se construyó un modelo de edad de alta resolución para el margen Atlántico del corredor Bético y se relacionaron los cambios en el ambiente de sedimentación de la cuenca del Guadalquivir con la evolución del corredor, y con los eventos regionales ocurridos durante el Mioceno tardío en el Atlántico Norte y en el Mediterráneo.

• Adicionalmente, se mejoró el marco cronoestratigráfico para los sedimentos acumulados durante el Mioceno tardío en la región Bética occidental, y se correlacionaron los cambios en el ambiente de depósito con la evolución del corredor.

Durante el Mioceno tardío, cuando el Estrecho de Gibraltar posiblemente aún no existía, la conexión entre el océano Atlántico y el mar Mediterráneo se estableció a través de dos canales: el corredor Bético a lo largo del sur de España, y el corredor Rifeño en el norte de Marruecos. La restricción progresiva y finalmente el cierre de dichos canales interoceánicos produjo importantes cambios tanto en la salinidad como en el nivel del Mediterráneo. Este evento se conoce como la Crisis de Salinidad del Mesiniense (CSM). A pesar de décadas de investigación enfocadas en entender la evolución geológica de los corredores, el momento exacto del cierre, su geometría y los patrones de interconexión de aguas aún son inciertos.

En el primer capítulo de esta Tesis se hace una revisión general de la evolución de dichos canales en el Mioceno tardío y la naturaleza de la conexión Atlántico-Mediterránea, con base en estudios enfocados en la caracterización de los sedimentos preservados dentro de los corredores y en la correlación estratigráfica con cuencas adyacentes. Además se discute el posible impacto que tuvo el intercambio de aguas en el clima Mediterráneo y global. Finalmente, se presentan los retos que supone investigar los patrones de intercambio Atlántico-Mediterráneo del pasado.

Los siguientes capítulos de esta Tesis se enfocan en el corredor Bético. La región oriental del corredor Bético se dividió en varias ramificaciones oceánicas, las cuales se cerraron una a una durante el Tortoniense tardío debido al relleno sedimentario y al levantamiento tectónico. Sin embargo, aún se desconoce el momento del cierre de la ramificación más occidental del corredor Bético. Esta ramificación se conoce como la cuenca de Guadalhorce y fue posiblemente la última conexión activa del corredor. Hacia al occidente, el corredor Bético está formado por la cuenca del Guadalquivir. Debido a que las masas de aguas que cruzaron el corredor Bético debieron cruzar a través de esta cuenca, se espera que cualquier cambio en la geometría del corredor haya influenciado

(indirectamente) los patrones de circulación de aguas y por consiguiente los procesos sedimentarios propios de la cuenca. En tal virtud, se considera que esta cuenca es el eslabón perdido en la investigación de la evolución del corredor Bético durante el Mioceno tardío.

En los capítulos 2 y 3 se presenta el modelo de edad de alta resolución que se construyó para el Mesiniense de la cuenca del Guadalquivir. Para construir este modelo, se utilizaron los cambios cíclicos detectados en la composición elemental de los sedimentos, los cuales se obtuvieron mediante fluorescencia de rayos X (XRF). El marco cronoestratigráfico resultante es producto de la calibración de los ciclos en la composición elemental con las curvas astronómicas de referencia, empleando como puntos de amarre diferentes datos magnetobioestratigráficos. Con base en el modelo de edad propuesto, se realizaron las siguientes consideraciones con respecto a la evolución de la cuenca, y su relación con eventos Atlánticos o Mediterráneos de escala regional y/o global.

- Se encontraron dos cambios significativos en la tasa de sedimentación. El primero ocurrió hace 5.55 Ma y coincidió con el inicio de la etapa final de la CSM y con una fuerte deglaciación. El segundo cambió ocurrió hace 5.33 Ma y corresponde con la transición del Mioceno-Plioceno y el fin de la CSM asociado con el total restablecimiento de las condiciones marinas del Mediterráneo. Esto sugiere que los eventos de la CSM, no solamente afectaron la cuenca Mediterránea, sino que probablemente influenciaron el margen Atlántico español. Hasta el momento, no es posible detallar claramente las causas o mecanismos que generaron los mismos patrones entre cuencas; no obstante, es posible sugerir que procesos tectónicos y/o cambios en las corrientes oceánicas generaron cambios sincrónicos en los procesos de sedimentación de ambos cuencas.
- El registro isotópico de oxígeno bentónico se correlaciona bien con registros previamente publicados para Ain el Beida, Loulja y la perforación ODP 982. Esta relación indica que durante la sedimentación del Mesiniense, existió una influencia directa del Agua Noratlántica Central, pero no así de la masa de Agua Mediterránea (Mediterranean Outflow Water-MOW). Sin embargo, se observa una desviación entre los registros de isótopos de oxígeno bentónicos del margen Atlántico español y del margen marroquí durante el último período glacial de Mesiniense (5.9 a 5.5 Ma) y coincidiendo con las primeras etapas de la crisis. Esta desviación podría ser el resultado de la disminución/cesación de los flujos de MOW en la región del Estrecho de Gibraltar.
- Se reconoció un cambio gradual en la naturaleza de las fluctuaciones de la composición elemental de los sedimentos. Dicha variación se asoció con una somerización de los ambientes de depósito producto de la progresiva colmatación de la cuenca del Guadalquivir. Cuando la sedimentación tuvo lugar

en zonas más distales, el carbonato biogénico fue diluido debido al influjo cíclico de material detrítico; mientras que en zonas proximales, la sedimentación tuvo mayores aportes continentales y por tanto estuvo dominada por el influjo cíclico de partículas de grano más grueso.

En el capítulo 4, se presenta una actualización del marco cronoestratigráfico de la cuenca de Ronda y la región de Antequera. Estas zonas son clave para entender la evolución del corredor de Guadalhorce, ya que son adyacentes y son áreas que probablemente conformaron la zona más septentrional del dicho corredor. El registro sedimentario de ambas áreas indica una somerización hacia el tope de la secuencia, que se identifica por el cambio de margas profundas a calcarenitas someras. La datación bioestratigráfica de las margas señaló en todos los casos una edad Tortoniense, anterior a 7.58 Ma. Estas nuevas edades sugieren que la cuenca de Guadalhorce probablemente se cerró durante el Tortoniense tardío-Mesiniense temprano. Los resultados encontrados concuerdan con los obtenidos para la cuenca de Arcos y el cierre de la cuenca de Granada durante el Tortoniense tardío. En consecuencia, se sugiere que el Tortoniense tardío correspondió con un periodo de levantamiento tectónico de la región Bética oriental, el cual inicialmente ocasionó el cierre de las ramificaciones orientales del corredor, y posteriormente continuó hacia el oeste y generó el levantamiento de la región Bética occidental. Este evento tectónico resultó en el cierre del corredor Bético durante el Tortoniense tardío-Mesiniense temprano, mucho antes del inicio de la Crisis de Salinidad del Mesiniense.

INTRODUCTION

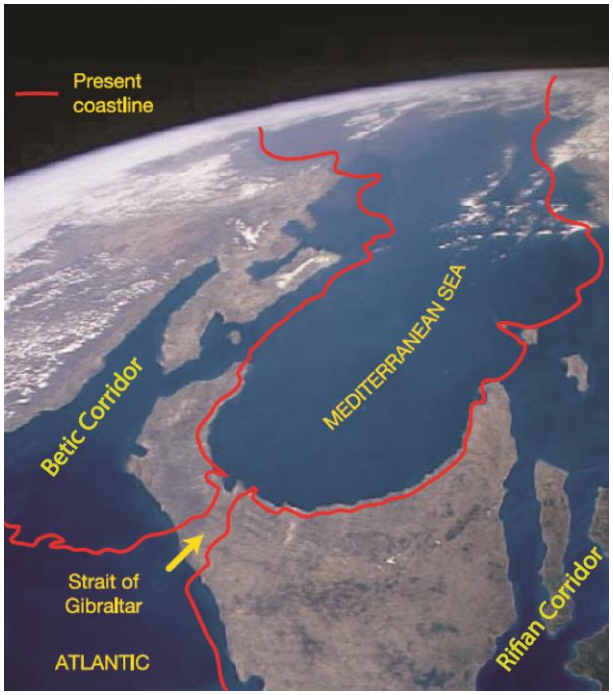

Figure 1. *Reconstruction of the Mediterranean gateways during the Messinian (the final stage of the Late Miocene period). In red is the present coastline (modified from Duggen et al., 2003).*

Sea strait evolution research

Sea straits have had a large influence on climate and oceans throughout the geological history. Opening and closing have led to major reorganisations in ocean currents, seawater characteristics, biological evolution and climate. For example, the opening of the Drake Passage between South America and Antarctica in the Eocene led to the onset of circum-Antarctic circulation and coincides with increased biological productivity, abrupt cooling and growing of Antarctic ice sheets (Livermore et al., 2007; Scher and Martin, 2006). More recently the closure of the Panama strait triggered the north Atlantic thermohaline circulation and probably intensification of the northern hemisphere glaciation (Bartoli et al., 2005; Haug and Tiedemann, 1998). To understand the earths system it is therefore essential to understand and reconstruct sea strait

evolution and their regional or global impact. This PhD thesis studies the evolution of the Betic Corridor, one of the former sea straits connecting the Mediterranean Sea with the Atlantic Ocean (Fig. 1).

Messinian Salinity Crisis

In the Late Miocene, 8 million years ago, the straits of Gibraltar probably did not exist. Instead, the Mediterranean Sea was connected to the Atlantic Ocean by at least two marine gateways: the Rifian Corridor through northern Morocco, and the Betic Corridor through southern Spain (Fig.1; Benson et al., 1991; Santisteban and Taberner, 1983). As a consequence of the collision between the African and the Eurasian plate and tectonic uplift of the Gibraltar Arc, progressive restriction and finally closure of these marine gateways led to reduced or absent (at times) Mediterranean-Atlantic exchange (Hsü et al., 1973), causing catastrophic changes in both Mediterranean sea-level and salinity. This event, known as the Messinian Salinity Crisis (MSC), saw ~6% of the world's sea salt sequestered in evaporite deposits across the Mediterranean Sea floor (McKenzie, 1999). Meanwhile, life nearly ceased to exist in the Mediterranean waters and the Mediterranean Sea experienced a sea level drop of at least a few hundred meters (Fig. 2). At the latest stage of the MSC –after its evaporitic phase– the Mediterranean shifted from hypersaline to brackish-water conditions, as shown by non-marine deposits. This period is known as the *Lago-Mare* event (Fig. 3), and it was followed by the opening or deepening of the Straits of Gibraltar at the Miocene-Pliocene boundary (Zanclean Flood, 5.33 Ma), which restored Mediterranean-Atlantic exchange (Blanc, 2002).

Figure 2. *Artist impression of the Messinian Salinity Crisis.*

Despite decades of research, the exact timing of closure, the geometry of the corridors, and the patterns of exchange through these corridors still remains uncertain. One of the most puzzling issues is that the Mediterranean-Atlantic gateways must have been severely restricted in order to have the right conditions for evaporite deposition in the

Mediterranean but at the same time must have facilitated the supply of compounds for the 1 km thick layer of salt that formed on the sea floor. Therefore the history of these corridors must have been more complex than is known so far. The different stages of the MSC, as defined by the most recent hypothesis, are summarised in Figure 3, which provides the current reference Messinian stratigraphic framework.

Medgate

In 2011 the European Union funded Medgate, a Marie Curie Initial Training Network, which studied this extraordinary event in order to try and reconstruct in detail the evolution of these gateways and how changes in Mediterranean-Atlantic exchange impacted the local, regional and global climate. At the same time the researchers were trained in multi-disciplinary scientific skills that are in high demand by both industry and academia. The Medgate team consisted of nine PhD students and a post-doctoral researcher. It brought together experts from universities and companies in the UK, the Netherlands, Spain, France and Morocco, while research ranged from geochemistry to micropaleontology and from modelling to paleogeography. Chapter 1 gives an overview on the state of the art of Late Miocene Mediterranean-Atlantic gateway research (Flecker et al., 2015).

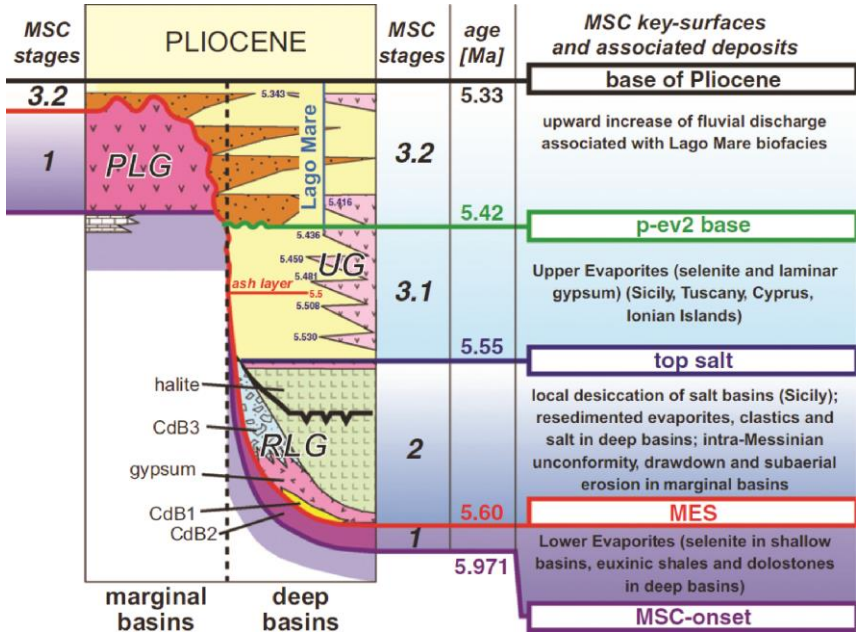

Figure 3. *CIESM Messinian Salinity Crisis stratigraphic framework (Manzi et al., 2013)*

The Betic Corridor

This thesis forms part of this project and focusses on the evolution of the Betic Corridor, which connected the Mediterranean with the Atlantic through southern Spain. The eastern part of this corridor was divided in several sea branches, of which each closed separately due to sedimentary infill and tectonic uplift, gradually restricting the Mediterranean-Atlantic exchange (Fig. 4; Flecker et al., 2015; Martín et al., 2014). The most northerly branch, known as the North Betic strait, closed at 7.8 Ma (Krijgsman et al., 2000), while the branch passing through the Granada Basin closed around 7.3 Ma (Corbí et al., 2012). The youngest marine sedimentation in the branch passing through the Guadix Basin is dated at 7.85 Ma, subsequently a hiatus of more than 2 Ma is present and therefore a later closure cannot be ruled out. Furthermore, it is suggested that the most western of these branches and probably the last existing, the Guadalhorce corridor, (Martín et al., 2001), has closed at 6.18 Ma (Pérez-Asensio et al., 2012a). However, this is based on indirect evidence through a change in benthic oxygen isotopes signatures in the sediments of the Guadalquivir Basin from typical Mediterranean towards more Atlantic values and therefore disputed.

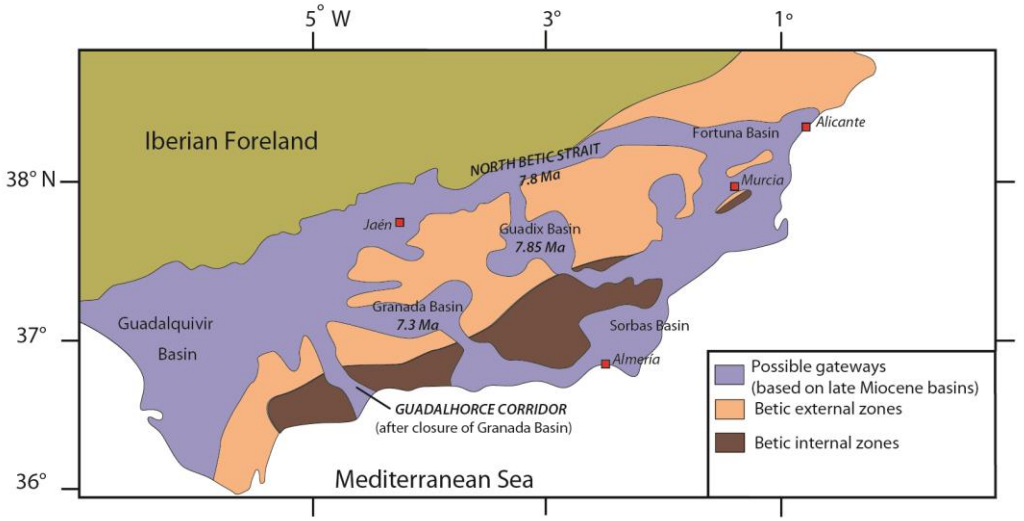

Figure 4. *Detail map of the Betic Corridor with closure ages of different branches.*

Determining the timing of gateway closure is complicated since direct evidence of this event from the corridor itself is, at best, scarce and in most cases non-existent. When a corridor shallows, shallow marine, coarse-grained sediments start to deposit which are very difficult to date. When the corridor is closed, the last marine sediments that were deposited, recording the closure, are also the first ones that will subsequently be eroded.

Assessing the timing of corridor closure by directly dating the corridor sediments is therefore complicated and uncertainties remain. Alternatively, one can assess corridor evolution by studying the sediments of nearby waterbodies and relate observations to the evolution of the corridor itself.

The Guadalquivir Basin

For the Betic Corridor, the Guadalquivir Basin is the most promising of these waterbodies. This foreland basin, located in southwest Spain formed the Atlantic part of the Betic Corridor during the Late Miocene (Fig. 4). The entire water mass passing through the corridor also passed through this basin so any change in the corridor geometry must have (indirectly) also influenced the water mass in the Guadalquivir Basin and hence, the sedimentation. As shown on figure 5, the Guadalquivir Basin is the missing link in Late Miocene corridor evolution research. Both sides of the Rifian corridor and the Mediterranean side of the Betic Corridor have been investigated, but research on the Atlantic side is lacking.

The sediments of the Guadalquivir Basin are not well exposed and most studies are reliant on seismic data, well logs and boreholes (Berástegui et al., 1998; Fernández et al., 1998; Larrasoaña et al., 2008; Ledesma, 2000; Pérez-Asensio et al., 2012b; Riaza and Martinez del Olmo, 1996). These indicate that the succession comprises marine and continental sediments, and range in age from lower Tortonian to recent (González-Delgado et al., 2004; Ledesma, 2000; Sierro et al., 1996). After closure of the Betic Corridor, the Guadalquivir Basin was established as a wide, marine embayment open to the Atlantic (Pérez-Asensio et al., 2012b) and marine sedimentation continued throughout the late Tortonian, Messinian and into the Pliocene. Recent studies of the Montemayor-1 borehole have resulted in a magnetobiostratigraphic framework (Larrasoaña et al., 2008), palaeo-environmental evolution based on benthic foraminifera (Pérez-Asensio et al., 2013; 2012a; 2012b) and reconstruction of vegetation and sea-level changes (Jiménez-Moreno et al., 2013). However, the chronostratigraphic framework used is a rough extrapolation of the magnetostratigraphic tie-points. A high resolution chronostratigraphic framework is needed to re-assess these results and possibly link them to precisely dated events within the Messinian Atlantic or Mediterranean region.

This thesis therefore focusses on two approaches assessing the evolution of the Betic Corridor: an indirect approach through constructing a high resolution age model for two boreholes in the Guadalquivir Basin and interpreting changes in deposition (chapter 2 & 3) and a direct approach by improving the chronostratigraphic framework of Late Miocene sediments in the western Betics and relate changes in their depositional environment to the evolution of the Guadalhorce corridor (chapter 4).

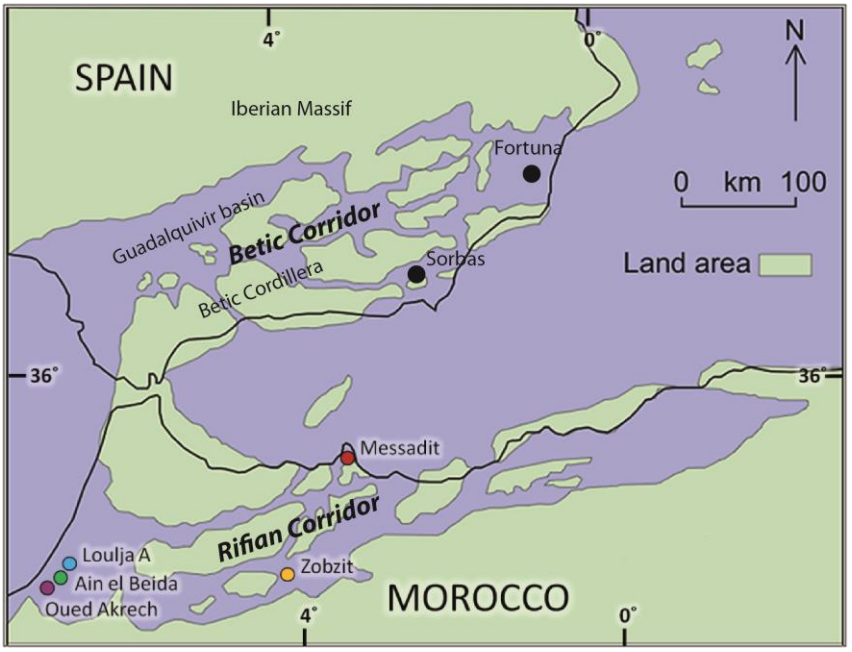

Figure 5. *Map of the western Mediterranean in Messinian times with locations of the key sections. The black line is the present day coast. Clearly, sections at the Atlantic side of the Betic Corridor are lacking.*

Methods

The studies in this thesis rely on a combination of cyclostratigraphy, biostratigraphy, XRF analyses, and fieldwork. Each of these will be further explained hereunder.

Cyclostratigraphy

Long-term changes in seasonal and latitudinal solar insolation are generated by periodic oscillations in the earth's orbit and tilt relative to the sun (Fig. 6). These cycles have a modulating effect on climate and ocean circulation patterns; a record of this signal can be found in a number of terrestrial and marine sedimentary sequences.

The shape of the earth's orbit around the sun and the orientation of the earth's rotational axis are defined by three orbital parameters: eccentricity, obliquity, and precession. These parameters are not constant but vary through time with different periodicities. Eccentricity is characterised by three main periodicities, the most prominent 413 ka (Berger, 1978), 100 ka (average of four periods), and 2.3 Ma (found in very long geological records), while the obliquity component with the largest amplitude has a period of 41 ka (Berger, 1977). The most dominant periodicities for climatic precession are 23 ka (average of the two most pronounced peaks at 23.7 and 22.4 ka)

and 19 ka (average of the following three periods), which are frequently found in geological records (Berger, 1977).

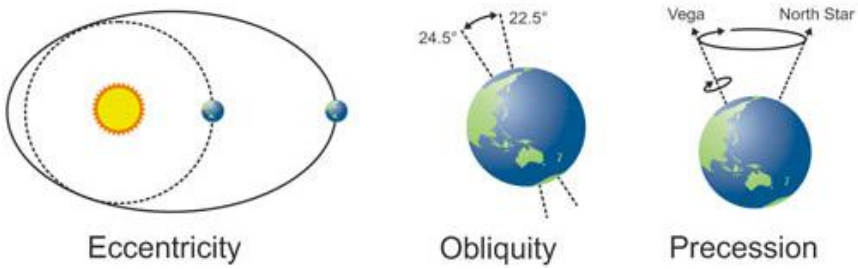

Figure 6. *The tree orbital parameters influencing seasonal and latitudinal solar insolation.*

Sediments are widely used as geo-archives of past climatic changes, but the interpretation of any geological record requires an accurate stratigraphy. Astronomical tuning and cyclostratigraphy can provide extremely precise chronostratigraphic frameworks, by matching orbitally-forced insolation cycles to sequences of sedimentary alternations, with the calibration to model-generated astronomical target curves. The Messinian geological record in the Mediterranean is commonly characterised by well-developed sedimentary alternations (e.g. Krijgsman et al., 1999). A robust high-resolution stratigraphic framework for these successions has been reconstructed through detailed studies on marine sections across the Mediterranean (Hilgen et al., 1995; Krijgsman et al., 1999), as well as within the Late Miocene corridors (e.g. Van der Laan et al., 2006). The use of astronomical tuning combined with an integrated stratigraphic approach can provide far higher resolution age controls than is typical for sediments of this age (Fortuin et al., 2000).

Biostratigraphy

Biostratigraphy is based on the evolution and migration of fauna through time. Within a region, the appearance, acme or disappearance of a certain marker species is often isochronous and can be tied to a certain age. This way it serves as a marker point within a stratigraphic section. In this study, biostratigraphy based on planktonic foraminifera is used.

XRF-analyses

Through X-Ray fluorescence (XRF) changes in elemental concentrations throughout boreholes or sections are measured. When elements are bombarded with an X-ray beam, they emit secondary X-rays with a wavelength characteristic for each element. This way, elemental concentrations for each stratigraphic level within a section can be measured. This can be used for cyclostratigraphy (by looking at the patterns of elements

throughout the section) or trends/abrupt changes in element concentration which could be related to, e.g., basin scale changes.

Fieldwork
In the field, sediment samples can be collected for the techniques stated above. In a direct approach to constrain the timing of closure of the Betic Corridor various basins were studied and sampled in order to assess their evolution and sedimentary filling, and construct a chronostratigraphic framework using planktonic and benthic foraminifera. By combining field observations, geological maps, literature and lab data, a detailed reconstruction can be made of the geological evolution of a certain area.

Chapter overview

Chapter 1 of this thesis consists of a published overview on the state of the art of Late Miocene Mediterranean-Atlantic gateways research (Flecker et al., 2015). It received contributions from all the members of the Medgate team to give a thorough review on all the different aspects of this subject.

Chapter 2 is focussed on the Montemayor-1 core. A late Messinian high resolution age model is constructed using cyclostratigrapic tuning of changes in elemental composition visualized by XRF. This age model is then used to improve the dating of the oxygen isotope and benthic foraminifera abundancy records. Subsequently these records are reinterpreted in terms of basin evolution, climate and evolution of Mediterranean Outflow Water (MOW). This chapter is published in *Global and Planetary change* (van den Berg et al., 2015).

Chapter 3 is focussed on the Huelva-1 core. Again a high resolution age model is constructed using cyclostratigraphy but for this borehole extending back to the latest Tortonian. Subsequently changes in sedimentation are related to events in the Messinian Mediterranean. This chapter is submitted to *Newsletters on Stratigraphy*.

In Chapter 4 the chronostratigraphic framework for the Arcos Basin, Ronda Basin and Antequera region is improved using biostratigraphy in an attempt to better date the closure of the most western and most disputed branch of the Betic Corridor, the Guadalhorce corridor.

CHAPTER 1

Evolution of the Late Miocene Mediterranean-Atlantic gateways and their impact on regional and global environmental change

Rachel Flecker[1], Wout Krijgsman[2], Walter Capella[2], Cesar de Castro Martín s[3], Evelina Dmitrieva[4], Jan Peter Mayser[3], Alice Marzocchi[1], Sevasti Modestou[5], Diana Ochoa Lozano[6], Dirk Simon[2], Maria Tulbure[2], Bas van den Berg[6], Marlies van der Schee[6], Gert de Lange[2], Robert Ellam[5], Rob Govers[2], Marcus Gutjahr[10], Frits Hilgen[2], Tanja Kouwenhoven[2], Johanna Lofi[12], Paul Meijer[2], Francisco J. Sierro[6] Naima Bachiri[7], Nadia Barhoun[7], Abdelwahid Chakor Alami[8], Beatriz Chacon[4], Jose A Flores[6], John Gregory[9], James Howard[11], Dan Lunt[1], Maria Ochoa[4], Rich Pancost[3], Stephen Vincent[11], Mohamed Zakaria Yousfi[7]

[1]BRIDGE, School of Geographical Sciences and Cabot Institute, University of Bristol, University Road, Bristol, UK
[2]Department of Earth Sciences, Utrecht University, PO Box 80.021, 3508 TA, Utrecht, The Netherlands
[3]School of Chemistry and Cabot Institute, University of Bristol, Cantock's Close, Bristol, BS8 1TS4, UK
[4]REPSOL Exploración, S.A., Paseo de la Castellana 280, 4B-28046- Madrid, Spain
[5]Scottish Universities Environmental Research Centre (SUERC), Scottish Enterprise Technology Park, Rankine Ave., East Kilbride, G75 0QF UK
[6]Department of Geology, University of Salamanca, Plaza de los Caídos s/n, 37008, Salamanca, Spain
[7]Université Hassan II Mohammedia, Fac Sci Ben MSik, Casablanca, Morocco
[8]Office National des Hydrocarbures et des Mines, 5, Avenue Moulay Hassan, BP 99 Rabat, Morocco
[9]PetroStrat Ltd, Tyttenhanger House, Tyttenhanger Park, St Albans, Hertfordshire, UK, AL4 0PG.
[10]GEOMAR Helmholtz Centre for Ocean Research Kiel, Wischhofstrasse 1-3, 24148 Kiel, Germany
[11]CASP, 181a Huntingdon Road, Cambridge, CB3 0DH, UK
[12]Géosciences Montpellier, UMR5243, Université Montpellier II, 34090 Montpellier, France, and Department of Geology / University of Leicester, Leicester LE1 7RH, UK

This chapter has been published in Earth Science Reviews

Abstract

Marine gateways play a critical role in the exchange of water, heat, salt and nutrients between oceans and seas. As a result, changes in gateway geometry can significantly alter both the pattern of global ocean circulation and associated heat transport and climate, as well as having a profound impact on local environmental conditions. Mediterranean-Atlantic marine corridors that pre-date the modern Gibraltar Strait, closed during the Late Miocene and are now exposed on land in northern Morocco and southern Spain. The restriction and closure of these Miocene connections resulted in extreme salinity fluctuations in the Mediterranean, leading to the precipitation of thick evaporites. This event is known as the Messinian Salinity Crisis (MSC). The evolution and closure of the Mediterranean-Atlantic gateways are a critical control on the MSC, but at present the location, geometry and age of these gateways is still highly controversial, as is the impact of changing Mediterranean outflow on Northern Hemisphere circulation. Here, we present a comprehensive overview of the evolution of the Late Miocene gateways and the nature of Mediterranean-Atlantic exchange as deduced from published studies focussed both on the sediments preserved within the fossil corridors and inferences that can be derived from data in the adjacent basins. We also consider the possible impact of evolving exchange on both the Mediterranean and global climate and highlight the main enduring challenges for reconstructing past Mediterranean-Atlantic exchange.

1.1 INTRODUCTION

During the late Tortonian (~11.6 to 7.2 Ma), several marine gateways through southern Spain, northern Morocco and potentially Gibraltar, connected the Mediterranean Sea with the Atlantic Ocean (Fig. 1.1). Plate tectonic convergence between Africa and Iberia, combined with subduction dynamics in the Alborán region, progressively closed these connections during the Messinian (e.g. Duggen et al., 2003; Gutscher et al., 2002). This tectonic forcing combined with eustatic (e.g. Manzi et al., 2013) and climatic (Hilgen et al., 2007) factors resulted in a complex history of varied Mediterranean-Atlantic exchange and high amplitude environmental fluctuations in the Mediterranean including the formation of the world's most recent saline giant (Warren, 2010).

Like other marginal basins, the Mediterranean's near-landlocked configuration makes it sensitive to subtle changes in climate (e.g. Thunell et al., 1988). Consequently, the first environmental responses to gradual restriction of exchange with the Atlantic recorded in the Mediterranean (e.g. faunal and isotopic changes; Fig. 1.2), predate any evaporite precipitation there by a million years or more. The most extreme palaeoenvironmental changes took place during the so-called Messinian Salinity Crisis (MSC; 5.97-5.33 Ma; Fig. 1.2) when extensive gypsum deposits precipitated in the Mediterranean's marginal basins and kilometre thick halite units formed in the deep basins (e.g. Hsü et al., 1973; Ryan et al., 1973). This was followed by a period during which the sediments recorded highly fluctuating conditions varying from brackish to hypersaline, before returning, in the Early Pliocene, to open marine conditions (Fig. 1.2; Hsü et al., 1972). These Late Miocene low salinity intervals, known as the Lago Mare, may be the product of an additional freshwater source supplied to the Mediterranean from Paratethys, the lacustrine precursor to the Black and Caspian seas. Like other major freshwater sources, this is a key component of the Mediterranean's freshwater budget, which combined with the gateway dimensions determine its salinity.

The large volume of salt preserved in the Mediterranean necessitates that one or more marine connections with the open ocean remained, at least until the end of the halite stage (5.55 Ma; Krijgsman and Meijer, 2008). However, the location of the last gateway(s) remains highly ambiguous. Field studies of the sedimentary basins in southern Spain (the Betic Corridor) and northern Morocco (the Rifian Corridor) thought to be part of the corridor network (Fig. 1.1), typically indicate that these areas were closed to marine exchange well before the MSC (e.g. Betzler et al., 2006; Ivanović et al., 2013a; Krijgsman et al., 1999b; Soria et al., 1999; van Assen et al., 2006), while the Gibraltar Strait is thought to have first opened at the beginning of the Pliocene (5.33 Ma) bringing the MSC to an end (e.g. Blanc, 2002; Garcia-Castellanos et al., 2009; Hsü et al., 1973; Hsü et al., 1977). The key problem is that it is extremely difficult to pinpoint the exact location or timing of closure from field data alone, because the sedimentary successions within the corridors have been uplifted and eroded (e.g. Hüsing et al., 2010).

Using other datasets to identify the location of each marine corridor, reconstructing its geometry and reducing uncertainty in the age of closure is therefore critical for constraining the process-response chain linking gateway evolution with the development of the Mediterranean's MSC succession. The Atlantic response to a change in gateway configuration is reliant on changes to the density and volume of Mediterranean outflow and consequently also depends on an ability to reconstruct gateway dimensions and the patterns of exchange.

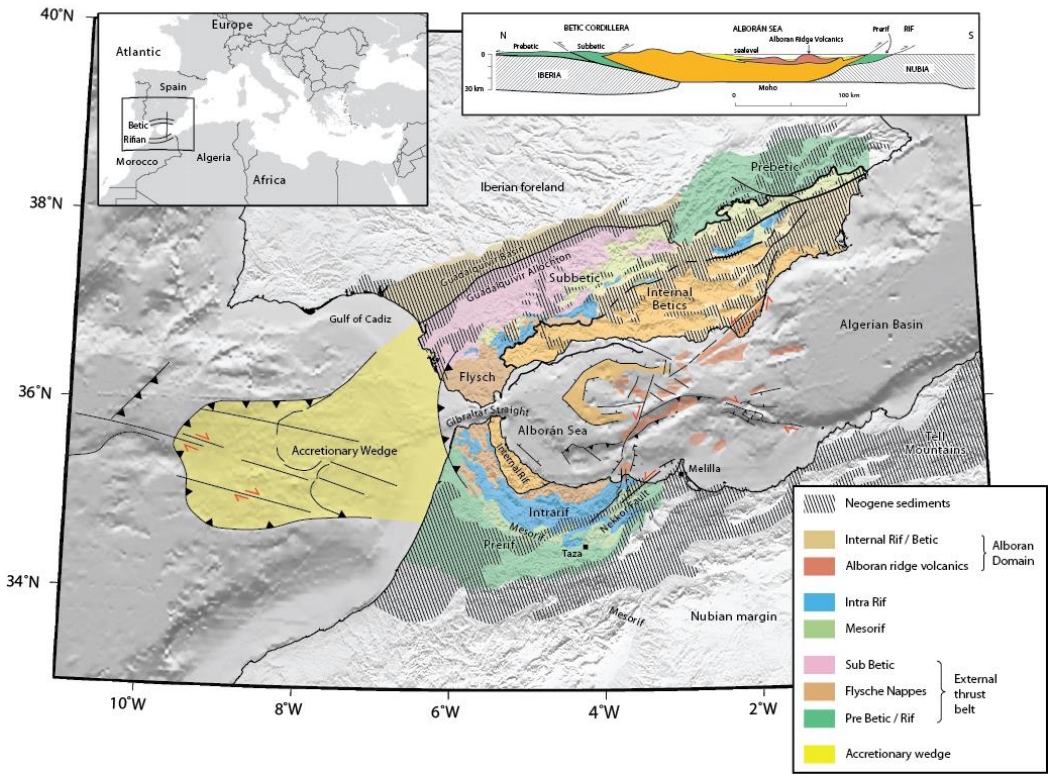

Figure.1.1. *The main structures and tectonic units of the Betic-Rif-Tell arc. Stippling represents the location of Late Miocene marine sediments which approximate the position of the pre-Gibraltar Strait connections between the Mediterranean and Atlantic. These connections are the Betic Corridor in southern Spain and the Rifian Corridor in northern Morocco.*

Several indirect approaches to the study of gateway evolution have been employed in the context of the MSC. These include for example, physics-based mathematical models that quantify gateway configuration (e.g. Meijer, 2006; Meijer and Krijgsman, 2005); and the use of isotopic proxies to elucidate changing connectivity (e.g. Flecker and Ellam, 1999; Ivanović et al., 2013a; Topper et al., 2011). Many other techniques have been applied to successions within the main Mediterranean Basin rather than the gateway

and the paleoenvironmental information they provide can be compared with similar data on the Atlantic side of the connection to constrain aspects of exchange. In this paper we review, synthesise and integrate both direct and indirect data relating to the Mediterranean-Atlantic gateways during Late Miocene. Our aim is to use this information to reconstruct exchange before, during and after the MSC, consider the regional and global implications and highlight enduring questions that may be amenable to new research methods.

1.2 BACKGROUND INFORMATION

1.2.1 Gateway control on Mediterranean water properties

At present, the Mediterranean Sea loses more water to the atmosphere by evaporation than it receives from rainfall and river runoff. As a result, its surface waters are subject to an increase in salinity and thus in density. This relatively dense water finds its way to the deeper levels of the Mediterranean. In addition, the Mediterranean is also a major heat sink for the Atlantic, (the temperature of Atlantic inflow is ~16°C, while Mediterranean outflow is ~12°C; Rogerson et al., 2012). Consequently, in the present-day gateway to the Atlantic, the Strait of Gibraltar, dense Mediterranean water is juxtaposed against lower density Atlantic water (Fig. 1.3). The resulting pressure gradient drives an outflow to the Atlantic Ocean which occupies, roughly speaking, the lower half of the 300 m deep and 13 km wide strait. Above the outflow, an inflow of Atlantic water occurs, pushed eastwards by the sea surface sloping down in that direction (in its turn a direct response of outflow). For a correct understanding of the working of this gateway-landlocked basin system, it is important to realise that the in- and outflow are much larger than the net evaporation through the sea surface. Of the 0.8-1.8 Sv (1 Sv = 10^6 m^3/s) worth of inflow, only about 0.05 Sv is "needed" to close the water budget of the Mediterranean Sea, while the rest flows out again. This description of what has been termed anti-estuarine exchange, relates to the situation averaged over several years. On a shorter (seasonal to tidal) time scale, significant deviations from this generalisation occur (Naranjo et al., 2014). The recent review by Schroeder et al. (2012) provides more background on the present-day strait-basin system, including specific references. Bryden and Stommel (1984) and Bryden and Kinder (1991) stand out from the vast literature on the two-way exchange at Gibraltar.

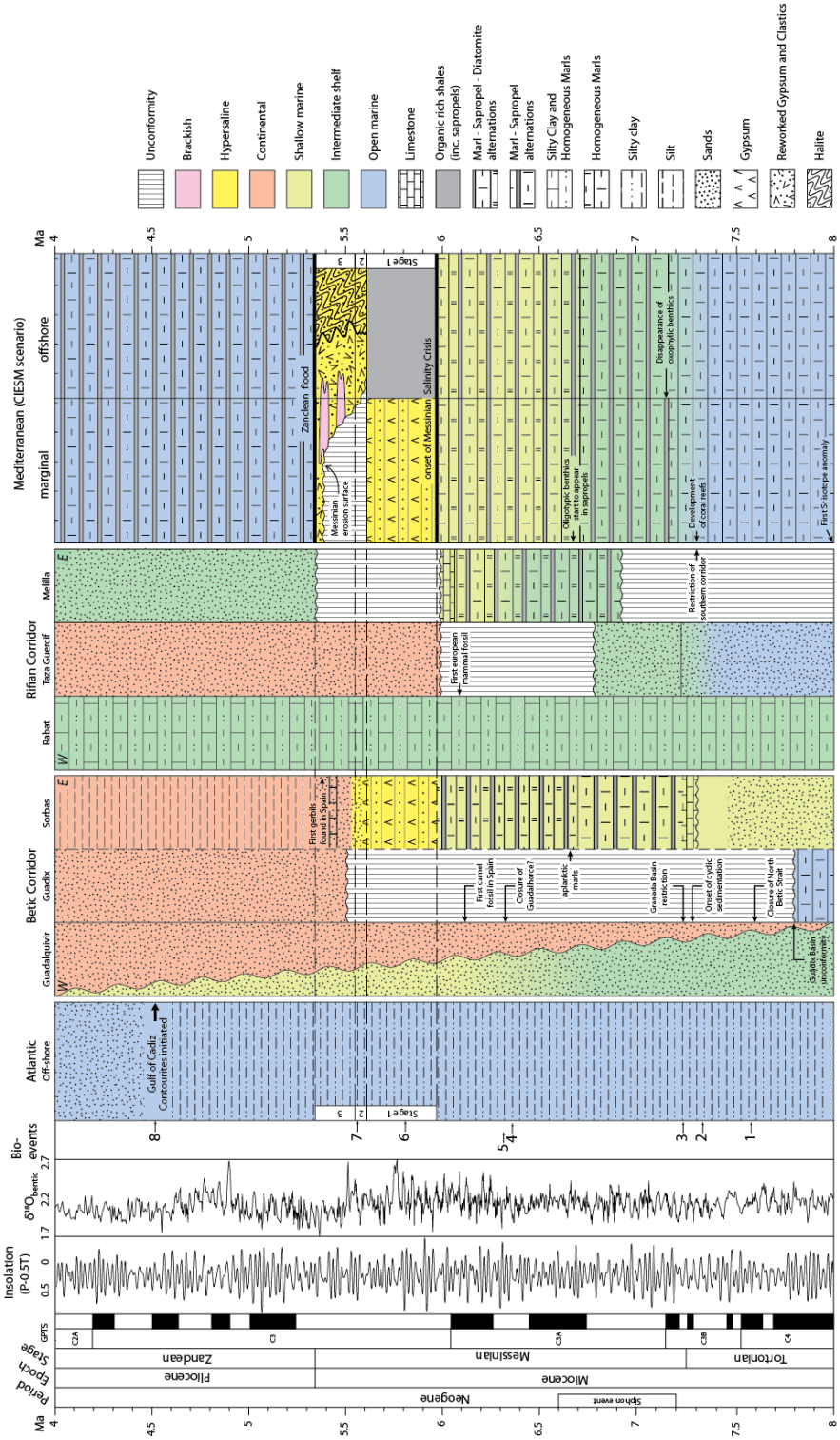
Unconformity
Brackish
Hypersaline
Continental
Shallow marine
Intermediate shelf
Open marine
Limestone
Organic rich shales (inc. sapropels)
Marl - Sapropel - Diatomite alternations
Marl - Sapropel alternations
Silty Clay and Homogeneous Marls
Homogeneous Marls
Silty clay
Silt
Sands
Gypsum
Reworked Gypsum and Clastics
Halite
Mediterranean (CIESM scenario)
marginal
offshore
Rifian Corridor
Betic Corridor
Atlantic
Off-shore
Bio-events
Insolation (P-0.5T)
Period
Epoch
Stage
Ma
Neogene
Miocene
Pliocene
Messinian
Tortonian
Zanclean
Stage 1
Stage 2
Stage 3
Sphon event
Zanclean flood
onset of Messinian Salinity Crisis
Messinian erosion surface
Gulf of Cadiz Contourites initiated
Guadalquivir
Guadix
Sorbas
Rabat
Taza Guercif
Melilla
First gerbils found in Spain
First camel fossil in Spain
Closure of Guadalhorce I
aplanktic marls
Granada Basin restriction
Onset of cyclic sedimentation
Closure of North Betic Strait
Guadix Basin unconformity
First european mammal fossil
Restriction of eastern corridor
Oligotypic benthics start to appear in sapropels
Development of coastal sabkhas
Disappearance of oxophylic benthics
First Sr isotope anomaly

Figure 1.2. *Summary of the Late Miocene- Early Pliocene stratigraphy of the Mediterranean, Atlantic gateway region. From left to right the columns are: Age; Geomagnetic Polarity Time Scale (GPTS); P-0.5T which is normalized precession minus half normalized obliquity. This is almost identical to summer insolation on 25th June at a latitude of 65° North and takes into account the time lag between astronomical forcing and climatic response for the different frequency bands (Lourens et al., 1996); Benthic foram □18O curve generated for the Rabat section, Morocco (Hodell et al., 2001) and the Plio-Pleistocene stack (Lisiecki and Raymo, 2005); Bioevents where 1= LCO G. menardii 4, 2= FCO of G. menardii 5, 3= FCO of G. miotumida group; 4= N. aconstaensis s/d, 5= FO G. margaritae, 6= bottom acme G. margaritae, 7= influx G. menardii sinistral, 8= FO G. puncticulata; sedimentation, environments and events in the Atlantic adjacent to the gateway area, Betic and Rifian corridors and the Mediterranean (split into shallow and deeper water settings according to the CIESM scenario; Roveri et al 2008).*

Today, Mediterranean salinity is about 38-39 ppt (1ppt = 1 gram of salt per kilogram of water, roughly equivalent to 1 gram per litre or 1psu, practical salinity unit), which is higher than at least 90% of the world ocean. During the MSC, Mediterranean salinity attained more extreme levels, reaching gypsum saturation (~130ppt) or even higher. As net evaporation during the Late Miocene was of a similar order as today (Gladstone et. al. 2007), it is clear that during the MSC the dimensions of the Atlantic-Mediterranean ocean gateway must have been significantly different from those of the present Gibraltar Strait.

1.2.2 Geodynamic framework of the gateway region

The Mediterranean is the last remnant of a much larger Tethys Ocean that formed in the Jurassic with the breakup of Pangea. Continental fragments rifted away from North Africa and collided with Eurasia to form the complex of Mesozoic to early Cenozoic basement that dominates the countries bordering the north Mediterranean coast. As late as the Early Miocene, there was still a marine corridor that linked the Mediterranean with the Indian Ocean (Hüsing et al., 2009b; Rogl, 1999). Closure of this eastern gateway fundamentally changed global oceanic circulation by shutting off the circum-equatorial current (Bryden and Kinder, 1991; Reid, 1979), changed salinity and temperature in both Mediterranean and Paratethys (Karami et al., 2011) and may have played a role in global Middle Miocene cooling (e.g. Flower and Kennett, 1993; Woodruff and Savin, 1989). In this broad context, the current corridor region of Gibraltar and adjacent Morocco and Spain has been the location of the western arm of the seaway and its link to the Atlantic since the inception of the Tethys Ocean.

The external thrust belt of the Gibraltar domain gives the Betic-Rif-Tell arc its characteristic horseshoe shape (Fig.1.1). It consists of the Pre- and Subbetic of southern Spain, the Prerif in Morocco and the Tell Mountains of northwest Algeria (Fig. 1.1). These thrust belts are mostly the remnants of the Iberian and Nubian (African) passive margins that were deformed by thin-skinned folding and thrusting during the Miocene (Fig. 1.1 insert). In addition, the thrust pile involves deep marine sediments, the Flysch nappes (Fig. 1.1), which are thought to be derived from a nearby oceanic basin. The

external thrust belt was activated in the Flysch Nappes and Subbetics during the Burdigalian and has accumulated up to 8.5 km crustal material and sediments since then (Fullea et al., 2010). The Rifian corridors in northern Morocco are thought to have been over-thrust by the external thrust belt in Morocco and the Tell Mountains while the accretionary wedge in the Gulf of Cadiz, which is largely continuous with the external thrust belt (Fig. 1.1), started building up in the Middle Miocene, initially as a result of westward over-thrusting by the Betic-Rifian belt on to the Atlantic margins (Medialdea et al., 2004).
The internal zone of the arc (Internal Betics of southern Spain and the Internal Rif in northern Morocco) over-thrusts Upper Cretaceous to Lower Miocene Flysch deposits of the Nubian and Iberian palaeomargins. This zone consists mainly of metamorphic rocks that were unroofed during Early Miocene extension that also affected the Alborán Basin (Comas et al., 1999). Remnants of the Guadalhorce gateway (see section 3.1) are located in the Internal Betic of southern Spain (Martín et al., 2001). The internal zone and the Alborán Basin (Fig. 1.1) are commonly considered to be genetically linked and are referred to as the Alborán Domain. Here, Miocene extension came to an end in the Tortonian, and strike-slip and thrust faulting were initiated (Lonergan and White, 1997; Platt and Vissers, 1989). Flat-lying Pliocene-Recent sediments that cover the Cadiz accretionary wedge (Iribarren et al., 2007) attest to a significant change in the regional tectonics west of Gibraltar at the end of the Miocene.

One driver of the regional deformation has been the convergence of Nubia and Eurasia. Following closure of the Iberian-Eurasian suture in the Pyrenees around 20 Ma (Vissers and Meijer, 2012), continuing convergence was accommodated in the Betic-Rif-Tell region. However, an additional tectonic driver is needed to explain the westward transport and extension of the Alborán Domain since the Miocene in this convergent setting (Dewey et al., 1989; Maldonado et al., 1999). The most likely driver is rollback of the east dipping Gibraltar slab (Gutscher et al., 2002; Lonergan and White, 1997) resulting from subduction that occurred mostly during the Miocene (see Gutscher et al., 2012; and Platt et al., 2013 for recent reviews). New seismological observations support the idea of Duggen et al. (2003) that delamination of the lithospheric mantle and upwelling of asthenosphere beneath northwest Africa and southern Spain accompanied the rollback of the slab (Thurner et al., 2014).

Figure 1.3 *Vertical east-west section along the Strait of Gibraltar showing the present-day salinity distribution a) between 0-300 m water depth and b) down to 2500 m. Depicted is the climatological field, averaged latitudinally across a 0.5 degree wide slice through the Strait (MEDAR Group, 2002); c) Cartoon of present day Mediterranean-Atlantic exchange where E = evaporation, P = Precipitation, R = river inflow and Q_{in} and Q_{out} are the exchange fluxes at the gateway.*

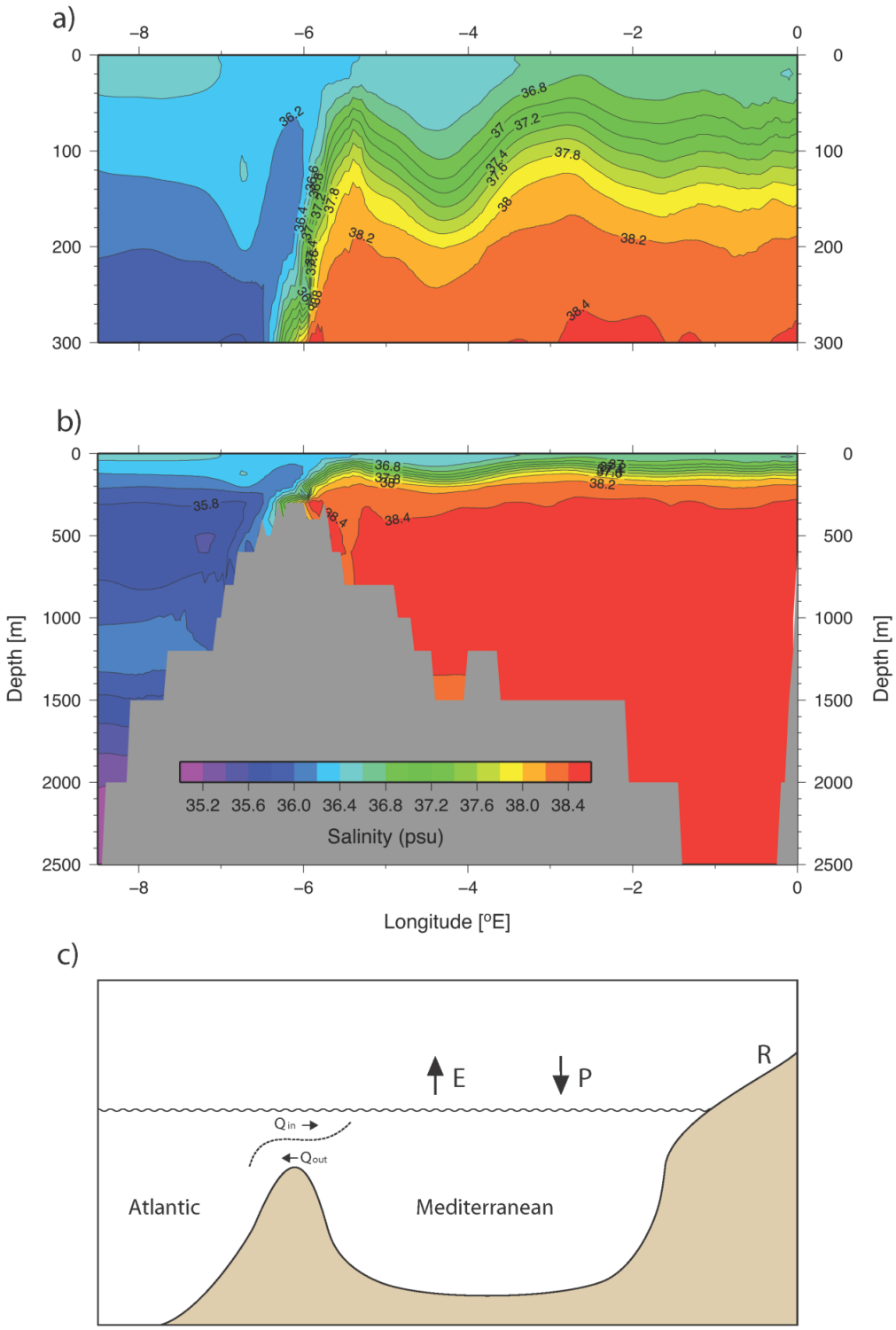
a)
−8
−6
−4
−2
0
100
200
300
36.2
36.8
37
37.2
37.4
37.6
37.8
38
38.2
38.4
b)
500
1000
1500
2000
2500
35.8
Depth [m]
35.2 35.6 36.0 36.4 36.8 37.2 37.6 38.0 38.4
Salinity (psu)
Longitude [ºE]
c)
E
P
R
Qin
Qout
Atlantic
Mediterranean

Regional GPS velocities (Koulali et al., 2011) and seismicity (Stich et al., 2006; Zitellini et al., 2009) suggest that the active plate boundary aligns with the boundary between the Alborán Domain and exterior thrust belt in southern Spain (Fig. 1.1). In northern Morocco, the active boundary follows the outer boundary of the Prerif in the south (Toto et al., 2012) and the Nekkor fault in the east (Fig. 1.1). GPS observations also indicate that the west Alborán-Cadiz block currently moves independently to the SW relative to Africa at a rate of a few mm/yr, i.e. velocities deviate significantly from the relative velocity of stable Africa with respect to stable Eurasia (4.3-4.5 mm/yr; Fernandes et al., 2003). This suggests that, in addition to the convergence of Africa and Iberia there is another driver for these motions (Gutscher et al., 2012).

1.2.3 Messinian stratigraphy of the Mediterranean and Atlantic basins

The stratigraphy that characterises the Late Miocene sediments of the Mediterranean-Atlantic gateway region results from the relative influence of both the adjacent basins and the tectonic evolution of the area itself. It is beyond the scope of this paper to describe in detail the extensive stratigraphic work that has been carried out on Late Miocene Mediterranean and Atlantic sediments (Roveri et al., 2014a). However, a brief description of the Messinian sedimentary sequences in both basins is provided here, along with a summary figure illustrating their relationship with the corridor sediments (Fig. 1.2).

Knowledge of the Late Miocene Mediterranean sedimentary evolution is heavily biased by the onshore exposures. Around the margins of the Mediterranean there are numerous sections of pre-MSC sediments and much of the lower part of the MSC succession is also exposed. A continuous deep basinal sedimentary succession is however still lacking as it has not yet been possible to drill in the deep Mediterranean and recover a complete MSC succession.

1.2.3.1 Mediterranean onshore successions

The pre-evaporite succession onshore consists of cyclic alternations of homogeneous marls, sapropels and diatomites (Fig. 1.2) that were deposited in response to astronomically-driven climate oscillations, predominantly precession, and were amplified as the Mediterranean became progressively isolated from the open ocean (Bellanca et al., 2001; Blanc-Valleron et al., 2002; Hilgen and Krijgsman, 1999; Hilgen et al., 1995; Krijgsman et al., 1999a; McKenzie et al., 1980; Sierro et al., 1999, 2001; Suc et al., 1995). This orbital signal combined with biostratigraphic and palaeomagnetic data allows the age of these sediments to be precisely constrained with an error of a single precessional cycle (+/-10 kyr; Krijgsman et al., 1999a).

The onset of the Messinian Salinity Crisis occurred at 5.97 Ma (Fig. 1.2; Manzi et al., 2013) with synchronous precipitation of gypsum in marginal basins around the

Mediterranean (Krijgsman et al., 2002, 1999a). This first period of the MSC (Stage 1; Fig. 1.2) is characterised by deposition of 16-17 gypsum horizons with interbedded laminated clastic sediments (Krijgsman et al., 2001; Lugli et al., 2010; Manzi et al., 2013). Little is known about coeval deposition in the deep basinal areas, but evidence from the Apennines and geochemical relationships suggest that organic-rich shales and dolomites rather than gypsum accumulated here (Fig. 1.2; de Lange and Krijgsman, 2010; Manzi et al., 2007; Roveri and Manzi, 2006).

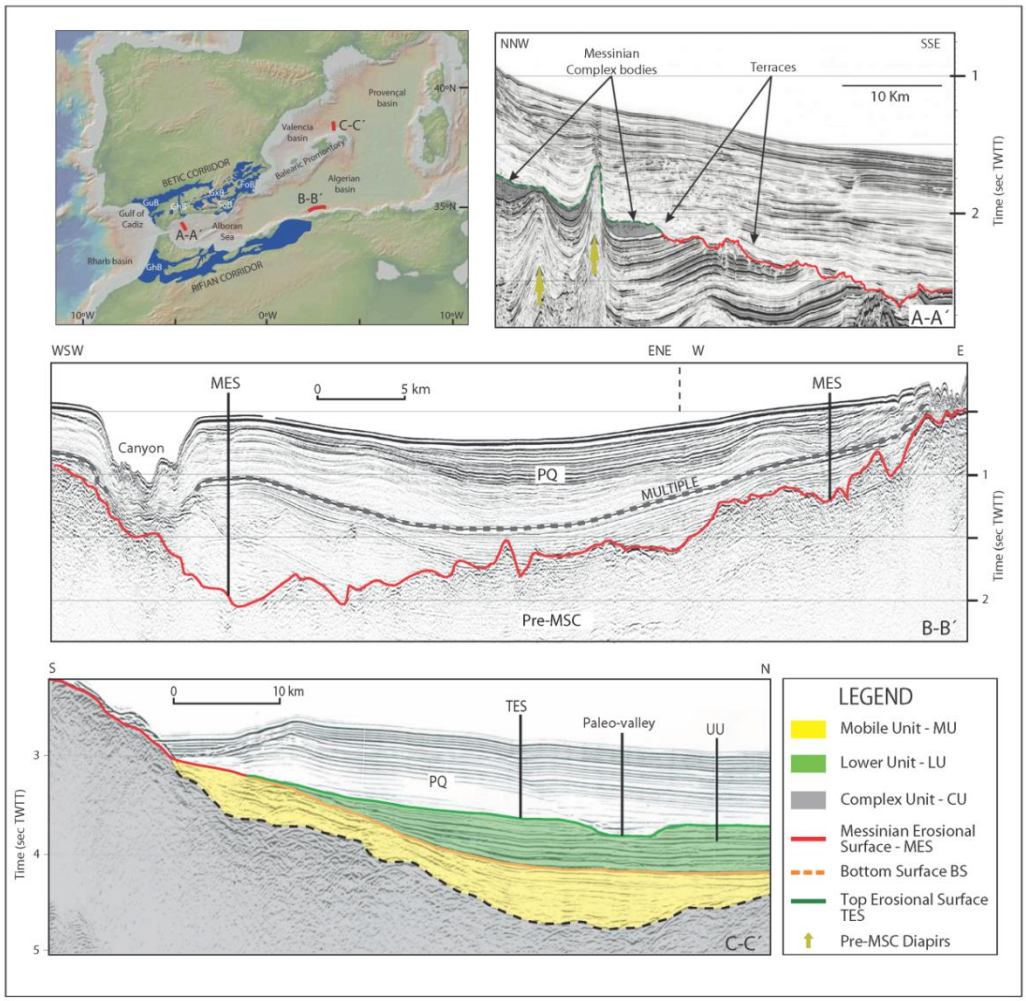

Figure 1.4. *a) Location map of the Atlantic and Mediterranean offshore basins adjacent to the gateway region and the location of seismic sections A-A', B-B' and C-C'. GuB Guadaquivir Basin, GhB Guadahorce Basin, SoB Sorbas Basin, GXB Guadix Basin, FoB Fortuna Basin, GhB Gharb Basin. b) Seismic section from the Alborán Sea close to the Guadalhorce corridor, part of the Betic connection. c) Seismic section from the Valencia Basin. d) Seismic section from the Algerian Basin close to onshore Neogene corridor sediments.*

Unsurprisingly, evaporite-bearing successions lack clear biostratigraphic markers and have a weak palaeomagnetic signal. Consequently, the independent age tie points that are used so successfully to confirm the age of pre- and post-MSC sediments are not available during the MSC itself. However, assuming precession also controlled the periodicity of gypsum cyclicity, the top of Stage 1 Lower Evaporites has been estimated at 5.61 Ma (Fig. 1.2; CIESM, 2008; Hilgen et al., 2007; Krijgsman et al., 2001; Roveri et al., 2014a).

In some marginal basins, the upper boundary of Stage 1 is marked by a major erosive event known as the Messinian Erosion Surface (MES; Fig. 1.2 and 1.4) which can also be traced offshore in seismic data where it splits into several surfaces not all of which are erosional (Fig. 1.4c; Lofi et al., 2011a; Lofi et al., 2011b). The marginal erosion surface is likely to have been caused by a sea-level drop which resulted in reworking and transport of sediments basinward, including significant gypsum, and their deposition in intermediate to deep basinal settings (Fig. 1.2; e.g. Clauzon et al., 1996; Lofi et al., 2005; Maillard et al., 2006; Manzi et al., 2005; Roveri et al., 2008). However, whether the associated seismic surfaces offshore were generated in subaerial or subaqueous environments is still highly contentious.

The halite phase of Stage 2 only developed in the deep basins (Fig. 1.2 and 1.4). By contrast, Stage 3 sediments which, in the upper part includes intervals known as the Lago Mare, have been recognized in many of the Mediterranean's marginal basins (Fig. 1.2). These sediments contain fauna thought to live in brackish water conditions (Bassetti et al., 2003; Bassetti et al., 2006; Orszag-Sperber, 2006); on Sicily, these deposits are interbedded with gypsum (Manzi et al., 2009; Rouchy and Caruso, 2006). In the western Mediterranean and within the Betic Corridor, however, the Lago Mare comprises grey to white marls interbedded with deltaic or fluvial conglomerates (Fig. 1.2; Fortuin and Krijgsman, 2003; Omodeo Salé et al., 2012). Material recovered from ODP and DSDP holes that correlates with the seismic Upper Unit, indicates that Lago Mare sediments overlie the deep sea evaporites (Hsü et al., 1973; Hsü et al., 1977; Orszag-Sperber, 2006; Roveri et al., 2014b). Unfortunately, the correlative relationship between these offshore deposits and the marginal sediments remains unclear. During Stage 3 the Mediterranean may have been isolated from the open ocean until the return to normal open marine conditions after the Miocene-Pliocene boundary (Fig. 1.2) at 5.33 Ma (Lourens et al., 1996).

1.2.3.2 Mediterranean offshore successions

The interpretation of the Mediterranean's basinal succession is mainly reliant on seismic data. These data show that in the deepest parts of the western basin, a seismic trilogy is developed comprising a bedded Lower Unit (LU) of unknown age and lithology with low frequency reflectors; a transparent Mobile Unit (MU; Fig. 1.4c) consisting mainly of halite and showing plastic deformation; and a bedded Upper Unit (UU) which occurs

just below Lower Pliocene sediments (Fig. 1.4; Lofi et al., 2011a; Lofi et al., 2011b). Of these, only the Upper Unit has been drilled (e.g. sites 122 and 372; Montadert et al., 1978; Ryan et al., 1973). The absence of well-ties and significant differences between the onshore and offshore MSC successions makes correlation highly controversial.

Seismic mapping of the Mobile Unit indicates that a large volume of salt, more than 2 km thick in some places, accumulated in the deepest parts of the Mediterranean (CIESM, 2008; Hsü et al., 1973; Lofi et al., 2005). It has been argued that this extensive salt deposit is equivalent in time to the major base-level drawdown that eroded the margins (e.g. Stage 2; Fig. 1.2; CIESM, 2008; Roveri et al., 2014a). This temporal coincidence suggests a major change in the pattern of Mediterranean-Atlantic exchange such that while Mediterranean outflow decreased to very low levels reducing salt export to the Atlantic, ocean inflow continued providing a constant supply of the ions required for gypsum and halite formation (Krijgsman and Meijer, 2008; Lugli et al., 2010; Meijer, 2006).

Mediterranean offshore succession adjacent to the corridors

The Western Mediterranean is made up of a series of basins that contain sediments deposited in both marginal and deep water settings during the MSC e.g. Alborán, Algerian, Provençal and Valencia basins (Fig. 1.4). They provide insight into the relationship between the marine corridors and the deeper Mediterranean Basin to which they were connected.

The Algerian Basin, located between the Alborán Basin to the west, Sardinia to the east, and the Balearic Promontory to the north (Fig. 1.4) has a complex geological history resulting from the Alpine orogeny (Mauffret et al., 2004). The basin is characterized by having young oceanic basement, relatively thin pre-MSC sediments and significant salt-driven deformation. The deep basin MSC trilogy has been identified offshore (Capron et al., 2011; Obone-Zué-Obame et al., 2011). The Messinian Erosion Surface is, as elsewhere, traced on the margin between pre-MSC and prograding Pliocene deposits, where it preserves several deep canyons (Fig. 1.4b; Obone-Zué-Obame et al., 2011). The connection between the onshore Algerian corridors and their offshore extension has yet to be fully explored.

The MSC seismic trilogy is absent from the Alborán Basin which is dominated by the presence of a widespread erosion surface (MES, Fig. 1.4a; eg. Estrada et al., 2011). The MES separates Miocene units from Plio-Quaternary sediments and appears as a prominent, high-amplitude, and laterally continuous reflector (Martínez-García et al., 2013) that occurs in terraces at different depths (Fig. 1.4a; Estrada et al., 2011). The origin of this erosional surface is thought to be polygenic since it has been shaped by multiple erosional stages related to erosion during the MSC acme and the Zanclean

reflooding through the Gibraltar Strait (Estrada et al., 2011; Martínez-García et al., 2013).

Where the basin has been drilled, the Pliocene typically unconformably overlies the pre-MSC series (e.g. Leg 13 site 121; Leg 161 sites 977, 978). Where MSC sediments are recovered (CU unit in Fig. 1.4a), they consist of pebbles, shallow-water carbonates, sandy turbidites and gypsum or anhydrite deposits (Iaccarino and Bossio, 1999; Jurado and Comas, 1992), which are interpreted as being deposited in small isolated lacustrine basins (Martínez-García et al., 2013) equivalent in age to the Lago Mare (Fig. 1.2).

Late Miocene marine sediments exposed along the north coast of Morocco adjacent to the Alborán Sea (Fig. 1.1) indicate the nature of this eastern extension of the Rifian Corridor. The sections near the Melilla volcanic centre (Fig. 1.6) record alternations of volcanic ashes interbedded with diatomites and marls that grade up and laterally into reef carbonates (Fig. 1.2; Cornée et al. 2002; Cunningham & Collins 2002; Cunningham et al. 1994; Cunningham et al. 1997; Münch et al. 2001; Münch et al. 2006; Roger et al., 2000; Saint Martín & Cornée 1996; Saint Martín et al. 1991; Van Assen et al. 2006; Azdimousa et al. 2006; Barhoun & Wernli 1999). Where the sections have been astronomically tuned and/or Ar/Ar dated, the resulting interpretation suggests that cyclic sedimentation began around 6.84 Ma (Van Assen et al., 2006). Sedimentation was terminated following exposure at or above sea level at ~6.0 Ma (Fig. 1.2; Münch et al. 2006; Van Assen et al. 2006). In the near-by Boudinar Basin (Fig. 1.6) clastic sedimentation began around late Tortonian (Azdimousa et al., 2006) followed by a transgressive-regressive sequence comprising alternations of marls and sands. The sequence is similar to that seen in the Melilla sections, but in the Boudinar Basin the top sandy-marl intervals are Early Pliocene in age (Barhoun and Wernli, 1999).

The southern limit of the Valencia Basin is formed by the Balearic Promontory which is considered to be the offshore continuation of the Betic Range (Fig. 1.4). The asymmetric basin formed during an Oligo-Miocene extensional phase linked to a concurrent transpressional-compressional system (Alfaro et al., 2002; Doglioni et al., 1997; Fontboté et al., 1990; Gueguen et al., 1998; Maillard and Mauffret, 2011, 2013; Roca and Guimerà, 1992; Vegas, 1992). The intermediate depth of the Valencia Basin and its location adjacent to well exposed onshore successions of Messinian Salinity Crisis sediments (e.g. in the Sorbas Basin) mean that it has great potential as a source of information linking marginal sequences with deep-marine seismic units (Fig. 1.2). In the Valencia Basin, seismic profiles show only an Upper Unit (generally < 200 m thick; Fig. 1.4c) rather than the complete deep basin MSC succession (Maillard et al., 2006) that is observed further east, in the Liguro-Provençal Basin. This Upper Unit overlies an erosion surface which truncates pre-evaporitic reflectors and is itself cut by an upper erosion surface which has been interpreted as having been generated during the latest Messinian (Maillard et al., 2006). Diachronism, a polygenetic origin, and local

expression of the MES hinder assessment of its exact relationship with the MSC event (Fig. 1.4c; Lofi et al., 2005; Maillard et al., 2006; Lofi et al., 2011b).

1.2.3.3 Atlantic successions

Late Miocene Atlantic sediments recovered from the present day Moroccan and Iberian shelf are dominated by nannofossil ooze, clays, marls and silty marls (Fig. 1.2, Hayes et al., 1972; Hinz et al., 1984). Where Atlantic margin sediments are exposed today onshore Morocco and Spain in the mouths of the two corridors, they comprise long and continuous successions of cyclic silty marls.

The Guadalquivir Basin

During the Middle and Late Miocene, all the Betic corridors were connected to the Atlantic Ocean through the Guadalquivir Basin which extends offshore into the Gulf of Cadiz (Fig. 1.1). The sediments of the Guadalquivir Basin are not well exposed on land and most studies are reliant on seismic data, well logs and boreholes (e.g. Berástegui et al., 1998; Fernández et al., 1998; Larrasoaña et al., 2008; Pérez-Asensio et al., 2012b; Riaza, 1996). These indicate that the succession comprises marine and continental sediments that range in age from late Tortonian to Recent (González-Delgado et al., 2004; Sierro et al., 1996). After closure of the North Betic strait, the Guadalquivir Basin was established as a wide marine embayment open to the Atlantic (Pérez-Asensio et al., 2012b), and marine sedimentation continued throughout the late Tortonian and Messinian into the Pliocene (Fig. 1.2). Recent studies of the Montemayor borehole have resulted in a magnetobiostratigraphic framework (Larrasoaña et al., 2008), a palaeoenvironmental scheme based on benthic foraminifera (Pérez-Asensio et al., 2013; 2012a; 2012b) and the reconstruction of local vegetation and sea level changes (Jiménez-Moreno et al., 2013). These results show a shallowing trend before and during the MSC (Fig. 1.2), with two distinct cooling periods and associated sea-level falls, one of which is identified as contributing to the onset of the MSC. However, the chronostratigraphic framework of the Montemayor borehole on which these results are based (Pérez-Asensio et al., 2012a) is constructed from magneto- and biostratigraphic tie-points combined with an age model based on extrapolation of stable isotope data. An improved age model by van den Berg et al. (2015) was based on astronomical tuning of the cycles found in the geochemical composition of the borehole sediments. This shows that the cooling period cannot be associated with the onset of the MSC since the oxygen isotope records follow global ocean trends. These results also imply that there was no direct influence of Mediterranean outflow on this part of the Guadalquivir Basin during the Late Messinian.

The Gharb-Prerif Basin and classic successions near Rabat

The Gharb-Prerif Basin (Fig. 1.1 and 6) straddles the Moroccan Atlantic coastline and is a Miocene foreland basin which developed parallel to the southern edge of the Rif (Michard, 1976; Flinch, 1993; Pratsch, 1996). During the Late Miocene and Early

Pliocene this area, the western extension of the Rifian corridor, was a large marine gulf (e.g. Esteban et al., 1996; Martín et al., 2009). The Gharb-Prerif Basin is commonly divided into two main areas. The northern part links onshore sub-basins in the Rifian corridor's northern strand or Prerif Zone (e.g. Taounate and Dar Souk) with the Gharb Basin which extends offshore (Fig. 1.1), while the southern arm comprises the Sais Basin west of Taza-Guercif and the South Rifian Trough, which also extends offshore. The stratigraphy of the Gharb-Prerif Basin is subdivided into Mesozoic pre-foredeep and Upper Miocene (mainly Messinian) to Pliocene foredeep successions in the north (Flinch, 1993) into the lower part of which deformed Triassic-Miocene sediments of the Prerif Nappes were emplaced (Michard, 1976; Flinch, 1993). During the late stages of the Rif-Betic orogeny,a series of satellite extensional mini-basins were generated within the Gharb Basin that are filled with thick Upper Tortonian to Pleistocene clastics (Flinch and Vail, 1998). These are deformed by a late Neogene phase of flexurally-induced normal faulting and syn- to post-thrusting of the Rif nappes (Zouhri et al., 2002) interpreted as being either coeval (Flinch, 1993), or as part of two episodes of deformation; an extensional Tortonian-Messinian and a compressional Plio-Quaternary episode (Litto et al., 2001).

In the South Rifian Trough (Fig. 1.1), the pre-foredeep succession is overlain by Middle to Late Miocene clastics (Wernli, 1987; Flinch 1993) thought to have been deposited in a shallow foreland basin (Michard, 1976; Flinch, 1993). Unlike the Gharb Basin, it is not disrupted by the Nappe system and the Neogene succession is almost structurally undeformed with a north dipping basement leading to a thicker Neogene and Quaternary succession to the north (e.g. Zouhri et al., 2002). In contrast with the relatively coarse clastic-rich, occasionally turbiditic successions that dominate the central areas of the Rifian corridor, the well-studied sections near Rabat on the Atlantic coast comprise regular alternations of indurated marls that are blue when freshly exposed and softer reddish clay-rich marls (Fig. 1.2) unconformably overlying Devonian limestones (Hilgen et al., 2000). These well exposed successions have been astronomically tuned and therefore have an exceptionally high resolution age model (Hilgen et al., 2000; Krijgsman et al., 2004). In offshore parts of the basin, data is sparse and interpretations are of much lower resolution and often restricted by poor quality seismic data.

Despite being outside the Mediterranean and consequently significantly buffered by the Atlantic Ocean, the tuning of these Late Miocene-Pliocene successions indicates a strong pattern of sedimentary response to precession with secondary components of obliquity and eccentricity (e.g. van der Laan et al., 2005). Fluctuations in the faunal assemblage that mirror this strong precessional signal are similar to, but of lower amplitude than those seen in time equivalent sediments in the Sorbas Basin (Fig. 1.2; van der Laan et al 2012). One possible explanation for the insolation-driven sedimentation that persists in the Rabat successions before, during and after the MSC is that the controlling

mechanism linking orbital forcing to its sedimentary response is, in this area, independent of the state of connectivity between the Atlantic and Mediterranean and therefore probably lies outside the Mediterranean. A possible explanation for the colour cycles are precession driven climate oscillations that are linked to the Atlantic system (Bosmans et al 2015; Brayshaw etal 2001; Tzedaks, 2007) rather than to the African monsoon as generally assumed for Mediterranean sapropels (Kutzbach et al., 2014). The Atlantic system brings rain in the winter-halfyear, and the dominantly precession controlled changes in this system may have been operative at least from 7.8 Ma to the Recent, although climatic interpretations differ (Sierro et al., 2000; Moreno et al., 2001; Bozzano et al., 2002; van der Laan et al., 2012; Hodell et al., 2013).

1.3 EVOLUTION OF THE ATLANTIC-MEDITERRANEAN GATEWAYS: DIRECT APPROACH

The distribution of Late Miocene marine sediments across Northern Morocco and Southern Spain resembles a complex network of channels connecting the Mediterranean and Atlantic (Fig. 1.1, 1.5 and 1.6) and it is this now uplifted area that is considered to be the Late Miocene gateway region (e.g. Santisteban and Taberner, 1983). It is less clear, however, how much of the bifurcating channel pattern reflects the primary configuration of the Late Miocene marine corridors and how much is a function of the preservation of the sediments after uplift and erosion. Much of the sedimentation of this region, particularly at either end of the corridors, is characterised by clay-silt grade material (Fig. 1.2) with few if any current structures. This is indicative of low energy conditions rather than the coarser material anticipated from high velocity currents such as those seen in the Gibraltar Strait today. Even in central areas of the corridors, where sands and conglomerates are common (Fig. 1.2), these may result from uplift-driven higher energy processes relating to slope transport for example, rather than being the direct product of inflow or outflow current transport and deposition. Here we present a summary of the sedimentological data preserved in the exposed gateway region.

1.3.1 The Betic Corridor

The Betic Corridor can be subdivided into four distinct connections that link the Atlantic with the Mediterranean during the Late Miocene: the North-Betic strait; the Granada Basin; the Guadix Basin and the Guadalhorce Basin (Fig. 1.5). All these basins contain large-scale palaeocurrent structures (Fig. 1.5) typically in coarse-grained sand or conglomeratic sediments indicating high energy currents (Martín et al., 2014). These coarse clastics which commonly form the last part of the preserved succesion are difficult to date. However, some of the Betic successions also contain evaporite and continental sediments that predate the MSC suggesting that these connections were

conduits for Mediterranean-Atlantic exchange before the formation of the Mediterranean's saline giant.

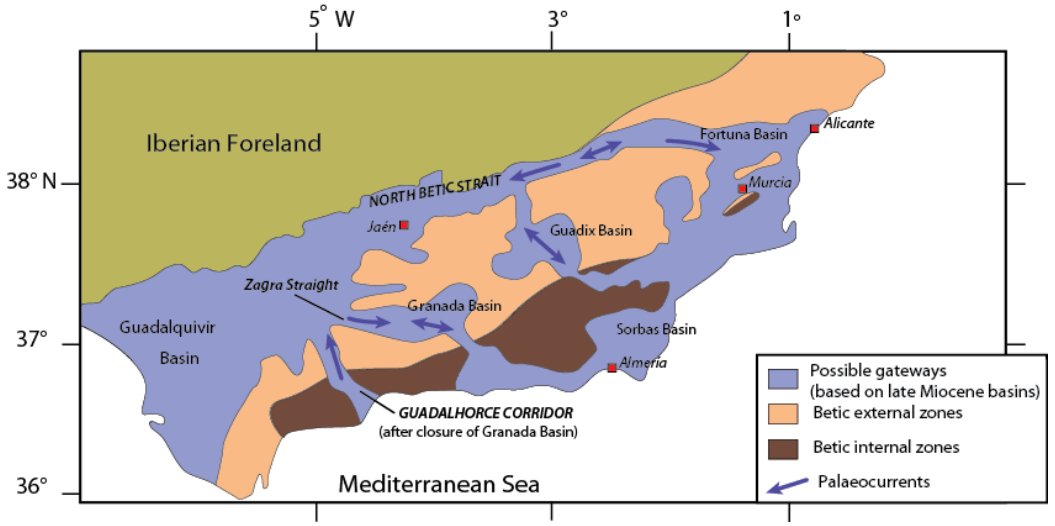

***Figure 1.5**. Detail map of the Betic Corridor showing the main geological units, corridors and palaeocurrent indicators (modified after Santisteban and Taberner, 1983). Palaeocurrents from Santisteban and Taberner (1983), Benson et al. (1991), Martín et al. (2001) and Martín et al. (2014).*

North Betic strait: This most northerly corridor connects the Guadalquivir Basin and the Mediterranean through the Fortuna and Lorca basins (Fig. 1.5; Martín et al., 2009). Müller and Hsü (1987) initially suggested that the North Betic strait was open throughout the Messinian, allowing an ocean water flux and providing the salt required for evaporite deposition to reach the Mediterranean. This flux was thought to have been modulated by glacio-eustatic sea level change Santisteban and Taberner (1983). By contrast, Benson et al. (1991) envisaged the North Betic Strait closing just before the onset of the MSC, but serving as a channel for unidirectional Mediterranean outflow during the precursor 'Siphon event'. Subsequently, integrated stratigraphic studies were carried out on the Fortuna Basin at the eastern end of the North Betic Strait (Garcés et al., 1998; Krijgsman et al., 2000b). These indicate that sedimentation changed from marls to diatomites and evaporites at 7.8 Ma (the 'Tortonian salinity crisis' of the eastern Betics; Krijgsman et al., 2000a), before deposition of continental deposits at ~7.6 Ma. The dating of this tectonically driven restriction event (Krijgsman et al., 2000a) suggests that the North Betic Strait cannot have been the route by which ocean water reached the Mediterranean during the MSC.

Granada Basin: The Granada Basin connects the Guadalquivir Basin to the Mediterranean via the Zagra strait (Martín et al., 2014). The stratigraphy of this basin was first described by Dabrio et al. (1978), who suggested tectonism caused basin restriction through the uplift of the present day Sierra Nevada, leading to the deposition of evaporites in the Granada Basin (Fig. 1.5) that pre-date the MSC (Fig. 1.2). According to Martín et al. (1984) this restriction took place around the Tortonian-Messinian transition. Braga et al. (1990) suggested instead that restriction began on the eastern side of the basin in the late Tortonian, spreading to the southern and western margins which uplifted around the Tortonian–Messinian boundary, gradually isolating and desiccating the basin and filling it with continental deposits. The restriction of the Granada Basin has recently been more precisely dated using biostratigraphy by Corbí et al. (2012) demonstrating that a short phase of evaporite precipitation occurred between 7.37 to 7.24 Ma, followed by a less well constrained phase of continental sedimentation. This confirms the conclusion of earlier studies that the Granada Basin was not a conduit for Mediterranean-Atlantic exchange for any part of the Messinian.

Guadix Basin: This was a relatively open marine passage (around 12-15km wide), probably permitting two-way flow, with coarse grained sediments deposited on the edges while marls accumulated in its central part. Later it evolved into a narrow strait with strong bottom currents flowing from the Mediterranean to the Atlantic, based on huge bioclastic sand and conglomerate dunes, displaying internally cross-bedding several meters high (Fig. 1.5; Betzler et al., 2006). Contemperanous with these bottom currents there were Atlantic surface current flowing southwards (Puga-Bernabeu et al., 2010). Although there is broad consensus that the Guadix Basin corridor, (or Dehesas de Guadix strait; Martín et al., 2014) was open during the late Tortonian (Betzler et al., 2006; Hüsing et al., 2010; Soria et al., 1999), the detailed timing of the closure is disputed. According to Betzler et al. (2006) the strait narrowed to about 2 km and was finally blocked at ~7.8 Ma by a tectonic swell fringed by reefs (7.8-7.4 Ma). This is contradicted by more recent magnetobiostratigraphic results for the same section (La Lancha, Hüsing et al., 2010) which show that there is a major hiatus of at least 2 Myr between open marine sediments of ~7.85 Ma and continental deposits, dated at 5.5 Ma (Fig. 1.2) in agreement with the presence of the MN13 mammal biostratigraphy (Hüsing et al., 2012; Minwer-Barakat et al., 2012). This unconformity means that closure of the Guadix Basin corridor is not recorded and consequently, the possibility that a shallow marine connection remained during MSC Stage 1 and 2 cannot be excluded.

Guadalhorce Corridor: The history of the Guadalhorce corridor (Fig. 1.5; Martín et al., 2001) is less well known than the other Betic basins. Its sedimentary record consists predominantly of siliciclastics containing unidirectional cross-beds (Fig. 1.2) with sets over 100m in length and ranging from 10 to 20m in thickness. These structures have been interpreted as indicating that the corridor was at least 60-120m deep and subject

to an extremely fast (1.0-1.5 m s^{-1}) unidirectional current flowing northwest (Fig. 1.5; Martín et al., 2001). Foraminifera-bearing marls intercalated with carbonates in one of the outcrops towards the bottom of this unit have an early Messinian age (7.2-6.3; Martín et al., 2001). Consequently, the Guadalhorce corridor was considered to be a conduit for Mediterranean outflow prior to the MSC in accordance with the 'siphon' model (Benson et al., 1991). Pérez-Asensio et al. (2012b) also took the view that Guadalhorce had an important role in Mediterranean to Atlantic outflow. These authors assume that ultimately all other corridors were closed during the MSC and only the Guadalhorce supplied Mediterranean water to the Atlantic via the Guadalquivir Basin during this period. They interpreted a change in benthic $\delta^{18}O$ record in the Guadalquivir Basin at 6.18 Ma, as indicating closure of the Guadalhorce corridor. However, as there are no MSC-aged sediments preserved evidence of this from within the Guadalhorce corridor itself remains to be found.

In summary, of the four possible Betic corridors that may have supplied Atlantic water to the Mediterranean during the Late Miocene, two are known to have been closed during the MSC (the North Betic Corridor and the Granada corridor) while the successions of the remaining two (Guadix and the Guadalhorce corridors) contain large unconformities and uncertainties that span the critical Late Miocene period. It is therefore not currently possible to rule out definitively an open or intermittent connection within the Betic Corridor area during the MSC.

1.3.2 The Rifian Corridor

The distribution of late Tortonian and Messinian sediments through northern Morocco is broadly divided into a northern and a southern strand (Fig. 1.6); the intramontane basins form the northern part of this gateway; the Nador - Taza-Guercif - Rabat axis forms the better-studied southern arm. These strands merge at their western end which, in the Late Miocene, formed a broad Atlantic-facing embayment (Fig. 1.6). By contrast, their eastern connections to the Mediterranean are distinct, with the northern strand reaching the Mediterranean between Boudinar and Melilla and the southern strand joining further east in Algeria. Given that the area between the two strands is a thrust nappe pile (Chalouan et al. 2008, Flinch 1993, Feinberg 1986) which is locally overlain by Late Miocene marine sediment, one possibility is that the Rifian corridor was in fact a single wide strait which has subsequently been uplifted and eroded leading to the preservation of a more complex and segmented pattern of Late Miocene marine sediments (Fig. 1.6). Detailed palaeogeographic data are required to distinguish between these two hypotheses.

Understanding of the evolution of the Rifian Corridor is strongly biased by the location of well-studied sections, some of which have been astronomically tuned. To be specific:

1. There is almost no published information about the onshore Algerian section of the corridor;
2. For reasons of exposure, nearly all information available regarding the western embayment comes from an area to the south, near Rabat (Fig. 1.6);
3. The only astronomically tuned section from the central part of the corridor is located near the southern margin of the southern strand, in the Taza-Guercif Basin (Fig. 1.6).

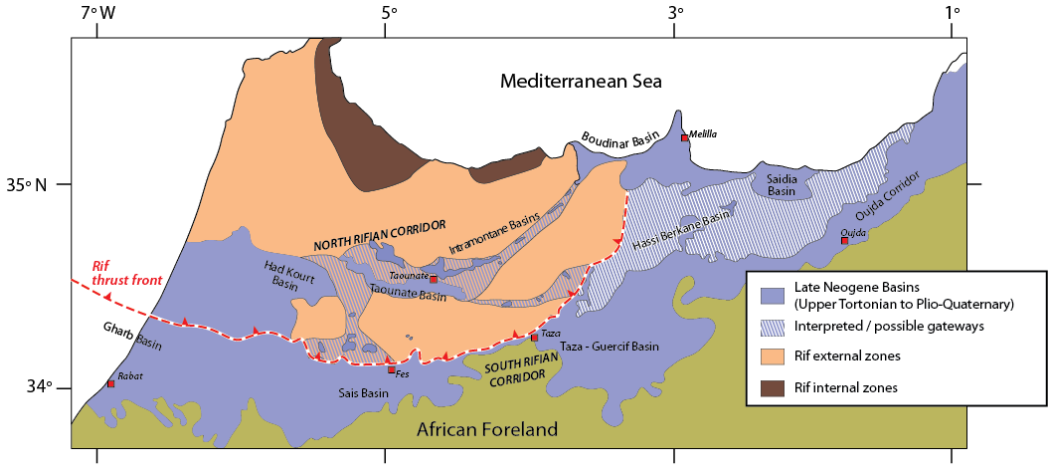

Figure 1.6 *Detail map of the Rifian Corridor showing the main geological units and corridors.*

North Rifian connection: The age of the northern strand of the Rifian Corridor currently relies on biostratigraphic analysis of marine sediments carried out during the eighties (Wernli, 1988). These sediments are all assigned to an undifferentiated Tortonian-Messinian marine zone (M6), which spans 11.6 to 5.3 Ma but does not allow more accurate age subdivisions. Nevertheless, the highly diverse faunal assemblage suggests sediments occurring in these apparently distinct subbasins (Taounate, Dhar Souk, Boured; Fig. 1.6) experienced open marine conditions during the Late Miocene. Sections near the town of Taounate and in the other intramontane basins record the onset of clastic sedimentation with poorly sorted conglomerates and sandy marls, followed by thick alternations of marls and sands which indicate abundant sediment input from the basin margins. The top of the marine sequence is generally truncated by erosion and covered by Quaternary deposits (Wernli 1988).

South Rifian Corridor: Astronomical tuning of the central southern Taza-Guercif Basin section (Fig. 1.6) indicates that closure of this part of the corridor (e.g. the transition from marine to continental sedimentation) occurred between 6.7 to 6.0 Ma (Fig. 1.2; Krijgsman and Langereis, 2000; Krijgsman et al., 1999b), but this evidence cannot preclude there being a concurrent Mediterranean-Atlantic connection further north. The Nd isotope data from the Taza-Guercif Basin suggests that restriction of the southern strand of the corridor took place to the east around 7.2 Ma, cutting the connection with the Mediterranean, but allowing the connection between the Taza–Guercif Basin and the Atlantic to persist (Ivanović et al., 2013a; see section 4.1.2). The timing is coincident with a significant shallowing event seen in the palaeobathymetric reconstructions for the thick clastic successions found in the central Taza-Guercif Basin (Krijgsman et al., 1999b). The sedimentation pattern in the Taza-Guercif Basin is consistent with a pre-MSC closure of the Rifian Corridor as a whole, for which there is a growing and diverse body of evidence including evidence from mammal fossils which indicates that rodents were able to migrate between Morocco and Spain before 6.1 Ma (Agustí et al., 2006; Benammi et al., 1996; Gibert et al., 2013).

Palaeomagnetic studies in the Rifian Corridor demonstrate that no vertical axis rotations have occurred in the Taza and Gharb foreland basins and in the post-thrusting Melilla Basin (Fig. 1.1) since the Tortonian-Messinian (Krijgsman and Garcés, 2004). In the Rifian part of the External Thrust Belt (Fig. 1.1), however, upper Miocene thrust top sequences show anticlockwise rotations (Cifelli et al., 2008). Southward propagation of the thrust load appears to be a significant driver of closure of the Rifian corridors along with regional uplift attributed to slab dynamics (Duggen et al., 2004).

1.3.3 Strait of Gibraltar

The Strait of Gibraltar connects the Mediterranean with the Atlantic today (Fig. 1.1) and is commonly assumed to have formed at the Miocene/Pliocene boundary (5.33 Ma; Hsü et al., 1973; Hsü et al., 1977) with rapid (5-800 days according to Garcia-Castellanos, 2009) refilling of the Mediterranean (Blanc 2002, Meijer & Krijgsman 2005, Loget & Van Den Driessche 2006, Garcia-Castellanos 2008). The assumption of a major 'Zanclean flood' is based on seismic evidence of an incised channel that dips from the Gibraltar Strait across the Alborán Sea and can be followed for at least 300 km towards the east (Estrada et al., 2011). Here, the deep U-shaped incision merges laterally with the Messinian Erosion Surface (MES) and is locally filled with Plio-Quaternary sediments (Campillo et al., 1992; Garcia-Castellanos et al., 2009). The cause of the initial rupture at Gibraltar is still debated. If a eustatic trigger is excluded (van der Laan et al., 2006), it may have been caused by tectonic collapse (Govers, 2009), possibly in combination with headward river erosion (Hsü et al., 1973; Blanc 2002, Loget & Van Den Driessche, 2006).

Detailed geomorphological studies (Esteras et al., 2000, Blanc 2002) revealed the asymmetric structure of the strait and identified an eastern and western domain. The eastern domain is narrower and deeper (750 to 960 m) while the western domain has an irregular bottom morphology composed of sharp submarine hills up to 80m high, large flat banks and ditches up to 650 m deep. To explain such physiography Esteras et al. (2000) suggested that large gravity slides of unknown age may have occurred, derived from both the Iberian and Moroccan margins. A major slide may have been contemporaneous with the Zanclean flood (Blanc, 2002). These gravitational collapses locally filled the two excavated channels with flysch mud-breccia, forming shallow sills.

Since the clastic sediments at the base of the canyon infill are not dated, and the age of the main erosion event that shaped the channels remains uncertain (Esteras et al., 2000), the possibility that (at least temporary) opening of the Strait of Gibraltar preceded the Miocene/Pliocene boundary cannot be ruled out. This missing information is arguably the main reason for the uncertainty around the evolution of Mediterranean-Atlantic exchange before, during and after the MSC.

1.3.4 Biotic evidence of corridor evolution

Faunal groups impacted by the evolution of the Mediterranean-Atlantic gateways include marine species utilising the marine corridors (e.g. foraminifera, fish, corals) and land-based species able to migrate when these corridors were closed (e.g. mammals). Analysis of faunal datasets provide insights into the dimensions of the marine gateways and the timing of closure.

1.3.4.1 Marine biota

From the perspective of gateway evolution, evidence from marine faunal palaeoecology contributes in two important areas: (1) palaeoecological differences between the Mediterranean and Atlantic sides of the corridors, and (2) palaeo-water depth reconstructions of the corridors themselves. During the Tortonian - earliest Messinian and from the Early Pliocene onwards, open Mediterranean-Atlantic connections resulted in similar planktic and benthic microfossil assemblages on both the Atlantic side of the gateways and in the homogeneous, marly sediments that span the entire Mediterranean Basin (most data pertain to foraminifera and calcareous nannoflora: (e.g. Baggley, 2000; Barbieri and Ori, 2000; Corbí et al., 2012; Feinberg, 1986; Hilgen et al., 2000; Hodell et al., 1989; Hodell et al., 1994; Hüsing et al., 2009a; Kouwenhoven et al., 2003; Kouwenhoven et al., 2006; Lozar et al., 2010; Pérez-Asensio et al., 2012b; Raffi et al., 2003; Santarelli et al., 1998; Sierro et al., 1993; Van de Poel, 1991; Zhang and Scott, 1996 and references therein). During the intervening Messinian interval, there are differences in the Mediterranean and Atlantic assemblages to a greater or lesser extent. These biological distinctions are sometimes mirrored by sedimentological differences which suggest synchronous chemical differentiation between the two basins. Many of the hypotheses that relate the Mediterranean's distinct Late Miocene sedimentary

record to its connectivity with the Atlantic are based on these observations and the inferences that can be drawn about the nature of exchange.

Stepwise restriction of Mediterranean-Atlantic exchange

Not all faunal groups record environmental changes at the same time. Benthic foraminifera (and stable isotope records; see section 4.2.2) indicate changing Mediterranean deep water environments as early as 7.17 Ma (Fig. 1.2), just after the Tortonian-Messinian boundary (7.251 Ma; Hilgen et al., 2000) with the disappearance of open marine, oxyphilic taxa (e.g. Kouwenhoven et al., 2003). This is more or less coincident with shallowing in the central Rifian Corridor (Fig. 1.2: Krijgsman et al., 1999b), although a causal relationship is not certain and changes in bottom water oxygenation are dependent on freshwater runoff as well as circulation. The first sapropel in the Faneromeni section (Crete, Hilgen et al., 1995) and the onset of cycle LA1 of the lower Abad marls in the Sorbas Basin (Sierro et al., 2001) indicate that restriction of water exchange occurred at this time such that the Mediterranean became sufficiently isolated to record a lithological response to subtle orbital variation. From 7.17 Ma onwards, benthic foraminifers typical of organic-rich suboxic waters and more tolerant to high environmental stress become increasingly abundant in bottom-water environments of the Mediterranean. In this development towards the MSC rather discrete steps are recognized around 6.7, 6.4 and 6.1 Ma (Seidenkrantz et al., 2000; Bellanca et al., 2001; Blanc-Valleron et al., 2002; Kouwenhoven et al., 2003, 2006; Iaccarino et al., 2008; Orszag-Sperber et al., 2009; Di Stefano et al., 2010; Lozar et al., 2010). Eventually oligotypic, *Bolivina-Bulimina* dominated faunas developed (Fig. 1.2) and deeper basins are barren of foraminifera (Sprovieri et al., 1996; Violanti, 1996; Kouwenhoven et al., 2003) whereas contemporaneous assemblages in the Atlantic are largely unaffected (Kouwenhoven et al., 2003; Pérez-Asensio et al., 2012b).

From ~6.7 Ma planktic assemblages within the Mediterranean mirror restriction of gateway exchange through decreasing abundances and amplification of the orbital-scale changes of the planktic communities (Santarelli et al., 1998; Sierro et al., 1999, 2003; Bellanca et al., 2001; Pérez-Folgado et al., 2003; Flores et al., 2005). Warm-water oligotrophic planktic foraminifera (summed as *Globigerinoides* spp.), and between 6.6 and 6.4 Ma *Globigerina bulloides* show 60-100% abundance shifts (Sierro et al., 1999, 2003). On the Atlantic side of the Rifian Corridor, in the Ain el Beida section (6.46-5.52 Ma) the amplitude of these precessional changes in warm-water planktic foraminifera abundance is in the order of 20% (van der Laan et al. 2012; Fig. 1.2). Decreasing abundances of Mediterranean planktic assemblages and a trend towards low diversity are attributed to increasingly adverse conditions of the surface waters preceding the MSC. Eventually, just below the MSC virtually barren samples are recorded (Sierro et al., 1993, 2003; Blanc-Valleron et al., 2002; Krijgsman et al., 2004; Lozar et al., 2010). The most extreme divergence between the planktic and benthic communities on the Mediterranean and Atlantic sides of the corridors is associated with the onset of

evaporite deposition at 5.971 Ma (Manzi et al., 2013), when marine organisms disappear from the Mediterranean. Although planktic and benthic micro- and macro-organisms have been described from Stage 1, their presence is probably mainly the result of reworking and most marly layers intercalated in the gypsum are barren (Rouchy & Caruso, 2006 and references therein).

Brackish-water assemblages are recorded during the Lago-Mare phase in the latest Messinian (section 2.3.1; e.g. Iaccarino & Bossio 1999; Aguirre & Sanchez-Almazo, 2004; Pierre et al., 2006; Orszag-Sperber, 2006; Rouchy et al., 2007; Guerra-Merchán et al., 2010). This period is also characterised by intervals containing well preserved fossil fish of open marine origin suggesting at least an episodic biological connection to the Atlantic during the Lago Mare phase (Carnevale et al., 2006).

Only after the Miocene-Pliocene boundary (5.33 Ma; Lourens et al., 1996; Van Couvering et al., 2000) did planktic and benthic communities of the Mediterranean recover (e.g. Wright, 1979; Thunell et al., 1991; Pierre et al., 2006; Rouchy et al., 2007; Sprovieri and Hasegawa, 1990; Sgarrella, 1997, 1999). Open ocean assemblages persist throughout the MSC in both the Guadalquivir (Spanish) and South Rifian (Moroccan) corridors (Feinberg 1986; Kouwenhoven et al., 2003; Pérez-Asensio et al., 2012b).

Biostratigraphic implications

Increasing restriction of Mediterranean-Atlantic exchange has impacted biostratigraphic datums. Biostratigraphic correlations within the Mediterranean and between the Mediterranean and Atlantic are unequivocal for most of the pre-MSC Messinian, up to the sinistral-to-dextral coiling shift of *Neogloboquadrina acostaensis* (e.g. Sierro et al., 1993, 2001; Hilgen et al., 2000; Krijgsman et al., 2004; Larrasoaña et al., 2008). However, the last common occurrence of *Globorotalia miotumida* at 6.28 Ma in the Atlantic (Sierro et al., 1993; Krijgsman et al. 2004) is a diachronous bioevent in the Mediterranean where the last influx of the species has been identified as early as 6.6 Ma, while some rare specimens were found in levels as young as 6.25 Ma (Sierro et al., 2001). This may relate to environmental sensitivity in planktic foraminifera. For the same reason, calcareous nannofossil datums have been found to deviate between Atlantic and Mediterranean strata (e.g. Raffi et al., 2003).

Palaeodepth reconstructions in the corridors

Reliable records of water-depth change in the Mediterranean-Atlantic corridors are critical to reconstructing gateway exchange. Several methods based on microfossils have been used to reconstruct palaeo-water depths, including (1) the ratio between planktic and benthic foraminifera (P/B ratios), (2) the occurrence of benthic foraminiferal species with restricted depth ranges that are assumed to be constant (e.g. Van Hinsbergen et al., 2005), and (3) transfer functions (e.g. Van der Zwaan et al., 1990; Hohenegger, 2005; Baldi & Hohenegger, 2008). For instance, vertical movements of the

Taza-Guercif Basin (Rifian Corridor), reconstructed using P/B ratios indicate rapid shallowing from outer shelf-upper slope (~ 400 m depth) to near–shore depths of ~40 m between 7.2 and 7.1Ma (Fig. 1.2; Krijgsman et al., 1999b). P/B ratios were also used to reconstruct palaeodepths in the Murcia-Cartagena and Sorbas basins, to constrain differential vertical movements and tectonic uplift in the Murcia Basin (Krijgsman et al., 2006). Problems associated with the exclusive use of P/B ratios are discussed in Van Hinsbergen et al. (2005) and Pérez-Asensio et al. (2012b). Apart from the effect of environmental factors such as oxygen and food on benthic assemblages (causing, among others, a correlation with astronomical cyclicity; Van Hinsbergen et al., 2005), these problems include reworking and downslope transport of sediment. In Late Miocene sediments from the Guadix section in the Betic Corridor, significant reworking of Cretaceous foraminifera and sediment transportation precluded the use of P/B ratios for depth reconstruction. Instead, depth-diagnostic species were used to approximate palaeodepths, suggesting a rather rapid shallowing from ~500 to ~200m (Hüsing et al., 2010). In the Guadalquivir area, palaeodepth reconstructions which also document shallowing as the basin infilled are based on a combination of methods including a transfer function (Pérez-Asensio et al., 2012b) or a transfer function alone (Pérez-Asensio et al., 2013). Despite each method having its limitations, valuable information can be extracted regarding differential vertical movements within the corridor area. Disentangling whether the shallowing seen is caused by tectonic uplift, sedimentary infill and/or Mediterranean sea-level fall remains challenging.

1.3.4.2 Terrestrial biota and mammal migration

The progressive closure of the Mediterranean-Atlantic marine connections should have created a land-bridge that permitted mammal migration between Africa and Spain. The continental (fossil mammal) biostratigraphic record is less detailed than the marine record, because the richest fossil localities are usually found in small scattered outcrops, and well-dated successions are scarce. Nevertheless, it has long been recognised that typical African species like camels and gerbils (desert rats) appear in the Messinian fossil records of Central Spain (Jaeger et al., 1975; Pickford et al., 1993; van Dam et al., 2006). Similarly, typical European rodent species are observed in the Messinian successions of northern Africa (Coiffait et al., 1985; Garcés et al., 1998; Jaeger, 1977).

One of the most significant Messinian mammalian events is marked by the entry into southern Spain of the murid *Paraethomys miocaenicus* (Agustí et al., 2006; Gibert et al., 2013) and camels of the genus *Paracamelus*. Camels originated in North America and *Paraethomys* in Asia, but the absence of their fossil remains in Western Europe suggest that they reached Iberia via Africa (Pickford et al., 1993; Van der Made et al., 2006). The first African immigrants (*Paraethomys* and *Paracamelus*) in Spain are magnetostratigraphically dated at ~6.2 Ma (Fig. 1.2; Garcés et al., 1998, 2001; Gibert et al., 2013). Another Messinian mammalian event is characterised by the dispersal of gerbils into Southern Spain. Gerbils are subdesertic rodents that today inhabit the dry

landscapes of northern Africa and southwestern Asia. Their first record in Spain is found just after the basal Pliocene transgression (Garcés et al., 2001) and their presence in Europe is probably directly related to the onset of the MSC and the spread of subdesertic conditions in the Western Mediterranean Basin. The identification of gerbils in the latest Messinian reddish continental beds of the Zorreras Formation, in the Sorbas Basin, is in agreement with this hypothesis (Fig. 1.2; Martín-Suárez et al., 2000).

The first age constraint on Africa-Iberia mammal exchange came from magnetostratigraphic dating of European mammalian fossils in the Aït Kandoula Basin of Morocco, which are correlated with chron C3An.1n at an age of ~6.2 Ma (Benammi et al., 1996). These data indicate that mammal exchange in the Gibraltar area took place in both directions more than 200 kyr before the onset of the MSC (Fig. 1.2) and this points to an ephemeral Messinian land bridge between Morocco and Spain, indicative of a pre-MSC (partial) closure of the Mediterranean-Atlantic gateways (Agustí et al., 2006; Gibert et al., 2013).

1.4. EVOLUTION OF THE MEDITERRANEAN-ATLANTIC GATEWAYS: INDIRECT APPROACH

The geological records of the Late Miocene marine connections that are now exposed on land are incomplete as a consequence of the unconformities associated with corridor closure and uplift (Fig. 1.2) and the uncertainty as to corridor location. As a result, important information about the nature and timing of Mediterranean-Atlantic exchange can only be derived from records outside the corridors that respond to some aspect of the exchange or the lack of it. In the Atlantic a variety of water mass tracing methods (contourites and Nd and Pb isotopes) capture aspects of Mediterranean outflow and consequently provide information about the timing of closure and the vigour of exchange. In the Mediterranean, Sr isotopes serve as an indicator of isolation from the global ocean. The successions preserved within the Mediterranean and elsewhere during the Late Miocene provide geological constraints for numerical modelling experiments, both those investigating the processes occurring during the MSC and those considering its consequences for global ocean circulation and climate. This section summarises the information about Mediterranean-Atlantic exchange that can be deduced from these diverse indirect approaches.

1.4.1 Evidence of Mediterranean-Atlantic connectivity from outside the Mediterranean

1.4.1.1 Mediterranean Outflow

As a mid-latitude semi-enclosed marginal basin, the Mediterranean Sea plays a fundamental role in supplying dense waters to the global ocean (Price and Baringer, 1994; Price et al., 1993) impacting the thermohaline structure of the North Atlantic (Artale et al., 2002; Hecht et al., 1997; Mauritzen et al., 2001) and ultimately global climate (Li, 2006). Today, two-layer flow exists in the Straits of Gibraltar, and colder, more saline Mediterranean water (Mediterranean Outflow/Overflow, MO) flows down the continental slope. En route it entrains significant quantities of Atlantic water (Baringer and Price, 1999) which decreases the density and velocity of the resulting water mass and causes it settle out into the Atlantic at intermediate depths (~500-1400 m; Fig. 1.3; Ambar and Howe, 1979). This distinctive water mass which is the combination of MO and ambient Atlantic water, we will refer to as Atlantic Mediterranean Water (AMW) as defined by Rogerson et al. (2012). Although MO undergoes rapid dilution due to mixing and entrainment processes (Dietrich et al., 2008), the resulting AMW remains a well-defined water mass in the Gulf of Cadiz (Figs. 1.1 & 1.7). Subsequently AMW divides into two distinct pathways and can be traced both westward to the Bermuda Rise and northward, over most of the central North Atlantic basin (Armi and Bray, 1982; Curry et al., 2003; Iorga and Lozier, 1999; Lozier and Stewart, 2008). AMW influences the heat and salt balance of the North Atlantic (Dietrich et al., 2008) and contributes to deep-water formation by keeping relatively high salinities at the surface (Price and Baringer, 1994; Reid, 1979).

The interaction of AMW with the Iberian margin's slope system results in an extensive contourite depositional system in the Gulf of Cadiz (Fig. 1.1), visible in both seismic profiles and bathymetry (García et al., 2009). Thick sedimentary deposits generated by these currents and by bottom currents on the eastern (Alborán Sea) side of the Gibraltar Straits, provide extensive records of past Mediterranean-Atlantic dynamics (Rogerson et al., 2010; Stow et al., 2013). These records, along with observational data suggest that Mediterranean-Atlantic exchange exhibits significant variability over seasonal (García Lafuente et al., 2007), interannual (Lozier and Sindlinger, 2009), and glacial-interglacial (Rogerson et al., 2005; Voelker et al., 2006) time scales.

Mediterranean-Atlantic exchange through the Straits of Gibraltar, is assumed to have been established immediately after the Zanclean flood (5.33 Ma; e.g. Iaccarino et al., 1999). However, to date, no direct evidence exists to enable the characterization of MO just after the opening of Gibraltar. IODP drilling in the Gulf of Cadiz recovered turbidites and debrites deposited between~4.5-4.2 Ma. These indicate the presence of relatively high flow strength in the Early Pliocene (Hernández-Molina et al., 2013; Hernández-Molina et al., 2014). From 3.8 Ma onwards these deposits developed into an

extensive contourite depositional system. AMW circulation strengthened from 3.2-2.1 Ma, where two major sedimentary hiatuses from 3.2-3.0 Ma and 2.4-2.1 Ma indicate strong bottom water currents (Hernández-Molina et al., 2014). The first hiatus has been linked with geochemical evidence of a rise in MO density and it has been suggested that this intensified Upper North Atlantic Deep Water (NADW) formation (Khélifi et al., 2009, 2014). Rogerson et al. (2012) concluded that a AMW pathway comparable to that of today (Fig. 1.7) could have been established around 1.8 Ma. (e.g. Llave et al., 2001; 2007; Llave 2003; Brackenridge et al., 2013). Finally, changes in the distribution and splitting of the upper and lower AMW is likely to have been caused by diapiric reactivation that can be correlated to tectonic events and sea level changes (García et al., 2009; Llave et al., 2007; Rodero et al., 1999).

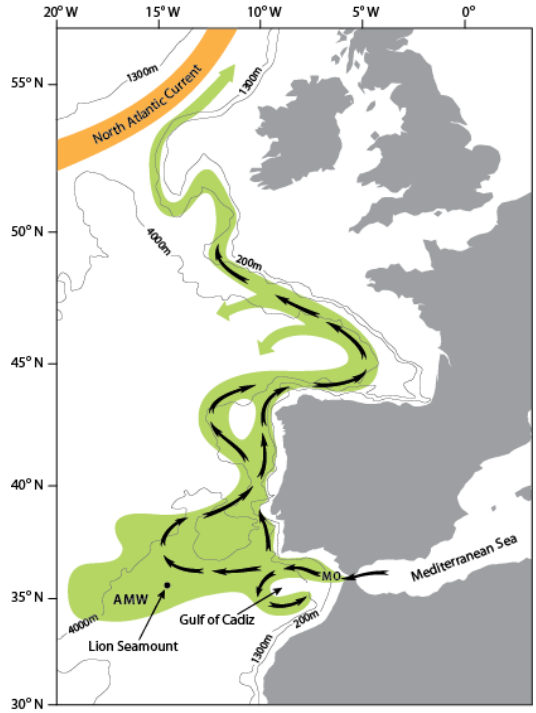

Figure 1.7 *Overview of the main circulation patterns of modern Mediterranean Outflow (MO) and its pathway in the North Atlantic (Iorga and Lozier, 1999) as Atlantic Mediterranean Water (AMW). In green is the saline tongue centred around 1000 m depth (Reid, 1979) and in orange is the surface North Atlantic Current (NAC). Arrows represent flow direction and the relevant bathymetric features are contoured in black.*

Consequently, exchange through the Late Miocene Mediterranean-Atlantic gateways may have been quite different to that seen today in the Gibraltar Strait, and the evolution of the Atlantic's sedimentary and geochemical response to MO may well reflect the evolution of the gateway itself. Three hypotheses can be formulated to explain the absence of evidence for MO before the earliest turbidites and debrites. Firstly, the outflow was insufficiently powerful to generate such current flow related deposits (Hernández-Molina et al., 2013). This is consistent with the interpretation of the onset of Gulf of Cadiz contourites and the geochemical signal of outflow as a strengthening or intensification of MO rather than its initiation (Hernández-Molina et al., 2013; Khélifi et al., 2009). Secondly, Mediterranean and Atlantic waters may have had physical properties too similar to leave traceable geochemical evidence of MO in the Atlantic (Rogerson et al., 2010). During the Early Pliocene global climate was warmer and the gateway may have been deeper (Raymo et al., 2006, Esteras et al., 2000). It is suggested that such conditions would not be met at

the time of the gateway opening, but there is no proof of this (Rogerson et al., 2012). A third possibility for the absence of Early Pliocene contourites from Leg 339 Sites is that Early Pliocene MO did exist, but AMW did not follow the present-day route along the Iberian margin and therefore it was not recovered during IODP Expedition 339. However, Rogerson et al. (2012b) demonstrated that the relationship between the salinity of Mediterranean Outflow and its flow pathway while not intuitive, is predictable. Increased salinity of MO could result in increased flow velocity and not in a variation of the plume's depth.

1.4.1.2 Geochemical tracers of Mediterranean Outflow – Nd and Pb isotopes

Attempts have been made to deduce the presence of MO in the Atlantic during the Miocene using geochemical tracers such as neodymium (Nd) and lead (Pb) isotopes. While Nd has a residence time in seawater on the order of 200-1000 years (Tachikawa et al. 1999), on a global average Pb is removed from the water column within 10-100 years (Henderson and Maier-Reimer, 2002). These relatively short residence times enable the Pb and Nd isotope systems to vary regionally in seawater. Nd isotopic compositions (expressed as εNd, the ratio of 143Nd/144Nd in a sample normalized to the bulk earth value in parts per 10^4; Jacobsen and Wasserburg, 1980) are used as water mass tracers for open ocean palaeocirculation reconstructions (e.g. Frank et al., 2002; Robinson et al., 2010; Thomas et al., 2003). Within the Mediterranean-Atlantic gateway region, clarifying εNd signal provenance is complicated by riverine and aeolian input (e.g. Henry et al., 1994; Sholkovitz and Szymczak, 2000) and boundary exchange at the sediment-bottom water interface (see Lacan and Jeandel, 2005). Nevertheless, since MO and Atlantic Inflow Water (AIW) have measurably different εNd (-9.4 and -11.8 respectively, Fig. 1.8; Piepgras and Wasserburg, 1983; Spivack and Wasserburg, 1988; Tachikawa et al., 2004), this isotope system theoretically has the potential to monitor past exchange. Two marine Nd archives have been exploited to investigate Late Miocene Mediterranean-Atlantic exchange: hydrogenous ferromanganese (FeMn) crusts derived from Atlantic seamounts and marine microfossils from Atlantic and palaeo-corridor locations.

FeMn crusts faithfully record both the Nd and Pb isotopic composition of overlying bottom seawater (Frank, 2002). Pb is commonly analysed alongside Nd as it contributes complimentary information such as insight into local changes related to continental weathering and other climate-induced signals (Christensen et al., 1997; Gutjahr et al., 2009; Harlavan and Erel, 2002). Pb and Nd isotope records from the Lion Seamount west of Gibraltar (Fig. 1.7) which is bathed in AMW today provide no evidence for the cessation of MO during the Messinian (Abouchami et al., 1999; Muiños et al., 2008). Unfortunately, the temporal resolution of both studies is too coarse to clearly rule out

changes in Atlantic-Mediterranean exchange during the different stages of the MSC (Fig. 1.7).

Marine fossils such as fish remains, teeth or bone fragments and foraminifera are an alternative target for Nd isotopic measurements with the potential for much higher resolution records. Ivanović et al. (2013a) studied this archive in sediment samples from the onshore Rifian Corridor. These authors independently estimated palaeo-MO and found palaeo-Atlantic εNd values which were not inconsistent with Fe-Mn crust studies (Fig. 1.8; Abouchami et al., 1999; Muiños et al., 2008) and showed that:

- Mediterranean water is likely to have reached the Atlantic through the Rifian Corridor until it closed between 6.64 and 6.44 Ma (Fig. 1.8), well before the onset of the MSC. This is consistent with other ages for the timing of closure, but provides tighter constraints;
- The prevailing water in the corridor was likely to have been a mixture of both Atlantic and Mediterranean water between 7.2 and 6.58 Ma (Fig. 1.8), directly contradicting the Siphon Event hypothesis which advocates that all water passing through the Rifian Corridor during this period was Atlantic in origin (Benson et al., 1991).

Further research is necessary to develop a more robust Nd and Pb isotope signature framework from this time period for the relevant water masses.

1.4.2 Reconstructing gateway history by comparing Mediterranean and Atlantic records

1.4.2.1 Sr isotopes

Sr isotope stratigraphy is an established marine carbonate dating tool. However, where semi-enclosed basins have limited exchange with the global oceans, they evolve an $^{87}Sr/^{86}Sr$ ratio that deviates from the global ocean water Sr isotope curve (McArthur et al., 2012) towards the $^{87}Sr/^{86}Sr$ of the basin's fluvial input. Such deviating Sr isotope records have been used to infer the connectivity history of various marginal marine systems (e.g. Baltic Sea and San Fransisco Bay, Andersson et al., 1994; Ingram and Sloan, 1992). For the Mediterranean, the $^{87}Sr/^{86}Sr$ will deviate measurably from global ocean values when the river discharge constitutes >25% of the total water flux (Topper et al., 2014). It has also been suggested that the changing concentration of Sr in groundwater could affect the $^{87}Sr/^{86}Sr$ values of marginal basins. During periods of aridity (occurring during low insolation), a build-up of Sr in groundwater may occur. On transition to wetter periods that occur during insolation maxima, this excess is flushed into marginal basins, causing $^{87}Sr/^{86}Sr$ to deviate away from global ocean values towards ratios that reflect the local geology (Schildgen et al., 2014). As a large proportion of geology around marginal Mediterranean sub-basins is composed of Mesozoic age

carbonate or igneous rock both of which have low $^{87}Sr/^{86}Sr$ ratios (e.g. Albarede and Michard, 1987; Flecker and Ellam, 1999; Schildgen et al., 2014), the resulting deviation would be towards values lower than those expected from the seawater curve for the age of deposition (McArthur et al., 2001).

Around 8 Ma, Sr isotope values from northern marginal basins indicate a divergence from global values e.g. in southern Turkey (Flecker and Ellam, 1999), the Adriatic, (Montanari et al., 1997), and Tyrrhenian Seas (Müller et al., 1990). Coeval records from central Mediterranean areas such as Sicily and Crete (Flecker et al., 2002; Flecker and Ellam, 2006; Sprovieri et al., 2003), maintain global values (Fig. 1.8). This has been interpreted as indicating significant restriction of these northern marginal basins from the main body of the Mediterranean prior to the MSC (Flecker and Ellam, 1999). At the onset of the MSC, the anomalously low Sr isotope values in the northern marginal basins return back to values within error of the ocean water curve (Flecker et al., 2002). Model analysis by Topper et al., (2011) indicates that although a marine transgression would generate these oceanic Sr isotope values (Flecker et al., 2002), a transgression alone would not account for gypsum precipitation which marks the onset of the MSC. Consequently gateway restriction must have played a dominant role in this transition (Topper et al., 2011).

During the MSC, the Mediterranean Basin responded to reduced exchange resulting in a deviation away from ocean $^{87}Sr/^{86}Sr$ ratios to lower, fluvial-like values, reflecting a decline in the proportion of ocean water reaching the basin (Fig. 1.8). The lowest values are recorded during Stage 3 throughout precipitation of the Upper Evaporites and Lago Mare. Recently, Roveri et al. (2014b) assessed the available $^{87}Sr/^{86}Sr$ data for the evaporites and determined correlations between marginal and deep basin evaporite units which, although potentially controversial at present, may lead to an enhanced understanding of evaporite deposition during the MSC. Sr isotope ratios returned abruptly to global ocean values at the Mio-Pliocene boundary (Fig. 1.8) indicating re-establishment of exchange with the Atlantic.

1.4.2.2 Stable isotopes and glacioeustatic sea level change

Open ocean oxygen isotopes provide a record of global glacioeustatic sea level change (Fig. 1.2). High resolution astronomically tuned age-models are available both for sections within the Mediterranean and on the adjacent Atlantic margin. This allows stable isotope records close to the Mediterranean-Atlantic gateway and further afield (e.g. Hodell et al., 2001; Shackleton et al., 1995a; Shackleton et al., 1995b) to be compared with the timing of key MSC events within the Mediterranean. This comparison provides a means to disentangle glacioeustatic and tectonic controls (e.g. Govers et al., 2009; Krijgsman and Meijer, 2008; Manzi et al., 2013; van der Laan et al., 2006). The idea that expansion of the Antarctic ice-sheet and associated glacio-eustatic sea-level lowering played a critical role in the restriction and subsequent isolation of the

Mediterranean during the latest Miocene goes back several decades (e.g. Adams et al., 1977). This early notion is consistent with what now may be called the Messinian glacial interval which is characterized by dominantly obliquity controlled glacial cycles, and started at 6.29 Ma with glacial stage C3An.1n0.16 and ended with a major deglaciation following glacial TG12 at 5.54 Ma (Hodell et al., 2001; van der Laan et al., 2005; van der Laan et al., 2006). Although it has become clear that tectonics are likely to have played a more important role than eustacy in the overall isolation of the Mediterranean, individual peak interglacials with sea-level changes in the order of tens of metres can still determine critical steps in the evolution of the MSC.

The oldest conspicuous Messinian glacial C3An.1n0.16 coincides with a marked change observed in the pre-evaporite succession towards higher surface water salinity and stressful conditions for the marine microfauna (Blanc-Valleron et al., 2002). The onset of evaporite (gypsum) formation at 5.96 Ma did not seem to be related to glacio-eustatic sea-level fall (Krijgsman et al., 2004), although such a claim has recently been made following the inclusion of a discontinuous older gypsum cycle in the Sorbas Basin in Spain (Manzi et al., 2013; Pérez-Asensio et al., 2013).

According to current high-resolution age models, the climax phase of the MSC during Stage 2 halite precipitation (Fig. 1.2) coincides with the twin peak glacials TG12 and 14. It has been suggested that these may correspond to unconformities in the succession when the connection with the Atlantic was fully blocked (Hilgen et al., 2007; Roveri et al., 2008). The onset of the Upper Evaporites may be coincident with the stepwise deglaciation following TG12, potentially explaining the marine faunas observed in this unit (van der Laan et al., 2006: Hilgen et al., 2007). The Zanclean reflooding of the Mediterranean following the MSC has also been related to deglaciation and glacio-eustatic sea-level rise, in this case of interglacial TG5 (Shackleton et al., 1995b; Suc et al., 1997). However, subsequent studies led to a revision of the tuning that did not confirm this causal connection (van der Laan et al., 2006).

1.4.3 Using Box Models to understand the Messinian Gateway Problem

Budget or box models based on the laws of physics and chemistry have provided valuable insight into some of the longstanding, first order questions about the Mediterranean's Late Miocene water and evaporite budgets and its gateways. Most of these studies are based on the notion of water conservation, which must be maintained for Mediterranean sea level to remain constant:

$$Q_{in} + \text{Precipitation} + \text{River input} = Q_{out} + \text{Evaporation} \quad (1)$$

where Q_{in} and Q_{out} are the fluxes from the Atlantic to the Mediterranean and from the Mediterranean to the Atlantic, respectively (Fig. 1.3).

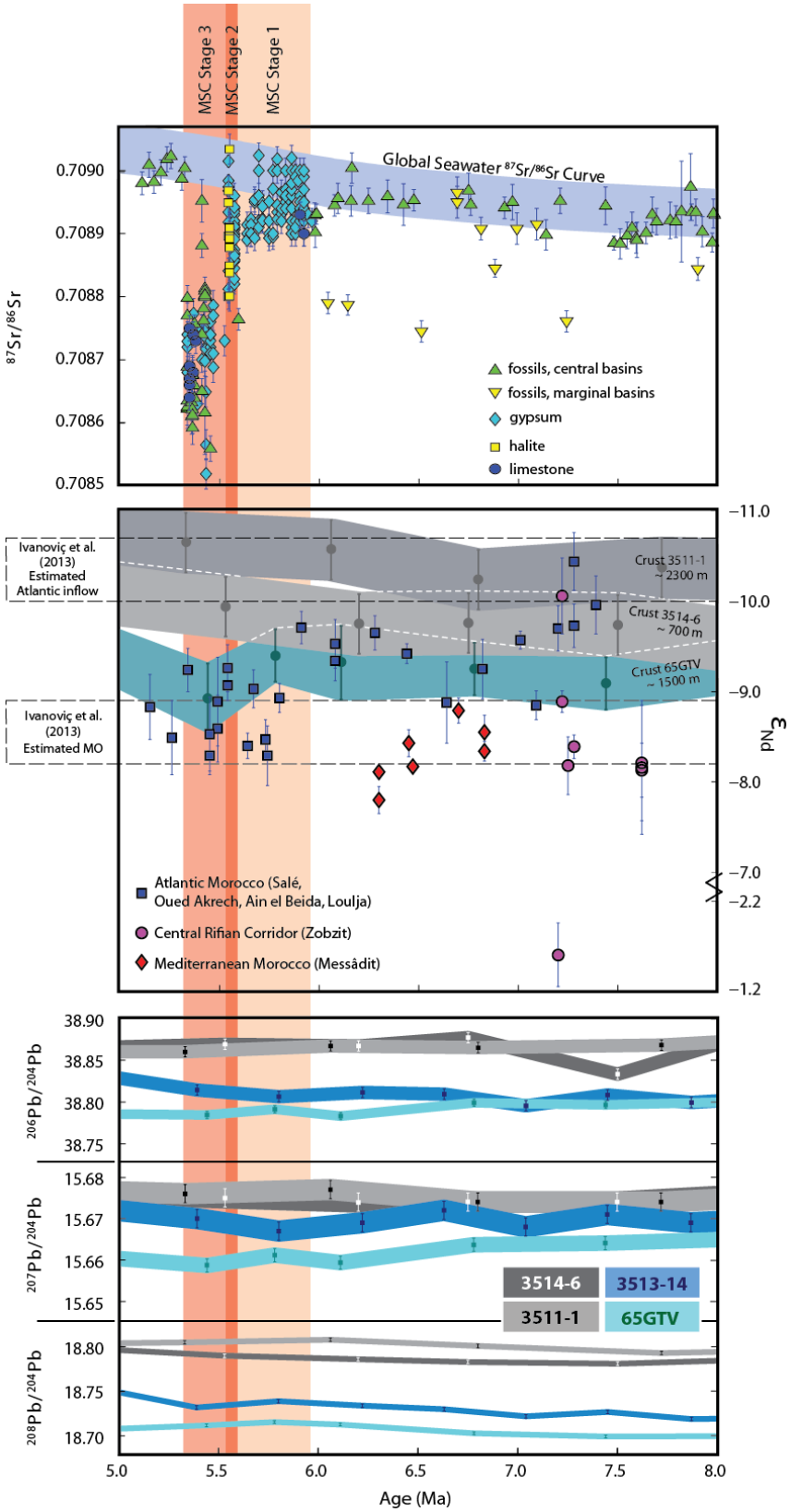
MSC Stage 3
MSC Stage 2
MSC Stage 1
Global Seawater $^{87}Sr/^{86}Sr$ Curve
$^{87}Sr/^{86}Sr$
0.7090
0.7089
0.7088
0.7087
0.7086
0.7085
fossils, central basins
fossils, marginal basins
gypsum
halite
limestone
Ivanoviç et al. (2013) Estimated Atlantic inflow
Ivanoviç et al. (2013) Estimated MO
Crust 3511-1 ~ 2300 m
Crust 3514-6 ~ 700 m
Crust 65GTV ~ 1500 m
−11.0
−10.0
−9.0
−8.0
−7.0
−2.2
−1.2
εNd
Atlantic Morocco (Salé, Oued Akrech, Ain el Beida, Loulja)
Central Rifian Corridor (Zobzit)
Mediterranean Morocco (Messâdit)
$^{206}Pb/^{204}Pb$
38.90
38.85
38.80
38.75
$^{207}Pb/^{204}Pb$
15.68
15.67
15.66
15.65
3514-6
3513-14
3511-1
65GTV
$^{208}Pb/^{204}Pb$
18.80
18.75
18.70
5.0
5.5
6.0
6.5
7.0
7.5
8.0
Age (Ma)

***Figure 1.8**. Radiogenic isotope records for the Mediterranean Sea and Mediterranean Outflow (MO) from 8 to 5 Ma, with Messinian Salinity Crisis stages. Top) $^{87}Sr/^{86}Sr$ ratios of Mediterranean water inferred from fossils, gypsum, halite, and limestone, plotted with the global $^{87}Sr/^{86}Sr$ seawater curve. Fossils are divided according to marginal or more central Mediterranean locations. Compilation based on Roveri et al. (2014) and Topper et al. (2011) and references therein. Middle) $\varepsilon_{Nd(t)}$. Point data represent inferred bottom water values at various locations from the Rifian Corridor (present day Northern Morocco), estimated from foraminiferal and fish tooth Nd (Ivanović et al., 2013). These data are compared to estimates for MO and North Eastern Atlantic Deep Water (NEADW) inferred from microfossils (Ivanović et al., 2013) and ferromanganese crusts (hereafter 'crusts'; Abouchami et al., 1999; Muiños et al., 2008). 65GTV and 3514-6 are thought to represent MO [4,5]; 3511-1 is thought to represent NEADW (Muiños et al., 2008). 65GTV values recalculated for post-deposition ingrowth of ^{143}Nd using $^{147}Sm/^{144}Nd = 0.115$ (assuming the value from Muiños et al., 2008) and ^{147}Sm $t_{1/2} = 1.06 \times 10^{11}$ y; all crust value ages recalculated using the latest ^{10}Be half-life of 1.387 Ma (Chmeleff et al., 2010). Bottom) Relatively flat Pb isotope ratio time series reported for major water masses outside the Gulf of Cadiz as inferred from crusts 65GTV and 3514-6 (potential AMW archives), 3511-1 (potential NEADW archive) and 3513-14 (potential Antarctic Bottom Water archive, Muiños et al., 2008). All errors for Nd and Pb isotope ratios are shown as 2 standard deviations of the external reproducibility, unless the internal reproducibility was larger.*

Components like evaporite minerals or Sr isotopic ratios which are controlled by the water budget and for which there are palaeo-records, are added to this equation to constrain modelled scenarios. This allows quantitative testing of many of the hypotheses that have been constructed to explain different aspects of the MSC.

Sonnenfeld and Finetti (1985) were the first to apply this approach to the MSC. These authors calculated the volume of fresh water that must be lost from seawater by evaporation in order for gypsum (81%) and halite (90%) to precipitate. This has been built on subsequently by a variety of authors interested in calculating the time taken for different saturation states to be reached (Debenedetti, 1982; Meijer, 2006), or for desiccation and refilling of the basin (Blanc, 2000; Blanc, 2002; Meijer and Krijgsman, 2005). As to the magnitude of the exchange fluxes, Meijer (2006) shows that in order to reach MSC saturations levels the exchange fluxes have to reduce to a few percent relative to modern values. Also, Krijgsman and Meijer (2008) and Topper et al (2011) show that during the precipitation of Stage 1 Primary Lower Gypsum (Fig. 1.2) the Mediterranean outflow must have continued, but may well have been cut off during Stage 2 halite formation.

Including hydraulic-control theory in box models allows the translation of gateway depth and the depth of the interface between the two water mass layers, to their corresponding exchange fluxes. These exchange fluxes can then be further linked to basin salinity or isotope ratios. Rohling et al. (2008) used this approach to calculate basin salinity as a function of strait depth and showed that the gypsum-clastic alternations that dominate Stage 1 of the MSC (Fig. 1.2) and had been widely considered to be driven by precession (e.g. Vai, 1997; Krijgsman et al., 1999a and b; Hilgen et al., 2007) could result from sea level variation (Rohling et al. 2008). The Mediterranean's

cyclic evaporites were also the target record of a study that explored the role of erosion and tectonic uplift on an open gateway to the Atlantic (Garcia-Castellanos and Villaseñor, 2011). Mediterranean sea-level variation related to eustatic changes combined with uplift in the gateway region have been modelled and compared to seismic data by Gargani and Rigollet (2007).

Further investigation of hydraulic-control theory by Meijer (2012) shows: (1) the depth of the marine corridor connecting to the Atlantic must be reduced to a few tens of metres to result in gypsum saturation in the Mediterranean; (2) blocked Mediterranean outflow results if the depth is reduced to a few metres and (3) the relationship between salinity and corridor depth is highly non-linear. This suggests that even a gradual shallowing of the gateway sill can result in an abrupt salinity rise in the enclosed basin leading to an apparent evaporite precipitation event.

Typically, Late Miocene budget calculations consider the Atlantic gateway to resemble Gibraltar (e.g. Meijer, 2012 and references therein). This is clearly a simplification given the evidence of more than one concurrent corridor and the possibility that these may have had multiple strands (Figs. 1.1, 1.5 & 1.6). In order to investigate the gateway dimension problem, Topper and Meijer (2015) used a regional ocean model to examine how a restricted Mediterranean-Atlantic connection would influence both Mediterranean thermohaline circulation and water properties. This study indicates that Mediterranean-Atlantic exchange is proportional to sill depth and the results of these simulations can therefore be used to interpret the Late Miocene sedimentary record both preceding and during the MSC Topper and Meijer (2015). Sill depths below 10 m result in blocked Mediterranean Outflow, which could represent a plausible scenario for the second stage of the MSC (Fig. 1.2), characterised by the rapid accumulation of halite in the Mediterranean (Topper and Meijer, 2015).

1.5. CAUSES AND CONSEQUENCES OF LATE MIOCENE MEDITERRANEAN-ATLANTIC EXCHANGE

1.5.1 Tectonic drivers of gateway evolution

There are a variety of different tectonic processes that contributed to the evolution of the Mediterranean-Atlantic connections during the Late Miocene-Pliocene. The main tectonic drivers of the location of the connections are likely to have been the combined influence of African-Iberian convergence with slab rollback and westward motion of the Alborán Domain. Regional uplift will also have played a significant role in the closure of these marine connections and this is likely to have resulted from lithospheric delamination and asthenospheric upwelling in the region (Duggen et al., 2003; Duggen

et al., 2004). In Morocco for example, southward propagation of the thrust load appears to be a significant driver of both formation and closure of the Rifian corridors (Fig. 1.1) along with regional uplift attributed to slab dynamics (Duggen et al., 2004).

During the MSC itself, loading and unloading of the lithosphere provides another tectonic mechanism for vertical movement in the gateway area. For example, loading of the lithosphere with thick evaporites results in flexural subsidence of the Mediterranean's basin and uplift of its margins contributing to reduced connectivity while sea level lowering has the opposite effect, but not necessarily by the same magnitude (Govers et al., 2009). The relative importance of these two processes depends on the thickness and location of evaporites precipitated, the amount of Mediterranean sea level fall and the relative timing of the two. All three of these are controversial with the largest degree of uncertainty associated with the relative timing of events during stage 2 (Fig. 1.2). This is perhaps best illustrated by the persistence of three contrasting scenarios for halite emplacement and sea level fall each of which would result in a different subsidence/uplift history for the marginal gateway region:

1. deep water emplacement where halite is precipitated during a moderate base level fall (Roveri et al., 2008);
2. halite precipitation during a large relative sea level fall (Lofi et al., 2011b; Ryan, 2009); and
3. halite precipitation after desiccation of the Mediterranean Basin (Bache et al., 2012; Clauzon et al., 1996).

Despite this ambiguity, it is clear that vertical lithospheric adjustment significantly affected river canyons, topographic slopes and erosion rates in and around the basin and was an important contributary driver of the Mediterranean's connectivity history through its impact on the gateway region. One extension of this was the work by Garcia-Castellanos and Villaseñor (2011) who explored the interplay between uplift of the gateway region and erosional deepening of the corridor as a result of Atlantic inflow. The numerical model they produced illustrates that this interplay provides a mechanism for maintaing at least Atlantic inflow over relatively long timescales despite progressive tectonic uplift. The harmonic behaviour of this interplay also led them to suggest that the cyclicity in the evaporites might have a tectonic-erosion origin rather than the widely held climatic one (Garcia-Castellanos and Villaseñor, 2011).

Another example of the possible role of tectonics and erosion in the evolution of the Mediterranean-Atlantic connectivity concerns the end of the MSC. At this point, as a result of evaporite loading, the Alborán Basin was bordered by a peripheral dam along the Spanish, Gibraltar and northwest Africa margins (Govers et al., 2009). This impeded the reconnection of the Mediterranean to the global oceans. Breaching this barrier with the opening of the Gibraltar Strait has been attributed to regional subsidence as a consequence of the evolution of the Gibraltar slab (Govers et al., 2009).

While no-one disputes the role of tectonics in the evolution of the Mediterranean-Atlantic gateway, disentangling the relative importance of the different processes for individual events is challenging. What the sedimentary record of the Mediterranean does allow us to do is identify key moments at which restriction or opening of the gateway must have occurred. It is then possible to evaluate the probable roles of tectonics, eustatic sea level change and erosion in effecting this change. These are summarised in Figure 1.9.

1.5.2 Climatic drivers of the MSC and their impact on Mediterranean-Atlantic exchange

It is clear that climate played an important role in the evolution of the MSC. Numerical modelling has been used to explore aspects of this relationship, particularly in relation to the Mediterranean's hydrologic budget at times of restricted Mediterranean-Atlantic connection and may help to explain the salinity fluctuations that took place during the MSC (see also Krijgsman and Meijer, 2008). As a consequence of salinity changes in the Mediterranean, the density contrast between the Mediterranean and Atlantic will have varied thus impacting the vigour of exchange. Using a global atmosphere-only GCM, Gladstone et al. (2007) demonstrated that the Mediterranean freshwater budget in the Late Miocene may have been closer to a neutral position than it is today making it easier for climatic change to switch the sign of the hydrologic budget from negative, which would result in higher salinities, to positive, which reduces Mediterranean salinity below ocean water values. Gladstone et al. (2007) also estimated river runoff around three times greater than today mostly as a consequence of input from North African rivers feeding the Eastern part of the basin. Many of these rivers, which are dry today, are thought to have transported water from the south (Griffin, 1999) as a result of a stronger African summer monsoon (Marzocchi et al., 2015; Gladstone et al., 2007). However, on precessional time scales, wetter periods in the Mediterranean region may also have resulted from enhanced wintertime storm track activity in the Atlantic and associated increased precipitation (Kutzbach et al., 2014). It is these two independent precession-driven processes which may be responsible for the formation of similarly cyclic Late Miocene sedimentation both within the Mediterranean, responding mainly to the North African monsoonal signal and outside it along the Atlantic coast where the driver is rainfall and runoff from Atlantic storms. Evaluation of the role of the Mediterranean's freshwater fluxes in controlling both its environmental evolution and exchange through its gateways is in its early stages, hampered by inadequate rainfall data as well as model-data mismatch on temporal as well as spatial scales.

Another modelling approach used is to combine GCMs with regional ocean-only models. This can be achieved by forcing ocean-only models with output from fully-coupled global simulations, and then running them at sufficiently high resolution to resolve more realistically the different gateway scenarios. For instance, Meijer and Tuenter (2007)

combined an intermediate complexity, global-scale atmosphere-ocean model with a more detailed regional model for the circulation of the Mediterranean Sea to investigate the consequences of precession-induced changes in the Mediterranean freshwater budget, linking it to the Late Miocene sedimentary cyclicity.

1.5.3 The impact of the MSC on global climate

Today MO entrained in the North Atlantic current is thought to contribute to North Atlantic circulation by supplying warm saline waters to sites of North Atlantic Deep Water formation in the Greenland-Iceland-Norwegian (GIN; Fig. 1.7) seas and northernmost Atlantic (McCartney and Mauritzen, 2001; Reid, 1978; Reid, 1979). This hypothesis has been investigated through the removal of MO water from several North Atlantic ocean circulation modelling experiments, both for the present day (Ivanović et al., 2014a; Wu et al., 2007; Kahana, 2005; Chan and Motoi, 2003; Artale et al., 2002; Rahmstorf, 1998) and the Quaternary (Rogerson et al., 2010; Bigg and Wadley, 2001). According to these studies, the presence of AMW in the North Atlantic appears to have a negligible effect on modern climate. An enduring question is therefore whether the MSC had any significant impact on global climate.

In order to answer this question it is first necessary to establish the differences between the Miocene and present day climatic system. Major changes include:

- A Central American Seaway that linked the Atlantic and Pacific oceans during the Late Miocene to Early Pliocene (Duquecaro, 1990; Keigwin, 1982; Osborne et al., 2014; Sepulchre et al., 2014). This implies a significant difference in ocean circulation patterns and may have resulted in considerably weaker Messinian North Atlantic Deep Water formation than today (Boehme et al., 2008; Herold et al., 2012; Lunt et al., 2008; Molnar, 2008; Murdock et al., 1997; Prange and Schulz, 2004; Schneider and Schmittner, 2006; Zhang et al., 2012).
- Major post-Miocene uplift of the Himalayas, Andes, Rockies, Alps and East African Plateau (see Bradshaw et al., 2012 and references therein) that will have impacted significantly on the patterns of atmospheric circulation.
- An extensive Late Miocene Antarctic ice-sheet (e.g. Lewis et al., 2008; Shackleton and Kennett, 1975), but more limited Northern Hemisphere glaciation than today (Kamikuri et al., 2007; Moran et al., 2006).
- In addition, despite the overall cooling trend during the Cenozoic (Zachos et al., 2001), the global climate proxy record for the Late Miocene suggests that it was generally hotter and/or wetter than today (Bradshaw et al., 2012; Bruch et al., 2007; Eronen et al., 2010; Pound et al., 2012; Pound et al., 2011; Utescher et al., 2011).

These significant differences in the climatic configuration mean that evaluation of the impact of the MSC on global climate requires Miocene specific model experiments.

Possible mechanisms for an MSC influence on climate include: extreme changes in MO density and volume reaching the Atlantic; a substantial reduction in sea level and evaporative flux during draw-down; associated changes in circum-Mediterranean vegetation; and a significant reduction in global ocean salinity as a result of salt sequestration in the Mediterranean. General Circulation Models (GCMs) are a powerful tool for simulating the interactions between the main components of the global climate system. They have therefore been used to assess some aspects of the possible impact of the MSC on global climate.

A significant reduction in Mediterranean outflow is an essential aspect of raising Mediterranean salinity and although removal of AMW in the North Atlantic has a negligible impact on modern climate (Ivanović et al., 2014a; 2014b; Wu et al., 2007; Kahana, 2005; Chan and Motoi, 2003; Artale et al., 2002; Rahmstorf, 1998), during stages of weaker Atlantic Meridional Overturning Circulation (AMOC) such as the Younger Dryas, it does impact North Atlantic Ocean circulation. This matches the Younger Dryas sea surface salinity and temperature records from the Iberian margin and Alborán Sea (Penaud et al., 2011; Voelker et al., 2006), and implies that, since AMOC was weaker in the Messinian, it should have been more sensitive to Atlantic salinity and temperature variations driven by AMW (Ivanović et al., 2014a; 2014b).

The impact of extreme changes in MO properties on ocean circulation and climate has also been investigated. Coupled ocean-atmosphere GCM simulations suggest that elevating Mediterranean salinity enhances salt export from the Mediterranean, which in turn modifies the rate of deep water formation and circulation in the Atlantic Ocean (Ivanović et al., 2014a; 2014b). In the model, this triggered cooling (9°C in the Boreal winter-spring) in Northern mid-high latitude surface air temperatures, but did not result in significant changes in atmospheric circulation or precipitation patterns (Ivanović et al., 2014b). However, episodes of extremely elevated or negative Mediterranean salt-export are most likely to have occurred only intermittently (Thierstein and Berger, 1978) and for short periods of time (Meijer and Krijgsman, 2005). This scenario is not well captured by published model experiments which maintain MO salinity levels for hundreds of years until climate equilibrium is achieved in the model. The modelling results of Ivanović et al. (2014b) exhibit an initial decadal-scale overshoot in ocean circulation, suggesting that the shorter-term (transient) ocean circulation impact of the MSC may therefore have been far more extreme than the multi-decadal averages calculated in these published studies.

The dimensions of the Straits of Gibraltar (nearly 60 km long, 12 km at its narrowest point, and with a maximum depth of 300 m; Candela et al., 1990) make realistically simulating the thin, dense current spilling over the sill (the MO) in numerical models very challenging (Dietrich et al., 2008). In models with a relatively coarse resolution where the model grid cannot resolve the features of the shallow, narrow strait, the

exchange is simulated either using a less realistic wider and deeper open seaway (Ivanović et al., 2013b; Rogerson et al., 2010; Bigg and Wadley, 2001), or using an empirical parameterisation of the exchange (Ivanović et al., 2013b; Wu et al., 2007; Chan and Motoi, 2003; Rahmstorf, 1998). Clearly, the same resolution problem also applies to both the Late Miocene Mediterranean-Atlantic seaways.

Climate-modifying aspects of the MSC other than MO have also been investigated through modelling. The impact of MSC-driven Mediterranean sea level and vegetation change have been explored using an atmosphere-only GCM and an intermediate complexity Earth system model, respectively. These experiments suggest that lowering Mediterranean sea level results in strong cooling over the North Pacific, which may have enhanced high latitude glaciation in the Late Miocene (Murphy et al., 2009). The vegetation experiments did not exhibit dramatic climate changes close to the margins of the Mediterranean Basin during the MSC, but instead indicated cooling in Central, Northern and Eastern Europe (Schneck et al., 2010).

In summary, the impact of the MSC on global climate remains poorly established. This is due partly to shortcomings in palaeoclimate model configurations (Ivanović et al., 2014b), partly to difficulties modelling a realistic MSC scenario with an appropriately small gateway, and more generally to sparse and irregular distribution of Late Miocene climate proxy data (Bradshaw et al., 2012) generating difficulties in evaluating the plausibility of model simulations.

1.5.4 The challenges of deducing palaeosalinity and its impact on reconstructing exchange

The main control on Mediterranean-Atlantic exchange is the salinity contrast between the two water masses and this is driven by the efficiency or size of the gateway and net evaporation (section 2.1). Quantifying the evolution of Mediterranean salinity is therefore a key step in reconstructing exchange. The current constraints on extreme palaeosalinity, however, only provide a few threshold values with which to reconstruct the Mediterranean's complex salinity history (e.g. 350g/L for halite; 130-180 g/L for gypsum; ~50g/L the upper tolerance limit of foraminifera; 5-20g/L for brackish water fauna). Consequently, it is not currently possible to quantify the pre-MSC salinity contrast between the Mediterranean and Atlantic. For example, the absence of planktic foraminifera in some intervals of the pre-evaporitic succession of the Sorbas Basin (Sierro et al., 2001), merely indicates that surface water salinity has exceeded their tolerance (e.g. ~49 psu; Fenton et al 2000 and references therein). Although these salinity thresholds are used to constrain specific exchange scenarios suitable for particular salinity conditions (e.g. gypsum or halite precipitation; Flecker et al., 2002;

Topper et al., 2011; Meijer 2006), another complication is that brine concentration is not always the only possible control on the mineralogical or biological changes observed.

An excellent example of this problem is the salinity reconstruction of the gypsum-clastic cycles that occur around the margins of the Mediterranean during the precipitation of Stage 1 Primary Lower Gypsum and Stage 3 Upper Gypsum (Fig. 1.2). The clastic intervals in these alternations may be organic rich. They are always either abiotic, or if they do contain foraminifera, these show signs of being reworked (e.g. Rouchy and Caruso, 2006). Three different salinity records are possible all of which have different implications for exchange at the time:

1. The clastic sediments between the gypsums may have been deposited when the brine was diluted by additional fresh or marine water generating salinity conditions that were too high to support marine fauna, but lower than the ~130g/L salinity and 5.25g/L $CaSO_4$ concentration (Topper and Meijer, 2013) required for gypsum precipitation. The density contrast with the Atlantic was therefore at its highest during gypsum precipitation implying the smallest, least efficient gateway with an increase in exchange during clastic deposition;
2. The clastic sediments between the gypsums may have been deposited during higher salinity conditions when brine concentration exceeded the maximum associated with gypsum precipitation (~180 g/L NaCl). Were this to have happened, exchange would have been most limited during deposition of the clastics;
3. Finally it is possible that the lithological variation does not reflect a change in salinity but rather the availability of sulphate (Natalicchio et al., 2014). Gypsum precipitates when sulphate is available and the salinity is between130-180g/L; once the sulphate is used up, it is not possible to precipitate gypsum and clastic sediments accumulate instead. This is the same process that leads to the lateral and depth related shift from shallow water gypsum to deeper water organic-rich shales during Stage 1 Primary Lower Gypsum phase (de Lange and Krijgsman, 2010). The consequences for exchange are that there is very little variation throughout this period.

1.6. EVOLUTION OF MEDITERRANEAN-ATLANTIC EXCHANGE DURING THE LATE MIOCENE

The Mediterranean's hydrologic budget is controlled by both the efficiency of the gateway(s) and net evaporation over the Mediterranean (precipitation + runoff – evaporation, P+R-E; section 2.1). The combination of these two drivers along with a Mediterranean circulation system where surface water flows east becoming more saline,

sinks in the Eastern Mediterranean and flows west at depth, typically results in a density contrast between Mediterranean and Atlantic water at the gateway where Mediterranean water is both more saline and colder than surface Atlantic water (Rogerson et al., 2012). It is this density contrast at the gateway that drives the pattern and vigour of Mediterranean-Atlantic exchange. While tectonic forcing is the dominant driver of the width, depth, length, location and age of the different gateways, with sea level a contributory factor, for any specific gateway configuration, variability in exchange is modulated by climate which drives the salinity (P+R-E) and temperature of the Mediterranean and hence its density contrast with the Atlantic (section 2.1). There is evidence from the Quaternary that illustrates the independent behaviour and impact of gateway efficiency and net evaporation. The Last Glacial Maximum (LGM) and its associated sea-level fall, provides an example of gateway efficiency dominating exchange and associated salinity rise. Modelling studies suggest that Mediterranean salinity rose to around 44 psu as a result of sea-level driven reduction in inflow and outflow during the LGM (e.g. Bethoux 1984; Rohling, 1999). There is no direct evidence of this salinity rise in the Mediterranean since it is not high enough to exceed the salinity tolerance of planktic foraminifera (~49psu; Fenton et al., 2000) and $\square^{18}O$ residuals which can be used for reconstructing palaeo-salinity elsewhere appear to be non-proportional to salinity and more influenced by run-off in the Mediterranean (Rohling, 1999; Rohling et al., 2015). However, the same LGM sea-level fall across the silled connection between the Red Sea and the Indian Ocean does reduce exchange sufficiently to produce high salinities that contribute to the development of aplanktic horizons in the Red Sea (Fenton et al., 2000). By contrast, Heinrich Events provide an example of climate-driven variation in exchange. These ice-rafting events generated fresher surface water in the North Atlantic. Coeval with Heinrich Events are episodes of coarser-grained contourites in the Gulf of Cadiz (Voelker et al., 2006). Since contourite grainsize is indicative of higher energy MO this succession is interpreted to result from a larger, climate driven density contrast between the Mediterranean and Atlantic as a result of reduced Atlantic salinity and consequently more vigorous exchange (Rogerson et al., 2010; Voelker et al., 2006) during a period when the gateway configuration remained effectively constant.

In the Late Miocene, before the onset of Northern Hemisphere glaciation, a mechanism for modifying Atlantic salinity does not appear readily available. Mediterranean-Atlantic exchange is likely to have varied in concert with Mediterranean salinity on a variety of timescales. Controlling factors include:

1. Tectonic driven changes to the gateways controlling Mediterranean salinity via exchange efficiency (Meijer, 2012);
2. Glacio-eustatic sea-level oscillations with an increasing impact on the efficiency of exchange as the gateways shallow;
3. Precessional fluctuations in the freshwater-flux relating to the supply of North African monsoonal rainfall (Marzocchi et al., 2015) to the Eastern

Mediterranean via the Esohabi and Nile rivers (Gladstone et al., 2007; Griffin, 1999, 2002);

4. Longer-term climate change resulting in changing net evaporative loss over the Mediterranean Basin.

During the Late Miocene there is little evidence of any significant, long-term change in climate that might account for triggering or terminating the MSC (Bertini, 2006; Bertini et al., 1998; Roveri et al., 2014a; Suc and Bessais, 1990; Suc et al., 1995). Consequently, using what is known about Late Miocene Mediterranean salinity, it is possible to reconstruct the history of Mediterranean-Atlantic exchange and consider the relative impact of tectonics and orbital variability in determining the evolution of the MSC (Fig. 1.9).

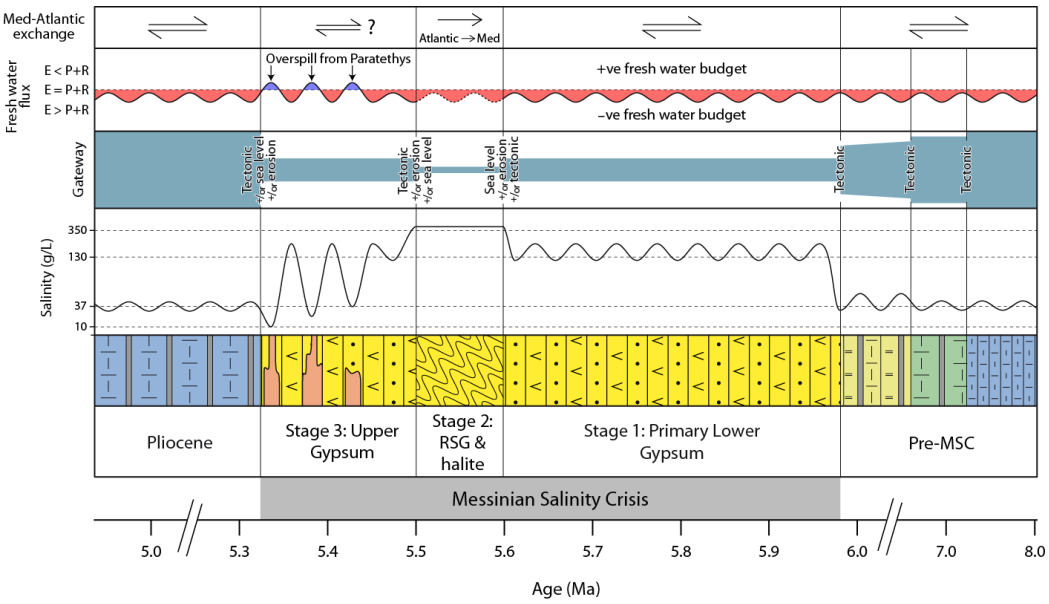

***Figure 1.9**. Summary figure illustrating the main features of the Mediterranean's exchange history in the Late Miocene-Pliocene including lithology, Mediterranean salinity, a qualitative representation of gateway size and the probable drivers (tectonics, erosion, sea level) of changing dimensions, the Mediterranean's fresh water flux where E and P = evaporation and precipitation over the Mediterranean respectively and R is the river discharge into the Mediterranean Sea, and arrows representing one-way or two-way exchange between the Mediterranean and Atlantic.*

Plio-Quaternary Mediterranean successions are dominated by strong precessional cyclicity that is visually enhanced by the barcode-like dark stripes of the sapropels (e.g. Rohling et al., 2015). Very similar sediments were also deposited in the Mediterranean

prior to the MSC (Fig. 1.2). This similarity combined with the observation that the sedimentary response is coupled to orbital variation, suggests that before and after the MSC the basin responded to orbital-induced climate change in essentially the same way despite the different gateway configurations (e.g. de la Vara et al., 2015) and the warmer and wetter Late Miocene conditions (Bradshaw et al 2012). Consequently, Late Miocene exchange is assumed to resemble that occurring through the Gibraltar Strait today, with a similar degree of restriction (Fig. 1.9) leading to an overall slightly enhanced salinity in the Mediterranean (38 g/L) relative to the Atlantic (35 g/L). Just as is seen in the Plio-Quaternary, this tectonically controlled exchange is modulated by precessional changes to the Mediterranean's freshwater flux (P+R-E) which remains negative throughout (Fig. 1.9).

Sediments deposited before the first evaporite precipitated contain evidence indicative of step-wise restriction of exchange. The progressive loss of oxic benthic faunal species (Kouwenhoven et al. 2003; Section 3.5.1; Fig. 1.2) and divergence of marginal basin Sr isotope values from coeval ocean values, (Flecker et al., 2002; section 4.2.1; Fig. 1.2 and 8) suggest enhanced water column stratification and reduction in Atlantic influence. The development of aplanktic marls similar to those seen in the Red Sea during the LGM (Fenton et al., 2000) incorporated into the precessional cyclicity of Sorbas Basin sediments (Sierro et al 2001; section 3.5.2; Fig. 1.2) shows that, here at least, the amplitude of salinity variation increased to levels above planktic foraminiferal tolerance (49 psu; Fenton et al., 2000; Fig. 1.9). This period between 8-5.97 Ma is the interval during which geological evidence demonstrates the closure of most strands of the Betic and Rifian corridors (Fig. 1.2). This suggests that exchange was progressively reduced with respect to earlier periods, probably by a series of tectonic events with superimposed ~100 and 405-kyr orbital cyclicity (e.g. Hüsing et al., 2009a; Krijgsman et al., 1999a) and the eustatic sea-level fall associated with glacial C3An.1n0.16 giving the step-wise pattern of restriction (Fig. 1.9). Precessional modulation of the freshwater flux continued (P-E+R) and remained negative (Fig. 1.9). However, this resulted in an increasingly high-amplitude salinity response in the Mediterranean (Fig. 1.9) as a consequence of reduced gateway efficiency.

Primary gypsum dominates both the Primary Lower Gypsum in Stage 1 (Fig. 1.2) and the Upper Gypsum in Stage 3. Gypsum precipitation requires salinities of 130-160 g/L. Modelling results suggest that maintaining this salinity can only be achieved if two-way exchange persists (Fig. 1.9), but is reduced significantly by decreasing the efficiency of the gateway, probably by shallowing it to a few tens of metres (Debenedetti, 1976; Meijer, 2012). Topper et al, (2011) demonstrated that the transition from pre-MSC sediments to gypsum at 5.97 Ma requires a reduction in gateway efficiency and consequently, we infer a further tectonic and/or sealevel-driven (Manzi et al 2013) reduction in the gateway as the trigger for the onset of the MSC (Fig. 1.9) although a significant increase in Mediterranean stratification may also play a role. Both Stage 1

and Stage 3 comprise regular gypsum-clastic alternations (Fig. 1.2 and 1.9) which are also thought to be precessionally driven (Hilgen et al., 2007; Krijgsman et al., 2001; Roveri et al., 2014a) and this suggests on-going precessional modulation of the freshwater flux (Fig. 1.9). However, because of the problems reconstructing palaeosalinity for these gypsum-clastic cycles (section 5.3), neither the amplitude nor the phasing of the salinity response is clear (see Topper and Meijer, 2013 for model-based insight).

Stage 2 gypsum is the reworked erosional product of Stage 1 primary gypsum (CIESM, 2008). This, combined with its association with the Messinian Erosion Surface (Figs. 1.2 and 1.4) indicates a Mediterranean base-level fall and the timing of Stage 2 is coincident with glacials TG12 and TG14. The implications for Mediterranean-Atlantic exchange are clear, but the scale of this sea-level drop is still contentious (see Roveri et al., 2014a for review). In the CIESM (2008) model, thick (~1.5km) halite precipitated in the deep Mediterranean Basin at the end of Stage 2. This required salinities of >350g/L and a supply of seawater, most easily sourced from the Atlantic. To achieve these high salinities, outflow must have been negligible so that one-way flow from the Atlantic to the Mediterranean is envisaged (Fig. 1.9). Because the deep basinal halite has not been drilled, the only direct access to part of this succession is through a mine on Sicily. Here, annual bands in the salt have been identified, but while the peak glacials may correspond to unconformities in the succession, a precessional signal has not so far been demonstrated (Lugli et al., 1999). Given that the precessional signal is clearly visible in Stage 3 and Plio-Quaternary sediments (Fig. 1.9), it is unlikely that precessional modulation to the freshwater flux was switched off during Stage 2. Alternative explanations include the possibility that this area around Sicily was in some way protected from the impacts of the freshwater flux driven by North African run-off; or that any salinity variation generated by the precessional freshwater flux was small by comparison with the extreme salinity of the Mediterranean as a whole at this time and consequently never moved the basin out of the halite window so that no sedimentary response to the freshwater flux is recorded (Fig. 1.9).

In terms of Mediterranean-Atlantic gateway exchange, the most enigmatic phase of the MSC is the Stage 3 Lago Mare association of local evaporites and sediments some of which contain fresh to brackish water fauna and flora. These low salinity assemblages which increase in abundance and diversity with time (Roveri et al., 2008) and spread progressively westward, resemble those found in the brackish-water Paratethyan lake system (Orszag-Sperber, 2006; Rouchy and Caruso, 2006; Roveri et al., 2008). This suggests prolonged and increasing connectivity between the Mediterranean and Paratethys, although the location of the Mediterranean's Paratethyan gateway at this time is just as enigmatic as its Atlantic counterpart. The traditional interpretation of the Lago Mare phase is that it occurred during a period when there was negligible connectivity with the Atlantic (e.g. Hsü et al., 1977; Orszag-Sperber, 2006). However,

Stage 3 successions also include a variety of features that suggest that the Mediterranean did receive at least periodic incursions of Atlantic water. These include the presence of Atlantic open marine fish (Carnevale, 2006; 2008), and dwarf foraminifera (Iaccarino et al., 2008). In addition, the same arguments that are used to infer two-way Mediterranean-Atlantic exchange for Stage 1 Primary Lower Gypsum (e.g. Meijer, 2012; Fig. 1.9) can also be invoked to explain the similar Stage 3 gypsum-clastic cycles. These indicators of at least episodic Atlantic connectivity, along with the reduction in Mediterranean salinity from its peak halite concentration, suggests that the transition from Stage 2 to 3 is triggered by more efficient Atlantic gateway exchange resulting either from a tectonic driver and/or erosional opening of the gateway and/or stepwise deglaciation following TG12 (Hilgen et al., 2007; Roveri and Manzi, 2006).

The paradox is that associated with this more efficient gateway are Sr isotope ratios indicative of an environment that is more dominated by continental run-off than at any other time during the MSC (Fig. 1.8). Consequently, although Stage 3 gypsum-clastic cycles resemble those of Stage 1, the geochemistry indicates distinctly different water sources. The obvious contender as an additional water source is Paratethys, with its low Sr isotope ratio (Flecker and Ellam, 2006; Major et al., 2006) and brackish water salinity and fauna. The Mediterranean during Stage 3 appears to be equivalent to the Black Sea today, with a Bosphorus-like connection with the Atlantic.

The mechanisms for achieving very low salinity conditions in the Mediterranean are either substantial dilution by fresh water from Paratethys (Orszag-Sperber, 2006; Rouchy and Caruso, 2006; Roveri et al., 2008) and/or a change in climate leading to a switching of the Mediterranean's hydrologic budget from negative to positive (Gladstone et al., 2007). Since the Mediterranean successions that contain these Lago Mare sediments commonly show the same strong cyclicity as the gypsum-clastic alternations with which they are interbedded (the Eraclea Minoa section on Sicily is a good example), it is likely that precessional modulation of the freshwater flux is still the driver of changes to both hyper and hypo-saline conditions in the Mediterranean (Fig. 1.9). The mechanism for this is not yet clear, but the cyclicity may suggest that precession-driven Mediterranean-Paratethys connectivity caused episodic fluctuations between negative and positive P-E+R (Fig. 1.9). Superimposed on this is the concept of on-going base-level rise in the Mediterranean which may or may not be related to latest Messinian deglaciation (see Roveri et al., 2014a). One possibility supported by the increasingly widespread evidence of low salinity in the Mediterranean is therefore that exchange with Atlantic involved only periodic inflow to a partially filled Mediterranean during Stage 3.

Once tectonic and/or erosional opening of the Atlantic gateway further increased gateway efficiency at the Mio-Pliocene boundary (Fig. 1.9), the Paratethyan component of the freshwater flux is no longer visible in the Mediterranean sedimentary record. This may be because Paratethys was no longer connected, but more likely, as it is today, the

more efficient Mediterranean-Atlantic gateway diminished the amplitude of the Mediterranean's response to subtle hydrologic change via its freshwater flux.

1.7. CONCLUSIONS

Marine gateways are an important control on both local environmental change and global climate. The Late Miocene Mediterranean gateway system that linked to the Atlantic is a good example of this and much can be learnt about the processes and impacts of gateway closure from the study of the sediments preserved within the ancient marine corridors in southern Spain and northern Morocco. Uplift and erosion resulting from the same tectonic drivers of gateway closure, has led to the preservation of incomplete sedimentary successions punctuated by unconformities. Despite this, it appears that the main channels, as deduced from the current distribution of Late Miocene sediment in the region, were closed before the precipitation in the Mediterranean of large volumes of halite during the Messinian Salinity Crisis. The whereabouts and dimensions of the connection that supplied Atlantic water to the Mediterranean during this period therefore remain currently unclear.

Additional constraints on Mediterranean-Atlantic exchange have been deduced from studying successions outside the immediate corridor region. Contourites in the Gulf of Cadiz are a direct consequence of Mediterranean Outflow and changes in their properties and location reflect fluctuations in the vigour of Mediterranean Outflow. Novel isotopic proxies that monitor connectivity have also been used to explore the presence of Mediterranean water in the Atlantic and the amount of Atlantic water reaching the Mediterranean. However, these records are currently too low resolution to capture the sub-precessional scale variability which is such a dominant feature of the hydrologic system active across the region. This in turn limits the constraints the data can provide for modelling experiments that explore both the gateway processes themselves and the impact of variable exchange on regional and global climate. In addition, the lack of a robust salinity proxy able to function across the wide range of salinities that were produced during the Messinian Salinity Crisis is currently a major problem that has consequences for reconstructing gateway exchange because this is driven by the density contrast between the Mediterranean and Atlantic.

Despite these challenges, an integrated review of the wide variety of information pertaining to Mediterranean-Atlantic exchange before, during and after the Messinian Salinity Crisis allows the first order reconstruction of gateway evolution (Fig. 1.9) and the role of exchange in driving the extreme environmental changes to be deduced.

Acknowledgements

The research leading to these results has received funding from the People Programme (Marie Curie Actions) of the European Union's Seventh Framework Programme FP7/2007-2013/ under REA Grant Agreement No. 290201 MEDGATE. The authors would like to thank Javier Hernández-Molina and Mike Rogerson for their helpful reviews and Dr Carla Sands, MEDGATE's superb Project Manager without whom much of the research would not have happened. CC Martins also thanks CAPES by scholarship support (BEX 5366/12-7).

CHAPTER 2

Astronomical tuning for the upper Messinian Spanish Atlantic margin: Disentangling basin evolution, climate cyclicity and MOW

Bas van den Berg[*], Francisco Sierro[a], Frits Hilgen[b], Rachel Flecker[c], Juan Cruz Larrasoaña[d], Wout Krijgsman[e], Jose Abel Flores[a]., Pilar Mata[f], E. Bellido Martín[f], Jorge Civis[f], Jose Angel González-Delgado[a]

[a]*Departamento de Geologia, Facultad de Ciencias, Universidad de Salamanca, 37008 Salamanca, Spain*
[b]*Stratigraphy/Paleontology, Faculty of Geosciences, Utrecht University, Budapestlaan 4, 3584 CD Utrecht, the Netherlands*
[c]*School of Geographical Sciences and Cabot Institute, University of Bristol, Bristol, UK*
[d]*Instituto Geológico y Minero de España, Unidad Zaragoza, Zaragoza, Spain.*
[e]*Paleomagnetic laboratory "Fort Hoofddijk", Budapestlaan 17, 3584 CD Utrecht, the Netherlands*
[f]*Instituto Geológico y Minero de España, Rios Rosas 23, Madrid, Spain.*

Abstract

We present a new high-resolution cyclostratigraphic age model for the Messinian sediments of the Montemayor-1 core. This core was drilled in the Guadalquivir Basin in southern Spain, which formed part of the marine corridor linking the Mediterranean with the Atlantic in the Late Miocene. Tuning of high-resolution geochemical records reveals a strong precessional cyclicity, with maximum clastic supply from river run off coinciding with maximum summer insolation. We recognize a gradual change in the nature of the typical cyclic fluctuations in elemental compositions of the sediments through the core, which is associated with a gradual change in depositional environment as the basin infilled. After applying the new age model, the upper Messinian glacial stages and deglaciation are clearly identified in the oxygen isotope records of the Montemayor-1 core. Reinterpretation of existing planktonic and benthic oxygen isotope records for the core and comparison with equivalent successions in the Rifian Corridor in northern Morocco allow the re-evaluation of the influence of the different water masses in the region: North Atlantic Central Water and Mediterranean Outflow Water. We observe no direct influence of MOW immediately before or during the Messinian Salinity Crisis.

This chapter has been published in Global and Planetary Change

2.1 Introduction

The Messinian Salinity Crisis (MSC, Hsü et al., 1973; Krijgsman et al., 1999; Roveri et al., 2014) is one of the most dramatic events in recent geological history. In less than 700 kyr, the Mediterranean Basin accumulated a succession of evaporites more than a kilometre thick as a consequence of the near-complete disconnection of the Mediterranean Sea from the Atlantic Ocean (Ryan, 2009). There is general consensus that the Atlantic Ocean was the water source that provided the chemical components needed for evaporite precipitation. However, the exact location and configuration (e.g. Simon and Meijer, 2015) of the marine gateway(s) that connected the Messinian Mediterranean with the Atlantic during the MSC remains elusive.

As a direct result of the gateway evolution, a number of modelling studies suggest that the Mediterranean Outflow Water (MOW) must have been active during the Early Messinian, but became weaker around 5.97 Ma, with the onset of the MSC and the precipitation of stage 1 primary gypsum (CIESM, 2008). It stopped completely at 5.55 Ma during the halite precipitation, i.e. the MSC acme (Krijgsman and Meijer, 2008; Meijer, 2006). Subsequently, the most commonly accepted model is that, at the Miocene-Pliocene boundary, the Zanclean deluge reconnected the Mediterranean with the Atlantic and re-established MOW through the Gibraltar Strait (e.g. Hsü et al., 1973; Roveri et al., 2014). However, other research based on the presence of marine fauna in the western and central Mediterranean, that is thought to be late Messinian in age, supports a marine reflooding event during the latest Miocene (Bourillot et al., 2010; Braga et al., 2006; Riding et al., 1998). Integrated Ocean Drilling Program (IODP) expedition 339 planned to investigate the evolution of Atlantic-Mediterranean water exchange from the Messinian to the Holocene close to the Gibraltar Strait in the Gulf of Cádiz (Fig. 2.1). In order to establish whether MOW was active or not and how it changed during the MSC, a number of sites both offshore (e.g. IODP Site U1387; Fig. 2.1) in the Gulf of Cádiz (van der Schee, in prep) and onshore (e.g. the Montemayor-1 core; Fig. 2.1) in the western part of the Guadalquivir Basin (this study), have been investigated.

During most of the Miocene, exchange with the Atlantic occurred through the Betic and Rifian corridors, located in southern Spain and northern Morocco, respectively (Fig. 2.1). To reconstruct the changes in flow patterns within, and the evolution of these corridors, well-dated reference sections at both ends of each corridor are required. These exist for the Rifian Corridor, where the Ain el Beida (Krijgsman et al., 2004) and Loulja (Van der Laan et al., 2006) sections on the Atlantic margin, and the Melilla (Van Assen et al., 2006) and Zobzit (Krijgsman and Langereis, 2000) sections at the Mediterranean side have been astronomically tuned. For the Betic corridors, the Sorbas Basin (Krijgsman et al., 2001; Sierro et al., 2001) serves as a reference section on the Mediterranean margin, but a well-dated reference section at the Atlantic end of the Betic

Corridor is currently lacking. The best region for establishing such a reference section is the Guadalquivir Basin (Fig. 2.1), which formed the connection between the Atlantic Ocean and all of the strands of the Betic Corridor to the east and south (Martín et al., 2014). A well-dated section in the Guadalquivir Basin could constrain the role of the Betic Corridor and evolution of MOW during the MSC. Unfortunately, outcrops exposing long sedimentary sequences in this basin are virtually non-existent because of the low lying, heavily vegetated landscape. Therefore we are reliant on subsurface data.

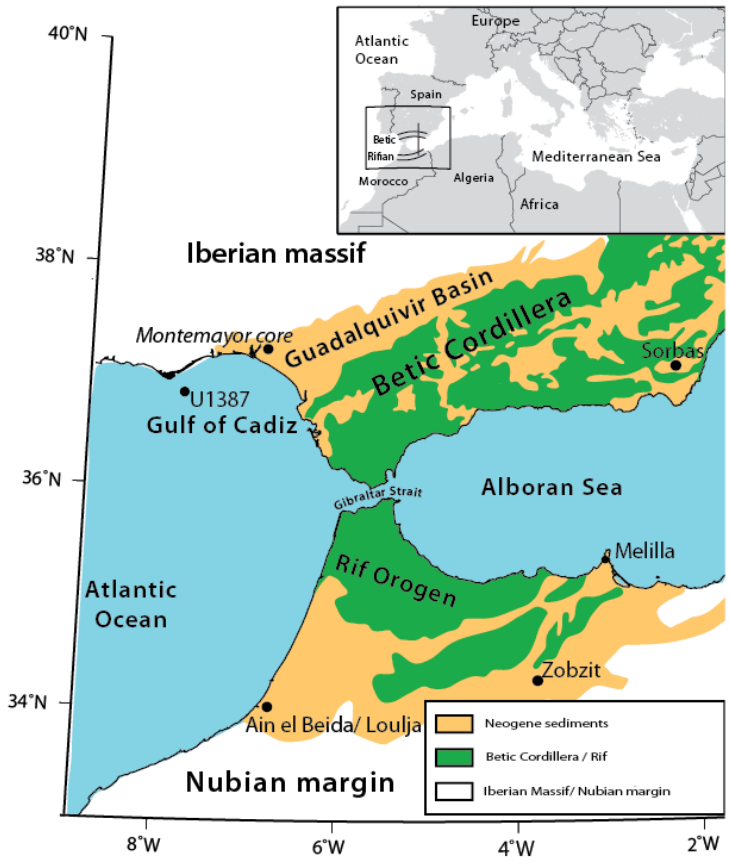

Figure 2.1. *Schematic geological map of the Gibraltar Strait region with the Neogene basins and the Betic and Rif Orogen. The location of the Montemayor-1 core as well as ODP Leg 339 drill sites and key Messinian sections are shown. The overview map in the in the upper right corner shows the locations of the Betic and Riffian corridors.*

The Montemayor-1 core was drilled in the northwest of the Guadalquivir Basin. Using this borehole, various paleoenvironmental studies, based on benthic foraminifera, environmental magnetism, stable isotopes and pollen analyses have investigated climate, vegetation and sea level changes during the Messinian, and the possible influence of MOW (Jiménez-Moreno et al., 2013; Larrasoaña et al., 2014; Pérez-Asensio et al., 2013; 2012a; 2012b, 2014). These results show that the Guadalquivir Basin shallowed before, during, and after the MSC. They also suggest that two major cold periods and associated sea level falls took place, one of which is thought to contribute to the onset of the MSC (Pérez-Asensio et al., 2013). Pérez-Asensio et al. (2012a) also suggested that the termination of MOW is recorded in the Montemayor-1 core at 6.18 Ma, and related this event to the closure of the Guadalhorce Corridor. The existing age models of the Montemayor-1 core on which these results are based use magnetobiostratigraphic tie-points (Larrasoaña et al., 2008; 2014) and the correlation of the oxygen isotope record to other, astronomically dated, isotope records in the Atlantic Ocean (Pérez-Asensio et al., 2012a). However, the identification of the marine isotope stages remains uncertain because of both the lack of high-resolution biostratigraphic age control in the critical interval above the C3A.1n–C3r reversal boundary and inconsistencies observed in the pattern of the benthic $\delta^{18}O$ record. The shift to lighter values above the distinct pair of $\delta^{18}O$ maxima identified as stages TG20 and TG22 by Pérez-Asensio et al. (2012a) is particularly inconsistent with the open ocean $\delta^{18}O$ record. Here we aim to improve the age model for the Montemayor-1 core, and evaluate the implications of this new age model for the interpretation of previously published records.

Astronomically induced changes in the amount of insolation result in cyclic changes in climate and therefore in cyclic sedimentary successions (Milankovitch, 1941; Strasser et al., 2006). This provides a powerful tool for constructing high-resolution chronologies. Our new age model is constructed using cyclostratigraphic analysis and tuning of high-resolution geochemical records combined with planktonic foraminiferal astrobiochronology. A similar approach was used for the Ain el Beida and Loulja sections in northern Morocco (Krijgsman et al., 2004; Van der Laan et al., 2006), which are equivalent in age and setting as the Montemayor-1 core (i.e. on the Atlantic margin of a foreland basin), and will therefore be referred to in this paper for comparison. In constructing an astronomically tuned reference section for the Atlantic side of the Betic Corridor, we are able to link major changes in the sedimentary succession of the Guadalquivir Basin to local, regional and global events. A number of paleoceanographic proxies can subsequently be used to reconstruct hydrological changes in the Atlantic margins and assess the influence of MOW.

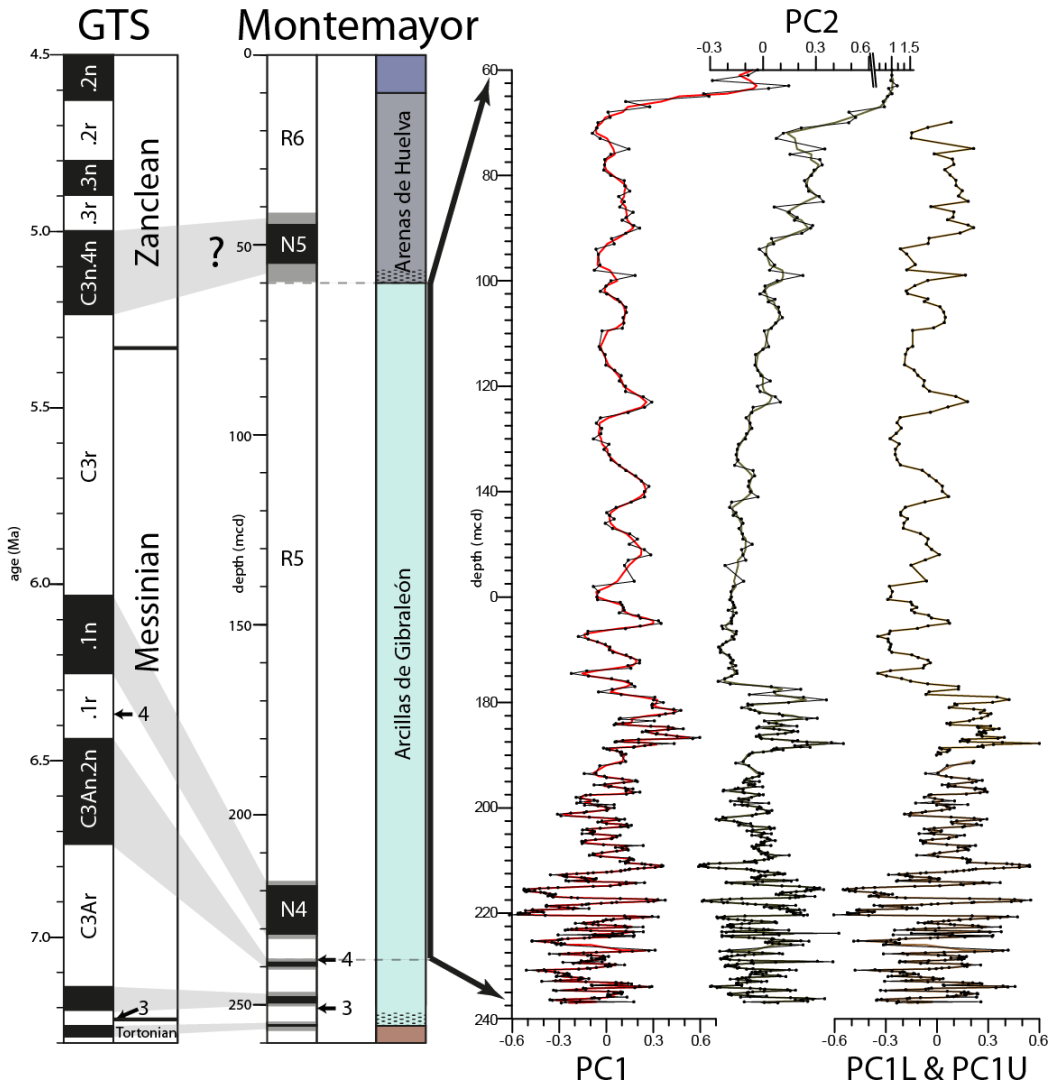

Figure 2.2: *<u>Left:</u> Tortonian-Zanclean magnetostratigraphic chrons and biostratigraphic events of the GTS (Lourens et al., 2004). Numbers denote planktonic foraminiferal events of Sierro et al. (1993). <u>Middle:</u> previously published magnetostratigraphic and biostratigraphic results for the Montemayor-1 core (Larrasoaña et al., 2008) with their relation to the GTS. The lithology column shows from bottom to top the Calcarenita de Niebla formation, Arcillas de Gibraleón formation, Arenas de Huelva formation and Arenas de Bonares formation, respectively. The small black dots represent the glauconite layers at 252 and 60 mcd. Black arrows indicate the part of the borehole addressed in this study. <u>Right:</u> PC1 and PC2, PC1L and PC1U data (black) with their 3 point moving average (red/green/brown/gold). Note the excellent agreement between the original data and the 3 point moving average. In subsequent figures only the 3 point moving average will be shown.*

2.2 Geological setting and core

The Guadalquivir Basin was formed in the Late Serravallian – Early Tortonian and evolved from foredeep to foreland basin throughout the Miocene by downward flexure of the basin as a response to loading of the imbricated Betic External units (Berástegui et al., 1998; García-Castellanos et al., 2002; Sanz de Galdeano and Vera, 1992; Sierro et al., 1996). The basin is bounded by the Iberian massif to the North, the subbetic thrust belt of the Betic Cordillera to the south, and is open to the Atlantic Ocean at its western end (Fig. 2.1). It has experienced continuous sedimentation from middle-Late Miocene up to the late early Pleistocene (González-Delgado et al., 2004; Salvany et al., 2011; Sierro et al., 1996). After the closure of the Betic corridors, the Guadalquivir Basin developed as an embayment to the Atlantic, gradually filling up from east to west, in a configuration that persists today in the Gulf of Cádiz.

The Montemayor-1 core was drilled in November 2001 near the village of Moguer in the northwest Guadalquivir Basin at 37°15.99'N; 6°48.62'W (Fig. 2.1). The core recovered marine sediments that correspond to the four lowermost lithostratigraphic units of the basin infill (Fig. 2.2; Sierro et al., 1996). The lowermost unit, the Niebla Formation, is Tortonian in age and consists of a mix of calcareous and siliciclastic sediments deposited during the marine transgression over the Paleozoic-Mesozoic basement. The middle unit, the Arcillas de Gibraleón Formation, covers the largest part of the borehole. It is Tortonian-Messinian in age and consists of nearly-continuous homogeneous bluish-green clays with some interbedded silty beds and a glauconite layer at its base (~252 mcd). This formation is the main focus of this study. Above this unit is the Arenas de Huelva Formation, which consists of lower Pliocene sands, with a pronounced glauconite layer at the base of the formation, at about 60 meter core depth (mcd). This unit is overlain by the transitional sands of the Arenas de Bonares Formation (Larrasoaña et al., 2008; 2014).

Based on the age model of Larrasoaña et al. (2008), the normal polarity chron observed at the top of the core (labelled N5) begins within the glauconite layer (Fig. 2.2). As glauconite typically forms during periods of very slow or negligible marine sedimentation, this glauconite layer probably corresponds to a condensed interval or hiatus (e.g. Jiménez-Moreno et al., 2013). If we examine closely the magneto-biostratigraphic results, bio-event 4 (Sierro et al., 1993) and the top of chron C3An.2n are found at almost the same core depth (237 mcd and 238 mcd, respectively), although these events are clearly separated in the Ain el Beida section and the GTS with an age difference of 70 kyr (Krijgsman et al., 2004; Lourens et al., 2004). Therefore this interval must also be condensed or associated with a (small) hiatus in this part of the core. In order to assess the cyclicity, continuous sedimentation is required. Consequently we will only consider the interval 60-237 mcd (Fig. 2.2) which spans ca.

6.4-5 Ma (Larrasoaña et al., 2008; 2014) capturing the entire duration of the MSC (5.97-5.33 Ma; Roveri et al., 2014).

2.3 Method

2.3.1 X-Ray Fluorescence (XRF) analyses

The strikingly homogeneous composition and lithology that dominates the Montemayor-1 core (Fig. 2.2), prevents the construction of a reliable cyclostratigraphic framework based on visually identifiable lithological cycles (e.g. grain size and lithology). Cyclic changes may, however, be apparent in the chemical composition of the sediments. To detect these, we measured a total of 527 samples using X-Ray Fluorescence (XRF) with a NITON XL3t900 GOLDD analyser. Measurements were done in 'mining Cu/Zn' mode, measuring time was 150 seconds per sample and Helium purging was used for optimal detection of light elements. The hand-held analyser was used while placed in its holder and the analyses were done on three different sample surfaces, which were smoothed and flattened using a scalpel. One sample was selected as a 'standard' and measured several times during the entire measurement campaign to be able to detect measurement anomalies or gradual deviations over time. Analysis of this standard data did not indicate any measurement inconsistencies. All samples were measured three times and the reproducibility was in general good with very few outliers. Since the clays forming the matrix throughout the entire studied section are very homogenous (except for the very top), anomalies due to changes in the matrix are not expected.

The use of fast, low-cost XRF methods is increasingly used for chemostratigraphy and/or geochemical shifts in sedimentary records. XRF core-scanning measurements have been widely applied when a well-preserved section is available. Validation and discussion of this method can be found in Jansen et al. (1998); Richter et al. (2006); Tjallingii et al. (2007). The reliability of geochemical data obtained from handheld XRF devices has been demonstrated previously, in both the field and laboratory data (Higueras et al., 2012; Kalnicky and Singhvi, 2001; Rowe et al., 2012; USEPA, 2006).

To assess the reliability of our data still further, we performed an additional calibration for the data obtained by the NITON XL3t900 GOLDD analyser using a conventional WD-XRF of the Instituto Geológico y Minero de España (IGME). For this calibration, major and trace element concentrations were determined by WD-XRF analysis using a MAGIX PANalytical equipped with an Rh x-ray tube at 2.4 Kw. Quantitative data were obtained using superQ PANalytical software. Major elements were measured on a lithium borate-fused disk (Spectromelt A1000, 0.3 g sample: 5.5 g flux) to avoid matrix effects typical of sediments and rocks. Trace elements were determined in a pressed powder pellet, with elvacite as a binding agent, and quantitative data were obtained with

pro-trace software, which includes chemical matrix effects correction, interference of spectral lines and background corrections.

Figure 2.3 shows the correlation plots for the three most important major elements, based on Principal Component Analysis loadings (see section 4.1): Calcium (R^2=0.78), Silicon (R^2=0.70) and Titanium (R^2=0.78), and the three trace elements used in this study: Strontium (R^2=0.96), Zirconium (R^2=0.77) and Rubidium (R^2=0.88) for a selection of 31 samples selected from the entire core. Only Silicon seemed to be largely influenced by the change in matrix at the bottom and top of the core, therefore for this element only the samples of the interval of homogeneous bluish-green clays used in this study are used. These correlations indicate that although the absolute values of element concentrations obtained with the NITON handheld analyser should be treated with caution, the relative changes in geochemical composition are robust.

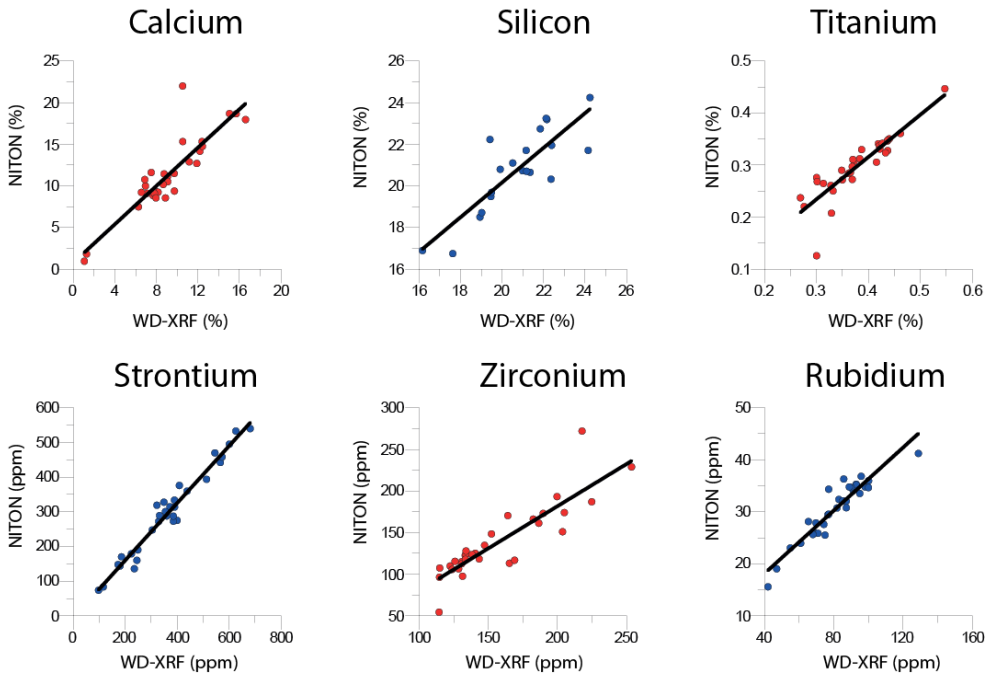

Figure 2.3. *Correlation curves for Calcium, Silicon, Titanium, Strontium, Zirconium and Rubidium measured by the WDS XRF vs. the NITON handheld XRF.*

2.3.2 Statistics

Dixon's test (Dean and Dixon, 1951; Rorabacher, 1991) was used to detect outliers with 95% confidence. Outliers were excluded and the remaining values were averaged for

each sample. A well-known problem with XRF measurements is that lighter elements emit a smaller signal when excited and their emission is therefore more prone to attenuation (Tjallingii et al., 2007). In order to account for the larger scattering of light elements like aluminium and silicon, only a three-point average of these measurements has been used (Fig. 2.4). Likewise, elements with very low concentrations (less than 100 ppm), in this case only rubidium, are subjected to enhanced scattering and consequently only a three-point average of this record has been used (Fig. 2.4). Since aluminium yields enhanced scattering, the common practice of Aluminium normalization will not be applied here. Instead, as proposed by Davis and Sampson (2002) and Aitchison (1986) we performed a centred log-ratio transformation, to make the dataset 'open' (i.e. remove all spurious correlations), and statistically robust. This involves dividing through the geometric mean, which is a type of normalization (Aitchison, 1986; Davis and Sampson, 2002), allowing direct comparison between the major oxides and trace elements. A centred log-ratio transformation also allows each of the elements to be represented in the Principal Component Analysis (PCA), which was conducted using the PAST version 3.01 software package (Hammer et al., 2001). Note that when using any element as a common denominator, this element cannot be considered further when performing PCA.

2.4 Results

2.4.1 Principal Component Analysis

All elements measured and used in this study are presented in figure 2.4. Principal component analysis was performed to simplify and visualize the data matrix. Elements with similar behaviour are combined into a few components, each of which represents a specific linear combination of elements, in such a way that the linear combination of the first principal component explains the largest possible amount of variance within the dataset. Subsequently, the second component explains the largest possible amount of the remaining variance, and so on (Davis and Sampson, 2002). This analysis yields two statistically significant components: the first principal component (PC1), describing 51% of the total variance and the second principal component (PC2) describing 37% of the total variance. The two most important negative loadings for PC1 are Ca and Sr (Fig. 5), while the positive loadings comprise Zr, Si, Ti, K and Fe (in descending order). For PC2, the two most important positive components are Zr and Ca. The negative loadings consist of Fe, Al, Rb, and K (Fig. 5). All elements that have a positive loading for PC1 are important components of aluminosilicate minerals. Ca and Sr are the major elements in biogenic carbonate, which visual inspection suggests is mainly associated with foraminifera and coccoliths. The relationship between the loadings of PC2 is unclear.

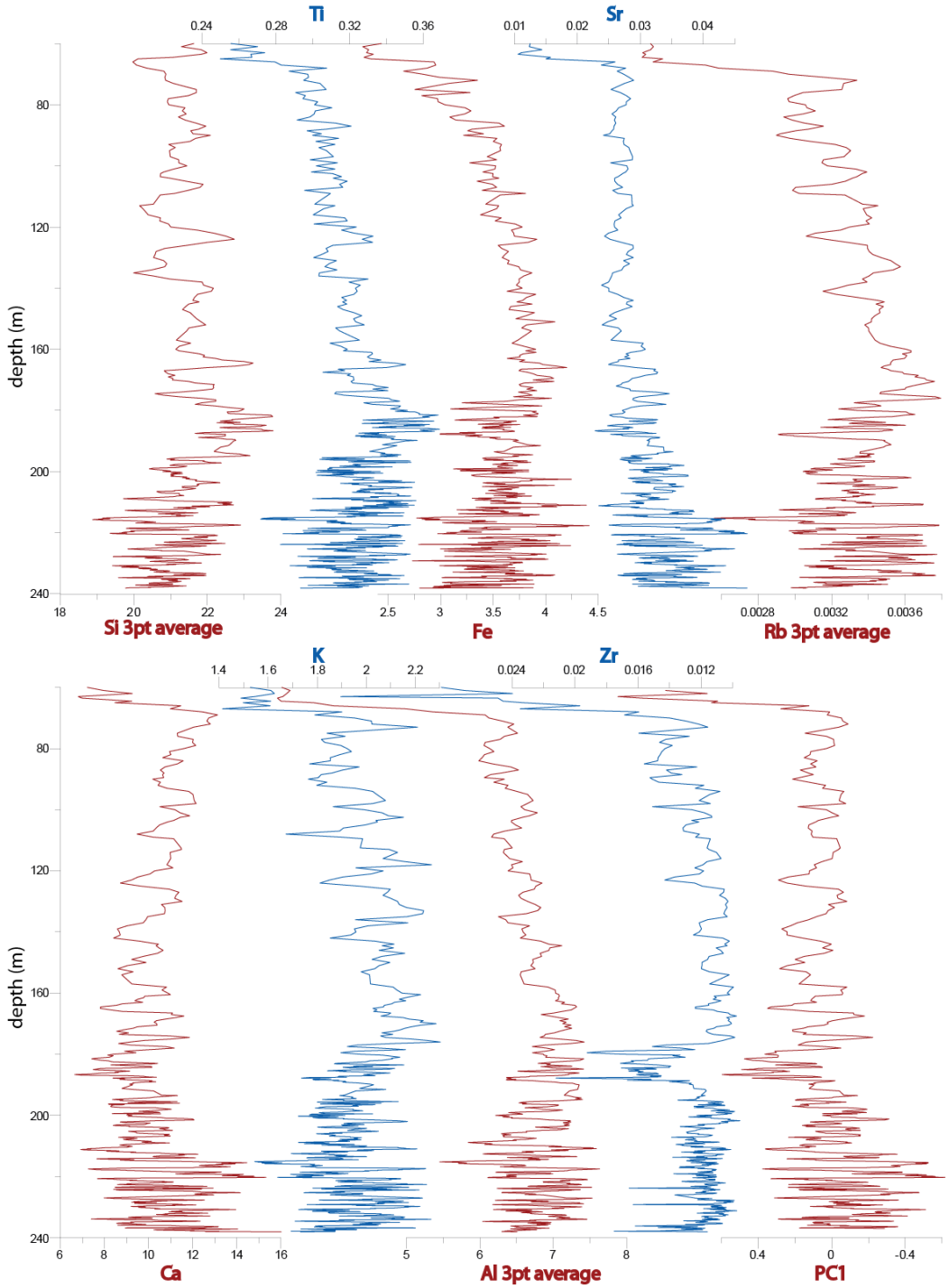

Figure 2.4: *Element concentrations in percentages for the individual elements used in this study.*

2.4.2 Geochemical records in depth domain

PC1 (Fig. 2.2) shows regular alternations, gradually thickening upwards, with a sudden increase in thickness around 175 mcd. The pattern is very similar to the observed patterns in all the individual element records (Fig. 2.4). In the bottom part (238-220 mcd), three groups of alternations can be distinguished, each separated by a pronounced minimum. The amplitude of the alternations becomes smaller towards the top of the core, especially above 120 mcd. The sudden increase at the top of the record (above 66 mcd) corresponds to a change in lithology, from clays to sands, just before the glauconite layer.

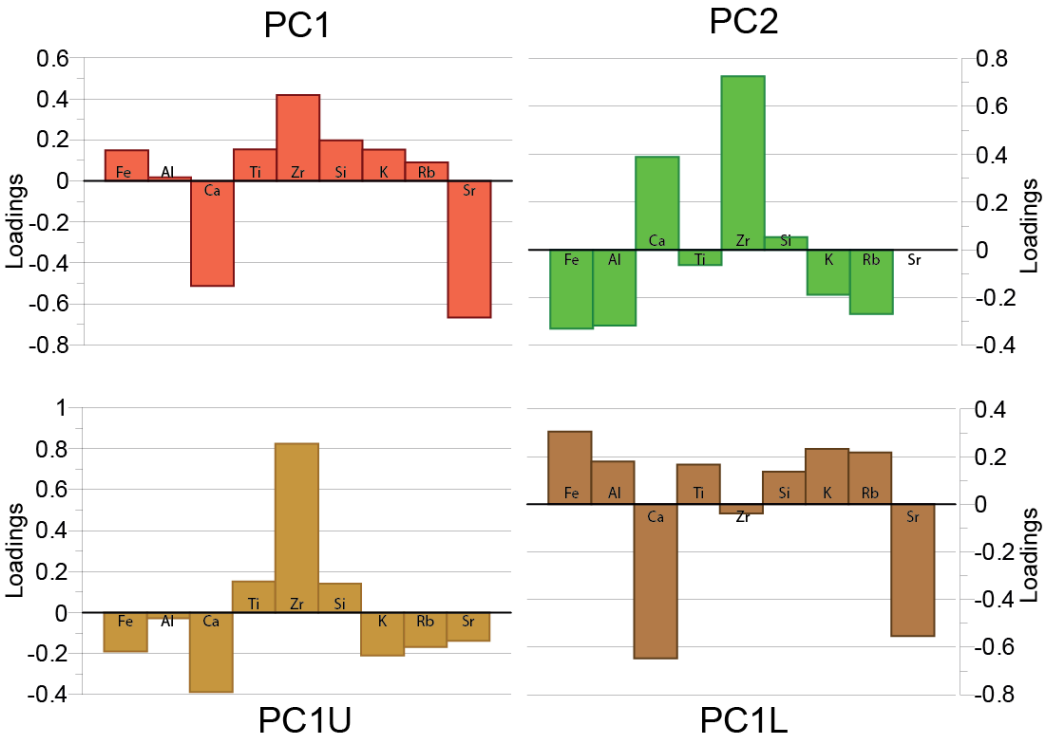

Figure 2.5: *Loadings of the Principal Components PC1 (top, left), PC2 (top, right), PC1U (bottom, left) and PC1L (bottom, right).*

In addition, to assess the nature of the regular alternations and changes therein, a principal component has been performed on both the lower (70-190 mcd) and the upper (190-237 mcd) part separately. The PC1 records of both intervals show identical regular alternations as the PC1 of the entire core. However, surprisingly, the loadings comprising these alternations change from the lower to the upper interval (Fig. 2.5). The first principal component of the lower part (PC1L) shows similar loadings to PC1, with Ca and Sr being the most important elements on the negative side and the aluminosilicates at the positive side, only the contribution of Zr to PC1U is negligible in

comparison to PC1. The first principal component for the upper part of the record (PC1U), however, consists of a very different combination of loadings. Here the most important positive loading is Zr, followed by Ti and Si, while the negative side consists predominantly of Ca followed by K, Fe and Rb which are commonly associated with clay minerals.

The benthic $\delta^{18}O$ record of the Montemayor-1 core (Fig. 2.6; Pérez-Asensio et al., 2012a) also shows regular alternations, with heavier values common in the 200-175 mcd interval and a sudden increase in thickness at 175 mcd. The top part of the $\delta^{18}O$ record (above 175 mcd) is in anti-phase with PC1. Below 175 mcd there is no clear phase relation. This could be due to the lower resolution of the record.

2.5 Age model

2.5.1 New biostratigraphic events

In order to build a more accurate biostratigraphic framework, we analysed and counted the keeled Globorotaliids, in particular changes in abundance of *Globorotalia margaritae* and *Globorotalia menardii* sin (Fig. 2.7). For the 170-180 mcd interval, where possible, 400 specimens per sample were counted, because in this interval the two influxes of *G. menardii* sin were identified which have a relatively low abundance (2-8%), the other intervals were extensively scanned to assure no influxes were missed. For the interval below 180 mcd, 100 specimens per sample were counted to reconstruct the acme of *G. margaritae* which has a much higher abundance (15-35%) and therefore 100 specimens per sample is sufficient to give a reliable representation. To justify this, the 95% confidence interval based on the binomial standard error (Dennison and Hay, 1967; Fatela and Taborda, 2002) is also plotted in figure 2.7, clearly showing the reliability of the two influxes of *G. menardii* as well as the acme of *G. margaritae*. Changes in abundance of these two species have been linked to specific astronomical cycles in the Ain el Beida and Loulja sections (Krijgsman et al., 2004; Van der Laan et al., 2006). Two influxes of *Globorotalia menardii*, found in Ain el Beida cycle 42 (5.55 Ma) and cycle 43 (5.53 Ma; Krijgsman et al., 2004, Fig. 2.2) and in the bottom of the Loulja section (Van der Laan et al., 2006), were recorded in the Montemayor-1 core at 176 and 172 mcd, respectively (Fig. 2.7). These two influxes of *G. menardii* sin were erroneously reported in Ain el Beida as *Globorotalia miotumida* (Krijgsman et al., 2004; Tulbure et al., in prep).

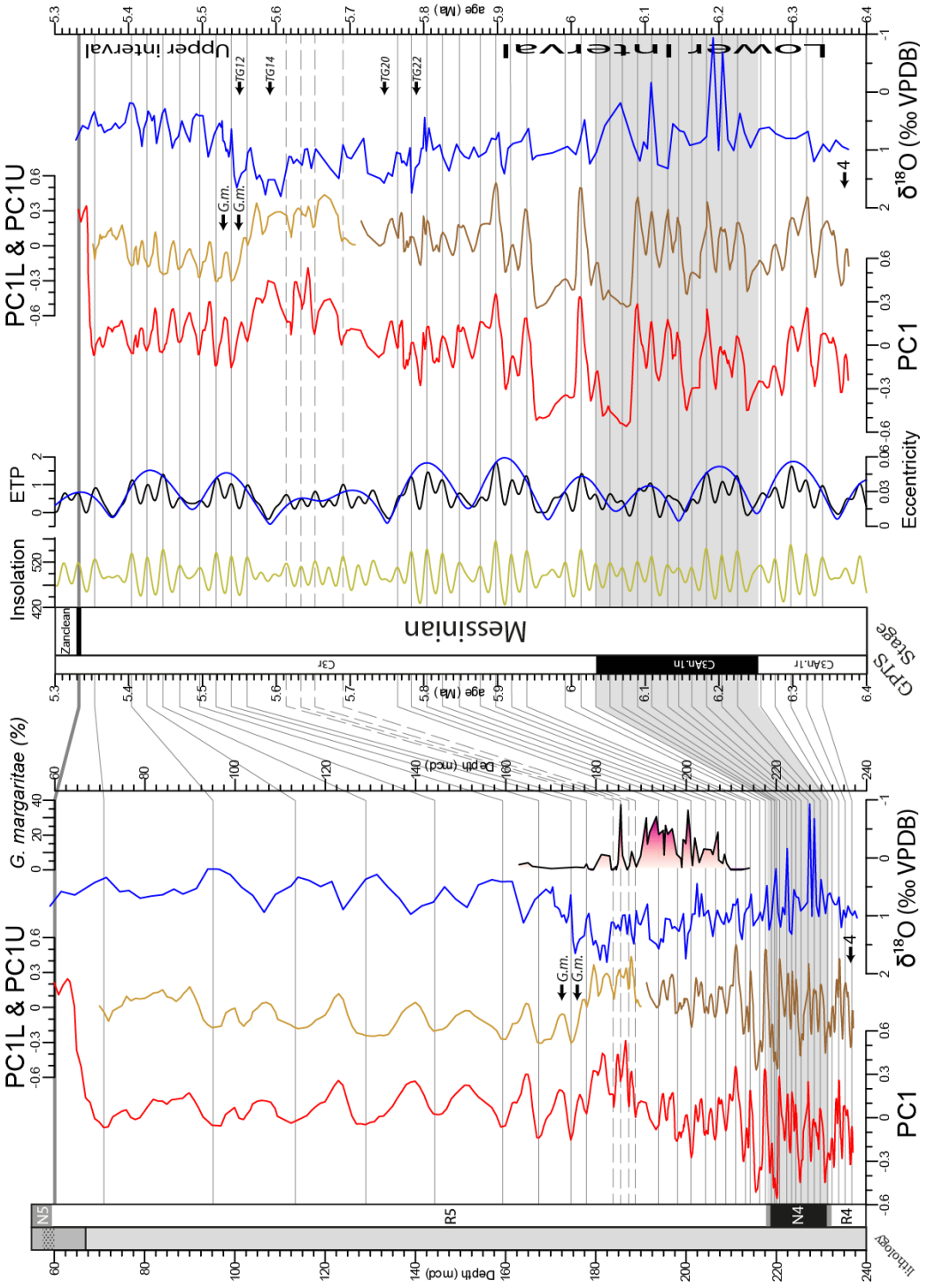
Lower interval
Upper interval
PC1L & PC1U
PC1
δ18O (‰ VPDB)
G. margaritae (%)
ETP
Insolation
Eccentricity
GPTS Stage
Messinian
Zanclean
C3r
C3An.1n
C3An.1r
lithology
Depth (mcd)
age (Ma)
G.m.
TG12
TG14
TG20
TG22
N5
R5
N4
R4
4

Figure 2.6: *PC1, PC1U, PC1L (all 3 point moving average) and $\delta^{18}O$ (Pérez-Asensio et al., 2013) records in the depth domain (left) converted to a cyclostratigraphic age model (right) using, the insolation, E+T-P and eccentricity (blue) curve (middle). Nomenclature of glacial stages is after Shackleton et al. (1995a). G.m. is influx of Globorotalia menardii sin, 4 is bio-event 4 of Sierro et al. (1993), i.e. coiling change of Neogloboquadrina acostaensis. The interval with uncertainty in phase relation is shown with dashed lines. In the lithology column (far left) the change from Clays (light grey) to sands (dark grey) is shown, with the glauconite layer (black dots).*

Two intervals of abundant *G. margaritae* are found in the 210-198 mcd interval, with a brief low abundance interval at 199.1 mcd (Fig. 2.7). Another short peak is found at 185.6 mcd. The two intervals with abundant *G. margaritae* may coincide with the *G. margaritae* acme at Ain el Beida which also shows two peaks in abundance, in cycles 33 and 35 (Krijgsman et al., 2004), corresponding to glacial stages TG20 and TG22.

For the 244-234 mcd interval, up to 40 specimens of *Neogloboquadrina acostaensis* were counted to estimate the sinistral to dextral ratio in order to confirm the depth of the main sinistral to dextral coiling change (Fig. 2.7). This marks the bottom end of the record analysed in this study.

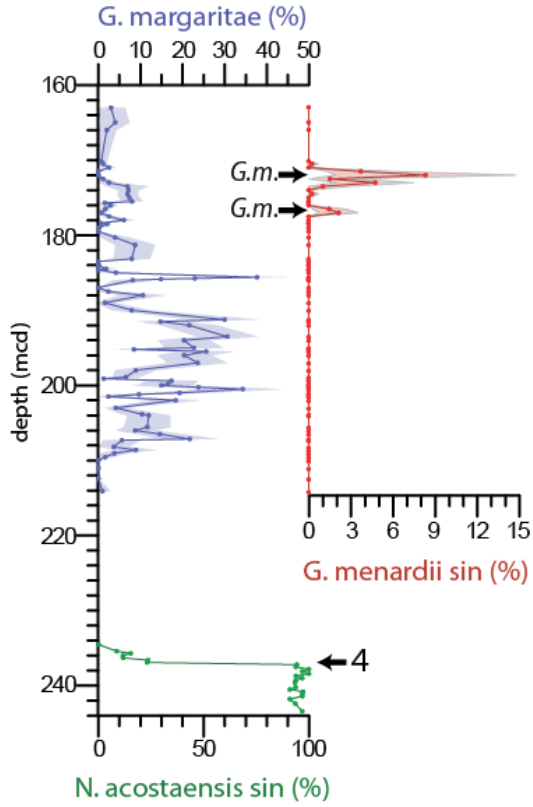

Figure 2.7: *Abundance of Globorotalia margaritae (blue) and Globorotalia menardii sin (red) including 95% confidence interval, and percentage of Neogloboquadrina acostaensis species that is sinistral (green), with indications of the core depth for the associated bio-events.*

2.5.2 Cyclostratigraphic age model.

To perform a cyclostratigraphic study of the geochemical records we first need to demonstrate that the alternations in the geochemical record are of astronomical origin, corresponding to the periods of precession, obliquity and/or eccentricity. To demonstrate this we used the depths and astronomical ages of the two bio-events that are furthest apart, together with the number of geochemical alternations between them. Between the coiling change of *N. acostaensis* (bio-event 4, 6.37 Ma) and the highest influx of *G. menardii* (5.53 Ma), which covers a time span of ~840 kyr, we identified ca. 38 cycles (Fig. 2.6). This means each cycle has an average period of ~22 kyr, which coincides well with the average precession period.

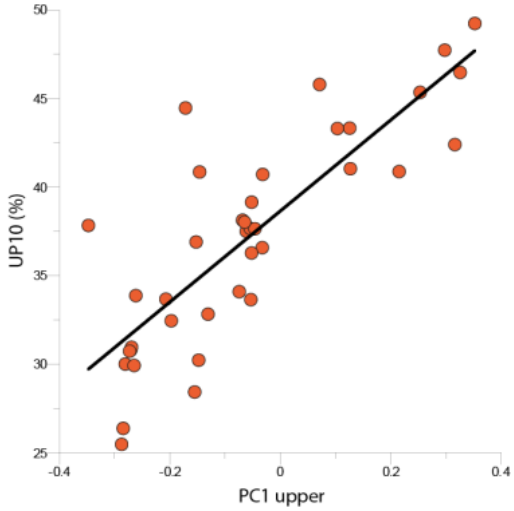

Figure 2.8: *Cross correlation of PC1U and UP10 for a random set of samples of the Montemayor-1 core, including a linear fit.*

Next we have to understand the nature of the geochemical cycles based on the PCA loadings and the phase relation with respect to the astronomical target curve. Since both the PCA loadings and the phase relation changes along the core, we will first consider the cycle nature, phase relation and subsequent tuning for individual parts of the record before interpreting the evolution of the record as a whole. In general, based on the loadings of the principal components (Fig. 2.5), PC1 as well as PC1L can both be considered as representing the juxtaposition of biogenic carbonate versus aluminosilicates (clay). In Ain el Beida, the same relationship is found for PC1, where maxima of fine grained aluminosilicates are found in the red layers, and minima in the beige layers (Van der Laan et al., 2012). At Ain el Beida, this is explained by terrigenous, fluvial influx of aluminosilicates into the basin during wet periods causing dilution of the biogenic carbonate content. The red layers with low carbonate content correspond to precession minima and summer insolation maxima, as they share many proxy signals with Mediterranean sapropels, while the beige layers with high carbonate content correspond to precession maxima and summer insolation minima.

Again, based on the loadings, our PC1U can be considered as a proxy for grain size of terrigenous particles, with Zr, Si and Ti on the positive axis typically representing the silty fraction, while the elements accompanying Ca on the negative axis are typically found in the clay fraction (Fig. 2.5). This relationship is confirmed by grain size measurements carried out on 38 samples from the upper part of the core, yielding a positive correlation between PC1U and UP10 (R^2=0.6727, P_{uncorr}= $3*10^{-10}$; Fig. 2.8). The UP10 size (i.e. the percentage of the sample consisting of particles coarser than 10 μm), which adds the fine sand subpopulation to the sortable silt size fraction (10-63 μm), is considered a proxy for paleocurrent intensity (McCave et al., 1995). Even though the correlation is clear, the R^2 value is not so high, probably due to the relative small number of samples. In conclusion, while PC1L shows the biogenic carbonate versus clay ratio, PC1U reflects the biogenic carbonate and clay versus silt ratio.

2.5.2.1 Tuning of the lower interval (238-210 mcd)

Based on the phase relation described above, we correlate insolation minima to maxima in calcium carbonate in the Montemayor core. Since calcium has a negative loading on

PC1, we tune PC1 minima to insolation minima, and PC1 maxima to insolation maxima (Fig. 2.6).

Our results are tuned to the La2004$_{(1,1)}$ solution (Laskar et al., 2004). The first order calibration involves tuning to eccentricity. Intervals with higher amplitude peaks should correspond to eccentricity maxima. In the depth domain, PC1 yields five intervals with high amplitude maxima (at 234, 228, 222, 218 and 211 mcd) which, based on the initial magnetobiostratigraphic age model (Larrasoaña et al., 2008), should correspond to the five ~100-ka eccentricity maxima between 6.37-5.88 Ma. The tuning is constrained by normal chron C3An.1n, the base of which is located at 232 mcd, just above the oldest of the five intervals with high amplitude variability in PC1, and the top at 218 mcd, just below the fourth interval (Fig. 2.6). The prominent maxima in the PC1 curve just below the base of C3An.1n should therefore be tuned to the four precession related peaks associated with the ~100-ka eccentricity maximum at 6.3 Ma. The three prominent maxima in the lower part of chron C3An.1n are tuned to the three precession related peaks in the eccentricity maximum at 6.2 Ma, while the four maxima in the upper part of this chron are tuned to precession related peaks in the eccentricity maximum around 6.1 Ma. This tuning to eccentricity is continued for the two youngest intervals with high amplitude variations located above C3An.1n. The small peaks flanking the prominent peak in PC1 at 6.1 Ma should also represent precession related cycles and thus correspond to precession driven insolation maxima. As shown by Van der Laan et al. (2005), sedimentation rates at Ain el Beida can be up to five times higher in the thickest and most prominent reddish marl layers as a consequence of the high amplitude insolation maxima and precession minima at times of maximum eccentricity. This can be explained by much-enhanced fluvial runoff and associated sediment supply during extreme insolation maxima. This link between sedimentation rate and the amplitude of precession, or more correctly, the amplitude of precession minima and, hence, summer insolation maxima, may explain the expanded thickness of high amplitude PC1 cycles while less pronounced cycles remain thin.

2.5.2.2 Tuning of the upper interval (60-178 mcd)

The PC1 and PC1U records in this interval are almost identical (Fig. 2.2), but each is based on a different set of loadings (Fig. 2.5). Since the loadings of PC1U must, by definition, represent this interval best, we will use these to explain the nature of the cycles. Maxima in carbonate now correspond to maxima in clay since carbonate and the clay minerals are found on the same side of the loadings axis. To evaluate the phase relation of these cycles with respect to insolation, we use the bio-events and the $\delta^{18}O$ record of Pérez-Asensio et al. (2012a). At Ain el Beida, the two influxes of *Globorotalia menardii* are found in successive beige layers and thus correspond to insolation minima. In our record these influxes coincide with PC1 maxima, which should therefore also correspond to insolation minima. This suggests that PC1's phase relationship with precession in the upper interval is different from its relationship with precession in the

lower interval (Fig. 2.6). This is confirmed by the benthic $\delta^{18}O$ record, which shows clear alternations in the upper part of the record where minima in the benthic $\delta^{18}O$ record are in phase with minima in PC1. Both the $\delta^{18}O$ record of Ain el Beida (Krijgsman et al., 2004) and the lower part of the Loulja $\delta^{18}O$ record (Fig. 2.9; Van der Laan et al., 2006) show clear precession-related cyclicity with minima in $\delta^{18}O$ corresponding to maxima in insolation. Therefore we also expect minima in the benthic $\delta^{18}O$ record of the Montemayor-1 core to correspond to maxima in insolation.

Unfortunately, as a result of the condensed glauconitic interval there is no reliable bio- or magnetostratigraphic tie point at the top of the record. However, since the geochemical alternations in the lower interval are invariably controlled by precession, we interpret the clear cycles in the upper interval to be precession related as well. This is confirmed by the bio-events and the benthic $\delta^{18}O$ record. Influxes of *Globorotalia menardii,* which are expected in successive precession maxima (Krijgsman et al., 2004; Lourens et al., 2004), are found in successive PC1 maxima. The benthic $\delta^{18}O$ record of Loulja (Van der Laan et al., 2006) has a strong precessional component for the influxes of the *Globorotalia menardii* interval and above. Likewise, the alternations in the upper interval of the Montemayor-1 benthic $\delta^{18}O$ record, in phase with PC1, should also be controlled by precession. Finally, if the alternations were related to obliquity the precessional component should still be, at least partly, distinguishable, e.g. see the benthic $\delta^{18}O$ records of Ain el Beida and Loulja (Van der Laan et al., 2005; 2006). However, the cycles in de PC1 as well as in the $\delta^{18}O$ record are very simple, i.e. there is no indication of interference patterns derived from both precession and obliquity. This all suggests that the cycles in the upper interval are precession related. Unfortunately, there is no clear eccentricity related pattern in this part of the record that would strengthen the tuning. Only the last complete alternation at the top is substantially thicker; this cycle is tuned to the eccentricity minimum at 5.38 Ma.

If the cycles are precessional and are used to constrain the age of the succession, the base of the glauconite layer at the top of our record corresponds exactly with the Miocene–Pliocene boundary (5.33 Ma; Fig. 2.6). Since the base of chron C3n is dated at 5.235 Ma (Fig. 2.2; Lourens et al., 2004), and assuming that polarity interval N5 correlates with chron C3n.4n (see Larrasoaña et al., 2008), this implies a condensed interval of at least 100 kyr, associated with the glauconite layer.

2.5.2.3 Tuning of the middle interval (210-178 mcd)

The tuning of the middle interval is more complicated as the signal amplitude is low and the observed change in cycle nature, expressed by the change in PCA loadings, takes place here. This change is gradual and it is therefore not possible to pinpoint its exact location. To calculate PC1L and PC1U we have set the division between the lower and upper interval at 190 mcd. Since we want to assess the nature of the patterns, and the patterns in PC1L and PC1U are very similar to the ones found in respectively the lower

and upper interval of PC1, this division is justified. For the top part of this middle interval (190-178 mcd), apart from some details, the general pattern in PC1U is the same as in PC1. Therefore, just like the upper interval, we will tune PC1 minima to insolation maxima. The insolation curve for this part is characterized by a 400 kyr eccentricity minimum, resulting in low amplitude precession cycles. As a result, not all cycles are expressed in the record. In addition, very few samples were available for XRF measurements in the 195-189 mcd interval, so the data resolution is too low to demonstrate a clear pattern. Both the low amplitude of the signal and the low sample resolution hamper a straightforward tuning, resulting in only a best possible fit for this part of the record. If we assume no major changes in sedimentation rate, at least two cycles are either missing or are not expressed in the 195-189 mcd interval. By also assuming that the low amplitude precession cycle, which is not expressed as a reddish layer above cycle 38 at Ain el Beida (Krijgsman et al., 2004), is not well expressed in the Montemayor core either, we can then tune the remaining alternations to the remaining precession cycles in this upper part of the middle interval. Due to all these uncertainties, this part of the tuning is marked with dashed lines in figure 2.6, and an extra uncertainty of one precession cycle (22 kyr) must be taken into account.

In the bottom part of this interval (190-210 mcd), the cycles are not so well expressed as in the lower interval of the entire core. However, the pattern of PC1 and PC1L is nearly identical for this interval, so we interpret that the nature of the cyclicity is the same and maxima in PC1 and PC1L should be tuned to insolation maxima (Fig. 2.6).

2.6 Discussion

2.6.1 Comparison with previous age models

The first age model was constructed by Larrasoaña et al. (2008), based on bio- and magnetostratigraphic tie points. Subsequently, Pérez-Asensio et al. (2012a) changed this age model by attempting to identify glacial stage TG22. We have improved the age model by adding extra biostratigraphic tie-points; the two influxes of *G. menardii* and the *G. margaritae* acme (Fig. 2.6). These tie-points suggest that a reinterpretation of the $\delta^{18}O$ record is required. The two heavy excursions in the $\delta^{18}O$ record, at 176 and 183 mcd, should be correlated to isotope stages TG12 and TG14 (Fig. 2.6), and not to TG20 and TG22 as proposed by Pérez-Asensio et al. (2012a). Consequently only two other maxima, i.e. at 193 and 199 mcd, remain candidates for isotope stages TG20 and TG22. This is confirmed by the *G. margaritae* acme (Fig. 2.6), which corresponds to the same glacial stages at Ain el Beida (Krijgsman et al., 2004). The acme of *G margaritae* was not used to construct the age model and therefore confirms independently our tuning.

As a consequence of the successfully tuning of the PC1 record, the uncertainty associated with the age model has been reduced to only a couple of thousands of years, except for

the interval between 5.7-5.6 Ma where, due to the tuning issues addressed in section 5.2.3, an extra uncertainty of one precession cycle must be taken into account.

2.6.2 Mechanisms driving sedimentary cycles

2.6.2.1 Lower interval (238-210 mcd; 6.37-5.9 Ma)

The geochemical cycles of the lower interval (Fig. 2.6) are mainly driven by precession forced cyclical changes in annual rainfall with more biogenic carbonate concentrated at times of Northern Hemisphere summer insolation minima when terrigenous supply is low. By contrast, enhanced amounts of terrigenous sediments, which in a distal setting are dominated by clays, are deposited at times of Northern Hemisphere summer insolation maxima when high rates of annual rainfall resulted in enhanced clay supply to the Guadalquivir Basin through intensified river run off. Plumes of fine-grained terrigenous material will dilute the biogenic carbonate-rich sediments. As a consequence, the sedimentary cycles are expressed by the regular alternations of carbonate-rich, more silty beds and carbonate-poor, clay rich layers, similar to those described in other Atlantic sections like Ain el Beida (Van der Laan et al., 2012) and Loulja (Van der Laan et al., 2006).

Similar astronomically-driven cyclical changes in gamma-ray and sonic logs have been recorded in the Gulf of Cádiz during the Pliocene (Sierro et al., 2000). High annual rainfall in southern Spain at times of maximum summer insolation resulted in enhanced detrital supply to the Gulf of Cádiz and deposition of clay-rich beds with high gamma ray and sonic values, while dryer climates at times of minimum insolation correspond to low gamma ray and sonic values. Iberian margin piston cores taken in the Atlantic Ocean also yield colour cycles that can be linked to precession (Hodell et al., 2013). These authors explain the precession-induced changes in sediment redness and alcohol ratios by changes in wind-driven processes (e.g. dust transport, upwelling or precipitation). However, a logical alternative explanation would be that these cycles are related to fluvial terrigenous input, with enhanced clay input causing increased sediment redness when oxidized. More recent carbonate cycles in cores spanning the last 225-250 kyr, recovered in the Atlantic Ocean off Morocco, share many similarities with the cycles described above (Bozzano et al., 2002; Moreno et al., 2001). Carbonate minima in these sediments show a similar in-phase relation with precession minima, and have also been interpreted as dilution cycles. These authors, like Hodell et al. (2013), attribute the carbonate dilution to an eolian rather than a fluvial source, due to the site location which is relatively far (200 km) from the Moroccan margin but in the pathway of present-day Saharan dust plumes. However, as stated by Van der Laan et al. (2012), the luminescence ages (von Suchodoletz et al., 2008; 2010) do not exclude an alternative interpretation with wetter periods corresponding to precession minima and yielding a

perfect fit with the much better dated last wet phase on Lanzarote between 15 and 8.5 kyr (e.g. Damnati et al., 1996; see von Suchodoletz et al., 2010). This phase, centered around the last precession minimum at 11-12 kyr, is consistent with our interpretation of carbonate minima being related to carbonate dilution caused by enhanced river runoff. When considering all these sections and sites, this kind of cyclicity is clearly not restricted to the Messinian Guadalquivir Basin, but found throughout the entire recent geological history and in at least the entire Mediterranean and the neighbouring Atlantic region.

2.6.2.2 Upper interval (178-60 mcd; 5.53-5.33 Ma)

The Principal Component Analyses show an up core change from biogenic carbonate versus clay cycles (PC1L) to cycles of biogenic carbonate and clay versus silt (PC1U, Fig. 2.5). On top of that, the records show an increase in sedimentation rate at around 180 mcd that is demonstrated by a clear increase in the thickness of the precession cycles, followed by a gradual increase in PC1U from 175 mcd to the top, reflecting a coarsening-upward sedimentary sequence (Fig. 2.2). Lastly, this interval coincides with an observed decrease in paleodepth from 400 to 100 meter (Pérez-Asensio et al., 2012b). All these features are consistent with a gradual east-west infilling of the Guadalquivir Basin in the Late Miocene (Iribarren et al., 2009; Sierro et al., 1996). The change in lithology and sedimentation rate at 180 mcd may reflect the transition from a more distal, deeper water environment to a shallower, more proximal one, probably associated with prodelta progradation and rapid infilling of the basin.

In this upper interval sedimentary cycles also seem to be driven by regular alternations in the rate of terrigenous supply to the basin. However, because of the proximity to the coast, the grain size of detrital particles is dominated here by silts in contrast to the clay rich deposits that characterize the lower part. In consequence, phases of higher input of silt material from the shelf dilutes the biogenic carbonate and clay, while a decrease of this coarser grained detrital supply would lead to a relative increase of the biogenic carbonate and clay component. This suggests that the relationship between local climate and detrital input is strongly affected by the distance to the coast. Distal marine settings can only be reached by the clay fraction that is transported in suspension far away from the coast, whereas coarser particles, such as silts or sands, remain on the shelf, and dominate the detrital input in more proximal settings.

Throughout the entire record detrital supply dilutes biogenic carbonate. However, the phase relationship between carbonate-rich beds and insolation changes from the lower to the upper part. This can be explained by changes in erosion rates. Summer insolation minima cause a colder and more arid climate. This may have a negative effect on the vegetation cover of the Guadalquivir Basin. Land with a permanent vegetation cover is characterized by soil losses which are generally more than an order of magnitude lower than those on arable land (Cerdan et al., 2010). Therefore loss in vegetation cover would

result in more erosion of the land during insolation minima. This would lead to an increased input of coarser-grained material to the shelf through increased sediment concentration in the river discharge at times of insolation minima due to more intense erosion of non-vegetated landscapes. Subsequently the core's environment at the outer shelf is reached by these sediments through storms and thereby diluting the biogenic carbonate and the clay during insolation minima, also explaining the concurrent increase in cycle thickness. Meanwhile, river discharge is higher at times of insolation maxima when a wetter climate and a more vegetated landscape prevailed in Southern Spain, however the sediment concentration, and therefore sediment input, was lower and consisted mainly of clays.

A similar mechanism is proposed to explain the cyclic depositional changes in the Plio-Quarternary continental deposits of the Guadix Basin (Pla-Pueyo et al., 2015). These authors explain cyclical changes between alluvial and fluvial deposits to changes in vegetation cover and subsequent erosion. Also, similar climatic dependencies on erosion and alluvial fan progradation have been observed in Nevada and California, USA (Harvey et al., 1999). So far this mechanism has only been attributed to cycles found in continental deposits, but since the setting of the Montemayor core is proximal for the upper interval, we propose that this mechanism can result in similar cyclicity in shallow marine deposits.

Two other models that cannot currently be ruled out can also explain the observed cyclicity. First, it may be the result of enhanced input of detrital, fine-grained carbonate to the basin during insolation maxima adding to the biogenic carbonate component. However since we observe an increase in the number of coccoliths and foraminifera in our samples during insolation maxima, implying that the carbonate is mainly of biogenic origin, this model is unlikely. Another alternative model is based on changes in bottom current strength. Stronger currents during insolation minima would cause winnowing of the fine-grained, lighter, non-cohesive particles, leaving an enriched layer of coarser grained particles and heavier minerals (McCave and Hall, 2006). The most likely candidate for changes in current strength on precessional timescales in concordance with the phase relation described here is MOW (Kaboth et al., 2015; Lofi et al., 2015). However, as we will conclude in section 6.3, we don't observe any direct influence of MOW on this part of the Montemayor-1 core; therefore also this model is unlikely.

The infilling of the Guadalquivir Basin, and consequently the change in cycle nature, is also supported by fluctuations in benthic foraminifera abundances in combination with the geochemical and oxygen isotope records. In the lower part of the record the coastline is still distant and input of fluvial-derived nutrients and terrestrial organic matter is relatively low, resulting in mesotrophic conditions in which *Uvigerina peregrina s.l.* thrives (Fig. 2.9; Pérez-Asensio et al., 2012b; 2014 and references therein).

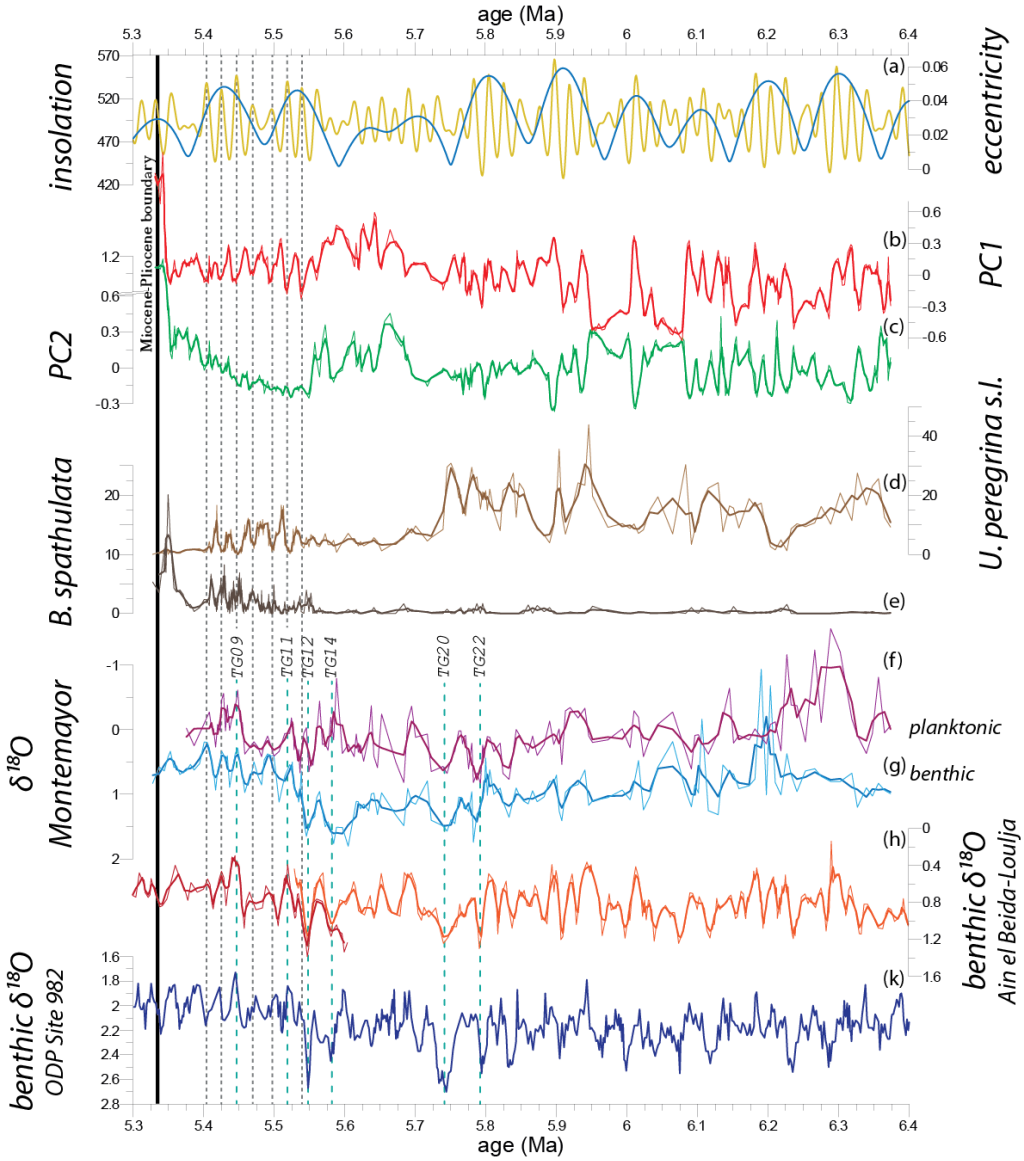

Figure 2.9: *(a) insolation (yellow) and eccentricity curve (blue), (b) PC1, (c) PC2, (d) relative abundance (%) of Uvigerina peregrina s.l., (e) relative abundance (%) of Brizalina spathulata, (f) planktonic and (g) benthic δ¹⁸O record, (h) benthic δ¹⁸O of Ain el Beida (Krijgsman et al., 2004; red) and Loulja (Van der Laan et al., 2006; orange) and (k) the benthic δ¹⁸O record of ODP Leg 982 (Hodell et al., 2001). For all records, except δ¹⁸O of ODP Leg 982, both the original data (thin) and a three point average (thick) are shown. All the records of the Montemayor-1 core are (re-)dated using the cyclostratigraphic age model from this paper. Correlations for the upper part (small dash) are shown, see text for further explanation. Glacial stages (wide dash) and Miocene-Pliocene boundary are put in for reference.*

As the depositional environment of the sediments of the Montemayor-1 core becomes more proximal, *U. peregrina s.l.* decreases in abundance and *Brizalina spathulata* increases along with *Bulimina aculeata* (Pérez-Asensio et al., 2014). These species are eutrophic, associated with conditions of high degraded organic matter input and low oxygen (Pérez-Asensio et al., 2012b; 2014 and references therein).

In the upper interval of the record we find a clear relationship between insolation, PC1, benthic foraminifera and the oxygen isotopes (dashed lines in Fig. 2.9). Precession minima are in phase with minima in PC1, relatively low abundances of *U. peregrina s.l.,* high abundances of *B. spathulata*, and light $\delta^{18}O$ values. The main factor driving these phase relationships is arguably changes in sea floor oxygen concentration, due to grain size fluctuations in the sediment input, forced by precession. During insolation minima (precession maxima) decreased vegetation cover leads to relatively high input of coarser-grained sediment. This results in higher porosity and therefore better oxygenated sediments at the seafloor, leading to lower abundance of eutrophic species like *B. spathulata* and higher abundances of *U. peregrina s.l.*, which is living less deep in the sediment and is more dependent on oxygen supply. At the same time, as Pérez-Asensio et al. (2014) argues, stronger winds may cause upwelling which could also result in an increase in fresh organic matter and also therefore higher abundances of *U. peregrina s.l.* Warm/wet periods during precession minima, on the other hand, will trigger enhanced input of clay (PC1U), leading to lower sediment porosities and therefore oxygen depleted conditions, resulting in higher abundances of *B. spathulata*. We therefore suggest that, in the upper interval where the depositional environment is more proximal, fluctuations in the benthic foraminifera assemblages are largely regulated by precession-related changes in oxygen input through sediment supply instead of glacio-eustatic fluctuations as stated by Pérez-Asensio et al. (2014).

2.6.3 Reinterpretation of stable isotope records

2.6.3.1 Stable isotope chronostratigraphy

The new high-resolution chronology allows a very precise correlation of the isotope records of the Montemayor-1 core with other astronomically-tuned isotope records. We focus particularly on comparison with the oxygen isotope records from Ain el Beida (Krijgsman et al., 2004), Loulja (Van der Laan et al., 2006) and Site 982 of ODP Leg 162 (Hodell et al., 2001; Fig. 2.9 & 2.10). In general, the benthic $\delta^{18}O$ record of the Montemayor-1 core shows increasingly heavier values up core, culminating in the glacial period of 5.9-5.5 Ma (Fig. 2.9). The same trend is also found in the planktonic $\delta^{18}O$ record, but is interrupted by a decrease at 5.75 Ma, after TG20. However, this increasing trend is not seen in the benthic $\delta^{18}O$ record from ODP Site 982 or Ain el Beida (Fig. 2.9). The sudden decrease towards lighter values at 5.53 Ma in the benthic $\delta^{18}O$ record of the

Montemayor-1 core coincides well with the deglaciation towards TG11 and finally TG9. This shift is greater than for the benthic $\delta^{18}O$ record of Ain el Beida and the open ocean benthic $\delta^{18}O$ record of ODP Site 982 (Fig. 2.10), which can be explained by a concurrent decrease in paleodepth (Pérez-Asensio et al., 2012b), generating a shallower and therefore warmer environment. The decrease in paleodepth is confirmed by a decrease in the offset between the planktonic and benthic $\delta^{18}O$ values. In the lower interval this offset is more than 1‰, but declines up core to values less than 0.5‰ (Fig. 2.9), corresponding to a decrease in temperature difference between bottom and surface waters of 2-3°C. (Shackleton, 1974). Assuming a stabilized vertical temperature gradient, this could correspond to a decrease in paleodepth from 400 to 100 meters (Criado-Aldeanueva et al., 2006), which is in agreement with the Montemayor-1 paleodepth curve of Pérez-Asensio et al. (2012b).

2.6.3.2 Water masses

The benthic and planktonic $\delta^{18}O$ records of the Montemayor-1 core follow very similar patterns and they are in phase with each other (Fig. 2.9). Similar parallel behaviour is also observed in Ain el Beida (Van der Laan et al., 2005) suggesting the presence of the same water mass throughout the water column on both the Moroccan and Iberian margins. Since this water mass follows the global ocean trend, represented by ODP Site 982 (Fig. 2.10), we agree with Pérez-Asensio et al. (2012a) that this water mass is likely to have been of Atlantic origin. The similar behaviour between the benthic and planktonic $\delta^{18}O$ records both in Morocco and Spain in combination with a relatively shallow paleodepth of a few hundred meters for both sites suggests the presence of NACW, similar to that existing today on both margins. However, this does not rule out the possibility that MOW was flowing further offshore during this time period.

Oxygen isotope data recently recorded at ODP Site U1387 (van der Schee, in prep), probably located at greater depth than the Guadalquivir Basin during the Messinian, has heavier benthic oxygen isotope values than those recorded in the Montemayor-1 core. This could be caused by colder water masses and/or advection of Mediterranean sourced heavy $\delta^{18}O$ water at this site. Colder temperatures suggest a vertical temperature gradient in the water column in the vicinity of the Atlantic-Mediterranean gateways during the Messinian, which might imply absence of MOW. In today's Gulf of Cádiz, due to the nearly constant temperature of MOW, there is currently no vertical temperature gradient at the 500-1500 m depth interval (Criado-Aldeanueva et al., 2006). The presence of a vertical temperature gradient, as has been argued here based on the difference in $\delta^{18}O$ between ODP Site U1387 and the Montemayor-1 core, may imply that MOW was absent in the uppermost Messinian. Other oxygen isotope records at intermediate depths in the northeast Atlantic margins close to the Messinian gateways are needed to reconstruct the vertical temperature and oxygen isotope gradients in the Guadalquivir Basin and Gulf of Cádiz, and address the evolution of MOW in this region.

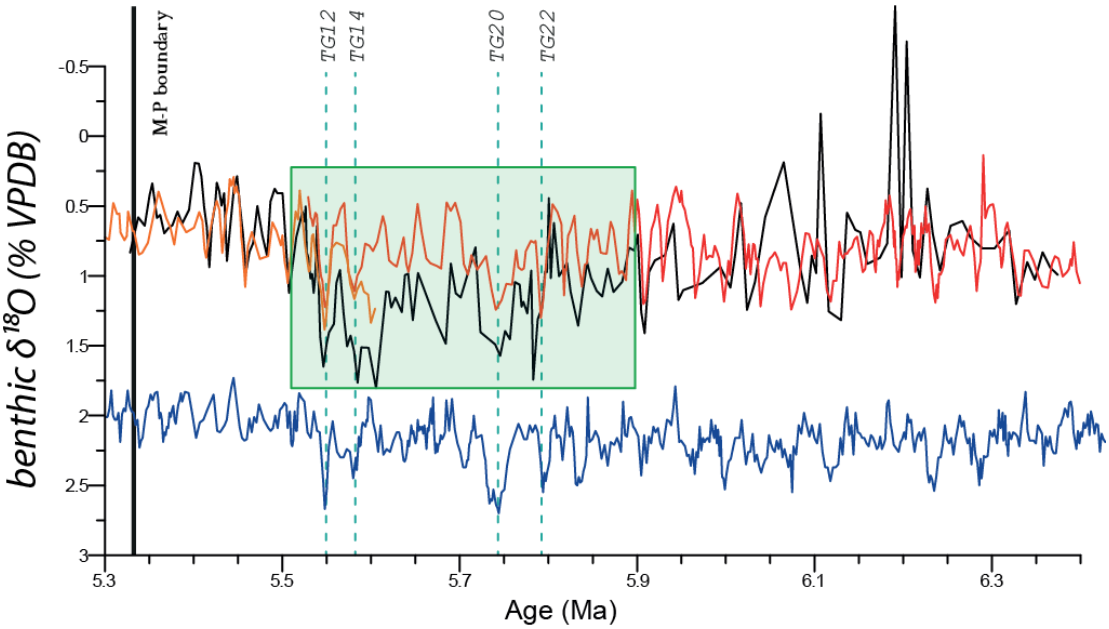

Figure 2.10: *Direct comparison between benthic δ¹⁸O records of the Montemayor-1 core (black), Ain el Beida (Krijgsman et al., 2004; red), Loulja (Van der Laan et al., 2006; orange) and ODP Leg 982 (Hodell et al., 2001; blue). Green box indicates period of deviation between Montemayor and Ain el Beida/Loulja oxygen isotope values, see section 6.3.2. Glacial stages (wide dash) and Miocene-Pliocene boundary are put in for reference.*

Due to the difference in trend in the benthic δ¹⁸O records of the Montemayor-1 core and Ain el Beida, stated in section 6.3.1, the benthic δ¹⁸O record of the Montemayor-1 core yields different mean values from Ain el Beida and Loulja between 5.9-5.5 Ma (green box in Fig. 2.10), which coincides with the latest Messinian glacial period (Hodell et al., 2001) and the first stages of the MSC (Roveri et al., 2014). During this time period the benthic δ¹⁸O values of the Montemayor-1 core are higher than at Loulja or Ain el Beida, approaching the North Atlantic values of ODP Site 982, especially during the most prominent glacial cycles TG12, TG14, TG20 and TG22 (Fig. 2.10). This might be the result of a decrease in or cessation of MOW so that cold North Atlantic Intermediate Water could penetrate shallower water depths resulting in a colder and therefore heavier δ¹⁸O signal. This is congruent with the deposition of the lower evaporites and halite in the Mediterranean Basin during this period, indicating at least a very restricted connection between the Atlantic and the Mediterranean with negligible outflow. Were this to be the case however, it is surprising that Ain el Beida does not show the same increase in δ¹⁸O values. An explanation might be that Ain el Beida was located at a slightly shallower depth, or experienced a concurrent shallowing, resulting in the influence of warmer, shallower water.

An alternative explanation could be that the influence of heavier oxygen isotope water flowing out of the saline Mediterranean results in heavier $\delta^{18}O$ values in the Guadalquivir Basin between 5.9 and 5.5 Ma. The increasing trend in the benthic $\delta^{18}O$ record may be caused by the advection of increasingly more saline MOW, counteracting the effect of the presumed reduction in outflow as a result of the very restricted connection during these first stages of the MSC. The northward bending of the MOW after exiting the Mediterranean due to Coriolis forcing should explain its greater influence along the Spanish margin relative to Morocco. However, during deposition of halite in the Mediterranean, a complete cessation of MOW at 5.60-5.55 Ma is required (Meijer, 2006) while we observe a maximum in oxygen isotope values. Another alternative could be upwelling in the Guadalquivir Basin, bringing deeper, colder waters to the surface during this time period. To be consistent with the lighter oxygen isotope values found at Ain el Beida, this process would have affected Morocco to a smaller degree. However, as indicated by low values of *U. peregrina* (Fig. 2.9), upwelling influence seems to be very low in this part of the Montemayor-1 record (Pérez-Asensio et al., 2014).

For our record in general we can conclude that the sediments of the Montemayor-1 core were not directly influenced by MOW, probably due to its relatively shallow paleodepth, based on the paleodepth curve of Pérez-Asensio et al. (2012b), which infers a maximum paleodepth of 450 meters. However, we cannot rule out presence of MOW at greater depths, and the indirect influence of MOW on the Montemayor-1 core mixing with the overlying NACW. This conclusion is in agreement with Pérez-Asensio et al. (2012a) who, based on various lines of evidence, concluded that the sediments of the Montemayor-1 core were only affected by MOW prior to 6.18 Ma. In particular, these authors point out the offset between, and different behaviour of the planktonic and benthic $\delta^{18}O$ records before 6.18 Ma, which they relate to the influence of Mediterranean derived waters at the bottom of the water column. In our record the interval before 6.18 Ma is too short (190 kyr), and the oxygen isotope data points too scarce (20 data points), to come to a conclusive statement as to whether MOW was present or not in this part of the record. A later date for MOW cessation, however, is not incompatible with our data, and would be supported by one of the interpretations of the deviation in benthic isotope record values of the Montemayor-1 core for the 5.9-5.5 Ma period.

Unfortunately the resolution of the Montemayor-1 stable isotope records in the lower interval is too low to draw any firm conclusions about the origin of any higher order fluctuations of these records. For example, one of the arguments Pérez-Asensio et al. (2012a) uses for MOW cessation at 6.18 Ma is the benthic oxygen isotope excursion in the Montemayor-1 core at this time (Fig. 2.9). However, a similar decrease in the benthic $\delta^{18}O$ is seen in the high resolution benthic oxygen isotope record of Ain el Beida (Fig. 2.9) and in this case is clearly linked to the high amplitude precession minima at times of eccentricity maxima (Krijgsman et al., 2004). Various pronounced minima and lower

mean values in the $\delta^{18}O$ are recorded at times of high amplitude insolation maxima during the two eccentricity maxima centered around 6.3 and 6.2 Ma (Fig. 2.9). The 100 kyr eccentricity maxima around 6.2 may therefore also have caused the concurrent abrupt decrease in the benthic oxygen isotope values of the Montemayor-1 core at 6.22 Ma, rather than the cessation of MOW. A high resolution study for the Montemayor-1 core, together with high resolution oxygen isotope records from other parts of the Guadalquivir Basin, are required to test different interpretations and evaluate better the evolution of Messinian MOW.

2.7 Conclusions

A new high-resolution chronostratigraphic age model for the Guadalquivir Basin at the Atlantic end of the Betic Corridor has been constructed by tuning cyclic changes in elemental composition of sediments from the Montemayor-1 core to insolation using magneto- and biostratigraphic tie points. This age model spans the late Messinian (6.37-5.33 Ma) and permits comparison of previously published records of stable isotopes and benthic foraminifera with global and regional equivalents. We recognize a gradual change in the nature of the typical fluctuations in geochemical composition of the sediments through the core, which is associated with a gradual change in depositional environment as the basin infilled. The lower part of the core yields alternations of biogenic carbonate layers with beds of terrigenous clay material. The terrigenous material dilutes the biogenic carbonate during periods of increased river runoff induced by maxima in Northern Hemisphere summer insolation. In the upper interval of the record, the nature of the cycles changes probably as a result of more proximal setting. In this shallow marine environment, sedimentation is dominated by coarser grained terrestrial input. Due to increased erosion rates caused by a loss in vegetation cover during insolation minima, enhanced input of silty detrital sediments dilutes the biogenic carbonate and the clay.

Based on the new age model, the benthic oxygen isotope records correlate well with the previously published records of Ain el Beida, Loulja and ODP Site 982. Glacial stages TG12, TG14, TG20 and TG22 as well as the deglaciation towards TG11 and finally TG9 are clearly expressed. Similar behaviour in the planktonic and benthic oxygen isotope records for Ain el Beida, Loulja and the Montemayor-1 core, together with general trends reflecting open ocean signals, suggest the presence of NACW and no direct influence of MOW on the sediments of the Montemayor-1 record. We recognize an offset between the benthic oxygen isotope records of the Montemayor-1 core and Ain el Beida for the last Messinian glacial period (5.9-5.5 Ma), concurrent with the first stages of the MSC. This might be the result of the decrease/cessation of the MOW in the Gibraltar Strait region, but could also be explained by the presence of more saline MOW or upwelling. Additional high-resolution records from the Atlantic margins near the

Gibraltar Strait are needed to reconstruct fully the role and evolution of MOW during the Messinian Salinity Crisis.

Acknowledgements

Jose Noel Pérez-Asensio is thanked for providing the stable isotope and benthic foraminifera data sets. All fellow Medgate ESR's, ER and supervisors are thanked for their valuable suggestions and discussions. Francisco Jimenez-Espejo, Tanja Kouwenhoven and two anonymous reviewers are thanked for their critical comments, which greatly improved the manuscript. The research leading to these results has received funding from the People Programme (Marie Curie Actions) of the European Union's Seventh Framework Programme FP7/2007-2013/ under REA Grant Agreement No. 290201 MEDGATE, and from the Guadaltyc project (MINECO, CGL2012-30875). Funding from JCYL project SA263U14 is also acknowledged.

CHAPTER 3

Imprint of Messinian Salinity Crisis events on the Spanish Atlantic margin

van den Berg, Bas C.J.[1,*], Sierro, Francisco J.[1], Hilgen, Frederik J.[2], Flecker, Rachel[3], Larrasoaña, Juan C.[4], Krijgsman, Wout[5], Flores, Jose A.[1], Mata, Maria P.[6]

[1]*Departamento de Geologia, Facultad de Ciencias, Universidad de Salamanca, 37008 Salamanca, Spain*
[2]*Stratigraphy/Palaeontology, Faculty of Geosciences, Utrecht University, Budapestlaan 4, 3584 CD Utrecht, the Netherlands*
[3]*School of Geographical Sciences and Cabot Institute, University of Bristol, Bristol BS8 1SS, UK*
[4]*Instituto Geológico y Minero de España, Unidad Zaragoza, Zaragoza, Spain*
[5]*Paleomagnetic laboratory "Fort Hoofddijk", Budapestlaan 17, 3584 CD Utrecht, the Netherlands*
[6]*Instituto Geológico y Minero de España, Rios Rosas 23, Madrid, Spain*

Abstract

One of the outstanding research questions regarding the Mediterranean's Messinian Salinity Crisis is whether mechanisms that generated Messinian events also have an expression outside the basin as a result of changes in ocean circulation, tectonics or isostasy. To assess this, a high resolution astronomically calibrated age model for the entire Messinian of the Guadalquivir Basin, on the Atlantic margin of Spain, has been constructed. Cyclic changes in the elemental composition of the Huelva-1 borehole, visualized through XRF, were tuned to astronomical target curves. In some intervals, the tuning was hampered as a consequence of the borehole's proximity to the basin margin, resulting in disturbances of the cyclic record; nevertheless three distinct correlations with Mediterranean events were observed. Firstly, the onset of cyclicity within the borehole at 7.16 Ma is synchronous with the first sign of Mediterranean-Atlantic gateway restriction; this may be related to the closure of the Betic Corridor. Secondly, the increase in sedimentation rate starting around 5.55 Ma coincides with the end acme of the Messinian Salinity Crisis (MSC). Lastly, and for the first time, a lithological expression has been found outside the Mediterranean which may have been generated by the same mechanism that terminated the Messinian Salinity Crisis. This level corresponds with the onset of a pronounced and extensive glauconite layer, indicating a sudden and significant decrease in sedimentation rates. Two causative mechanisms, or a combination of them, are proposed for the interbasinal correlations during the MSC. The first is based on tectonic events in the Betic region that influence sedimentation within the Guadalquivir Basin while altering the Atlantic-Mediterranean connection. The second explains the increase in sedimentation rate at 5.55 Ma as a consequence of local basin infill and the condensation at 5.33 Ma by sediment winnowing as a result of increased current strength with the opening, or deepening, of the Gibraltar Strait.

This chapter has been submitted to Newsletters on Stratigraphy

3.1 Introduction

3.1.1 Messinian gateway restrictions

The Messinian stage (7.246-5.332 Ma; Gradstein et al., 2012; Mayer-Eymar, 1868) is one of the most intriguing time periods in the geological history of the Mediterranean Basin. During the Messinian the connection to the Atlantic Ocean became progressively restricted, culminating into the Messinian Salinity Crisis (MSC;; chapter 1; Krijgsman et al., 1999; Roveri et al., 2014). During this dramatic event, life nearly ceased to exist in the Mediterranean waters, vast quantities of evaporites were deposited across the entire Mediterranean Basin, and the Mediterranean Sea experienced a sea level drop of at least a few hundred meters. The onset of this event, i.e. restriction of the Mediterranean-Atlantic gateways and decreased water exchange, commenced more than 1 Myr before the MSC, directly after the Tortonian-Messinian boundary (Kouwenhoven et al., 2003; Kouwenhoven and van der Zwaan, 2006). The effect of different degrees of Messinian gateway restriction has been investigated inside the Mediterranean Basin, by studying the sedimentary deposits, reconstructing their paleoenvironment and relating them to changes in Mediterranean-Atlantic exchange (Chapter 1; Meijer and Krijgsman, 2005; Roveri et al., 2014; Simon and Meijer, 2015). However, the precise evolution of these gateways remains debated. One method of investigating these outstanding controversies is to investigate the imprint of gateway evolution on the Atlantic side of the connecting corridors.

The effects of gateway restriction on the Atlantic Ocean were more muted than in the Mediterranean, making these types of studies at the Atlantic end of the corridor less straight forward. However, whatever the driving mechanism for gateway change, be that tectonics, isostasy or changes in ocean circulation and composition, it should also impact the Atlantic side of the gateway. For example, Eurasian–African oblique NW–SE relative plate convergence, ongoing from the Cretaceous to present, was the main driver for Atlantic-Mediterranean gateway narrowing and the formation of the Betic-Rif Orogen (Dewey et al., 1989; Rosenbaum et al., 2002; Sanz de Galdeano and Alfaro, 2004). In addition, within the Alboran domain subcrustal tectonics such as slab roll back, asthenospheric upwelling, and delamination of the lithospheric mantle have probably played an important role since the late Tortonian (Comas et al., 1999; Duggen et al., 2003; Lonergan and White, 1997; Platt et al., 2003). Govers (2009) showed that a major Mediterranean sea level lowering during the MSC acme could induce gateway closure and sizable regional uplift in the marginal Gibraltar region as a result of isostatic feedback to basin unloading. Lastly, gateway evolution can have a significant effect on ocean composition and circulation and therefore on sedimentary environments. A model study showed that, in- and outflow patterns in the Betic and Rifian corridors were substantially determined by gateway geometries and bathymetries during the pre-MSC (de la Vara et al., 2015). Furthermore, changes in Mediterranean Outflow Water (MOW)

have not only a significant effect on detrital deposits in the nearby Gulf of Cadiz (Hernández-Molina et al., 2014), but also, on a larger scale, contributes to North Atlantic circulation (McCartney and Mauritzen, 2001; Reid, 1979).

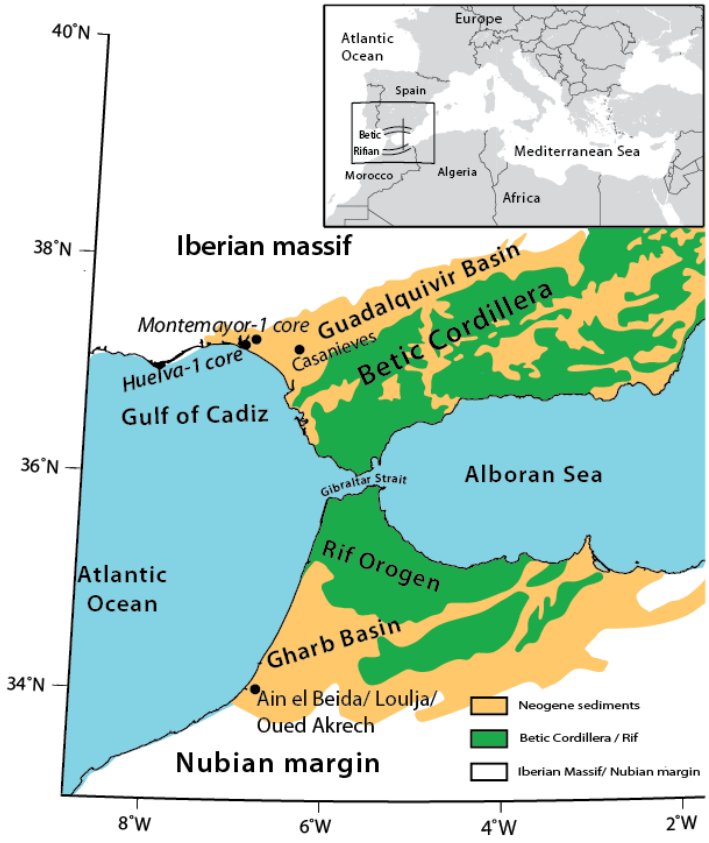

Figure 3.1. *Schematic geological map of the Gibraltar Strait region with the Neogene basins and the Betic and Rif Orogen. The location of the Huelva-1 core, Montemayor-1 core, as well as the Casanieves well and key Moroccan sections are shown. The overview map in the upper right corner shows the locations of the Betic and Rifian corridors.*

However, expressions of gateway restriction on the Atlantic side of the gateways have only rarely been observed. To study these kind of expressions and influence of climate and/or the Atlantic ocean on the MSC, Messinian sections on the Moroccan Atlantic margin, at the western end of the Rifian Corridor, have been astronomically tuned and studied (Hilgen et al., 2000; Krijgsman et al., 2004; Van der Laan et al., 2005; 2012; 2006). In the Ain el Beida section, a prominent planktonic carbon isotope excursion is

associated with the closure of the Rifian Corridor at 6.0 Ma, just before the onset of evaporite deposition in the Mediterranean Basin (Van der Laan et al., 2012). A marked Ti/Al maximum (Van der Laan et al., 2012) and a corresponding peak in sedimentation rate (Van der Laan et al., 2005) in the same section coincide with the onset of the MSC, but their relation is poorly understood. In the northern Atlantic, ODP site 982 provides a valuable template to record the evolution of the open ocean during the Messinian (Hodell et al., 2001). This study showed that peak glacials TG12 and TG14 occur within the Messinian acme (5.6-5.55 Ma). Moreover, there are prominent lows in gamma ray bulk density and several weight percent $CaCO_3$ minima at this site that correspond with the onset and first phase of the MSC, which could be related to a shoaling of the lysocline in response to rapid extraction of calcium carbonates and sulphates during the MSC (Hodell et al., 2001). However, expressions of other Messinian events and/or the Zanclean flooding at the Miocene-Pliocene boundary are not observed outside the Mediterranean Basin. The reason for this could be the scarcity of Messinian records in the Gibraltar region, particularly on the Spanish margin where outcrop is minimal. It is therefore essential to obtain a complete stratigraphic record with a high resolution age model that covers the late Tortonian to early Pliocene from the Spanish Atlantic margin.

3.1.2 The Montemayor-1 and Huelva-1 boreholes

The western part of the Guadalquivir Basin was the westernmost part of the Betic Corridor and is located relatively close to Gibraltar. The Montemayor-1 borehole has been drilled in this part of the basin (Fig. 3.1) and several paleoenvironmental studies using pollen data, stable isotopes, environmental magnetism, benthic foraminifera and XRF data have been carried out (Jiménez-Moreno et al., 2013; Larrasoaña et al., 2014; Pérez-Asensio et al., 2013; Pérez-Asensio et al., 2012a; 2012b, 2014; van den Berg et al., 2015). These studies demonstrate important cooling events, astronomically induced climate change and continuous infilling of the basin from east to west. Sea level changes and an excursion in benthic oxygen isotope values are attributed to the onset of the of the MSC (Jiménez-Moreno et al., 2013; Pérez-Asensio et al., 2013) and to the closure of the Betic Corridor (Pérez-Asensio et al., 2012a), respectively. However, based on an improved, astronomically tuned age model, van den Berg et al. (2015) related these events to global climate instead of Mediterranean events. Changes in cyclicity and sedimentation rate were also observed, most notably a glauconite layer that correlated with the Miocene-Pliocene boundary (chapter 2), but the spatial scale of these changes and their causative relationship with regional or global events was not tested. Also, the tuned Montemayor-1 record covers only the late Messinian (6.37-5.33 Ma) so another record is required to evaluate the evolution of the Atlantic Margin during the early Messinian.

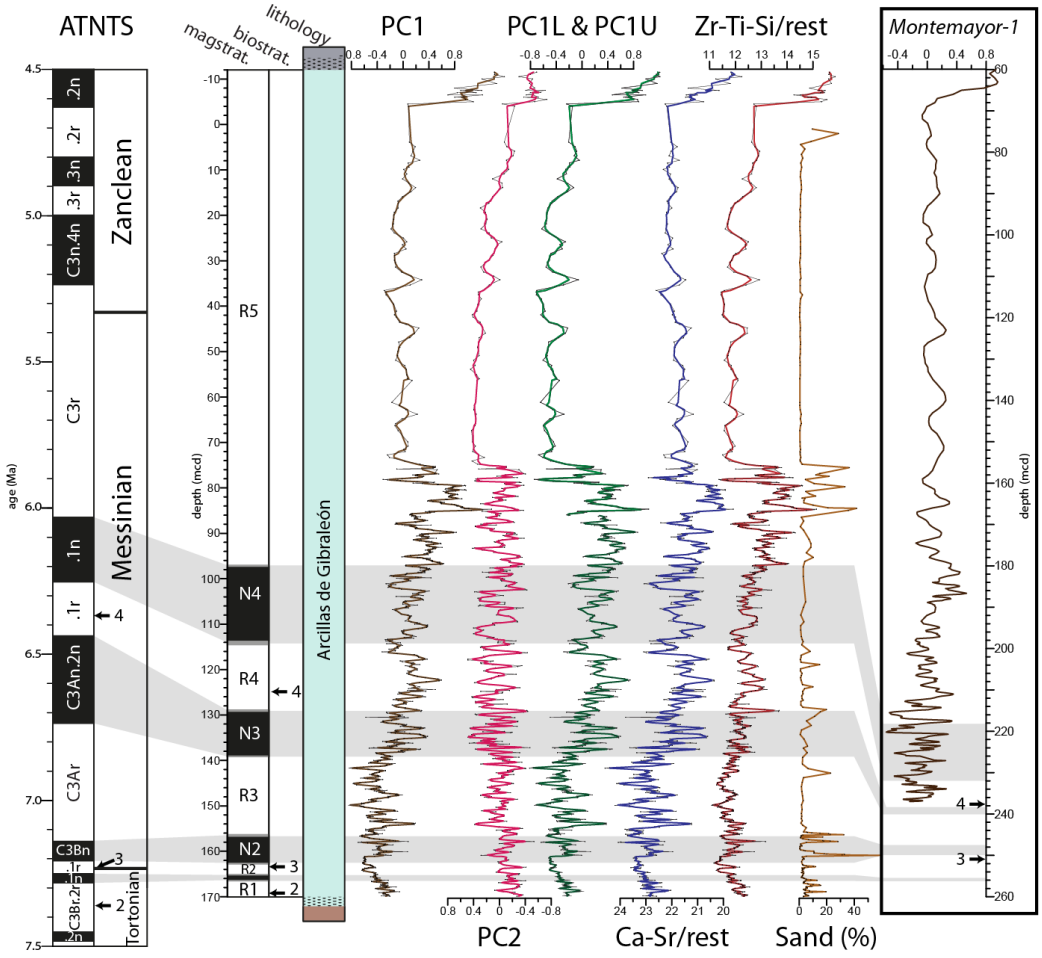

Figure 3.2. *Left: Tortonian-Zanclean magnetostratigraphic chrons and biostratigraphic events of the ATNTS (Lourens et al., 2004). Numbers denote planktonic foraminiferal events of Sierro et al. (1993). Middle: previously published magnetostratigraphic and biostratigraphic results for the Huelva-1 core (Larrasoaña et al., 2008) with their relation to the ATNTS. The lithology column shows from bottom to top the Niebla formation, Arcillas de Gibraleón formation, and Arenas de Huelva formation, respectively. The small black dots represent the glauconite layers at 170 mcd and 12 m. Right: PC1 and PC2, PC1L and PC1U Ca-Sr and Zr-Ti-Si data (black) with their three-point moving average (brown/pink/dark green/light green/blue/red), and sand fraction data (orange). Note the excellent agreement between the original data and the three-point moving average. In subsequent figures only the three-point moving average will be shown. Far right: PC1 data (dark brown) of the Montemayor-1 core (chapter 2) for comparison.*

Fortunately, the entire Messinian succession has been recovered in the Huelva-1 core, which is also located in the western Guadalquivir Basin, 12 km west of the Montemayor-1 core. The Huelva-1 core has been dated using bio- and magnetostratigraphy and is characterized by higher accumulation rates than the Montemayor-1 core throughout the

entire Messinian (Larrasoaña et al., 2008; 2014). Here, we aim to improve the previous magnetobiostratigraphic age model of the Huelva-1 core by tuning cyclic changes in sediment composition to astronomically induced changes in insolation with the aid of new biostratigraphic tie points and extend the high resolution chronostratigraphic framework for the Guadalquivir Basin down to the latest Tortonian. By constructing an astronomically tuned reference section for the Messinian Spanish Atlantic margin, we can assess the relevance of observed environmental changes in the region and their relationship with the Messinian Mediterranean and Atlantic Ocean.

3.2 Geological background and core setting

The Guadalquivir Basin formed in the Late Serravallian-Early Tortonian and evolved from a foredeep to a foreland basin of the Betic Cordillera during the Miocene. Loading of the imbricated Betic External units resulted in downward flexure of the Iberian basement and subsequent infilling (Berástegui et al., 1998; García-Castellanos et al., 2002; Ledesma, 2000; Sanz de Galdeano and Vera, 1992; Sierro et al., 1996). The basin is triangular, opens to the Atlantic Ocean at its western end, and is bounded by the Iberian massif to the north and the subbetic thrust belt of the Betic Cordillera to the south (Fig. 3.1). It has mainly experienced continuous sedimentation, gradually filling up from east to west, during middle-Late Miocene up to the present day (González-Delgado et al., 2004; Salvany et al., 2011; 1996; Sierro et al., 1990). After the closure of the Betic Corridor, the Guadalquivir Basin developed as an embayment open to the Atlantic, a configuration that persists today in the Gulf of Cádiz.

The Huelva-1 core was drilled in 1997, next to the bullring in the town of Huelva in the north-western part of the Guadalquivir Basin (37°15.914'N, 6°57.058'W; Fig. 3.1). The core recovered marine sediments that correspond to the two lowermost lithostratigraphic units of the basin infill (Fig. 3.2; Civis et al., 1987; González-Delgado et al., 2004; Sierro et al., 1996). The lower unit is the Niebla Formation and is Tortonian in age. It consists of a mix of calcareous and siliciclastic sediments deposited during the marine transgression over the Paleozoic-Mesozoic basement. The upper unit, which covers the largest part of the borehole, is the Arcillas de Gibraleón Formation. This formation is late Tortonian-Messinian in age and consists of homogeneous bluish-green clays with some interbedded silty beds and a glauconite layer at its base. This formation is the main focus of this study and continues in the cliff adjacent to the borehole's location. In this cliff, above the Arcillas de Gibraleón Formation, we find the Arenas de Huelva Formation, which consists of lower Pliocene sands. This formation also contains a pronounced glauconite layer at its base (~12 m; Larrasoaña et al., 2008; 2014; Sierro, 1985; 1996; 1990). In this article, locations or intervals within the core are denoted as meters core depth (mcd) while locations in the Huelva cliff are denoted in meters (m). Both are calculated with respect to ground level. As glauconite is typically found in high

concentrations during periods of very slow or negligible marine sedimentation (Kidwell, 1991; Loutit, 1988), both glauconite layers probably correspond to condensed intervals or hiatuses (Jiménez-Moreno et al., 2013; 1996; Sierro et al., 1990). In order to assess cyclicity, continuous sedimentation is required. Consequently we will focus on the Gibraleón Formation between the two glauconite layers (12 m – 170 mcd, Fig. 3.2), an interval which spans ca. 7.4-5 Ma (Larrasoaña et al., 2008; 2014) capturing the entire Messinian.

3.3 Methods

The rather homogeneous lithology that dominates the Huelva-1 borehole (Fig. 3.2) prevents the construction of a reliable cyclostratigraphic framework based on visually identifiable lithological cycles. Cyclic changes may, however, be apparent in the chemical composition of the sediments, as is the case for the Montemayor-1 core (chapter 2). To detect these changes, a total of 856 samples were measured using X-ray Fluorescence (XRF) with a NITON XL3t900 GOLDD analyser. Sample preparation, measurement characteristics and detection and treatment of outliers was carried out in exactly the same way as for the Montemayor-1 record (chapter 2). Since the clays forming the matrix throughout the entire studied section are in general homogenous (except for the very top and the 75-90 mcd interval), anomalies due to changes in the matrix are not anticipated. For an in-depth justification of this method, including an additional calibration using a conventional WD-XRF, the reader is referred to the method section of van den Berg et al. (2015). Note that the sediments of the Montemayor-1 core, on which this calibration is performed, originate from the same formation and region and are therefore very similar to the Huelva-1 core sediments.

A well-known problem with XRF measurements is that lighter elements emit a smaller signal when excited and their emission is therefore more prone to attenuation (Tjallingii et al., 2007). In order to account for the larger scattering of relatively light elements, i.e. aluminium and silicon, a three-point average of these measurements is used. Likewise, elements with very low concentrations (less than 100 ppm), in this case rubidium, are also subject to enhanced scattering and consequently a three-point average of this record has been used (Fig. 3.3). Since aluminium yields enhanced scattering, the common practice of aluminium normalization will not be applied here. Instead, as proposed by Davis and Sampson (2002) and Aitchison (1986), a centred log-ratio transformation was performed to make the dataset ‘open’ (i.e. remove all spurious correlations) and statistically robust. This includes dividing through the geometric mean, which is a type of normalization (Aitchison, 1986; Davis and Sampson, 2002), allowing direct comparison between the major oxides and trace elements. A centred log-ratio transformation also allows each of the elements to be used when performing a Principal Component Analysis (PCA). Note that when using any element as a common denominator to normalize the dataset, this element cannot be considered further when

performing PCA. Subsequently, a PCA was performed using the PAST version 3.01 software package (Hammer et al., 2001) to simplify and visualize the data matrix.

Also, a sand fraction record (>63 μm; Fig. 3.2) was obtained by weighing, washing, sieving and drying the samples, and weighing them again.

3.4. Results

3.4.1 Principal Component Analysis

The concentrations of all elements acquired by XRF and used in this study are presented in Figure 3.3. The PCA analysis yields two statistically significant components: the first principal component (PC1), describing 73% of the total variance, and the second principal component (PC2) describing 21% of the total variance (Fig. 3.2). The two negative loadings for PC1 are Ca and Sr, while the positive loadings comprise of Zr, Si, Ti, Fe, K and Al (in descending order). For PC2, the two most important negative components are Zr and Ca. The positive loadings consist of elements Fe, Rb, K, Al (Fig. 3.4). All elements that have a positive loading for PC1 are typical elements found in siliciclastic minerals. Ca and Sr are elements associated with biogenic carbonate and visual inspection suggests they are mainly related to foraminifera and coccoliths. The relationship between the loadings of PC2 seems to be aluminosilicates on the positive axis versus carbonate and (coarser grained) silicates on the negative axis.

3.4.2 Geochemical records in depth domain

PC1 shows regular alternations, gradually thickening upwards, with a sudden increase in thickness around 75 mcd (Fig. 3.2). Preceding this increase we observe an 11 meter interval of enhanced PC1 values, coinciding with increased sand content. The pattern is very similar to the observed patterns in all the individual element records (Fig. 3.3). In the 90-124 mcd and the 142-161 mcd intervals, distinct bundles of 3-5 alternations can be distinguished, each separated by a pronounced minimum. The amplitude of the alternations becomes smaller towards the top of the core, especially above 20 mcd. The sudden increase at the top of the record (above 5 m) corresponds to a change in lithology, from clays to sands, but also coincides with the change to samples taken from the Huelva cliff, which might be more weathered than those of the Huelva-1 core. PC2 shows similar regular alternations, however, between 50-75 mcd the alternations completely disappear.

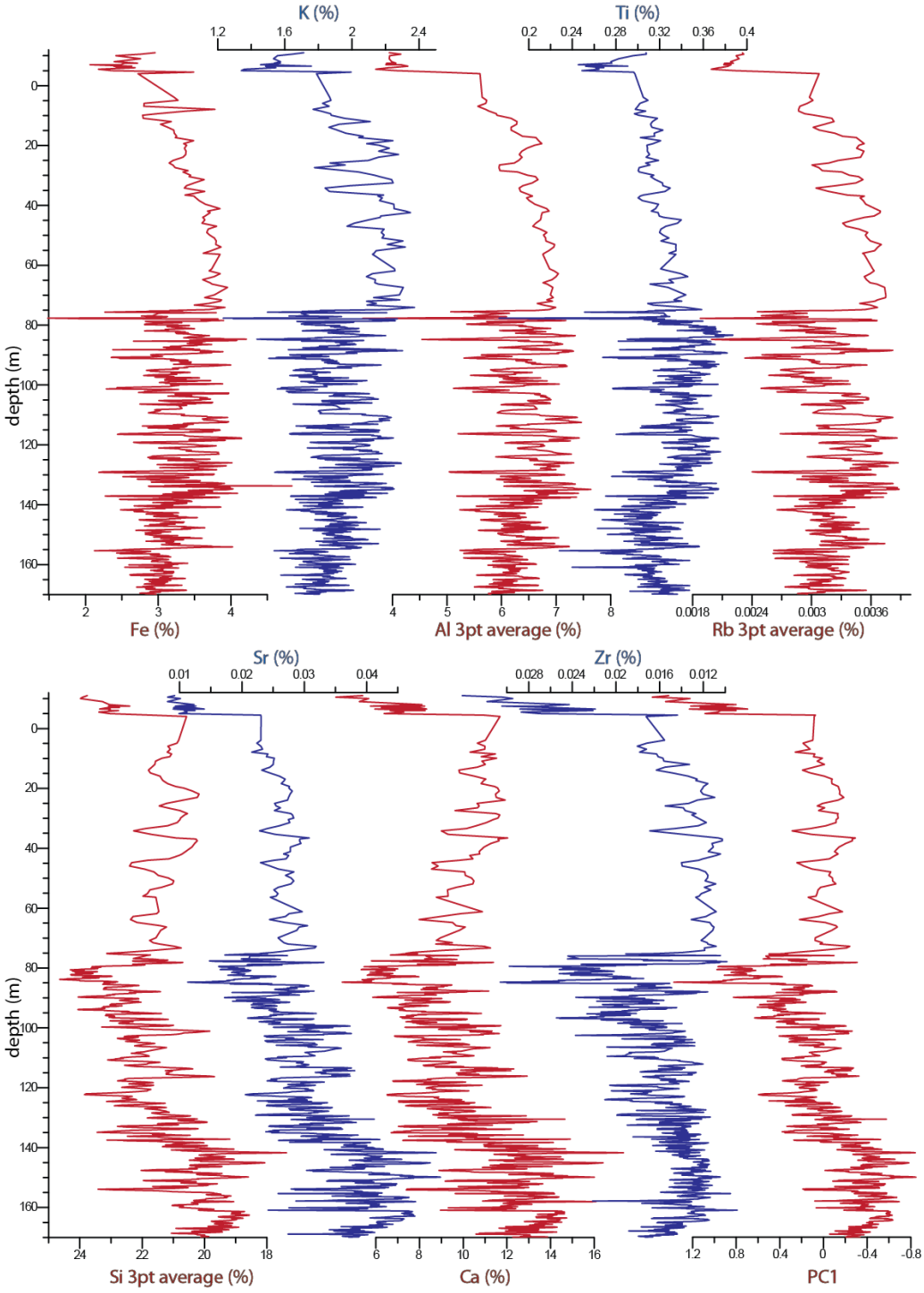

Figure 3.3. *Element concentrations in percentages for the individual elements used in this study.*

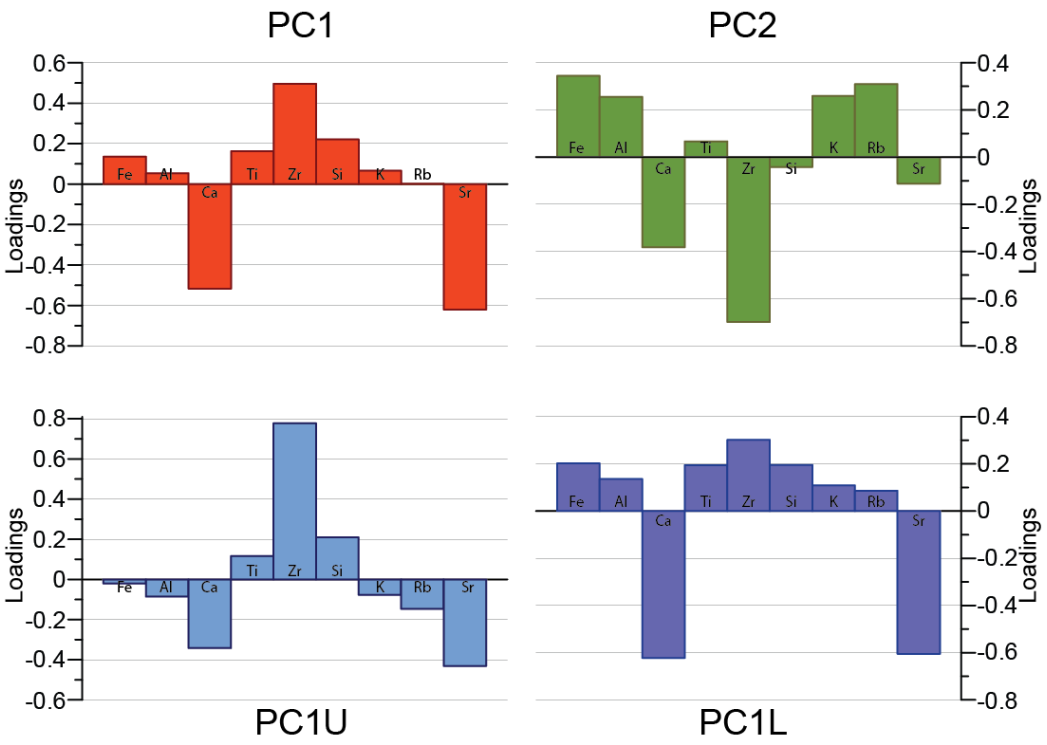

Figure 3.4. *Loadings of the Principal Components PC1 (top, left), PC2 (top, right), PC1U (bottom, left) and PC1L (bottom, right).*

In addition, to assess the nature of the regular alternations and changes therein, principal component analyses have been performed on both the lower (170 mcd-86 mcd) and the upper (86 mcd-12 m) part separately. The division is made at 86 mcd since we observe at this position the first distinct change in the PC1 pattern, accompanied by increased sand content (Fig. 3.2), followed by the observed increase in the thickness of regular alternations at 75 mcd. A change in sedimentary environment is expected at one or both of these stratigraphic positions. Both the lower and upper interval generate a first principal component that is identical to regular alternations shown in the PC1 of the entire core (Fig. 3.2). However, as was the result after applying the same technique on the Montemayor-1 core (chapter 2), the loadings, i.e. elements, comprising these alternations change from the lower to the upper interval (Fig. 3.4). The first principal component of the lower part (PC1L) shows similar loadings to PC1, with Ca and Sr being the most important elements on the negative side and the siliciclastic elements at the positive side. The first principal component for the upper part of the record (PC1U), however, consists of a very different combination of elements. Here the most important positive loading is Zr, followed by Si and Ti, representing the coarse-grained siliciclastic

fraction, while the negative side consists predominantly of Ca and Sr, representing biogenic carbonates, followed by Rb, Al and K, which are commonly associated with clay minerals (aluminosilicates).

When performing PCAs for even shorter intervals, the two sets of loadings described above, i.e. representing PC1L and PC1U, always comprise the first and second principal component for any given interval, only changing in the amount of total variance each represents. Therefore, we assume that the two most important processes controlling the sedimentary sequence in this core are represented by these two sets of loadings. The only problem is that these are not the same as PC1 and PC2. With PC1L and PC1U we can only evaluate these two processes for, respectively, the lower and the upper part of the record and not for the record as a whole (Fig. 3.2). To solve this problem and be able to evaluate these two processes throughout the entire record, we decided to go from PCA back to element ratios but now with the knowledge, acquired by PCA, on the most important processes. Using that information we constructed two records by manually assembling the two sets of loadings representing PC1L and PC1U (Fig. 3.2). 'Ca-Sr/rest' or 'Ca-Sr' was constructed by taking the logarithm of the product of normalized Ca and Sr values divided by the product of the normalized siliciclastic elements, which can therefore be interpreted as a measure of carbonate versus siliciclastic sediments. 'Zr-Ti-Si/rest' or 'Zr-Ti-Si' was constructed in a similar way by taking the logarithm of the product of normalized Zr, Ti and Si values divided by the product of the remaining normalized elements and can therefore be interpreted as a measure of coarser grained siliciclastic versus finer grained siliciclastic and carbonate sediments. As is evident from Fig. 3.2, the patterns of the corresponding intervals of the resulting records are very similar to the PC1L and PC1U records, subsequently. By following this approach no information is lost using these records and at the same time the involved sedimentary processes can now be studied over the entire length of the record. Besides, an element-ratio record leads to a more intuitive understanding as from these records the behaviour of any element is directly visible.

3.4.3 Additional biostratigraphic events

In order to build a higher resolution biostratigraphic framework than currently exists (Larrasoaña et al., 2008), all samples were scanned for keeled Globorotaliids, to identify the presence and changes in abundance of *Globorotalia margaritae* and *Globorotalia menardii* sin (Fig. 3.5) as these can provide key biostratigraphic tie points (Krijgsman et al., 2004; Sierro et al., 1993; chapter 2). *G. menardii* sin was only found in the interval between 70 and 80 mcd and shows two distinct peaks at 72 and 77 mcd. *G. margaritae* was found throughout the 25-110 mcd interval with the two most prominent peaks (>10%) at 85 and 87.3 mcd (Fig. 3.5).

3.5 Age model

3.5.1 New Biostratigraphic events

The abundance patterns in *G. menardii* sin and *G. margaritae* can be correlated with similar patterns in the Montemayor-1 core and in the Ain el Beida and Loulja sections in Morocco (chapter 2; Krijgsman et al., 2004; Van der Laan et al., 2006). There, changes in abundance of these two species have been correlated to specific astronomical cycles and/or time periods. Two influxes of *G. menardii* sin have been recorded in cycle 42 (5.55 Ma) and cycle 43 (5.53 Ma) of the Ain el Beida section, and to corresponding cycles in the bottom of the Loulja-A section. The two influxes found in the Montemayor-1 core have been assigned the same age as the influxes in the Moroccan sections; we have therefore correlated the two peaks observed in the Huelva-1 core to these same points on the astronomical cycle.

The abundance pattern of *G. margaritae* varies in detail between the Montemayor-1 core (chapter 2) and the Ain el Beida section (Krijgsman et al., 2004). However, at both localities the species does record an acme with two distinct peaks at glacial stages TG20 (5.75 Ma) and TG22 (5.79 Ma; Shackleton et al., 1995b; Van der Laan et al., 2012). Consequently, we correlate the two distinct peaks (>12%) that we observe in the Huelva-1 core with these two glacial stages (Fig. 3.5).

3.5.2 Cyclostratigraphic age model

The nearby located Montemayor-1 core (chapter 2) and the sonic data from the Casanieves well log (Ledesma, 2000) located more in the centre of the Guadalquivir Basin (Fig. 3.1), show that sedimentation in the basin was controlled by precessional related climate change during the Messinian and most of the Pliocene (Sierro et al., 2000). Furthermore, we have already observed bundling of 3-4 alternations in some intervals of the Huelva-1 records which is typical for precession cycles with superposed eccentricity amplitude modulation (section 4.2). We therefore assume that the cycles in the Huelva-1 record are also controlled by precession.

Since the sets of loadings for PC1U and PC1L (Fig. 3.4) are very similar to the loadings of the PC1U and PC1L of the Montemayor-1 core (Fig. 2.5), we assume that the phase relation with respect to the astronomical target curve and the nature of the geochemical cycles in the Huelva-1 core is also the same. This means that PC1L and the Ca-Sr record represent the juxtaposition of biogenic carbonate versus aluminosilicates, where the maximum carbonate concentration is correlated with insolation minima and maximum concentration in siliciclastics occurs during insolation maxima. In the same way, PC1U and Zr-Ti-Si in the Huelva-1 core and PC1U in Montemayor-1 (chapter 2) represent the juxtaposition of coarser grained siliciclastic sediments versus biogenic carbonate and clay with the peaks in coarser grained siliciclastics tuned to insolation minima and peaks in biogenic carbonate and clay correlated with insolation maxima.

3.5.2.1 Tuning of upper part (12 m - 90 mcd)

We tune our records to the La2004$_{(1,1)}$ solution (Laskar et al., 2004). When we compare the upper interval of the upper part (12 m-75 mcd) with the cycles of the upper part (70-176 mcd) of the Montemayor-1 record (chapter 2; Fig. 3.5), we find the influxes of *G. menardii* sin in the silt-rich bed of two adjacent cycles in both records. In between these two influxes both cores show an abrupt increase in cycle thickness. Above these influxes are 6.5 cycles followed by a decline in biogenic carbonate and an increase in coarser grained siliciclastics (Fig. 3.5) overlain by the glauconite layer that marks the end of the record. This pattern is exactly the same in the Montemayor-1 core. These identical patterns relative to the astronomical target curve suggest that the glauconite layers at the top of both records are synchronous and correlate with the Miocene-Pliocene boundary (Fig. 3.5).

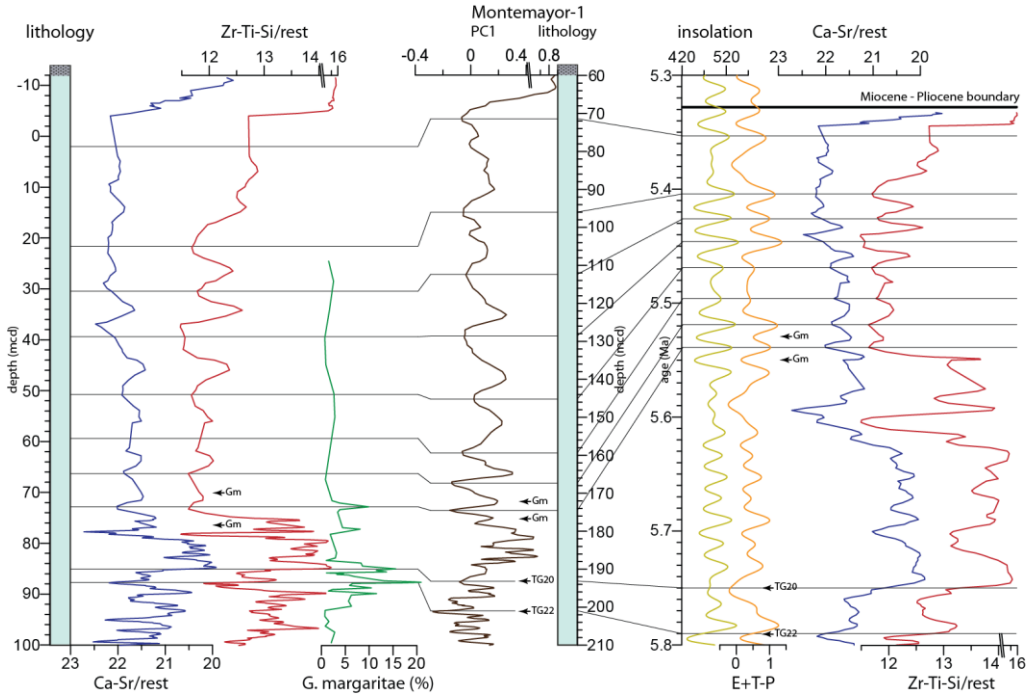

Figure 3.5. *lithology, Ca-Sr and Zr-Ti-Si (both their three-point moving average) and abundance of G. margaritae records in the depth domain (left) for the upper part of the Huelva-1 core (100 mcd -12 m), correlated to the lithology and PC1 record of the Montemayor-1 core (middle) and subsequently converted to a cyclostratigraphic age model using the insolation and E+T-P curves (right). The small black dots in the lithology columns denote the glauconite layers. Nomenclature of glacial stages is after Shackleton et al. (1995a). Gm is peak influx of Globorotalia menardii sin. Lines denote the tie points used for the age model of this interval.*

The part just below the two influxes of *G. menardii* sin (75-90 mcd) is characterized by higher Zr-Ti-Si values, implying larger grain size, which is confirmed by a pronounced

increase in the sand fraction of the sediments (Fig. 3.2). This change in matrix increases the uncertainty of the XRF results. In the Montemayor-1 core this corresponds to the 'transitional interval' which van den Berg et al. (2015) interpreted as a change from deeper-water environments dominated by detrital (i.e. clay and silt) dilution of biogenic carbonate, to shallower environments where clay and carbonate are diluted by silt input. Tuning on precession time scale over this interval was not possible for the Montemayor-1 core. Since the same change in loadings is observed at the transition between the lower and upper interval in the Huelva-1 core as is seen in the Montemayor-1 core, we expect a similar transition complicating the pattern of the geochemical cycles. Consequently, only the bio-events (i.e. the two peaks in *G. margaritae* and the two influxes of *G. menardii* sin) are used to constrain the age model for this interval (Fig. 3.5).

3.5.2.2 Tuning of lower part (90-170 mcd)

Two intervals in the lower part (90-124 mcd and 142-161 mcd) show bundles of 3-5 cycles which may reflect the imprint of the ~100 kyr eccentricity cycle on precession (Fig. 3.2). To illustrate this, following the method by Hilgen (1991), we took the Ca-Sr record, in which we clearly recognize this bundling, and calculated the 11 point moving average to remove any higher order fluctuations and emphasize the pattern produced by the bundling (Fig. 3.6, left). With the aid of the magnetobiostratigraphic tie points (Fig. 3.6), these intervals can be tuned to eccentricity where eccentricity minima are linked to the most pronounced biogenic carbonate maxima. In most cases tuning is straightforward and if there is any doubt, e.g. at 164 mcd, the best fitting maxima based on the magnetobiostratigraphic framework has been used.

However, the 124-142 mcd interval, which includes chron N3, is problematic. The magnetobiostratigraphic framework of Larrasoaña et al. (2008) suggests that the lower part of the core contains substantial variations in sedimentation rate, especially during normal chron N3 where the sedimentation rate appears to be very low by comparison with intervals at either side (Fig. 3.2). No clear bundling is observed in this interval and we count only 13 geochemical cycles while, if this part of the record is also forced by precession, 22 cycles are expected from the corresponding interval of the insolation curve. As a result one possible tuning for this interval is shown, denoted by dashed lines (Fig. 3.6) and we take into account an uncertainty of two precession cycles.

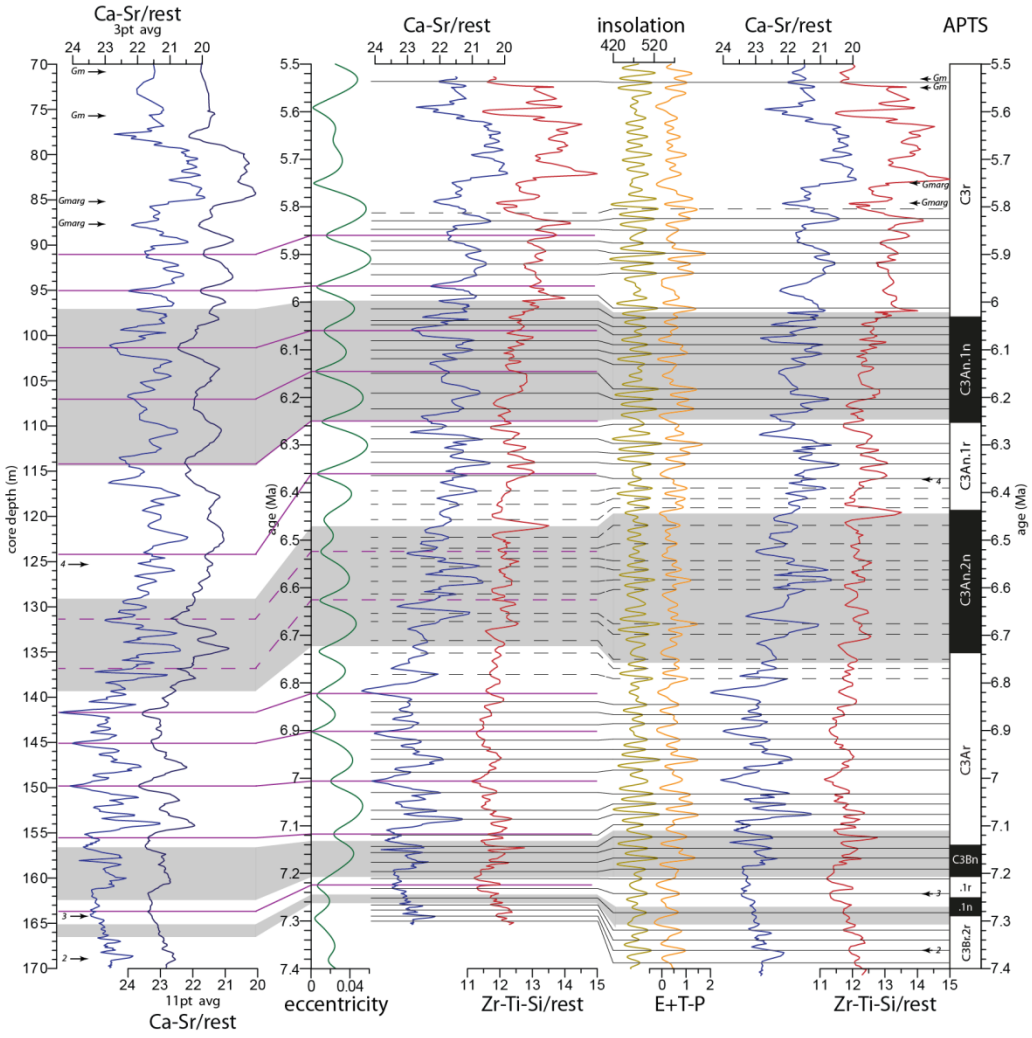

Figure 3.6. *A preliminary age model based on tuning to eccentricity (middle) of the three-point average and 11-point average of the Ca-Sr record (left). From this age model the Ca-Sr and Zr-Ti-Si records are tuned to precession (right) using the insolation and E+T-P curve. Numbers denote planktonic foraminiferal events of Sierro et al. (1993). Gm and Gmarg are influxes of Globorotalia menardii sin and Globorotalia margaritae, respectively. The reversed geomagnetic polarity intervals after Larrasoaña et al. (2008) are shown in grey shades. The interval with greater uncertainty is denoted with dashed lines (see text). Far right: The polarity timescale of the ATNTS2004 (Lourens et al., 2004).*

Using the cyclostratigraphic tie points resulting from this first order tuning to eccentricity, a preliminary age model has been constructed (Fig. 3.6, middle). From here, correlations are made on a precessional scale, where possible. Since the tuning of both the Montemayor-1 and Ain el Beida PC1 records show that the strongest insolation

peak correlates with the thickest/most pronounced peak in the PC1 records (chapter 2; Van der Laan et al., 2012), this relationship is also applied to the Huelva-1 core. The large number of magnetobiostratigraphic tie points (161-170 mcd) permits the bottom interval to be tuned to precession in spite of the lack of cycle bundling in both the sedimentary records and the astronomical target curve as a result of a 400kyr and 2.4Ma eccentricity minima. In this interval the cycles in the Zr-Ti-Si record are more pronounced and have higher amplitude than the Ca-Sr cycles, so the Zr-Ti-Si record is used for tuning of this interval. For the 142-161 mcd interval the Ca-Sr record demonstrates clear patterns on a precessional scale that can be tuned to insolation. The 90-124 mcd interval is tuned using the expression of eccentricity and the high amplitude precession cycles in the Ca-Sr record.

3.6 Discussion

3.6.1 Improvement of the age model

Even though tuning of the Huelva-1 record to the astronomical solution cannot be resolved on a precessional scale for all intervals, the resolution and precision of the age model greatly improves on the previous age model of Larrasoaña et al. (2008). That age model was based on 11 magnetobiostratigraphic tie points, giving a resolution of ca. 200 kyr. By comparison, the new age model has a resolution of ca. 2 precession cycles (40 kyr) or better, depending on the interval. This permits precise correlation with regional or global events at high temporal resolution. The ages of the reversals based on this age model are in good agreement with the ATNTS2004 (Lourens et al., 2004; Fig. 3.6). Mismatches do not exceed 40 kyr and can therefore be attributed to uncertainties in the position of the reversal due to measurement resolution or delayed remanence acquisition (Larrasoaña et al., 2014).

3.6.2 Mechanisms driving sedimentary cyclicity

Since the cycles in the Huelva-1 core, including their elemental loadings and changes therein, are very similar to those observed at Montemayor-1, only a summary of the mechanisms that drive these sedimentary cycles will be given here. For a full review the reader is referred to section 6.2 of van den Berg et al. (2015).

Both records consist dominantly of homogeneous marls with small changes in geochemical composition observed through XRF (Fig. 3.3 and 3.4). This is similar to the sediments of the Ain el Beida section in Morocco (Krijgsman et al., 2004), where identical cyclic changes in geochemical composition (fig. 3.7), i.e. an identical set of loadings for its PC1-ICP record as found for the PC1L records of both Montemayor-1 and Huelva-1, correspond with colour, stable isotope values, biological proxies and magnetic susceptibility (Van der Laan et al., 2005; 2012). Based on these proxies, and their correspondence with climate proxy signals observed in Mediterranean sapropel

formation (Krijgsman et al., 2004), these cycles were interpreted as dilution of biogenic carbonate by detrital clay input of fluvial origin; the reddish layers correspond to enhanced fluvial input associated with increased precipitation during insolation maxima (Van der Laan et al., 2012). The cycles of the lower interval of both records on the Spanish margin are interpreted the same way. These kind of dilution cycles are found throughout the recent geological history across the Mediterranean and the neighbouring Atlantic region (e.g., Bozzano et al., 2002; Hodell et al., 2013; Moreno et al., 2001; Sierro et al., 2000).

The upper intervals of both the Huelva-1 and Montemayor-1 cores are based on a different set of loadings than the lower intervals (Fig. 3.4 and 2.5). In the Montemayor-1 core this is explained by a change from more distal, open marine sedimentary conditions, to a more proximal pro-delta environment (chapter 2). This is in agreement with the paleodepth record for the Montemayor-1 core (Pérez-Asensio et al., 2012b) and the westward infilling of the Guadalquivir Basin (Iribarren et al., 2009; Sierro et al., 1996). This change is gradual and cannot be pinpointed to one specific time. We observe the same change in loadings and cycle amplitude in the Huelva-1 core, and even though we cannot demonstrate that the changes are synchronous, both occur within the 6-5.5 Ma interval. Since the Montemayor-1 and Huelva-1 cores are located only 12 km apart, a near-isochronous change is likely.

The set of loadings for the upper interval is very similar to the PC1U loadings of the Montemayor-1 core where it is explained as dilution of carbonate and clay by silt (chapter 2). Due to the more proximal setting of the Huelva-1 core, silt is able to reach the core site, possibly aided by storms, dominating the siliciclastic input. According to the model proposed by van den Berg et al. (2015), periods of Northern hemisphere summer insolation minima lead to relatively arid summers, and therefore result in decreased hinterland vegetation cover. This facilitates increased erosion and hence increases coarse-grained river runoff resulting in enhanced silt input. Similar models have been proposed for cyclic continental deposits elsewhere (Harvey et al., 1999; Pla-Pueyo et al., 2015).

3.6.3 Huelva-1 - Montemayor-1 comparison

We observe two distinct synchronous changes in sedimentation rate in both cores (Fig. 3.8). This implies that these changes are not merely local and might be associated with regional or even global events (see section 6.4). The first change occurs at 5.55 Ma and is marked by an abrupt increase in stable sedimentation rates from around 0.1 m/kyr to higher rates peaking at 0.9 m/kyr (Fig. 3.8). The second change is a sharp decrease in sedimentation rate in both the Huelva-1 and Montemayor-1 core from ca. 0.5 and 0.7 m/kyr, respectively (on average over the last 100 kyr of the Messinian), to a level with

increased glauconite concentration implying virtually no sedimentation at 5.33 Ma, coinciding with the Miocene-Pliocene boundary. This glauconite-rich layer can be traced for more than 100 km and is characterized by abundant biogenic and authigenic grains (Sierro et al., 2008). Glauconite typically forms on the outer shelf with water depths ranging from 50 to 500 m, usually during transgressive system tracts and/or high stand conditions, and is considered to represent a stratigraphic condensation within marine sediments (Amorosi et al., 2012; Banerjee et al., 2015; Harris and Whiting, 2000; Sierro et al., 2008; 1996; Sierro et al., 1990). Galán et al. (1989) has studied this particular glauconite layer in outcrop near Bonares and, based on the observed fauna which are typical for the sublittoral-circalittoral zone, concluded that it formed in situ at ca. 50 meter water depth during a transgressive pulse within a generally regressive system. This water depth is consistent with the 40-50 m estimated by Pérez-Asensio et al. (2012b) for this interval on the basis of benthic foraminifera. The duration of increased glauconite concentration is unclear. In the Montemayor-1 core a magnetic reversal is found just above the glauconite layer which could be tentatively correlated to the first reversal in the Pliocene, at 5.235 Ma (Larrasoaña et al., 2008). This would imply that this layer comprises a duration of ca. 100 kyr (Fig. 3.7). However, the FCO of *Globorotalia puncticulata* dated at 4.52 Ma (Lourens et al., 2004) is also found in this borehole only 20 meters above the reversal. This means that either the glauconite interval comprises a much longer time interval or that there is a hiatus within the interval between the glauconite layer and the FCO of *G. puncticulata* (see Larrasoaña et al., 2008).

The 6.37-7.3 Ma interval is very condensed in the Montemayor-1 core, precluding the construction of an astronomical age model based on tuning cyclic variations in the elemental composition of the sediments for that part of the record (Fig. 3.2). In the Huelva-1 core there are also problems with the tuning in the equivalent interval. However, because the sedimentation rate is higher, tuning is possible at least on the eccentricity scale. The difference in sedimentation rate is probably caused by the different locality of the two sites, resulting in a slight difference of sedimentary environment. Indeed, this change in sedimentation rate is not observed in the entire Guadalquivir Basin, as shown by the sonic data of the Casanieves hole (Fig. 3.7; Ledesma, 2000). The cycles in the Casanieves record are all well expressed and almost identical to the insolation curve. This well was drilled in a more central part of the basin suggesting that the tuning problems may have been caused by the proximity of both the Huelva-1 and Montemayor-1 cores to the basin margin.

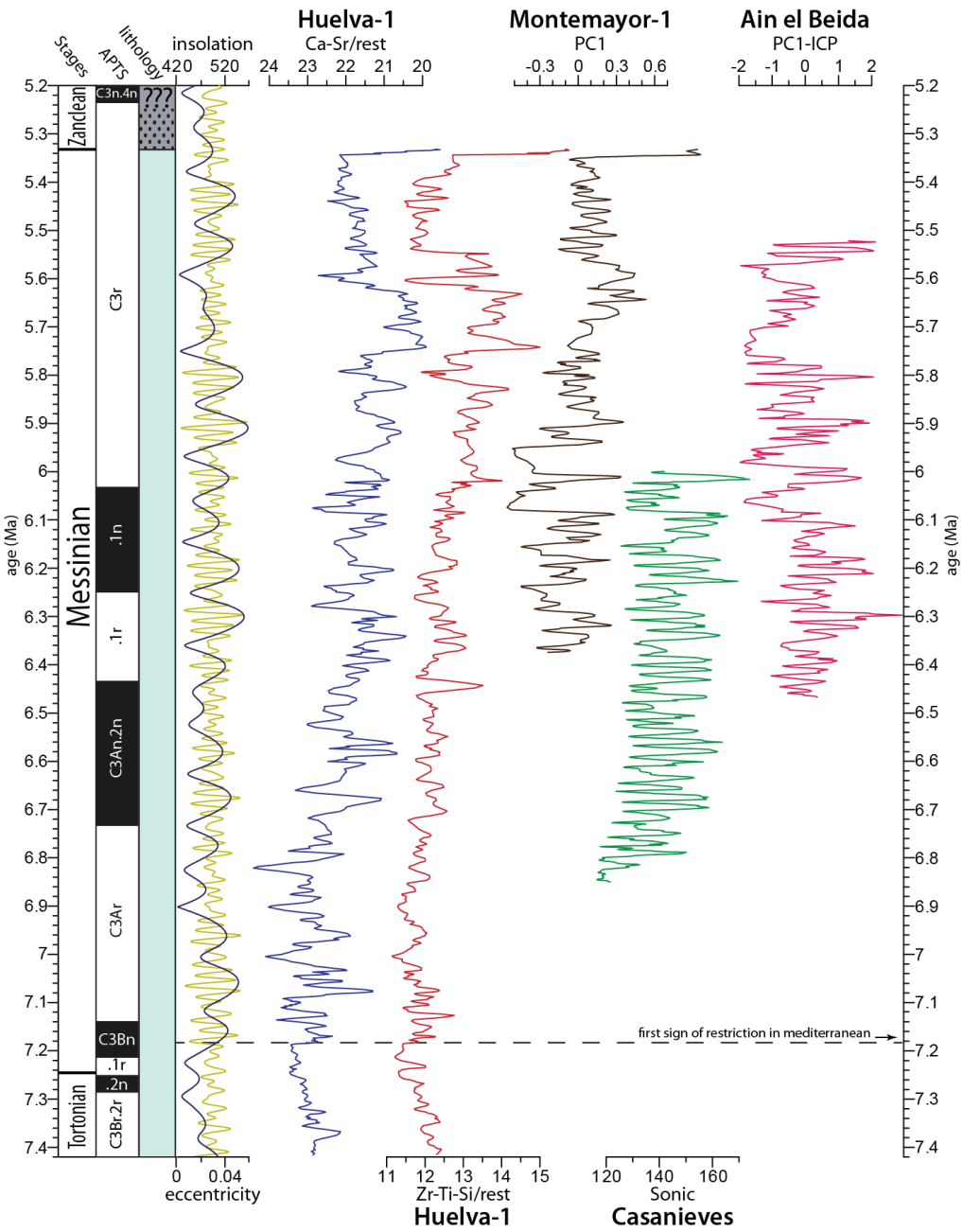

Figure 3.7: *Comparing the records from this study with similar records from the region. From left to right: geological stages, GPTS, Huelva-1 core lithology, insolation (yellow) and eccentricity (dark blue), Huelva-1 core Ca-Sr (blue) and Zr-Ti-Si (red) records, Montemayor-1 PC1 record (chapter 2; brown), Casanieves sonic record (Ledesma, 2000; green), Ain el Beida PC1-ICP record (Van der Laan et al., 2012; pink), all in the time domain. The event mentioned in the text is shown as a dashed line. In the lithology column the changes from clays (light grey) to sands (dark grey) and the glauconite layers (black dots) are shown.*

3.6.4 Correlation to regional/global events

3.6.4.1 Onset cyclicity at 7.16 Ma

In the basal part of both the Ca-Sr and Zr-Ti-Si records of the Huelva-1 core a decreasing trend and minor amplitude changes are observed, which changes abruptly to more stable values and high amplitude variability. This change occurs at 7.18 Ma, just after the Tortonian-Messinian boundary (Fig. 3.7). At the same time, the first evidence of reduced deep marine ventilation in the Mediterranean (2003; Kouwenhoven et al., 1999; Seidenkrantz et al., 2000) and the oldest opal-rich layer in the lower Abad marls of the Sorbas Basin (Sierro et al., 2001) are found, both of which have been related to the onset of Mediterranean gateway restriction. These events are also associated with the first marked increase in the amplitude of precession following a prolonged period of reduced amplitudes caused by a 400 kyr eccentricity minimum, superimposed on a 2.4 Myr eccentricity minimum, between 7.30 and 7.20 Ma (Kouwenhoven et al., 2003). The first high amplitude change in the Ca-Sr record is correlated to the same precession cycle, at 7.16 Ma (Fig. 3.6).

The increase in cycle amplitude in the Huelva-1 core represents an amplification of variability in the geochemical composition of the sediment. This can be related to more prominent changes in sediment input as a result of enhanced reaction to climate forcing. A similar increasingly pronounced reaction of the environment to climatic changes was observed in the Mediterranean Basin in the remainder of the pre-evaporitic part of the Messinian and was associated with progressive restriction (Sierro et al., 2003). Therefore, the 7.18 Ma event in the Huelva-1 core could be associated with a restriction of the Guadalquivir Basin and, consequently, of the Betic Corridor. In addition, the last olistostrome emplacement in the Guadalquivir Basin occurred around the same time and can also be linked to this restriction phase (Ledesma, 2000). Since all branches of the Betic Corridor except for the Guadalhorce were probably already closed by the late Tortonian (Chapter 1; Martín et al., 2014), the restriction might represent the final closure of the Betic Corridor. This is 1 Myr earlier than the closure of the Betic Corridor based on the oxygen isotope record of the Montemayor-1 core (Pérez-Asensio et al., 2012a). As this event is only found in the Huelva-1 core and is solely based on an increase in cycle amplitude, the lateral continuity of the expression of this apparent restriction event and its connection to the Betic Corridor should be further investigated.

3.6.4.2 Increase in sedimentation rate around 5.55 Ma

There are two abrupt changes in sedimentation rates that are isochronous in both the Montemayor-1 and Huelva-1 core and may therefore be related to regional or global events.

At 5.55 Ma, an abrupt and synchronous increase in sedimentation rate is recorded coincident with a decrease in paleodepth inferred from P/B ratios in the Montemayor-1

core (Pérez-Asensio et al., 2012b). At this time, the Guadalquivir Basin is filling up from east to west (Iribarren et al., 2009; Sierro et al., 1996) and it is reasonable to anticipate that the cores' locations experience a more proximal setting and an increase in sedimentation rate. However, the timing of the increase correlates exactly with the onset of MSC stage 3 in the Mediterranean Basin (Roveri et al., 2014), marking the deposition of the upper evaporites and Lago Mare after a short period of halite deposition (MSC stage 2, 5.6-5.55 Ma; Fig. 3.8). Therefore, a connection with these major events in the adjacent Mediterranean Basin that mark a major regional reorganization cannot be excluded. During halite deposition in the Mediterranean, a severely restricted connection with one-way inflow of Atlantic water is envisaged (CIESM, 2008) as outflow must have been negligible to achieve sufficiently high salinities (Meijer, 2006). Subsequently, following the same reasoning as Meijer (2012) for explaining the deposition of MSC stage 1 primary lower gypsum, two-way flow must have been re-established although in a still severely restricted setting to reduce salinities from halite to, at most, gypsum saturation. This change from one-way to two-way flow probably happened at the onset of MSC stage 3. At the same time, a major deglaciation took place from glacial stage TG12 (5.55 Ma) towards interglacial TG11 (5.52 Ma), which is recorded in oxygen isotope records from the open ocean (Fig. 3.8; Hodell et al., 2001; chapter 2; Van der Laan et al., 2006; Vautravers, 2014). This resulted in a, debated, glacio-eustatic sea-level rise in the order of tens of meters (Shackleton et al., 1995b; Vidal et al., 2002), reducing basin restriction and improving gateway exchange. Despite this sea-level rise and likely headward erosion threatening to deepen the strait (Garcia-Castellanos and Villaseñor, 2011), the Mediterranean-Atlantic connectivity must have remained restricted to facilitate evaporite formation during MSC stage 3.

The most likely explanation for both the increase in sedimentation rate in the Guadalquivir Basin and the prolonged restriction of the Mediterranean-Atlantic exchange is by tectonic uplift in the Betic and Gibraltar region. The concomitant decrease in paleodepth observed in the Montemayor-1 core can be considered as an independent argument for our explanation. Uplift of the Betics would lead to an increase in erosion rates of the mountain range, resulting in an increase in sediment supply to the Guadalquivir Basin. At the same time, accompanying uplift of the gateway area could explain the prolonged restriction of the Mediterranean Basin. Since there probably is a lag between the uplift and the resultant increase in sedimentation rate in the western Guadalquivir Basin, the timing of this tectonic event cannot be pinpointed exactly, but could be tentatively associated with the Messinian Erosional Surface (MES) and onset of halite deposition in the Mediterranean Basin, both dated at 5.6 Ma. The MES is recognized as a major erosional surface cutting into older deposits throughout the Mediterranean Basin. This erosion is either associated with a major sea-level drop (Clauzon, 1982; Lofi et al., 2005; Ryan and Cita, 1978) or with tectonics (Omodeo Salé et al., 2012; Roveri et al., 2008; Roveri and Manzi, 2006) in view of the angular

unconformity observed in several basins (Roveri and Manzi, 2006). In southern Spain this erosional surface has been found and dated in the Nijar Basin (Fortuin and Krijgsman, 2003), and is associated with a tectonically active period in this area (Omodeo Salé et al., 2012). The tectonic explanation is in agreement with the fact that MSC stage 2 is marked by a phase of Mediterranean-wide tectonic activity (Roveri et al., 2014 and references therein).

3.6.4.3 Onset of glauconite accumulation at 5.33 Ma

The other change, an abrupt decrease in sedimentation rate, occurs right at the Miocene-Pliocene boundary (Fig. 3.8). At this time fully marine conditions are re-established in the Mediterranean, ending the MSC. The return to fully marine conditions is geologically instantaneous and synchronous over the entire Mediterranean Basin (Roveri et al., 2014 and references therein). It is often related to the opening or deepening of the Gibraltar Strait which may have been accompanied by a catastrophic flood (Garcia-Castellanos et al., 2009). The correlation of the glauconite layer at the base of the Huelva Formation with the Miocene-Pliocene boundary makes the first time that a lithological expression has been found outside the Mediterranean that could possibly be associated with the end of the MSC due to their concurrence.

The return to open marine conditions does not correlate with any major deglaciation and/or climate event and is therefore considered more likely to have been caused by a tectonic event (Hilgen et al., 2007; Sierro et al., 2008; Van der Laan et al., 2006) or headward/downcutting erosion (Garcia-Castellanos and Villaseñor, 2011). A tectonic event could not only have caused an opening/deepening of the Gibraltar Strait, but at the same time could have lowered part of the western Guadalquivir Basin. Since the Guadalquivir Basin is, at present, very flat, a small relative sea level rise would result in a major landward migration of the coastline. This could trap sediment higher on shelf and result in a strong decrease in sedimentation rate at Montemayor-1 and Huelva-1 boreholes permitting glauconite accumulation.

One possible agent which could lead to uplift of the Betics and subsequent subsidence in the Gibraltar arc region is the rollback of the east dipping Gibraltar slab (Gutscher et al., 2002; Lonergan and White, 1997). The westward movement of slab rollback started in the eastern Betics and the accompanying delamination of the lithospheric mantle and upwelling of asthenosphere beneath southern Spain may have led to uplift of the Betic mountain chain (Duggen et al., 2003). Subsequently, the rollback process, and steepening of the slab may have caused a depression within the Gibraltar arc region, leading to sill lowering and the re-establishment of a marine connection at the end of the MSC (Duggen et al., 2003; Govers, 2009). However, no evidence for this hypothesis and the associated tectonic event causing the Zanclean flood has been found.

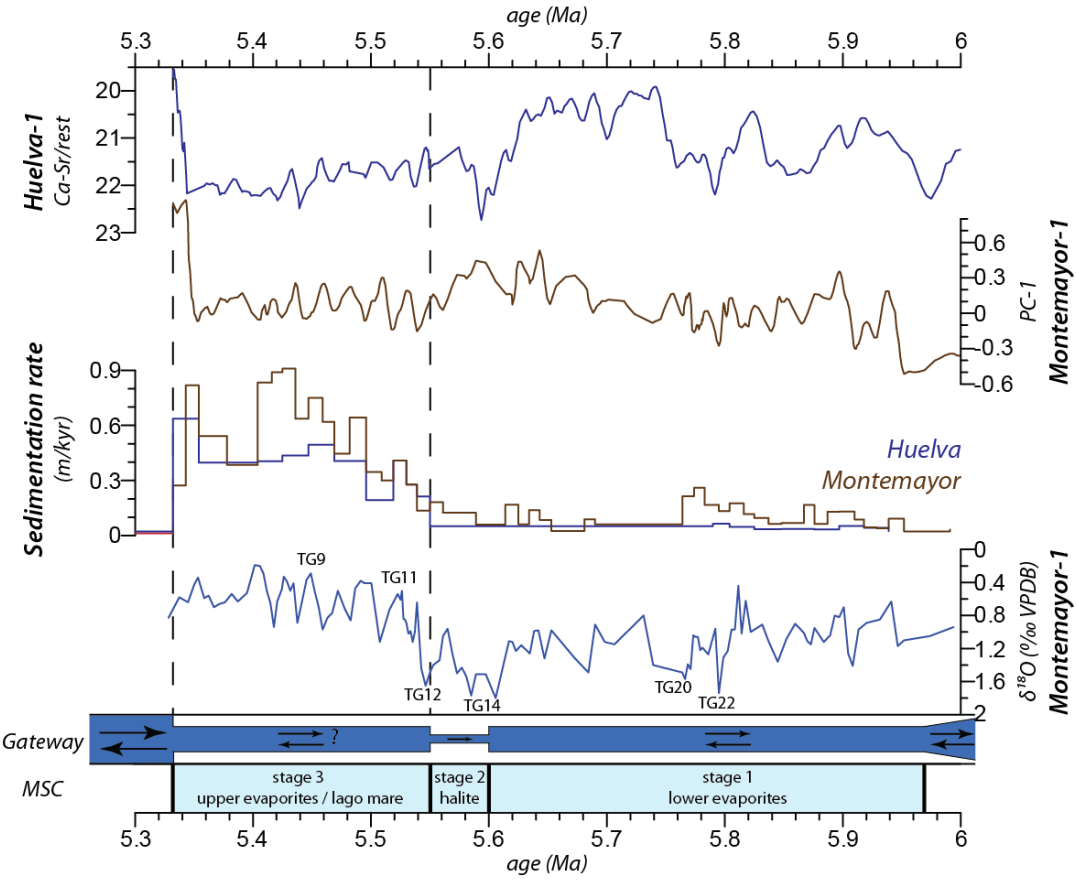

Figure 3.8. *Correlation between changes in the western Guadalquivir Basin records and Messinian Salinity Crisis events. From top to bottom: Huelva-1 Ca-Sr (blue) and Montemayor-1 PC1 (brown) records, sedimentation rates for Huelva-1 core (blue) and Montemayor-1 core (brown), oxygen isotope record of the Montemayor-1 core (chapter 2; blue) with assigned glacial/interglacial stages (Shackleton et al., 1995a), and gateway evolution with type of exchange and MSC stages (after Fig. 1.9). Correlations are shown with dashed lines.*

An alternative model for explaining the drop in sedimentation rate at the Miocene-Pliocene boundary is based on winnowing by currents. The western Guadalquivir Basin can be considered as the Messinian Gulf of Cadiz. This area has been strongly affected by currents flowing in and out of the Gibraltar Strait over the last 5 million years (e.g., Ambar et al., 2002; Bahr et al., 2014; García-Lafuente et al., 2006; Hernández-Molina et al., 2014; Lofi et al., 2015). Changes in gateway exchange impacting the current regime in the Gibraltar region, could also explain changes in the Guadalquivir Basin. Winnowing of the fine fraction by enhanced currents of North Atlantic Central Water flowing towards the Gibraltar Strait would only leave sands. This is in agreement with the sandy character of the glauconite layer observed in the Montemayor-1 core (Galán et al., 1989), but it is not clear why this would result in glauconite formation.

A final possible explanation comes from isostatic response to lithospheric loading (by evaporites) and unloading (through sea level fall) in the Mediterranean during the MSC (Govers, 2009). However, since no halite is found in the Alboran Sea (Comas et al., 1999), the change in loading is probably minor in the westernmost part of the Mediterranean. In addition, due to the mechanical properties of the lithosphere, the wavelength of the flexural response to these changes in loading is too short to affect the Betic mountain chain or the Guadalquivir Basin significantly. For both these reasons, the amplitude of isostatic rebound will be negligible in the Guadalquivir Basin (Govers, 2009) and consequently, this process is unlikely to have brought about the glauconite precipitation in the Huelva-1 and Montemayor-1 cores.

3.7 Conclusions

A high-resolution age model for the entire Messinian of the Spanish Atlantic Margin has been constructed by tuning cyclical changes in the elemental composition of sediments of the Huelva-1 core to astronomical target curves using magnetobiostratigraphic tie points. Most intervals can be tuned to precession and for these intervals the age model has an uncertainty of a few thousand years. For other intervals (i.e., 6.82-6.37 and 5.86-5.55 Ma), tuning was only possible on an eccentricity scale and an uncertainty of two precession cycles (ca. 40 kyr) should be observed. These complexities in the tuning probably result from synsedimentary changes in depositional environment and the marginal position of the core in the Guadalquivir Basin. The XRF record is strikingly similar to the XRF record of the nearby Montemayor-1 core.

The increase in cycle amplitude observed near the bottom of the Huelva-1 record is coeval with the first restriction of the Mediterranean Basin, at the base of the Messinian. This could be related to restriction of the Betic Corridor but further investigation is needed. Two significant changes in sedimentation rate are found in both the Huelva-1 and Montemayor-1 core; these may be related to regional or global events. The relatively abrupt increase in sedimentation rate around 5.55 Ma correlates well with the onset of the final stage of the MSC and a major deglaciation. The most likely mechanism explaining this correlation is a tectonic event, uplifting the region, which results in increasing erosion rates in the Guadalquivir Basin as well as restricting Mediterranean-Atlantic gateway exchange. The subsequent abrupt decrease in sedimentation rate coincides with the Miocene-Pliocene boundary and the reestablishment of fully marine conditions in the Mediterranean. The coeval change in sedimentation rate on the Spanish Atlantic margin may be linked to events within the Mediterranean that terminated the Messinian Salinity Crisis as a result of either regional tectonic subsidence, a change in localised ocean circulation associated with the opening, or deepening, of the Gibraltar strait, or both.

Acknowledgements

All fellow Medgate ESRs and supervisors are thanked for their valuable suggestions and discussions. Rob Govers and Dirk Simon are thanked for valuable discussions regarding isostasy. The research leading to these results has received funding from the People Programme (Marie Curie Actions) of the European Union's Seventh Framework Programme FP7/2007-2013/ under REA Grant Agreement No. 290201 MEDGATE, and also from the Guadaltyc project (MINECO, CGL2012-30875). Funding from Castilla y Leon Regional Government is also acknowledged (SA263U14).

CHAPTER 4

Improved biostratigraphic dating of Upper Miocene sediments in western Betics suggests late Tortonian closure of the Betic Corridor

In Collaboration with: Marlies van der Schee, Walter Capella, Dirk Simon, Evelina Dmitrieva, Francisco Sierro, Wout Krijgsman and Stephen Vincent

Abstract

The Betic Corridor connected the Mediterranean Sea with the Atlantic Ocean during the Upper Miocene but its timing of closure and therefore its role prior and during the Messinian Salinity Crisis is still under debate. Especially the timing of closure of the Guadalhorce Corridor, which was probably the last existing branch connecting the Mediterranean with the Guadalquivir Basin is disputed. Difficulties assessing the timing and evolution of the Guadalhorce Corridor are caused by the lack of adequate deposits to constrain precise age determination through integrated stratigraphy. Therefore, we have to rely on dating of sediments of adjacent basins and assessing their possible relationship with this corridor. Here we present new biostratigraphic age constraints on the Upper Miocene sediments of the Ronda Basin and Antequera region. These key areas formed the northern part of the gateway and both indicate a shallowing upward sedimentary succession from sandy marls to calcarenites. Biostratigraphic dating of the marls resulted in all cases in a late Tortonian age, older than 7.58 Ma. This suggests that the Guadalhorce Corridor probably closed during the late Tortonian-early Messinian. Our observations are in line with results from the Arcos Basin and the previous published late Tortonian closure of the Granada Basin. This suggests that the late Tortonian period of tectonic uplift in the eastern Betics, closing the eastern branches of the Betic Corridor, extended westward and also shallowed and subsequently closed the western branches of this corridor. This resulted in a late Tortonian-early Messinian closure of the Betic Corridor, well before the onset of the Messinian Salinity Crisis.

4.1 Introduction

The Betic Corridor connected the Mediterranean Sea with the Atlantic Ocean during the Late Miocene and plays an important role in the history of the Mediterranean Basin. Stepwise restriction of this corridor and the Rifian Corridor, located in northern Morocco, led to the extraordinary event of the Messinian Salinity Crisis (MSC; 5.97-5.332 Ma; (Chapter 1; Hsu et al., 1973; Roveri et al., 2014). However, the precise role of this corridor on the onset and progress of the MSC is still under debate.

The western part of the Betic Corridor consisted of the Guadalquivir Basin, the foreland basin of the Betic Cordillera, which experienced continuous marine sedimentation from Middle-Late Miocene up to the present day (González-Delgado et al., 2004; Salvany et al., 2011; Sierro et al., 1996). The eastern part was divided in several sea branches (Fig. 4.1), of which each closed separately due to sedimentary infill and tectonic uplift, gradually restricting the Mediterranean-Atlantic exchange through southern Spain (Chapter 1; Martín et al., 2014). The most northerly branch, known as the North Betic strait, closed at 7.8 Ma (Krijgsman et al., 2000), while the branch passing through the Granada Basin closed around 7.3 Ma (Corbí et al., 2012). The youngest marine sedimentation in the Guadix Basin is dated at 7.85 Ma, even though subsequently a hiatus of more than 2 Ma is present and therefore a later closure cannot be ruled out (Hüsing et al., 2010). It is suggested that the westernmost and probably last remaining of these branches, the Guadalhorce Corridor (Martín et al., 2001), has closed at 6.18 Ma (Pérez-Asensio et al., 2012). The timing of this closure, however, is only based on indirect evidence through a change in benthic oxygen isotopes signatures in the Guadalquivir Basin from typical Mediterranean towards more Atlantic characteristics, which suggests the closure of the last active Betic gateway.

Difficulties assessing the timing and evolution of the Guadalhorce Corridor are caused by the lack of adequate deposits to constrain precise dating through integrated bio-, magneto- and/or cyclostratigraphy. Currently, the sedimentary deposits in the Guadalhorce Corridor are dated on the geological map (MAGNA 50, 2ª Serie - IGME) as late Tortonian, based on regional lithostratigraphic correlations to nearby deposits close to Antequera, 12 km to the ENE, which include marly intercalations containing microfauna typical of the basal late Tortonian (López-Garrido and Sanz de Galdeano, 1999; Lozano, 1979). However, Martín et al. (2001) attributes the sediments of the Guadalhorce gateway to the early Messinian (7.2-6.3 Ma) based on the occurrence of the planktonic foraminifera assemblage found in the Peñarrubia exposures (Fig. 4.2). To resolve these age determination disputes, other nearby outcrops and basins that are laterally associated with the sedimentation found in this potential corridor are therefore essential.

The adjacently lying Ronda Basin is one of those associated basins and also formed part of the Betic Corridor as a satellite basin of the Guadalquivir Basin. It is located west of the Guadalhorce Corridor, in the external zone of the Betic Cordillera, and is commonly assumed to have a Tortonian-Messinian basin fill (Gläser and Betzler, 2002; Rodríguez Fernández, 1982; Ruiz-Constán et al., 2009; Lozano, 1979) with a typical shallowing upwards sequence from deep marine marls towards shallower marine calcarenites (Gläser and Betzler, 2002). The dating of these sediments is mainly based on the biostratigraphic framework of Lozano (1979), which does not connect with the astronomically-tuned biostratigraphic frameworks for sections or boreholes in the Mediterranean and nearby Atlantic margin (Chapter 2 & 3; Krijgsman et al., 2004; Sierro, 1985; Sierro et al., 2000, 1996, 1993; Van der Laan et al., 2006; Van der Schee et al., 2016). Therefore, the dating of the Ronda sedimentary sections together with the sediments associated with the Guadalhorce Corridor is essential and must be tested again within the current biostratigraphic framework to be placed within the context of Betic Corridor evolution.

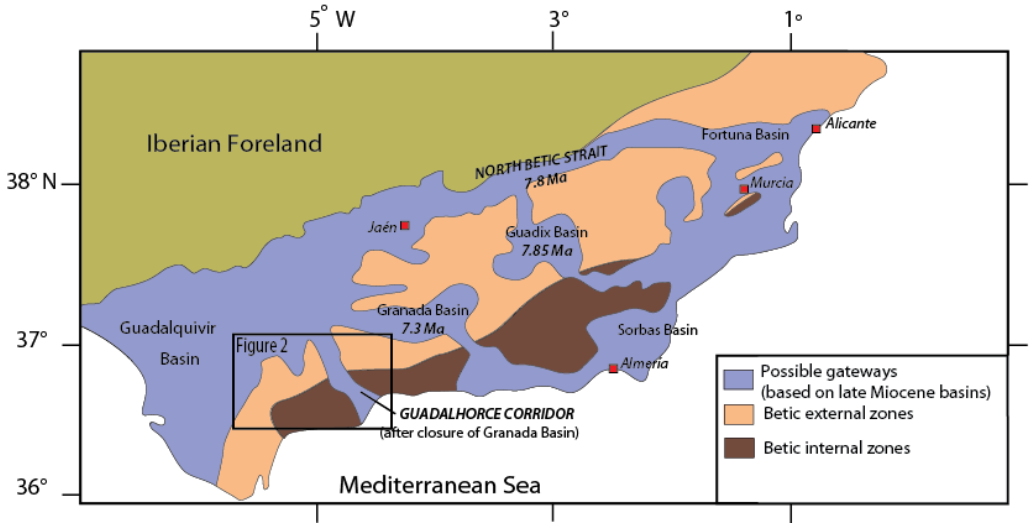

***Figure 4.1**. Detail map of the Betic Corridor showing the main geological units, corridors and closure dates of different branches (modified after Santisteban and Taberner, 1983).*

The area around Arcos was a satellite basin of the Guadalquivir Basin located west of the Ronda Basin and contains a similar shallowing upwards sequence in Late Miocene sediments. Also here precise dating of sediments using the current biostratigraphic framework is lacking. Therefore, Upper Miocene sediments from this basin will be dated and used to test if the changes in depositional environment are consistent throughout the Late Miocene basins of the Southwest Betic external zones.

To summarize, we will re-assess and improve the chronostratigraphy for the sediments of the Arcos and Ronda basins, the Antequera and Guadalhorce area, based on the most up-to-date and detailed biostratigraphic framework for this region. Subsequently, we will place these findings within the local geological framework and the evolution of the Betic Corridor.

4.2 Methods

We revisited the basins and areas described above and looked for outcrops or sections in areas marked 'Tortonian', 'Messinian' or 'Andalusian' on the MAGNA 50 (2ª Serie) - Mapa Geológico de España a escala 1:50.000 from the Instituto Geológico y Minero de España (IGME). The 'Andalusian' is an obsolete stage in geological history used in the western part of the Guadalquivir Basin and considered to be the uppermost Miocene sediments (Berggren and Haq, 1976; Perconig and Granados, 1973). Sections and areas were (re-)assessed in terms of their depositional environment using sediment characteristics and sedimentary structures.

By taking into account basin configurations and bedding planes, biostratigraphic samples were targeted to be as young as possible in sections and outcrops in each area or basin. A total of 54 samples from sandy to silty marls have been analyzed. Samples were carefully positioned from finer grained sediments if possible, to increase the probability of finding microfossils. For qualitative planktonic biostratigraphy, samples of ~100 gram were disintegrated in water and washed over a >150 µm sieve. To date the Tortonian-Messinian sediments, biomarkers from early Pliocene until the late Tortonian are reported if present. These include *Globorotalia margaritae, Globorotalia miotumida, Neogloboquadrina acostaensis, Globorotalia menardii 4* and *5*, *Globorotalia scitula* and *Sphaeroidinellopsis* with corresponding coiling directions.

4.3 Results

4.3.1 Arcos

The lower part of the Upper Miocene sequence found in the Arcos Basin is comprised of grey, fine to coarse grained marls, which are later replaced by sandy calcarenites. The marls contain microfossils, while the calcarenites are rich in bioclastic content, red algae, bryozoans and shell fragments. The calcarenites contain meter scale channels, tabular-cross and through-cross stratified sands. Some layers show intense bioturbation. Throughout the ~50 m exposure at the Arcos section (Fig. 4.3), a general trend is observed that the foreset-thicknesses decrease from several meters to few decimeters towards the top. Samples taken from grey, sandy marls just below the onset of the calcarenites at both Arcos and Espera contain the planktonic foraminiferal biomarkers *G. menardii* 4 sinistral, *G. scitula* sinistral/dextral and mainly sinistral coiling *N. acostaensis.*

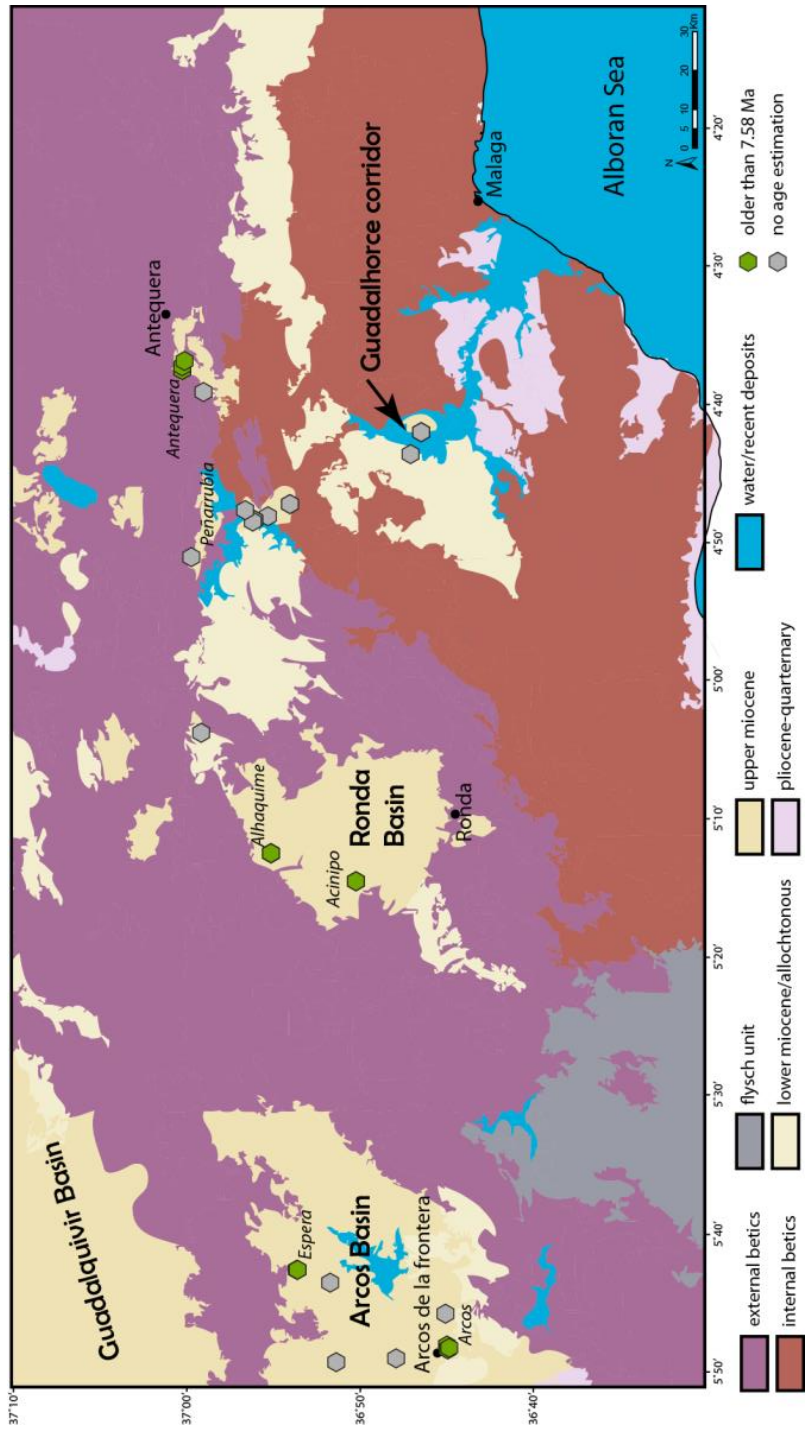

Figure 4.2. *Detail geological map of the southwest Betics with Late Miocene basins, sections, and sample locations.*

***Figure 4.3**. Overview of the calcarenites at the Arcos section*

4.3.2 Ronda

In the Ronda Basin, we studied the uppermost sequences of the Late Miocene infilling. The Alhaquime section (Fig. 4.4d) comprises of Fm. La mina (clay and marls) and Fm. De Setenil (Lozano, 1979) and are respectively marked Sequence 2 and 3 (equivalent to sections S13 and S14) in the lithostratigraphical subdivision presented by Gläser and Betzler (2002). The Acinipo section presented in this paper is equivalent to a combination of section S7 and S8 (Gläser and Betzler, 2002), and is referred to as Fm. Las Mesas by Lozano (1979). Sequence 2, at the lowest part of the Alhaquime section, consists of grey marls which become coarser-grained up sequence, forming lenses within the lowest calcarenitic layers (Fig. 4.4f). An erosional surface, which marks the boundary between Sequence 2 and 3, is associated with a relative sea level lowering and a tectonic event forming the anticline of the Sierra de las Salinas (Gläser and Betzler, 2002). Sequence 3 consists of increasingly thicker (up to 20 m) deposits of sandy bryozoan calcarenites and brown to yellow siliciclastic sandstone intercalated with marls. In these sandy intervals both tabular-cross and trough-cross bedding were observed. Set thicknesses of the cross stratifications vary from ~50 cm to 3 m and foreset planes dip towards the west and northwest (Fig. 4.4e). Red algal limestones dominate Sequence 3 in the Acinipo section. Biostratigraphic samples were taken from the marls below and in between the calcarenitic alternations at Alhaquime, and just below the limestones at Acinipo. Only the samples in the marls of Sequence 2 contained planktonic biomarkers: *G. menardii* 4 sinistral, *G. scitula* sinistral/dextral and mainly sinistral coiling *N. acostaensis.*

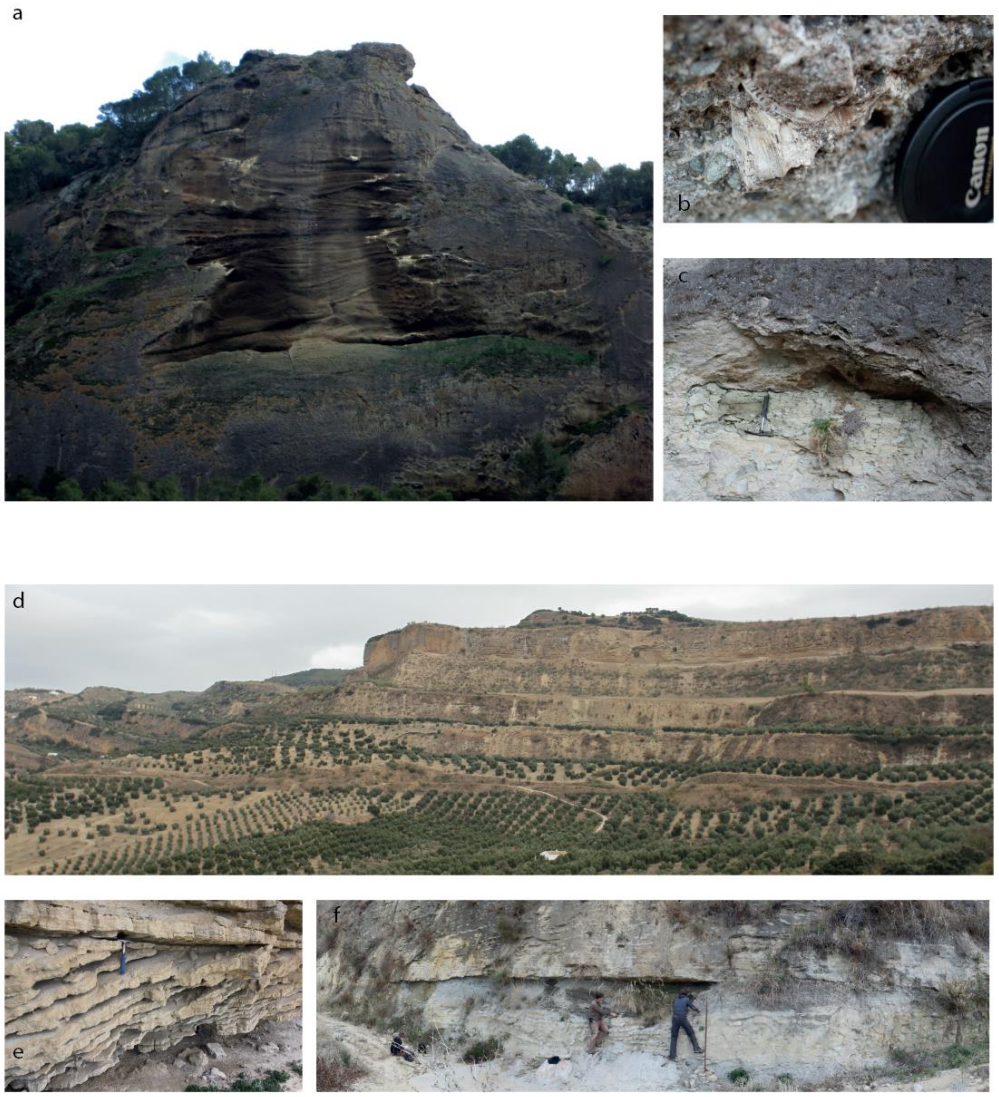

Figure 4.4. *a) cross-trough bedding in the Guadalhorce Corridor. b) close-up of barncle fragments. c) example of a rip-up mud clast. d) overview of the Alhaquime section (Ronda Basin). e) large scale foresets. f) claylenses within the calcarenite at the Alhaquime section.*

4.3.3 Antequera

The lowest part of the Antequera sequence contains grey, fine grained to very sandy marls (Fig. 4.5) which are subsequently replaced by sandy calcarenites with the marls containing microfossils, while the calcarenites show large bryozoan, ostracods, benthic foraminifera, red algae and shell fragments. The calcarenites of Antequera are more massive compared to the Ronda and Arcos basins; they show faint tabular bedding and

only locally through-cross stratification. However, ubiquitous indicators of paleocurrent directions are generally lacking. The samples taken in the marls contain planktonic biomarkers *G. menardii* 4 sinistral, *G. scitula* sinistral/dextral and mainly sinistral coiling *N. acostaensis*.

Figure 4.5 *Outcrop with Late Miocene sandy marls near Antequera*

4.3.4 Guadalhorce

The outcrops within and just north of the Guadalhorce area are slightly different from the other three key localities. The Upper Miocene sequence starts from the lowest part of the valley with coarse to very coarse grey sands and conglomerates with large scale erosional features (Fig. 4.4a). Lobes of grain-supported, coarser and more angular conglomerates are found within polymict, matrix-supported conglomerates and coarse sandstones. These attest to debris flows from the basin margins. Within the lower part of the sequence some centimeter to decimeter scale rip-up mud clasts are found (Fig.4.4c). Towards the top, coarse sandstones show large scale cross-bedding, pointing predominantly to the NW, as described in Martín et al. (2001). Despite the great amount of samples taken from outcrops within and just north of the Guadalhorce area, no planktonic foraminiferal biomarker species were found.

4.4 Discussion

4.4.1 Biostratigraphic dating

4.4.1.1 Late Tortonian age determination

The preservation of the foraminifera is generally good, however, in many biostratigraphic samples microfauna is scarce or samples are sterile. Some samples did contain microfossils but no marker species were found. The matrix of the samples consists of, (rounded) quartz grains, silts, (secondary) gypsum, bioclastic fragments, (reworked) glauconite, detrital wood and shell fragments. These types of coarse-grained sediment severely limit the possibilities for reliable dating, due to the fact that the used biostratigraphic marker species generally live in deeper marine environments, while silty to sandy sediments are more often deposited in shallow and high energy environments, where these planktonic species do not dwell. This is evident from the

amount of samples that are taken and unsuccessfully studied for age constraints (Fig. 4.2).

All samples that contain marker species consisted of marls and sandy marls. The same planktonic biomarkers, i.e. *G. menardii* 4 sinistral, *G. scitula* sinistral/dextral and mainly sinistral coiling *N. acostaensis* were observed in these samples. This indicates that all these samples are older than the Last Common Occurrence (LCO) of *G. menardii 4*, dated at 7.58 Ma (Krijgsman et al., 1994; Lourens et al., 2004; Sierro, 1985) and definitely older than the First Occurrence (FO) of *G. menardii 5* (7.355 Ma; Hilgen et al., 1995; Krijgsman et al., 1994; Lourens et al., 2004). This is consistent with the first sinistral coiling of *N. acostaensis*, of which sinistral to dextral coiling changes are reported from around 6.35 Ma (Lourens et al., 2004). Consequently, all the sediments in this study that were previously reported as 'Tortonian', 'Messinian' or 'Andalusian' on the MAGNA 50 (2ª Serie) geological maps and can reliably be dated are in fact late Tortonian and should not be related to the Messinian.

The dated marine silty marls in the Arcos and Ronda basins and Antequera region are subsequently replaced by calcarenites that can be in certain places up to 100 meters thick. Since there is no available method to reliably date these calcarenites, we cannot assess the exact time at which the observed marine sedimentation terminates in these basins. However, based on the fact that coarse grained deposits typically have high sedimentation rates and the reliable late Tortonian age determination of the deeper marine sediments below, the calcarenites are probably also deposited during the late Tortonian. We consider it as unlikely for the top of these sediments to reach up to an early Messinian age and highly unlikely that they are deposited during the Messinian Salinity Crisis. Unfortunately, it can neither be assessed how much (marine) sediment has been deposited and subsequently eroded on top of this late Tortonian sequence. Nonetheless, since Tortonian marine deposition is vast in the studied region, we find it unlikely that, if there was major Messinian marine sedimentation, it got completely eroded.

Despite numerous attempts, we did not succeed in finding samples from within the Guadalhorce area that provide a reliable age determination. This is probably due to the coarse grained and shallow environmental character of the deposits found within this region. We agree with Lopez-Garrido and Sanz de Galdeano (1999) that, based on their similarities in lithology, the Guadalhorce sandy deposits should be associated with the coarse-grained calcarenitic deposits in nearby regions like Ronda and Antequera. Since we assigned a late Tortonian age to these coarse grained sediments in these regions, probably the sediments within the Guadalhorce region were also deposited in the late Tortonian.

4.4.1.2 Comparison with previous studies

All datable samples indicate a late Tortonian age, older than 7.58 Ma. These samples were found in different basins and outcrops in the studied area, and should therefore represent well the ages of the deposition of Upper Miocene deep marine sediments north and west of the Guadalhorce Corridor. This is in contrast with the age determinations of previous studies done within this region (Gläser and Betzler, 2002; Martín et al., 2001; Lozano, 1979), which states that at least the upper part of the deep marine infilling was Messinian. Gläser and Betzler (2002) rely on the work of Lozano (1979) to assign a Tortonian-Messinian age to the deposits of the Ronda Basin. Martin et al., (2001) based their Messinian age determination for the Guadalhorce corridor on the occurrence of *Globoratalia* gr. *miotumida*, *G. conomiozea* and sinistral *N. acostaensis* in the Peñarrubia exposure. Despite extensive research and sampling in this area, we were not able to find a late Tortonian-early Messinian assemblage with planktonic foraminifera marker species in the same location. Also, we note that specimens of the group of *G. miotumida* and *G. conomiozea* have also been found during the late Tortonian well before the Tortonian-Messinian boundary, coexisting with sinistral *N. acostaensis* in the eastern Betic Lorca and Fortuna basins (Krijgsman et al., 2000).

4.4.2 Sedimentological interpretation

Regardless of smaller scale sea level fluctuations, e.g. in the Ronda Basin (Gläser and Betzler, 2002) within all basins and outcrops in the study area a change from deep marine marls, containing ample amount of benthic and planktonic foraminifera, towards coarse grained calcarenites with many shell fragments, algae and flow structures, and no, or only benthic foraminifera is observed, suggesting a general shallowing upwards trend. This is supported by evidence of very shallow environment depositions at the top of some sequences, with high percentages of benthic foraminifera and mollusk fragments. The youngest deep marine sediments in these basins and areas just north of the Guadalhorce Corridor are dated as late Tortonian, older than 7.58 Ma, therefore this shallowing trend must have occurred around that same time period, resulting in a late Tortonian age estimation for the shallower marine calcarenites and probably also for the deposits within the Gaudalhorce corridor. The age of this shallowing trend leads to the suggestion that this branch of the Betic Corridor closed in the latest Tortonian instead of the Messinian as suggested by previous studies (Martín et al., 2001; Pérez-Asensio et al., 2012). Due to the uncertainties described above it cannot be excluded that a restricted, shallow connection persisted after the major shoaling phase.

4.4.3 Placement of this shallowing event within the tectonic context of the Betics

The observed late Tortonian shallowing event in the western part of the Betics can be related to the regional tectonic uplift event which shallowed and subsequently closed the basins in the eastern Betics. In the Lorca and Fortuna basins a late Tortonian change towards continental sedimentation proves closure of the North Betic Strait (Krijgsman et al., 2000; Martín et al., 2009). In the Guadix Basin, a hiatus is observed at about 7.85 Ma, suggesting a late Tortonian closure of the branch passing through this basin (Betzler et al., 2006; Hüsing et al., 2010). The Granada Basin, just west of Antequera, closed in the latest Tortonian (7.3 Ma; Corbí et al., 2012). The late Tortonian age estimation for the observed shallowing trend, around the same time period as the eastern Betic range, implies a late Tortonian tectonic uplift over the entire Betic region. Ongoing uplift which eventually have led to the complete closure of the Betic Corridor might be related to the latest olistostrome emplacement in the Guadalquivir Basin around the Tortonian-Messinian boundary (Ledesma, 2000; Sierro et al., 1996) and the first sign of restriction in the Mediterranean Basin in the form of reduced deep marine ventilation at 7.18 Ma (Kouwenhoven et al., 1999; Seidenkrantz et al., 2000) and results from the Huelva-1 record (chapter 3) suggesting earliest Messinian signs of Betic Corridor restriction.

5. Conclusion

The studied area in south west Spain comprises four Upper Miocene key sections or basins, i.e. Arcos, Ronda, Antequera, and Guadalhorce, all indicating a shallowing upward trend. At Ronda, Arcos and Antequera a regression from sandy marls to calcarenitic deposits is observed. Biostratigraphic dating of the marls resulted in all cases in a late Tortonian age, older than 7.58 Ma. The Guadalhorce Corridor consists of similar calcarenitic deposits as found above the marls in the other sections. A reliable age estimation for these deposits was not found. The observed late Tortonian regression is interpreted as a restriction and subsequent closure of the most western branch of the Betic Corridor. Due to dating difficulties of the overlying calcarenites, marking the shallow marine phase and uncertainties in erosion rates, the exact timing of cessation of marine sedimentation in this area cannot be pinpointed. However, based on typical sedimentation rates for calcarenites, marine sedimentation in this part of the Betic Corridor probably terminated in the late Tortonian-early Messinian. We suggest that the late Tortonian period of tectonic uplift in the Eastern Betics, which caused the closure of the eastern branches of the Betic Corridor, extended westward, uplifting the western Betics from the Granada Basin up to the Arcos Basin. This resulted in a late Tortonian-early Messinian closure of the Betic Corridor, well before the onset of the Messinian Salinity Crisis.

CONCLUSIONS

Marine gateways are an important control on both local environmental change and global climate. The Late Miocene Mediterranean gateway system that linked to the Atlantic is a good example of this and much can be learnt about the processes and impacts of gateway closure from the study of the sediments preserved within the Betic Corridor (southern Spain) and the Rifian corridor (northern Morocco).

Through a high-resolution age model for the entire Messinian of the Guadalquivir Basin, representing the Atlantic side of the Betic Corridor, we can precisely date and thereby assess the relevance of environmental changes in this part of the corridor. This high-resolution age model was constructed for the Montemayor-1 and Huelva-1 cores, drilled in the NW Guadalquivir Basin, using cyclostratigraphy. However, tuning to the astronomical target curves is only possible when sedimentary cyclicity is perceptible, while the apparent homogeneous marls, predominating both cores, prevented tuning of visually identifiable sedimentary cycles. Therefore, cyclical changes in the elemental composition of the sediments were visualized through XRF measurements of 1383 samples using a handheld XRF gun. This novel method was tested for outlier detection, reproducibility and reliability, while an additional calibration was performed using conventional XRF, all proving that the relative changes in geochemical composition acquired though this method are robust. Subsequently, the high-resolution age model was constructed by tuning these cyclical changes to the astronomical target curves using magnetobiostratigraphic tie points.

Based on the age model the following observations were done and their regional or global relevance through possible linkage with Atlantic or Mediterranean events was considered.

- Two significant changes in sedimentation rate are found in both the Huelva-1 and Montemayor-1 core, therefore these may be related to regional or global events. The relatively abrupt increase in sedimentation rate around 5.55 Ma correlates well with the onset of the final stage of the Messinian Salinity Crisis (MSC) and a major deglaciation. The most likely mechanism explaining this correlation is a tectonic event, uplifting the region, which resulted in increasing erosion rates in the Guadalquivir Basin as well as restricting Mediterranean-Atlantic gateway exchange. The subsequent abrupt decrease in sedimentation rate coincides with the Miocene-Pliocene boundary and the reestablishment of fully marine conditions in the Mediterranean, terminating the MSC. This correlation may be linked through either regional tectonic subsidence, a change

in localised ocean circulation associated with the opening or deepening of the Gibraltar strait, or both.

- The increase in cycle amplitude observed near the bottom of the Huelva-1 record is coeval with the first restriction of the Mediterranean Basin at the base of the Messinian. This could be related to restriction of the Betic Corridor but further research is needed.
- A gradual change in the nature of the typical fluctuations in geochemical composition of the sediments through both records was recognized, which is associated with a gradual change in depositional environment as the Guadalquivir Basin infilled. The lower interval of both records show alternations of biogenic carbonate layers with beds of terrigenous clay material. The terrigenous material dilutes the biogenic carbonate during periods of increased river runoff induced by maxima in Northern Hemisphere summer insolation. In the upper interval of both records, the nature of the cycles changes probably as a result of a more proximal setting. In this shallow marine environment, sedimentation is dominated by coarser-grained detrital input. Due to increased erosion rates caused by a loss in vegetation cover during insolation minima, enhanced input of silty detrital sediments dilutes the biogenic carbonate and the clay.
- Based on the new chronostratigraphic framework, the benthic oxygen isotope record of the Montemayor-1 core correlates well with the previously published Atlantic records of Ain el Beida, Loulja and ODP Site 982. Glacial stages TG12, TG14, TG20 and TG22 as well as the deglaciation towards TG11 and finally TG9 are clearly expressed. Similar behaviour in the planktonic and benthic oxygen isotope records for Ain el Beida, Loulja and the Montemayor-1 core, together with general trends reflecting open ocean signals, suggest the presence of North Atlantic Central Water and no direct influence of Mediterranean Outflow Water (MOW) on the sediments of the Montemayor-1 record.
- An offset is recognized between the benthic oxygen isotope records of the Montemayor-1 core and Ain el Beida for the late Messinian glacial period (5.9-5.5 Ma), concurrent with the first stages of the MSC. This might be the result of the decrease/cessation of the MOW in the Gibraltar Strait region, but could also be explained by the presence of more saline MOW or upwelling. Additional high-resolution records from the Atlantic margins near the Gibraltar Strait are needed to reconstruct fully the role and evolution of MOW during the MSC.

Uplift and erosion resulting from tectonic drivers of gateway closure, has led to the preservation of incomplete sedimentary successions within the corridors themselves. Despite this, it appears that the main channels, as deduced from the current distribution of Late Miocene sediment in the region, were closed well before the precipitation of large volumes of halite during the MSC. However, the closure date of the most western

channel of the Betic Corridor, the Guadalhorce corridor, is still disputed. The Ronda Basin and Antequera region, which are located adjacent to the Guadalhorce corridor and probably formed the northern part of that gateway, both indicate a shallowing upward sedimentary succession from marls to calcarenites. Biostratigraphic dating of the marls in these key areas result in all cases in a late Tortonian age, older than 7.58 Ma. This late Tortonian regression leads to the suggestion that the Guadalhorce corridor closed during the latest Tortonian-earliest Messinian.

A similar late Tortonian regression as found in the Ronda Basin and Antequera region is also observed in the Arcos Basin, located west of Ronda. These observations are contemporary with the late Tortonian uplift and subsequent closure of the Granada Basin, east of Antequera. Therefore it is suggested that the late Tortonian period of tectonic uplift in the eastern Betics, causing the closure of the eastern branches of the Betic Corridor, continued westward and also uplifted the western Betics from the Granada Basin up to the Arcos Basin. This resulted in a latest Tortonian-earliest Messinian closure of the Betic Corridor, well before the onset of the Messinian Salinity Crisis. The timing of this closure is in agreement with results from the Huelva-1 core suggesting earliest Messinian signs of Betic Corridor restriction.

The whereabouts and dimensions of the connection that supplied Atlantic water to the Mediterranean during this crisis therefore remain currently unclear, but is just one of the many remaining uncertainties and unknowns in this marine gateway research. For example, recent studies with novel isotopic proxies that monitor connectivity explore the presence of Mediterranean water in the Atlantic and the amount of Atlantic water reaching the Mediterranean. However, these records are currently of too low resolution to capture the sub-precessional scale variability which is such a dominant feature of the hydrologic system active across the region. This in turn limits the constraints the data can provide for high resolution modelling experiments that explore both the gateway processes themselves and the impact of variable exchange on regional and global climate. In addition, the lack of a robust salinity proxy, able to function across the wide range of salinities that were produced during the MSC, is currently a major problem that has consequences for reconstructing gateway exchange since this is driven by the density contrast between the Mediterranean and Atlantic. Further research is needed to resolve these complex issues.

In short, this thesis gives a review on the Late Miocene Mediterranean-Atlantic gateways as a whole and new results, ideas and constraints on the Betic Corridor in particular. The most notable results are that the Mediterranean Messinian Salinity Crisis events also influenced the Spanish Atlantic margin, and Mediterranean Outflow Water was probably not present within the Messinian Guadalquivir Basin, which is in line with a late Tortonian closure of the Betic Corridor.

CONCLUSIONES

Los estrechos marítimos tienen una influencia importante tanto en los ambientales locales como en el clima regional y global. Un buen ejemplo del impacto que estos sistemas de conexión oceánica pueden llegar a tener lo brindan los estrechos marítimos Bético y Rifeño que durante el Mioceno tardío conectaron el Mar Mediterráneo con el Océano Atlántico. A partir del estudio de los sedimentos conservados en los corredores Bético (en el sur de España) y Rifeño (en el norte de Marruecos) se puede avanzar en el conocimiento sobre los procesos físicos y el impacto regional/global que tuvo el cierre de dichos estrechos.

A través de la construcción de un modelo de edad de alta resolución para el Mesiniense de la cuenca del Guadalquivir, la cual está localizada en el margen Atlántico del corredor Bético, se consiguió datar con alta precisión los cambios ambientales ocurridos en esta parte del corredor, así como evaluar su relevancia en un marco global. Dicho modelo de edad fue construido a partir de la calibración de los ciclos sedimentarios (cicloestratigrafía) presentes en los sedimentos de los sondeos Montemayor-1 y Huelva-1, que fueron perforados en el noroeste de la cuenca de Guadalquivir. Las margas aparentemente homogéneas que predominan en ambos sondeos, impidieron que la calibración de los ciclos con las curvas astronómicas se hiciese por inspección visual. Por lo tanto, se emplearon los cambios en la composición elemental de los sedimentos, los cuales se detectaron con fluorescencia de rayos X (XRF) a través del análisis de 1383 muestras. El método de XRF se calibró para detectar y quitar valores atípicos y para garantizar la reproducibilidad y fiabilidad de los valores elementales obtenidos con una pistola manual. Además se realizó una calibración extra mediante XRF convencional para comprobar que los cambios relativos en la composición geoquímica adquiridos manualmente son robustos. Finalmente, el modelo de edad se construyó calibrando dichas variaciones elementales con las curvas astronómicas, empleando como puntos de amarre varias dataciones magnetobioestratigráficas.

Con base en el modelo de edad propuesto, se realizaron varias interpretaciones sobre la evolución geológica de la Cuenca del Guadalquivir, y se evaluó su posible importancia regional y global mediante la relación con eventos propios del Océano Atlántico y el Mar Mediterráneo.

- Se encontraron dos cambios significativos en la tasa de sedimentación en ambos sondeos, Huelva-1 y Montemayor-1. Por lo tanto se consideró que éstos podrían

tener una relación con eventos regionales o globales. El primer cambio consiste en un aumento relativamente brusco de la tasa de sedimentación hace aproximadamente 5.55 Ma, el cual coincide con el inicio de la etapa final de la Crisis de Salinidad del Mesiniense (CSM) y con una fuerte desglaciación. El mecanismo más probable para explicar este cambio regional es un evento tectónico, el cual levantaría tectónicamente la región y promovería así un aumento de las tasas de erosión en la cuenca del Guadalquivir, así como la restricción de la conexión marítima Atlántico-Mediterránea. El segundo cambio abrupto en la tasa de sedimentación coincide con el límite Mioceno-Plioceno y con el restablecimiento de las condiciones marinas en el Mediterráneo, concluyendo la CSM. Estos eventos coetáneos pueden estar causados por subsidencia tectónica regional, cambios locales en la circulación oceánica asociados con la apertura y/o profundización del estrecho de Gibraltar.

- El aumento en la amplitud de los ciclos observado en la parte inferior del registro de Huelva-1 coincide con una primera restricción de la cuenca Mediterránea durante el Mesiniense temprano. Es posible que este cambio sedimentario este también relacionado con la restricción del corredor Bético, no obstante, se necesitan nuevos estudios para soportar esta hipótesis.
- Se reconoció un cambio gradual en la naturaleza de las fluctuaciones de la composición geoquímica de los sedimentos. Esta variación se asocia con un cambio paulatino en el ambiente de sedimentación de la cuenca del Guadalquivir, a medida que ésta progresivamente se colmataba. La parte inferior de ambos sondeos muestra una alternancia entre capas de carbonato biogénico y capas de material arcilloso terrígeno. El material terrígeno diluyó el carbonato biogénico durante los períodos de mayor flujo de ríos, inducidos por aumentos en la cantidad de insolación recibida durante los veranos del hemisferio norte. En el intervalo superior del registro, la naturaleza de los ciclos es diferente, probablemente como resultado de la somerización de la cuenca. En este ambiente marino somero, la sedimentación estuvo dominada por influjos de material terrestre de grano más grueso. La contribución de sedimentos limosos de origen detrítico aumentó debido al incremento de las tasas de erosión asociadas con una reducción de la cobertura vegetal durante los mínimos de insolación, lo que finalmente conllevó a la dilución del carbonato biogénico y la arcilla.
- Con base en el nuevo modelo de edad establecido para el sondeo Montemayor-1, se evidenció que el registro isotópico de oxígeno obtenido de foraminíferos bentónicos se correlaciona bien con registros previos del Atlántico, como son Ain el Beida, Loulja y la perforación ODP 982. Así mismo, los periodos glaciales TG12, TG14, TG20 y TG22, así como la deglaciación hacia TG11 y finalmente TG9 se expresan claramente en el registro del sondeo Montemayor-1. Las similitudes en los patrones de los registros isotópicos de oxígeno bentónico y

planctónico observadas entre Ain el Beida, Loulja y el sondeo Montemayor-1 reflejan señales típicas de mar abierto, sugiriendo una influencia directa de la masa de Agua Noratlántica Central y la ausencia total de Aguas Mediterráneas (Mediterranean Outflow Water-MOW) durante la sedimentación Mesiniense del sondeo Montemayor-1.

- Sin embargo, se observa una desviación entre los registros isotópicos de oxigeno bentónicos del sondeo Montemayor-1 y Ain el Beida para el último período glacial de Mesiniense (5.9 a 5.5 Ma), coincidiendo con las primeras etapas de la crisis. Esto podría ser el resultado de la disminución/cesación de la MOW en la región del estrecho de Gibraltar. No obstante, este desviación isotópica también podría ser consecuencia de la presencia de un flujo de MOW más salino o con mayor surgencia. Para entender completamente la evolución de MOW durante la CSM, se necesitan registros adicionales de alta resolución localizados en el margen Atlántico cerca del Estrecho de Gibraltar.

El levantamiento y la erosión resultante de los movimientos tectónicos que promovieron el cierre de los estrechos interoceánicos Bético y Rifeño, ha generado que la preservación de las secuencias sedimentarias dentro de los mismos corredores sea incompleta. No obstante, a partir de la distribución actual de sedimentos del Mioceno tardío en la región, se puede deducir que los principales canales interoceánicos se cerraron completamente antes de la precipitación de grandes volúmenes de halita durante la CSM. Sin embargo, la fecha de cierre del canal más occidental del corredor Bético, conocido como el corredor del Guadalhorce, es aún incierta. La cuenca de Ronda y la región de Antequera hacen parte de la región adyacente al corredor del Guadalhorce, conformando probablemente la zona más septentrional de este canal. En esta región, la secuencia sedimentaria muestra una somerización gradual del ambiente de depósito, identificado en el registro con el paso de margas a calcarenitas. Las nuevas dataciones bioestratigráficas realizadas en las margas señalaron en todos los casos una edad Tortoniense, anterior a 7.58 Ma. En consecuencia, es posible que la somerización de estas cuencas este asociada con una regresión regional durante el Tortoniense tardío, sugiriendo que el Corredor de Guadalhorce probablemente se cerró completamente durante el Tortoniense tardío-Mesiniense temprano.

Una regresión similar a la del Tortoniense tardío descrita para la cuenca de Ronda y la región de Antequera, ocurrió en la cuenca de Arcos, que está situada hacia al oeste de la cuenca de Ronda. Estas observaciones son contemporáneas con el levantamiento Tortoniense tardío y cierre de la cuenca de Granada, al este de Ronda. Por lo tanto, se sugiere que el periodo de levantamiento tectónico ocurrido durante el Tortoniense tardío en la región Bética oriental y que ocasionó el cierre de las ramificaciones orientales del corredor Bético, continuó hacia el oeste y elevó la región Bética occidental desde la cuenca de Granada hasta la cuenca de Arcos. Estos movimientos tectónicos

resultaron en el cierre del corredor Bético durante el Tortoniense tardío-Mesiniense temprano, mucho antes del inicio de la Crisis de Salinidad del Mesiniense. Estos resultados están en concordancia con los sedimentos de la base del sondeo Huelva-1, los cuales muestran que las primeras señales de restricción del corredor Bético ocurrieron durante el Mesiniense temprano.

La ubicación exacta y las dimensiones del canal (canales) que suministró agua del Océano Atlántico al Mar Mediterráneo durante la crisis son aún desconocidas, pero éstas son sólo algunas de las muchas incertidumbres que aún persisten en la investigación de los estrechos marítimos del Mioceno tardío. Estudios recientes basados en registros isotópicos, que buscan identificar el grado de conectividad de las aguas, han intentado reconstruir la presencia de aguas Mediterráneas en el Atlántico, así como las variaciones en el flujo de aguas Atlánticas que llegan al Mediterráneo. Sin embargo, estos nuevos registros tienen aún baja resolución temporal para capturar la variabilidad a escala sub-precesional de los flujos de aguas. Entender dicha variabilidad es fundamental ya que es una característica dominante del sistema hidrológico vigente en la región. La baja resolución de estos valores isotópicos además condiciona la interpretación que los registros sedimentarios pueden proporcionar a los experimentos de modelización que exploran a nivel teórico tanto los procesos que ocurren dentro de los estrechos, como el impacto que las variaciones en el intercambio de aguas tienen en el clima regional y global. La reconstrucción de intercambio en los corredores se ve además limitada por la falta de un indicador de salinidad que sea capaz de medir la amplia gama de salinidades que se produjeron durante la CSM, y que por tanto permita reconstruir los flujos de agua a partir de los contrastes de densidad entre corrientes de origen Mediterráneo o Atlántico. En consecuencia, es evidente que se necesitan nuevas investigaciones que permitan determinar las complejas características del intercambio de aguas Atlántico-Mediterráneas durante el Mioceno tardío.

En resumen, esta tesis brinda una visión general sobre los estrechos interoceánicos Atlántico-Mediterráneo que funcionaron durante el Mioceno tardío, prestando especial atención al corredor Bético, para el cual se presentan nuevos resultados cronoestratigráficos y evidencias en torno a su evolución geológica. Los resultados más notables son que los eventos de la CSM tuvieron también un efecto en el margen Atlántico español, sin embargo las aguas provenientes del Mediterráneo (MOW) probablemente no influenciaron los procesos sedimentarios de la cuenca del Guadalquivir durante el Mesiniense, lo cual concuerda con la hipótesis de cierre del corredor Bético durante el Tortoniense tardío-Mesiniense temprano.

Acknowledgements

These last four years since the Medgate interviews in Utrecht where it all started have been a real rollercoaster ride. The amount of new impressions and adventures I had, friends I made, skills I acquired, wonders I encountered, travels I enjoyed, problems I faced, in short experiences I have experienced, is enough for a lifetime. Even though it was great and worth every second of it, it wasn't always easy. Still, I can say now that it was a big success and the end is near, but I definitely did not do it alone, and could never have done it alone. Therefore there are a few (or actually many) people I would like to thank.

First of all, Paco Sierro. Thanks for being a supervisor who is kind, enthusiastic but critical, encouraging and flexible, all with a good sense of humour. Your door was always open if I needed something and at the same time you gave me the freedom to work also part time in Utrecht. I needed that. Thanks a lot.

Also thanks to Jose Abel Flores, not only for being my copromotor but also for introducing me to the great game of Padel. We were a great team and the conversations and discussion before and after the matches were very valuable.

Many thanks to all the great people at, or closely connected to, GGO: Anna, Blanca, Rocío, Jose Ignacio, Marta, Margarita, Montse, Eloy, German, Javi, Aleix, Raúl, Angelo, Felipe, Gloria, Miguel Angel, David, Lines, Chuchi and Misaki. Thanks for all the long coffee breaks in the bar (Gracias Vicente y Alberto!) the fun pincho nights and weekends away, and all the help whenever I needed that. A special thanks to Anna and Blanca, for being my cheerful and fun office mates, always providing sunshine and making it a warm, happy, place as well as providing me accommodation at their house when desperately needed. Unas gracias especiales para Jose Ignacio por introducirme en el mundo de música electrónica de los años 70.

Since Utrecht was practically my second home, thank you Frits Hilgen and Wout Krijgsman for being practically my 2nd and 3rd supervisors. It was great to have such outstanding researchers and great persons for any question that I had, from fieldwork ideas to trips, tuning problems, research focus, until whether we should have another beer (of course!). Thanks for always pushing and helping me into the right direction with any doubt I had.

Rachel Flecker and Carla Sands, thank you for Medgate. Thanks first of all for initiating this whole project, for bringing this amazing group of people together, for creating the positive, open atmosphere, for inexhaustible enthusiasm and energy and ideas, and doing that all in a structured and clear way, in short: Thanks for making Medgate what it was. Also thanks to all the supervisors and experts from other institutions that were so

willing to share their knowledge and expertise with us. This way, having 20 supervisors is a good thing.

But, this Medgate project was especially great, because of the great researchers that were in it. Evelina 'VIP' Dmitrieva, Dirk 'basically/this is great./modelling cobra' Simon, Alice 'onfire' Marzocchi, Jan Peter 'It's awesome!/so cool!' Mayser, Maria 'Hellooooooo/movie night/one more sample' Tulbure, Sevi 'I think we should go back to the hotel' Modestou and Walter 'mr./when does the work start/did you take sample /Medgate to heaven/fieldwork tiger/do you have powa?' Capella. There is only one way to summarize the ride we have been on, and that's by more of these shout outs we share and we should never forget: 'one more spoon!, what do you see?, 50 shades of clay, maybe we can model this, stupid PhDs, paper of the week, if you want to…, Gibraltar is the answer, reached, what's next?!' You were there. You know it. Enough said. Thanks.

A special thanks to Diana 'how are you today' Ochoa for all the great discussions and nights out we had in Salamanca, and helping me out when I needed it. Watching football matches or being airport VIPs together I will both never forget. One day we are still going to win the pub quiz!

But most of all a very special thanks to Marlies, because in the end there was no one more important for making my Spanish adventure into a success. Thanks for all the great lunches together, all the weekends hiking, all the parties, all the fieldtrips, all the heated discussions, all the critical questions, all the pinchos, all the mental support during writing, all the crazy plans, all the laughs about Spanish customs, all the advice on any kind of subject, all the laughter, all the caring. A PhD project is a personal journey but I always felt we were in this together.

Además, Muchas gracias a mi 'familia Española' de club tenis de mesa Salesianos Pizarrales y Peñaranda. Sois muy grandes y un grupo muy simpático con lo que ese deporte es algo mucho más grande que solo un deporte. No sabéis que importante habéis sido para mí por sentirme parte de vosotros y de Salamanca. Gracias por todo!

Ik wil al mijn vrienden in Amsterdam en omstreken bedanken voor het feit dat ze er altijd voor me waren, zelfs als ik er niet was, en altijd weer klaar stonden om me met open armen te ontvangen, al was het soms maar voor even. Er is veel veranderd in ons leven de afgelopen 4 jaar, maar dit niet, dit blijft, dat is zeker en dat is mooi.

Tom en Brigitte bedankt voor jullie rotsvaste vertrouwen in mij en alle lol, belangstelling en ondersteuning die jullie hebben gegeven. We zijn een geweldig team.

Jan en Sandra, bedankt voor de niet aflatende belangstelling in mij en mijn onderzoek. Jullie waren vaak een perfect klankbord voor mij om de voortgang en problemen in gewone-mensen-taal uit te leggen, wat soms ook voor mij zeer verhelderend was. Bedankt dat ik sowieso altijd bij jullie terecht kon.

Pap en mam, zonder jullie was ik er waarschijnlijk niet eens aan begonnen. Bedankt voor dat laatste zetje en ondersteuning wanneer ik het echt nodig had. Het is echt fijn om, hoeveel je ook weg bent, altijd ergens een warm nest te hebben met een rust en liefde die bijna vanzelfsprekend is.

Lieve Door, we did it! Samen! En hoe! bedankt voor je geloof in mij, je enthousiasme, liefde, doorzettingsvermogen, en je gigantische support, waarvan je het vaak zelf denk ik niet eens doorhad. Een 'komt wel goed' van jou doet meer dan je voor mogelijk houdt.

A police officer sees a man intently searching the ground near a lamppost and asks him the goal of his quest. The man replies that he is looking for his car keys, and the officer helps for a few minutes without success, then he asks whether the man is certain that he dropped the keys near the lamppost.

"No," is the reply, "I lost the keys somewhere across the street." "Why look here?" asks the surprised and irritated officer. "The light is much better here," the man responds with aplomb.

What's next?!

Bibliography

Abouchami, W., Galer, S.J.G. and Koschinsky, A., 1999. Pb and Nd isotopes in NE Atlantic Fe-Mn crusts: Proxies for trace metal paleosources and paleocean circulation. Geochimica Et Cosmochimica Acta, 63(10), 1489-1505.

Adams, C.G., Benson, R.H., Kidd, R.B., Ryan, W.B.F. and Wright, R.C., 1977. The Messinian salinity crisis and evidence of late Miocene eustatic changes in the world ocean. Nature, 269(5627), 383-386.

Aguirre, J. and Sánchez-Almazo, I.M., 2004. The Messinian post-evaporitic deposits of the Gafares area (Almerı´a-Nı´jar basin, SE Spain). A new view of the "Lago-Mare" facies. Sedimentary Geology, 168(1), 71-95.

Agustí, J., Garcés, M. and Krijgsman, W., 2006. Evidence for African–Iberian exchanges during the Messinian in the Spanish mammalian record. Palaeogeography, Palaeoclimatology, Palaeoecology, 238(1), 5-14.

Aitchison, J., 1986. The statistical analysis of compositional data. Springer.

Albarède, F. and Michard, A., 1987. Evidence for slowly changing 87Sr86Sr in runoff from freshwater limestones of southern France. Chemical Geology, 64(1), 55-65.

Alfaro, P., Delgado, J., Estévez, A., Soria, J. and Yébenes, A., 2002. Onshore and offshore compressional tectonics in the eastern Betic Cordillera (SE Spain). Marine Geology, 186(3), 337-349.

Ambar, I. and Howe, M., 1979. Observations of the Mediterranean outflow—II The deep circulation in the vicinity of the Gulf of Cadiz. Deep Sea Research Part A. Oceanographic Research Papers, 26(5), 555-568.

Ambar, I., Serra, N., Brogueira, M.J., Cabeçadas, G., Abrantes, F., Freitas, P., Gonçalves, C. and Gonzalez, N., 2002. Physical, chemical and sedimentological aspects of the Mediterranean outflow off Iberia. Deep-Sea Research Part II: Topical Studies in Oceanography, 49(19), 4163-4177.

Amorosi, A., Guidi, R., Mas, R. and Falanga, E., 2012. Glaucony from the Cretaceous of the Sierra de Guadarrama (Central Spain) and its application in a sequence-stratigraphic context. International Journal of Earth Sciences, 101(2), 415-427.

Andersson, P.S., Wasserburg, G., Ingri, J. and Stordal, M.C., 1994. Strontium, dissolved and particulate loads in fresh and brackish waters: the Baltic Sea and Mississippi Delta. Earth and Planetary Science Letters, 124(1), 195-210.

Armi, L. and Bray, N., 1982. A standard analytic curve of potential temperature versus salinity for the western North Atlantic. Journal of Physical Oceanography, 12(4), 384-387.

Artale, V., Calmanti, S. and Sutera, A., 2002. Thermohaline circulation sensitivity to intermediate-level anomalies. Tellus Series a-Dynamic Meteorology and Oceanography, 54(2), 159-174.

Azdimousa, A., Poupeau, G., Rezqi, H., Asebriy, L., Bourgois, J. and Ait Brahim, L., 2006. Géodynamique des bordures méridionales de la mer d'Alboran; application de la stratigraphie séquentielle dans le bassin néogène de Boudinar (Rif oriental, Maroc). Bulletin de l'Institut Scientifique, Rabat(28), 9-18.

Bache, F., Popescu, S.M., Rabineau, M., Gorini, C., Suc, J.P., Clauzon, G., Olivet, J.L., Rubino, J.L., Melinte-Dobrinescu, M.C. and Estrada, F., 2012. A two-step process for the reflooding of the Mediterranean after the Messinian Salinity Crisis. Basin Research, 24(2), 125-153.

Baggley, K.A., 2000. The Late Tortonian-Early Messinian foraminiferal record of the Abad Member (turre formation), Sorbas Basin, Almeria, south-east Spain. Palaeontology, 43, 1069-1112.

Bahr, A., Jiménez-Espejo, F.J., Kolasinac, N., Grunert, P., Hernández-Molina, F.J., Röhl, U., Voelker, A.H., Escutia, C., Stow, D.A. and Hodell, D., 2014. Deciphering bottom current velocity and paleoclimate signals from contourite deposits in the Gulf of Cádiz during the last 140 kyr: An inorganic geochemical approach. Geochemistry, Geophysics, Geosystems, 15(8), 3145-3160.

Baldi, K. and Hohenegger, J., 2008. Paleoecology of benthic foraminifera of the Baden-Sooss section (Badenian, Middle Miocene, Vienna Basin, Austria). Geologica Carpathica, 59(5), 411-424.

Banerjee, S., Bansal, U. and Thorat, A., 2015. A review on palaeogeographic implications and temporal variation in glaucony composition. Journal of Palaeogeography.
Barbieri, R. and Ori, G.G., 2000. Neogene palaeoenvironmental evolution in the Atlantic side of the Rifian Corridor (Morocco). Palaeogeography Palaeoclimatology Palaeoecology, 163(1-2), 1-31.
Barhoun, N. and Wernli, R., 1999. Biostratigraphy from the Mio-Pliocene of the Boudinar basin by planktic foraminifera (northeastern Rif, Morocco). Revue de Paleobiologie, 18(2), 491-508.
Baringer, M.O. and Price, J.F., 1999. A review of the physical oceanography of the Mediterranean outflow. Marine Geology, 155(1-2), 63-82.
Bartoli, G., Sarnthein, M., Weinelt, M., Erlenkeuser, H., Garbe-Schönberg, D. and Lea, D.W., 2005. Final closure of Panama and the onset of northern hemisphere glaciation. Earth and Planetary Science Letters, 237(1–2), 33-44.
Bassetti, M.A., Miculan, P. and Lucchi, F.R., 2003. Ostracod faunas and brackish-water environments of the late Messinian Sapigno section (northern Apennines, Italy). Palaeogeography Palaeoclimatology Palaeoecology, 198(3-4), 335-352.
Bassetti, M.A., Miculan, P. and Sierro, F.J., 2006. Evolution of depositional environments after the end of Messinian Salinity Crisis in Nijar Basin (SE Betic Cordillera). Sedimentary Geology, 188, 279-295.
Bellanca, A., Caruso, A., Ferruzza, G., Neri, R., Rouchy, J.M., Sprovieri, M. and Blanc-Valleron, M.M., 2001. Transition from marine to hypersaline conditions in the Messinian Tripoli Formation from the marginal areas of the central Sicilian Basin. Sedimentary Geology, 140(1-2), 87-105.
Benammi, M., Calvo, M., Prevot, M. and Jaeger, J.J., 1996. Magnetostratigraphy and paleontology of Ait Kandoula Basin (High Atlas, Morocco) and the African-European late Miocene terrestrial fauna exchanges. Earth and Planetary Science Letters, 145(1-4), 15-29.
Benson, R.H., Rakic-El Bied, K. and Bonaduce, G., 1991. An important current reversal (influx) in the Rifian Corridor (Morocco) at the Tortonian-Messinian boundary: The end of Tethys Ocean. Paleoceanography, 6(1), 165-192.
Berástegui, X., Banks, C.J., Puig, C., Taberner, C., Waltham, D. and Fernández, M., 1998. Lateral diapiric emplacement of Triassic evaporites at the southern margin of the Guadalquivir Basin, Spain. Geological Society, London, Special Publications, 134(1), 49-68.
Berger, A., 1977. Support for the astronomical theory of climatic change. Nature, 269(5623), 44-45.
Berger, A., 1978. Long-term variations of caloric insolation resulting from the Earth's orbital elements. Quaternary Research, 9(2), 139-167.
Berggren, W. and Haq, B.U., 1976. The Andalusian stage (Late Miocene): biostratigraphy, biochronology and paleoecology. Palaeogeography, Palaeoclimatology, Palaeoecology, 20(1), 67-129.
Bertini, A., Londeix, L., Maniscalco, R., Di Stefano, A., Suc, J.P., Clauzon, G., Gautier, F. and Grasso, M., 1998. Paleobiological evidence of depositional conditions in the Salt Member, Gessoso-Solfifera Formation (Messinian, Upper Miocene) of Sicily. Micropaleontology, 44(4), 413-433.
Bertini, A., 2006. The Northern Apennines palynological record as a contribute for the reconstruction of the Messinian palaeoenvironments. Sedimentary Geology, 188, 235-258.
Béthoux, J., 1984. Paleoceanographic changes in the Mediterranean-Sea in the last 20,000 years. Oceanologica Acta, 7(1), 43-48.
Betzler, C., Braga, J.C., Martín, J.M., Sánchez-Almazo, I.M. and Lindhorst, S., 2006. Closure of a seaway: stratigraphic record and facies (Guadix basin, Southern Spain). International Journal of Earth Sciences, 95(5), 903-910.
Bigg, G.R. and Wadley, M.R., 2001. Millennial-scale variability in the oceans: an ocean modelling view. Journal of Quaternary Science, 16(4), 309-319.
Blanc, P.L., 2000. Of sills and straits: a quantitative assessment of the Messinian Salinity Crisis. Deep-Sea Research Part I-Oceanographic Research Papers, 47(8), 1429-1460.

Blanc, P.-L., 2002. The opening of the Plio-Quaternary Gibraltar Strait: assessing the size of a cataclysm. Geodinamica Acta, 15(5-6), 303-317.

Blanc-Valleron, M.M., Pierre, C., Caulet, J.P., Caruso, A., Rouchy, J.M., Cespuglio, G., Sprovieri, R., Pestrea, S. and Di Stefano, E., 2002. Sedimentary, stable isotope and micropaleontological records of paleoceanographic change in the Messinian Tripoli Formation (Sicily, Italy). Palaeogeography Palaeoclimatology Palaeoecology, 185(3-4), 255-286.

Böhme, M., Ilg, A. and Winklhofer, M., 2008. Late Miocene "washhouse" climate in Europe. Earth and Planetary Science Letters, 275(3), 393-401.

Bosmans, J.H.C., Drijfhout, S.S., Tuenter, E., Hilgen, F.J., Lourens, L.J. and Rohling, E.J., 2015. Precession and obliquity forcing of the freshwater budget over the Mediterranean. Quaternary Science Reviews, 123, 16-30.

Bourillot, R., Vennin, E., Rouchy, J.-M., Blanc-Valleron, M.-M., Caruso, A. and Durlet, C., 2010. The end of the Messinian Salinity Crisis in the western Mediterranean: Insights from the carbonate platforms of south-eastern Spain. Sedimentary Geology, 229(4), 224-253.

Bozzano, G., Kuhlmann, H. and Alonso, B., 2002. Storminess control over African dust input to the Moroccan Atlantic margin (NW Africa) at the time of maxima boreal summer insolation: a record of the last 220 kyr. Palaeogeography, Palaeoclimatology, Palaeoecology, 183(1), 155-168.

Brackenridge, R.E., Hernandez-Molina, F.J., Stow, D.A.V. and Llave, E., 2013. A Pliocene mixed contourite-turbidite system offshore the Algarve Margin, Gulf of Cadiz: Seismic response, margin evolution and reservoir implications. Marine and Petroleum Geology, 46, 36-50.

Bradshaw, C.D., Lunt, D.J., Flecker, R., Salzmann, U., Pound, M.J., Haywood, A.M. and Eronen, J.T., 2012. The relative roles of CO2 and palaeogeography in determining late Miocene climate: results from a terrestrial model-data comparison. Climate of the Past, 8(4), 1257-1285.

Braga, J.C., Martín, J.M., Riding, R., Aguirre, J., Sánchez-Almazo, I.M. and Dinarès-Turell, J., 2006. Testing models for the Messinian salinity crisis: the Messinian record in Almería, SE Spain. Sedimentary Geology, 188, 131-154.

Brayshaw, D.J., Rambeau, C.M.C. and Smith, S.J., 2011. Changes in Mediterranean climate during the Holocene: Insights from global and regional climate modelling. Holocene, 21(1), 15-31.

Bruch, A.A., Uhl, D. and Mosbrugger, V., 2007. Miocene climate in Europe - Patterns and evolution - A first synthesis of NECLIME. Palaeogeography Palaeoclimatology Palaeoecology, 253(1-2), 1-7.

Bryden, H. and Stommel, H., 1984. Limiting processes that determine basic features of the circulation in the Mediterranean-Sea. Oceanologica Acta, 7(3), 289-296.

Bryden, H.L. and Kinder, T.H., 1991. Steady two-layer exchange through the Strait of Gibraltar. Deep Sea Research Part A. Oceanographic Research Papers, 38, S445-S463.

Campillo, A., Maldonado, A. and Mauffret, A., 1992. Stratigraphic and tectonic evolution of the western Alboran Sea: Late Miocene to Recent. Geo-Marine Letters, 12(2-3), 165-172.

Candela, J., Winant, C. and Ruiz, A., 1990. Tides in the Strait of Gibraltar. Journal of Geophysical Research: Oceans, 95(C5), 7313-7335.

Capron, A., Deverchere, J., Gaullier, V., Le Roy, S., Mecier de Lepinay, B. and Yelles, A.K., 2011. Algerian Margin: Regional Settings. In: J. Lofi. (Ed.), Seismic atlas of the Messinian Salinity Crisis markers in the Mediterranean and Black Seas, Mémoire de la Société Géologique, pp. 1-72.

Carnevale, G., Landini, W. and Sarti, G., 2006. Mare versus Lago-mare: marine fishes and the Mediterranean environment at the end of the Messinian Salinity Crisis. Journal of the Geological Society, 163(1), 75-80.

Carnevale, G., Longinelli, A., Caputo, D., Barbieri, M. and Landini, W., 2008. Did the Mediterranean marine reflooding precede the Mio–Pliocene boundary? Paleontological and geochemical evidence from upper Messinian sequences of Tuscany, Italy. Palaeogeography, Palaeoclimatology, Palaeoecology, 257(1), 81-105.

Cerdan, O., Govers, G., Le Bissonnais, Y., Van Oost, K., Poesen, J., Saby, N., Gobin, A., Vacca, A., Quinton, J. and Auerswald, K., 2010. Rates and spatial variations of soil erosion in Europe: a study based on erosion plot data. Geomorphology, 122(1), 167-177.
Chalouan, A., Michard, A., El Kadiri, K., Negro, F., de Lamotte, D.F., Soto, J. and Saddiqi, O., 2008. The Rif Belt. Springer.
Chan, W.-L. and Motoi, T., 2003. Effects of stopping the Mediterranean outflow on the southern polar region. Polar meteorology and glaciology, 17, 25-35.
Chmeleff, J., von Blanckenburg, F., Kossert, K. and Jakob, D., 2010. Determination of the Be-10 half-life by multicollector ICP-MS and liquid scintillation counting. Nuclear Instruments & Methods in Physics Research Section B-Beam Interactions with Materials and Atoms, 268(2), 192-199.
Christensen, J.N., Halliday, A.N., Godfrey, L.V., Hein, J.R. and Rea, D.K., 1997. Climate and ocean dynamics and the lead isotopic records in Pacific ferromanganese crusts. Science, 277(5328), 913-918.
CIESM, 2008. The Messinian salinity crisis from mega-deposits to microbiology. in: F. Briand (Ed.), A consensus report, in 33ème CIESM Workshop Monographs, 33CIESM, 16, bd de Suisse, MC-98000, Monaco(33), 1-168.
Cifelli, F., Mattei, M. and Porreca, M., 2008. New paleomagnetic data from Oligocene–upper Miocene sediments in the Rif chain (northern Morocco): insights on the Neogene tectonic evolution of the Gibraltar arc. Journal of Geophysical Research: Solid Earth, 113(B2).
Civis, J., Sierro, F., González-Delgado, J., Flores, J., Andrés, I., Porta, J.d. and Valle, M., 1987. El Neógeno marino de la provincia de Huelva, antecedentes y definición de las unidades litoestratigráficas. Paleontología del Neógeno de Huelva, 9-21.
Clauzon, G., 1982. Le canyon messinien du Rhone; une preuve decive du" desiccated deep-basin model"(Hsue, Cita and Ryan, 1973). Bulletin de la Société géologique de France(3), 597-610.
Clauzon, G., Suc, J.P., Gautier, F., Berger, A. and Loutre, M.F., 1996. Alternate interpretation of the Messinian salinity crisis: Controversy resolved? Geology, 24(4), 363-366.
Coiffait, B., Coiffait, P.E. and Jaeger, J.J., 1985. DISCOVERY OF THE GENERA STEPHANOMYS AND CASTILLOMYS (MURIDAE) IN NORTHERN AFRICA, IN A NEW DEPOSIT OF NEOGENIC MICROVERTEBRAE FROM EASTERN ALGERIA - ARGOUB-KEMELLAL. Proceedings of the Koninklijke Nederlandse Akademie Van Wetenschappen Series B-Palaeontology Geology Physics Chemistry Anthropology, 88(2), 167-183.
Comas, M., Platt, J., Soto, J. and Watts, A., 1999. 44. The origin and Tectonic History of the Alboran Basin: Insights from Leg 161 Results, Proceedings of the Ocean Drilling Program Scientific Results, pp. 555-580.
Corbí, H., Lancis, C., García-García, F., Pina, J.-A., Soria, J.M., Tent-Mancís, J.E. and Viseras, C., 2012. Updating the marine biostratigraphy of the Granada Basin (central Betic Cordillera). Insight for the Late Miocene palaeogeographic evolution of the Atlantic-Mediterranean seaway. Geobios, 45(3), 249-263.
Cornee, J.J., Roger, S., Munch, P., St Martin, J.P., Feraud, G., Conesa, G. and Pestrea-St Martin, S., 2002. Messinian events: new constraints from sedimentological investigations and new Ar-40/Ar-39 ages in the Melilla-Nador Basin (Morocco). Sedimentary Geology, 151(1-2), 127-147.
Criado-Aldeanueva, F., García-Lafuente, J., Vargas, J.M., Del Río, J., Vazquez, A., Reul, A. and Sánchez, A., 2006. Distribution and circulation of water masses in the Gulf of Cadiz from in situ observations. Deep Sea Research Part II: Topical Studies in Oceanography, 53(11), 1144-1160.
Cunningham, K.J., Farr, M. and Rakic-El Bied, K., 1994. Magnetostratigraphic dating of an upper Miocene shallow-marine and continental sedimentary succession in northeastern Morocco. Earth and Planetary Science Letters, 127(1), 77-93.
Cunningham, K.J., Benson, R.H., Rakic-El Bied, K. and McKenna, L.W., 1997. Eustatic implications of late Miocene depositional sequences in the Melilla Basin, northeastern Morocco. Sedimentary Geology, 107(3), 147-165.

Cunningham, K.J. and Collins, L.S., 2002. Controls on facies and sequence stratigraphy of an upper Miocene carbonate ramp and platfonn, Melilla basin, NE Morocco. Sedimentary Geology, 146(3-4), 285-304.
Curry, R., Dickson, B. and Yashayaev, I., 2003. A change in the freshwater balance of the Atlantic Ocean over the past four decades. Nature, 426(6968), 826-829.
Dabrio, C.J., Fernández, J., Peña, J.A., Ruiz Bustos, A. and Sanz de Galdeano, C.M., 1978. Rasgos sedimentarios de los conglomerados miocénicos del borde noreste de la Depresión de Granada. Estudios Geológicos, 34, 89-97.
Damnati, B., Petit-Maire, N., Fontugne, M., Meco, J. and Williamson, D., 1996. Quaternary palaeoclimates in the eastern Canary Islands. Quaternary International, 31, 37-46.
Davis, J.C. and Sampson, R.J., 2002. Statistics and data analysis in geology. Wiley New York.
de la Vara, A., Topper, R.P., Meijer, P.T. and Kouwenhoven, T.J., 2015. Water exchange through the Betic and Rifian corridors prior to the Messinian Salinity Crisis: A model study. Paleoceanography, 30(5), 548-557.
de Lange, G.J. and Krijgsman, W., 2010. Messinian salinity crisis: A novel unifying shallow gypsum/deep dolomite formation mechanism. Marine Geology, 275(1-4), 273-277.
Dean, R. and Dixon, W., 1951. Simplified statistics for small numbers of observations. Analytical Chemistry, 23(4), 636-638.
Debenedetti, A., 1976. Messinian salt deposits in the Mediterranean; evaporites or precipitates? Bollettino della Societa Geologica Italiana, 95(5), 941-948.
Debenedetti, A., 1982. THE PROBLEM OF THE ORIGIN OF THE SALT DEPOSITS IN THE MEDITERRANEAN AND OF THEIR RELATIONS TO THE OTHER SALT OCCURRENCES IN THE NEOGENE FORMATIONS OF THE CONTIGUOUS REGIONS. Marine Geology, 49(1-2), 91-114.
Debenedetti, A., 1982. The problem of the origin of the salt deposits in the Mediterranean and of their relations to the other salt occurrences in the Neogene formations of the contiguous regions. Marine Geology, 49(1-2), 91-114.
Dennison, J.M. and Hay, W.W., 1967. Estimating the Needed Sampling Area for Subaquatic Ecologic Studies. Journal of Paleontology, 41(3), 706-708.
Dewey, J., Helman, M., Knott, S., Turco, E. and Hutton, D., 1989. Kinematics of the western Mediterranean. Geological Society, London, Special Publications, 45(1), 265-283.
Di Stefano, A., Verducci, M., Lirer, F., Ferraro, L., Iaccarino, S.M., Husing, S.K. and Hilgen, F.J., 2010. Paleoenvironmental conditions preceding the Messinian Salinity Crisis in the Central Mediterranean: Integrated data from the Upper Miocene Trave section (Italy). Palaeogeography Palaeoclimatology Palaeoecology, 297(1), 37-53.
Dietrich, D.E., Tseng, Y.-H., Medina, R., Piacsek, S.A., Liste, M., Olabarrieta, M., Bowman, M.J. and Mehra, A., 2008. Mediterranean Overflow Water (MOW) simulation using a coupled multiple-grid Mediterranean Sea/North Atlantic Ocean model. Journal of Geophysical Research-Oceans, 113(C7).
Doglioni, C., Gueguen, E., Sabat, F. and Fernandez, M., 1997. The Western Mediterranean extensional basins and the Alpine orogen. Terra Nova, 9(3), 109-112.
Duggen, S., Hoernle, K., van den Bogaard, P., Rupke, L. and Phipps Morgan, J., 2003. Deep roots of the Messinian salinity crisis. Nature, 422(6932), 602-606.
Duggen, S., Hoernle, K., van den Bogaard, P. and Harris, C., 2004. Magmatic evolution of the Alboran region: The role of subduction in forming the western Mediterranean and causing the Messinian Salinity Crisis. Earth and Planetary Science Letters, 218(1-2), 91-108.
Duque-Caro, H., 1990. Neogene stratigraphy, paleoceanography and paleobiogeography in northwest South America and the evolution of the Panama Seaway. Palaeogeography, Palaeoclimatology, Palaeoecology, 77(3), 203-234.
Eronen, J.T., Puolamaki, K., Liu, L., Lintulaakso, K., Damuth, J., Janis, C. and Fortelius, M., 2010. Precipitation and large herbivorous mammals I: estimates from present-day communities. Evolutionary Ecology Research, 12(2), 217-233.

Esteras, M., Izquierdo, J., Sandoval, N. and Mamad, A., 2000. Evolución morfológica y estratigráfica plio-cuaternaria del Umbral de Camarinal (Estrecho de Gibraltar) basada en sondeos marinos. Rev Soc Geol España, 13(3/4), 539-550.
Estrada, F., Ercilla, G., Gorini, C., Alonso, B., Vázquez, J.T., García-Castellanos, D., Juan, C., Maldonado, A., Ammar, A. and Elabbassi, M., 2011. Impact of pulsed Atlantic water inflow into the Alboran Basin at the time of the Zanclean flooding. Geo-Marine Letters, 31(5-6), 361-376.
Fatela, F. and Taborda, R., 2002. Confidence limits of species proportions in microfossil assemblages. Marine Micropaleontology, 45(2), 169-174.
Feinberg, H., 1986. Les séries tertiaires des zones externes du Rif (Maroc): biostratigraphie, paléogéographie et aperçu tectonique. Éditions du Service géologique du Maroc.
Fenton, M., Geiselhart, S., Rohling, E.J. and Hemleben, C., 2000. Aplanktonic zones in the Red Sea. Marine Micropaleontology, 40(3), 277-294.
Fernandes, R., Ambrosius, B., Noomen, R., Bastos, L., Wortel, M., Spakman, W. and Govers, R., 2003. The relative motion between Africa and Eurasia as derived from ITRF2000 and GPS data. Geophysical Research Letters, 30(16).
Fernández, M., Berástegui, X., Puig, C., García-Castellanos, D., Jurado, M.J., Torné, M. and Banks, C., 1998. Geophysical and geological constraints on the evolution of the Guadalquivir foreland basin, Spain. Geological Society, London, Special Publications, 134(1), 29-48.
Flecker, R. and Ellam, R.M., 1999. Distinguishing climatic and tectonic signals in the sedimentary successions of marginal basins using Sr isotopes: an example from the Messinian salinity crisis, Eastern Mediterranean. Journal of the Geological Society, 156, 847-854.
Flecker, R., de Villiers, S. and Ellam, R.M., 2002. Modelling the effect of evaporation on the salinity-Sr-87/Sr-86 relationship in modern and ancient marginal-marine systems: the Mediterranean Messinian Salinity Crisis. Earth and Planetary Science Letters, 203(1), 221-233.
Flecker, R. and Ellam, R.M., 2006. Identifying Late Miocene episodes of connection and isolation in the Mediterranean-Paratethyan realm using Sr isotopes. Sedimentary Geology, 188, 189-203.
Flecker, R., Krijgsman, W., Capella, W., de Castro Martíns, C., Dmitrieva, E., Mayser, J.P., Marzocchi, A., Modestu, S., Ochoa, D., Simon, D., Tulbure, M., van den Berg, B., van der Schee, M., de Lange, G., Ellam, R., Govers, R., Gutjahr, M., Hilgen, F., Kouwenhoven, T., Lofi, J., Meijer, P., Sierro, F.J., Bachiri, N., Barhoun, N., Alami, A.C., Chacon, B., Flores, J.A., Gregory, J., Howard, J., Lunt, D., Ochoa, M., Pancost, R., Vincent, S. and Yousfi, M.Z., 2015. Evolution of the Late Miocene Mediterranean–Atlantic gateways and their impact on regional and global environmental change. Earth-Science Reviews, 150, 365-392.
Flinch, J.F., 1994. Tectonic evolution of the Gibraltar Arc, Rice University.
Flores, J.A., Sierro, F.J., Filippelli, G.M., Barcena, M.A., Perez-Folgado, M., Vazquez, A. and Utrilla, R., 2005. Surface water dynamics and phytoplankton communities during deposition of cyclic late Messinian sapropel sequences in the western Mediterranean. Marine Micropaleontology, 56(1-2), 50-79.
Flower, B. and Kennett, J., 1993. Middle Miocene ocean-climate transition: High-resolution oxygen and carbon isotopic records from Deep Sea Drilling Project Site 588A, southwest Pacific. Paleoceanography, 8(6), 811-843.
Fontboté, J., Guimerà, J., Roca, E., Sàbat, F., Santanach, P. and Fernández-Ortigosa, F., 1990. The Cenozoic geodynamic evolution of the Valencia trough (western Mediterranean). Revista de la Sociedad Geológica de españa, 3(2), 7-18.
Fortuin, A., Krijgsman, W., Hilgen, F. and Sierro, F., 2000. Late Miocene Mediterranean desiccation: topography and significance of the 'Salinity Crisis' erosion surface on-land in southeast Spain: Comment. Sedimentary Geology, 133(3), 167-174.
Fortuin, A.R. and Krijgsman, W., 2003. The Messinian of the Nijar Basin (SE Spain): sedimentation, depositional environments and paleogeographic evolution. Sedimentary Geology, 160(1–3), 213-242.

Frank, M., 2002. Radiogenic isotopes: Tracers of past ocean circulation and erosional input. Reviews of Geophysics, 40(1).
Frank, M., Whiteley, N., Kasten, S., Hein, J.R. and O'Nions, K., 2002. North Atlantic deep water export to the Southern Ocean over the past 14 Myr: Evidence from Nd and Pb isotopes in ferromanganese crusts. Paleoceanography, 17(2).
Fullea, J., Fernandez, M., Afonso, J.C., Verges, J. and Zeyen, H., 2010. The structure and evolution of the lithosphere-asthenosphere boundary beneath the Atlantic-Mediterranean Transition Region. Lithos, 120(1-2), 74-95.
Galán, E., González, I., Mayoral, E. and Vázquez, M., 1989. Caracterizacion y origen de la facies glauconitica de la cuenca del Guadalquivir. Estudios geológicos, 45(3-4), 169-175.
Garcés, M., Krijgsman, W. and Agustí• , J., 1998. Chronology of the late Turolian deposits of the Fortuna basin (SE Spain): implications for the Messinian evolution of the eastern Betics. Earth and Planetary Science Letters, 163(1), 69-81.
Garcés, M., Krijgsman, W. and Agustí, J., 2001. Chronostratigraphic framework and evolution of the Fortuna basin (Eastern Betics) since the Late Miocene. Basin Research, 13(2), 199-216.
Garcia, M., Hernandez-Molina, F.J., Llave, E., Stow, D.A.V., Leon, R., Fernandez-Puga, M.C., del Rio, V.D. and Somoza, L., 2009. Contourite erosive features caused by the Mediterranean Outflow Water in the Gulf of Cadiz: Quaternary tectonic and oceanographic implications. Marine Geology, 257(1-4), 24-40.
García Lafuente, J., Sánchez Román, A., Díaz del Río, G., Sannino, G. and Sánchez Garrido, J., 2007. Recent observations of seasonal variability of the Mediterranean outflow in the Strait of Gibraltar. Journal of Geophysical Research: Oceans, 112(C10).
Garcia-Castellanos, D., Estrada, F., Jiménez-Munt, I., Gorini, C., Fernández, M., Vergés, J. and De Vicente, R., 2009. Catastrophic flood of the Mediterranean after the Messinian salinity crisis. Nature, 462(7274), 778-781.
Garcia-Castellanos, D. and Villaseñor, A., 2011. Messinian salinity crisis regulated by competing tectonics and erosion at the Gibraltar arc. Nature, 480(7377), 359-363.
García-Castellanos, D., Fernandez, M. and Torné, M., 2002. Modeling the evolution of the Guadalquivir foreland basin (southern Spain). Tectonics, 21(3), 9-1-9-17.
García-Lafuente, J., Delgado, J., Criado-Aldeanueva, F., Bruno, M., del Río, J. and Vargas, J.M., 2006. Water mass circulation on the continental shelf of the Gulf of Cadiz. Deep Sea Research Part II: Topical Studies in Oceanography, 53(11), 1182-1197.
Gargani, J. and Rigollet, C., 2007. Mediterranean Sea level variations during the Messinian salinity crisis. Geophysical research letters, 34(10).
Gibert, L., Scott, G.R., Montoya, P., Ruiz-Sánchez, F.J., Morales, J., Luque, L., Abella, J. and Lería, M., 2013. Evidence for an African-Iberian mammal dispersal during the pre-evaporitic Messinian. Geology, 41(6), 691-694.
Gladstone, R., Flecker, R., Valdes, P., Lunt, D. and Markwick, P., 2007. The Mediterranean hydrologic budget from a Late Miocene global climate simulation. Palaeogeography Palaeoclimatology Palaeoecology, 251(2), 254-267.
Gläser, I. and Betzler, C., 2002. Facies partitioning and sequence stratigraphy of cool-water, mixed carbonate-siliciclastic sediments (Upper Miocene Guadalquivir Domain, southern Spain). International Journal of Earth Sciences, 91(6), 1041-1053.
González-Delgado, J.A., Civis, J., Dabrio, C.J., Goy, J.L., Ledesma, S., Pais, J., Sierro, F.J. and Zazo, C., 2004. Cuenca del Guadalquivir. Geología de España: Madrid, Sociedad Geológica Española, Instituto Geológico y Minero Español, 543-550.
Govers, R., 2009. Choking the Mediterranean to dehydration: the Messinian salinity crisis. Geology, 37(2), 167-170.
Gradstein, F.M., Ogg, G. and Schmitz, M., 2012. The Geologic Time Scale 2012 2-Volume Set. Elsevier.
Griffin, D.L., 1999. The late Miocene climate of northeastern Africa: unravelling the signals in the sedimentary succession. Journal of the Geological Society, 156, 817-826.

Griffin, D.L., 2002. Aridity and humidity: two aspects of the late Miocene climate of North Africa and the Mediterranean. Palaeogeography Palaeoclimatology Palaeoecology, 182(1-2), 65-91.
Group, M., 2002. Medatlas 2002: Mediterranean and Black Sea Database of Temperature, Salinity and Biochemical Parameters—Climatological Atlas. Comm. Mar. Sci. and Technol. Programme (MAST), Ifremer, Brest, France.(Available at www. ifremer. fr/sismer/program/medar/).
Gueguen, E., Doglioni, C. and Fernandez, M., 1998. On the post-25 Ma geodynamic evolution of the western Mediterranean. Tectonophysics, 298(1-3), 259-269.
Guerra-Merchan, A., Serrano, F., Garces, M., Gofas, S., Esu, D., Gliozzi, E. and Grossi, F., 2010. Messinian Lago-Mare deposits near the Strait of Gibraltar (Malaga Basin, S Spain). Palaeogeography Palaeoclimatology Palaeoecology, 285(3-4), 264-276.
Gutjahr, M., Frank, M., Halliday, A.N. and Keigwin, L.D., 2009. Retreat of the Laurentide ice sheet tracked by the isotopic composition of Pb in western North Atlantic seawater during termination 1. Earth and Planetary Science Letters, 286(3-4), 546-555.
Gutscher, M.-A., Malod, J., Rehault, J.-P., Contrucci, I., Klingelhoefer, F., Mendes-Victor, L. and Spakman, W., 2002. Evidence for active subduction beneath Gibraltar. Geology, 30(12), 1071-1074.
Gutscher, M.A., Dominguez, S., Westbrook, G.K., Le Roy, P., Rosas, F., Duarte, J.C., Terrinha, P., Miranda, J.M., Graindorge, D., Gailler, A., Sallares, V. and Bartolome, R., 2012. The Gibraltar subduction: A decade of new geophysical data. Tectonophysics, 574, 72-91.
Hammer, Ø., Harper, D. and Ryan, P., 2001. PAST: Paleontological Statistics Software Package for education and data analysis. Palaeontolia Electronica 4.
Harlavan, Y. and Erel, Y., 2002. The release of Pb and REE from granitoids by the dissolution of accessory phases. Geochimica Et Cosmochimica Acta, 66(5), 837-848.
Harris, L. and Whiting, B., 2000. Sequence-stratigraphic significance of Miocene to Pliocene glauconite-rich layers, on-and offshore of the US Mid-Atlantic margin. Sedimentary Geology, 134(1), 129-147.
Harvey, A.M., Wigand, P.E. and Wells, S.G., 1999. Response of alluvial fan systems to the late Pleistocene to Holocene climatic transition: contrasts between the margins of pluvial Lakes Lahontan and Mojave, Nevada and California, USA. Catena, 36(4), 255-281.
Haug, G.H. and Tiedemann, R., 1998. Effect of the formation of the Isthmus of Panama on Atlantic Ocean thermohaline circulation. Nature, 393(6686), 673-676.
Hayes, D.E., Pimm, A.C., Beckmann, J.P., Benson, W.E., Berger, W.H., Roth, P.H., Supko, P.R. and von Rad, U., 1972. Site 135, Initial Reports of the Deep Sea Drilling Project. XIV, 15-48.
Hecht, M., Holland, W., Artale, V. and Pinardi, N., 1997. North Atlantic model sensitivity to Mediterranean waters. Assessing Climate Change: Results from the Model Evaluation Consortium for Climate Assessment, 169-191.
Henderson, G.M. and Maier-Reimer, E., 2002. Advection and removal of Pb-210 and stable Pb isotopes in the oceans: A general circulation model study. Geochimica Et Cosmochimica Acta, 66(2), 257-272.
Henry, F., Jeandel, C., Dupre, B. and Minster, J.-F., 1994. Particulate and dissolved Nd in the western Mediterranean Sea: sources, fate and budget. Marine chemistry, 45(4), 283-305.
Hernández-Molina, F., Stow, D., Alvarez-Zarikian, C., Acton, G., Bahr, A., Balestra, B., Ducassou, E., Flood, R., Flores, J.-A. and Furota, S., 2013. IODP Expedition 339 in the Gulf of Cadiz and off West Iberia: decoding the environmental significance of the Mediterranean outflow water and its global influence. Scientific Drilling, 16, 1-11.
Hernández-Molina, F.J., Stow, D.A., Alvarez-Zarikian, C.A., Acton, G., Bahr, A., Balestra, B., Ducassou, E., Flood, R., Flores, J.-A. and Furota, S., 2014. Onset of Mediterranean outflow into the North Atlantic. Science, 344(6189), 1244-1250.
Herold, N., Huber, M., Müller, R. and Seton, M., 2012. Modeling the Miocene climatic optimum: Ocean circulation. Paleoceanography, 27(1).
Higueras, P., Oyarzun, R., Iraizoz, J., Lorenzo, S., Esbrí, J. and Martínez-Coronado, A., 2012. Low-cost geochemical surveys for environmental studies in developing countries: Testing a

field portable XRF instrument under quasi-realistic conditions. Journal of Geochemical Exploration, 113, 3-12.
Hilgen, F.J., 1991. Extension of the astronomically calibrated (polarity) time scale to the Miocene/Pliocene boundary. Earth and Planetary Science Letters, 107(2), 349-368.
Hilgen, F.J., Krijgsman, W., Langereis, C.G., Lourens, L.J., Santarelli, A. and Zachariasse, W.J., 1995. Extending the astronomical (polarity) time scale into the Miocene. Earth and Planetary Science Letters, 136(3-4), 495-510.
Hilgen, F.J. and Krijgsman, W., 1999. Cyclostratigraphy and astrochronology of the Tripoli diatomite formation (pre-evaporite Messinian, Sicily, Italy). Terra Nova, 11(1), 16-22.
Hilgen, F., Bissoli, L., Iaccarino, S., Krijgsman, W., Meijer, R., Negri, A. and Villa, G., 2000. Integrated stratigraphy and astrochronology of the Messinian GSSP at Oued Akrech (Atlantic Morocco). Earth and Planetary Science Letters, 182(3), 237-251.
Hilgen, F., Kuiper, K., Krijgsman, W., Snel, E. and van der Laan, E., 2007. Astronomical tuning as the basis for high resolution chronostratigraphy: the intricate history of the Messinian Salinity Crisis. Stratigraphy, 4(2–3), 231-238.
Hinz, K., Winterer, E.L., Baumgartner, P.O., Bradshaw, M.J., Channell, J.E.T., Jansa, L.F., Jaffrezo, M., Leckie, R.M., Moore, J.N., Rullkotter, J., Schaftenaar, C., Steiger, T.H., Vuchev, V.T. and Wiegand, G.E., 1984. INITIAL REPORTS OF THE DEEP-SEA DRILLING PROJECT, VOL 79, COVERING LEG-79 OF THE CRUISES OF THE DRILLING VESSEL GLOMAR-CHALLENGER LAS-PALMAS, GRAND-CANARY-ISLAND, TO BREST, FRANCE APRIL MAY 1981 - SITE-547. Initial Reports of the Deep Sea Drilling Project, 79(NOV), 223-361.
Hodell, D.A., Benson, R.H., Kennett, J.P. and Bied, R.E., 1989. Stable isotope stratigraphy of latest Miocene sequences in northwest Morocco: the Bou Regreg section. Paleoceanography, 4(4), 467-482.
Hodell, D.A., Benson, R.H., Kent, D.V., Boersma, A. and Bied, R.E., 1994. Magnetostratigraphic, biostratigraphic, and stable isotope stratigraphy of an Upper Miocene drill core from the Salé Briqueterie (northwestern Morocco): A high-resolution chronology for the Messinian stage. Paleoceanography, 9(6), 835-855.
Hodell, D.A., Curtis, J.H., Sierro, F.J. and Raymo, M.E., 2001. Correlation of late Miocene to early Pliocene sequences between the Mediterranean and North Atlantic. Paleoceanography, 16(2), 164-178.
Hodell, D., Crowhurst, S., Skinner, L., Tzedakis, P.C., Margari, V., Channell, J.E., Kamenov, G., Maclachlan, S. and Rothwell, G., 2013. Response of Iberian Margin sediments to orbital and suborbital forcing over the past 420 ka. Paleoceanography, 28(1), 185-199.
Hohenegger, J., 2005. Estimation of environmental paleogradient values based on presence/absence data: a case study using benthic foraminifera for paleodepth estimation. Palaeogeography Palaeoclimatology Palaeoecology, 217(1-2), 115-130.
Hsu, K., 1972. Origin of saline giants: a critical review after the discovery of the Mediterranean evaporite. Earth-Science Reviews, 8(4), 371-396.
Hsü, K., Ryan, W. and Cita, M., 1973. Late Miocene desiccation of the Mediterranean. Nature, 242(5395), 240-244.
Hsü, K.J., Montadert, L., Bernoulli, D., Cita, M.B., Erickson, A., Garrison, R.E., Kidd, R.B., Mèlierés, F., Müller, C. and Wright, R., 1977. History of the Mediterranean salinity crisis. Nature, 267(5610), 399-403.
Hüsing, S.K., Kuiper, K.F., Link, W., Hilgen, F.J. and Krijgsman, W., 2009. The upper Tortonian-lower Messinian at Monte dei Corvi (Northern Apennines, Italy): Completing a Mediterranean reference section for the Tortonian Stage. Earth and Planetary Science Letters, 282(1-4), 140-157.
Hüsing, S.K., Zachariasse, W.-J., Van Hinsbergen, D.J., Krijgsman, W., Inceöz, M., Harzhauser, M., Mandic, O. and Kroh, A., 2009. Oligocene–Miocene basin evolution in SE Anatolia, Turkey: constraints on the closure of the eastern Tethys gateway. Geological Society, London, Special Publications, 311(1), 107-132.
Hüsing, S.K., Oms, O., Agustí, J., Garcés, M., Kouwenhoven, T.J., Krijgsman, W. and Zachariasse, W.J., 2010. On the late Miocene closure of the Mediterranean-Atlantic gateway through

the Guadix basin (southern Spain). Palaeogeography, Palaeoclimatology, Palaeoecology, 291(3), 167-179.
Hüsing, S.K., Oms, O., Agustí, J., Garcés, M., Kouwenhoven, T.J., Krijgsman, W. and Zachariasse, W.-J., 2012. On the Late Miocene continentalization of the Guadix Basin: More evidence for a major Messinian hiatus. Geobios.
Iaccarino, S., Castradori, D., Cita, M., Di Stefano, E., Gaboardi, S., McKenzie, J., Spezzaferri, S. and Sprovieri, R., 1999. The Miocene/Pliocene boundary and the significance of the earliest Pliocene flooding in the Mediterranean. Mem. Soc. Geol. Ital, 54(10), 109-131.
Iaccarino, S.M. and Bossio, A., 1999. 42. Paleoenvironment of Uppermost Messinian sequences in the Western Mediterranean (Sites 974, 975, and 978), Proceedings of the Ocean Drilling Program: Scientific Results, pp. 529-541.
Iaccarino, S.M., Bertini, A., Di Stefano, A., Ferraro, L., Gennari, R., Grossi, F., Lirer, F., Manzi, V., Menichetti, E., Lucchi, M.R., Taviani, M., Sturiale, G. and Angeletti, L., 2008. The Trave section (Monte dei Corvi, Ancona, Central Italy): an integrated paleontological study of the Messinian deposits. Stratigraphy, 5(3-4), 281-306.
Ingram, B. and Sloan, D., 1992. Strontium isotopic composition of estuarine sediments as paleosalinity-paleoclimate indicator. Science, 255(5040), 68.
Iorga, M.C. and Lozier, M.S., 1999. Signatures of the Mediterranean outflow from a North Atlantic climatology 1. Salinity and density fields. Journal of Geophysical Research-Oceans, 104(C11), 25985-26009.
Iribarren, L., Verges, J., Camurri, F., Fullea, J. and Fernandez, M., 2007. The structure of the Atlantic-Mediterranean transition zone from the Alboran Sea to the Horseshoe Abyssal Plain (Iberia-Africa plate boundary). Marine Geology, 243(1-4), 97-119.
Iribarren, L., Vergés, J. and Fernández, M., 2009. Sediment supply from the Betic–Rif orogen to basins through Neogene. Tectonophysics, 475(1), 68-84.
Ivanovic, R.F., Flecker, R., Gutjahr, M. and Valdes, P.J., 2013. First Nd isotope record of Mediterranean–Atlantic water exchange through the Moroccan Rifian Corridor during the Messinian salinity crisis. Earth and Planetary Science Letters, 368, 163-174.
Ivanovic, R.F., Valdes, P.J., Flecker, R., Gregoire, L.J. and Gutjahr, M., 2013. The parameterisation of Mediterranean-Atlantic water exchange in the Hadley Centre model HadCM3, and its effect on modelled North Atlantic climate. Ocean Modelling, 62, 11-16.
Ivanovic, R.F., Valdes, P.J., Flecker, R. and Gutjahr, M., 2014. Modelling global-scale climate impacts of the late Miocene Messinian Salinity Crisis. Climate of the Past, 10(2), 607-622.
Ivanovic, R.F., Valdes, P.J., Gregoire, L., Flecker, R. and Gutjahr, M., 2014. Sensitivity of modern climate to the presence, strength and salinity of Mediterranean-Atlantic exchange in a global general circulation model. Climate Dynamics, 42(3-4), 859-877.
Jacobsen, S.B. and Wasserburg, G., 1980. Sm-Nd isotopic evolution of chondrites. Earth and Planetary Science Letters, 50(1), 139-155.
Jaeger, J.-J., 1975. Les rongeurs du Miocène moyen et supérieur du Maghreb.
Jaeger, J.J., Michaux, J. and Thaler, L., 1975. OCCURRENCE OF A NEW MURID RODENT, PARAETHOMYS-MIOCAENICUS NOV-SP, IN UPPER TUROLIAN OF MOROCCO AND SPAIN - PALEOGEOGRAPHIC IMPLICATIONS. Comptes Rendus Hebdomadaires Des Seances De L Academie Des Sciences Serie D, 280(14), 1673-&.
Jansen, J., Van der Gaast, S., Koster, B. and Vaars, A., 1998. CORTEX, a shipboard XRF-scanner for element analyses in split sediment cores. Marine Geology, 151(1), 143-153.
Jiménez-Moreno, G., Pérez-Asensio, J.N., Larrasoaña, J.C., Aguirre, J., Civis, J., Rivas-Carballo, M.R., Valle-Hernández, M.F. and González-Delgado, J.A., 2013. Vegetation, sea-level, and climate changes during the Messinian salinity crisis. Geological Society of America Bulletin, 125(3-4), 432-444.
Jurado, M. and Comas, M., 1992. Well log interpretation and seismic character of the Cenozoic sequence in the northern Alboran Sea. Geo-Marine Letters, 12(2-3), 129-136.
Kaboth, S., Bahr, A., Reichart, G.-J., Jacobs, B. and Lourens, L.J., 2015. New insights into Upper MOW variability over the last 150 ka from IODP 339 Site U1386 in the Gulf of Cadiz. Marine Geology, in press.

Kahana, R., 2005. Modelling the interactions between the Mediterranean and the Global Thermohaline Circulations, University of East Anglia.
Kalnicky, D.J. and Singhvi, R., 2001. Field portable XRF analysis of environmental samples. Journal of hazardous materials, 83(1), 93-122.
Kamikuri, S.-i., Nishi, H. and Motoyama, I., 2007. Effects of late Neogene climatic cooling on North Pacific radiolarian assemblages and oceanographic conditions. Palaeogeography Palaeoclimatology Palaeoecology, 249(3-4), 370-392.
Karami, M.P., de Leeuw, A., Krijgsman, W., Meijer, P.T. and Wortel, M.J.R., 2011. The role of gateways in the evolution of temperature and salinity of semi-enclosed basins: An oceanic box model for the Miocene Mediterranean Sea and Paratethys. Global and Planetary Change, 79(1-2), 73-88.
Keigwin, L., 1982. Isotopic paleoceanography of the Caribbean and East Pacific: role of Panama uplift in late Neogene time. Science, 217(4557), 350-353.
Khelifi, N., Sarnthein, M., Andersen, N., Blanz, T., Frank, M., Garbe-Schoenberg, D., Haley, B.A., Stumpf, R. and Weinelt, M., 2009. A major and long-term Pliocene intensification of the Mediterranean outflow, 3.5-3.3 Ma ago. Geology, 37(9), 811-814.
Khelifi, N., Sarnthein, M., Frank, M., Andersen, N. and Garbe-Schoenberg, D., 2014. Late Pliocene variations of the Mediterranean outflow. Marine Geology, 357, 182-194.
Kidwell, S., 1991. Condensed deposits in siliciclastic sequences: expected and observed features. Cycles and events in stratigraphy, 682-695.
Koulali, A., Ouazar, D., Tahayt, A., King, R.W., Vernant, P., Reilinger, R.E., McClusky, S., Mourabit, T., Davila, J.M. and Amraoui, N., 2011. New GPS constraints on active deformation along the Africa-Iberia plate boundary. Earth and Planetary Science Letters, 308(1-2), 211-217.
Kouwenhoven, T.J., Seidenkrantz, M.S. and van der Zwaan, G.J., 1999. Deep-water changes: the near-synchronous disappearance of a group of benthic foraminifera from the Late Miocene Mediterranean. Palaeogeography, Palaeoclimatology, Palaeoecology, 152(3–4), 259-281.
Kouwenhoven, T., Hilgen, F. and Van der Zwaan, G., 2003. Late Tortonian–early Messinian stepwise disruption of the Mediterranean–Atlantic connections: constraints from benthic foraminiferal and geochemical data. Palaeogeography, Palaeoclimatology, Palaeoecology, 198(3), 303-319.
Kouwenhoven, T.J., Morigi, C., Negri, A., Giunta, S., Krijgsman, W. and Rouchy, J.M., 2006. Paleoenvironmental evolution of the eastern Mediterranean during the Messinian: Constraints from integrated microfossil data of the Pissouri Basin (Cyprus). Marine Micropaleontology, 60(1), 17-+.
Kouwenhoven, T.J. and van der Zwaan, G.J., 2006. A reconstruction of late Miocene Mediterranean circulation patterns using benthic foraminifera. Palaeogeography, Palaeoclimatology, Palaeoecology, 238(1–4), 373-385.
Krijgsman, W., Hilgen, F., Langereis, C. and Zachariasse, W., 1994. The age of the Tortonian/Messinian boundary. Earth and Planetary Science Letters, 121(3), 533-547.
Krijgsman, W., Hilgen, F.J., Raffi, I., Sierro, F.J. and Wilson, D.S., 1999. Chronology, causes and progression of the Messinian salinity crisis. Nature, 400(6745), 652-655.
Krijgsman, W., Langereis, C.G., Zachariasse, W.J., Boccaletti, M., Moratti, G., Gelati, R., Iaccarino, S., Papani, G. and Villa, G., 1999. Late Neogene evolution of the Taza-Guercif Basin (Rifian Corridor, Morocco) and implications for the Messinian salinity crisis. Marine Geology, 153(1-4), 147-160.
Krijgsman, W. and Langereis, C., 2000. Magnetostratigraphy of the Zobzit and Koudiat Zarga sections (Taza-Guercif basin, Morocco): implications for the evolution of the Rifian Corridor. Marine and Petroleum Geology, 17(3), 359-371.
Krijgsman, W., Fortuin, A., Hilgen, F. and Sierro, F., 2001. Astrochronology for the Messinian Sorbas basin (SE Spain) and orbital (precessional) forcing for evaporite cyclicity. Sedimentary Geology, 140(1), 43-60.
Krijgsman, W., Blanc-Valleron, M.M., Flecker, R., Hilgen, F.J., Kouwenhoven, T.J., Merle, D., Orszag-Sperber, F. and Rouchy, J.M., 2002. The onset of the Messinian salinity crisis in

the Eastern Mediterranean (Pissouri Basin, cyprus). Earth and Planetary Science Letters, 194(3-4), 299-310.
Krijgsman, W., Gaboardi, S., Hilgen, F., Iaccarino, S., De Kaenel, E. and Van der Laan, E., 2004. Revised astrochronology for the Ain el Beida section (Atlantic Morocco): no glacio-eustatic control for the onset of the Messinian Salinity Crisis. Stratigraphy, 1(1), 87-101.
Krijgsman, W. and Garces, M., 2004. Palaeomagnetic constraints on the geodynamic evolution of the Gibraltar Arc. Terra Nova, 16(5), 281-287.
Krijgsman, W. and Meijer, P.T., 2008. Depositional environments of the Mediterranean "Lower Evaporites" of the Messinian salinity crisis: Constraints from quantitative analyses. Marine Geology, 253(3–4), 73-81.
Kutzbach, J.E., Chen, G., Cheng, H., Edwards, R.L. and Liu, Z., 2014. Potential role of winter rainfall in explaining increased moisture in the Mediterranean and Middle East during periods of maximum orbitally-forced insolation seasonality. Climate Dynamics, 42(3-4), 1079-1095.
Lacan, F. and Jeandel, C., 2005. Neodymium isotopes as a new tool for quantifying exchange fluxes at the continent-ocean interface. Earth and Planetary Science Letters, 232(3-4), 245-257.
Lafuente, J.G., Roman, A.S., del Rio, G.D., Sannino, G. and Garrido, J.C.S., 2007. Recent observations of seasonal variability of the Mediterranean outflow in the Strait of Gibraltar. Journal of Geophysical Research-Oceans, 112(C10).
Larrasoaña, J.C., González-Delgado, J.A., Civis, J., Sierro, F.J., Alonso-Gavilán, G. and Pais, J., 2008. Magnetobiostratigraphic dating and environmental magnetism of Late Neogene marine sediments recovered at the Huelva-1 and Montemayor-1 boreholes (lower Guadalquivir basin, Spain). Geo-Temas, 10, 1175-1178.
Larrasoaña, J.C., Liu, Q., Hu, P., Roberts, A.P., Mata, P., Civis, J., Sierro, F.J. and Pérez-Asensio, J.N., 2014. Paleomagnetic and paleoenvironmental implications of magnetofossil occurrences in late Miocene marine sediments from the Guadalquivir Basin, SW Spain. Frontiers in microbiology, 5.
Laskar, J., Robutel, P., Joutel, F., Gastineau, M., Correia, A. and Levrard, B., 2004. A long-term numerical solution for the insolation quantities of the Earth. Astronomy & Astrophysics, 428(1), 261-285.
Ledesma, S., 2000. Astrobiocronología y estratigrafía de alta resolución del Neógeno de la Cuenca del Guadalquivir-Golfo de Cádiz. Ph Degree. Universidad de Salamanca, 464.
Lewis, A.R., Marchant, D.R., Ashworth, A.C., Hedenas, L., Hemming, S.R., Johnson, J.V., Leng, M.J., Machlus, M.L., Newton, A.E., Raine, J.I., Willenbring, J.K., Williams, M. and Wolfe, A.P., 2008. Mid-Miocene cooling and the extinction of tundra in continental Antarctica. Proceedings of the National Academy of Sciences of the United States of America, 105(31), 10676-10680.
Li, L.Z.X., 2006. Atmospheric GCM response to an idealized anomaly of the Mediterranean sea surface temperature. Climate Dynamics, 27(5), 543-552.
Lisiecki, L.E. and Raymo, M.E., 2005. A Pliocene-Pleistocene stack of 57 globally distributed benthic delta O-18 records. Paleoceanography, 20(1).
Litto, W., Jaaidi, E., Medina, F. and Dakki, M., 2001. Seismic study of the structure of the northern margin of the Gharb Basin (Morocco): Evidence for a late Miocene distension. Eclogae Geologicae Helvetiae, 94(1), 63-74.
Livermore, R., Hillenbrand, C.D., Meredith, M. and Eagles, G., 2007. Drake Passage and Cenozoic climate: An open and shut case? Geochemistry, Geophysics, Geosystems, 8(1).
Llave, E., Hernandez-Molina, F.J., Somoza, L., Diaz-del-Rio, V., Stow, D.A.V., Maestro, A. and Dias, J.M.A., 2001. Seismic stacking pattern of the Faro-Albufeira contourite system (Gulf of Cadiz): a Quaternary record of paleoceanographic and tectonic influences. Marine Geophysical Researches, 22(5-6), 487-508.
Llave, E., 2003. Análisis morfosedimentario y estratigráfico de los depósitos contorníticos del Golfo de Cádiz: implicaciones paleoceanográficas. Serie de Geología. Instituto Geológico y Minero de España.

Llave, E., Hernandez-Molina, F.J., Stow, D.A.V., Fernandez-Puga, M.C., Garcia, M., Vasquez, J.T., Maestro, A., Somaza, L. and Del Rio, V.D., 2007. Reconstructions of the Mediterranean Outflow Water during the quaternary based on the study of changes in buried mounded drift stacking pattern in the Gulf of Cadiz. Marine Geophysical Researches, 28(4), 379-394.

Lofi, J., Déverchère, J., Gaullier, V., Gillet, H., Gorini, C., Guennoc, P., Loncke, L., Maillard, A., Sage, F. and Thinon, I., 2011. Seismic atlas of the Messinian Salinity Crisis markers in the Mediterranean and Black Seas. Mémoire de la Société Géologique ns, 179, 1-72.

Lofi, J., Sage, F., Deverchere, J., Loncke, L., Maillard, A., Gaullier, V., Thinon, I., Gillet, H., Guennoc, P. and Gorini, C., 2011. Refining our knowledge of the Messinian salinity crisis records in the offshore domain through multi-site seismic analysis. Bulletin De La Societe Geologique De France, 182(2), 163-180.

Lofi, J., Voelker, A.H.L., Ducassou, E., Javier Hernández-Molina, F., Sierro, F.J., Bahr, A., Galvani, A., Lourens, L.J., Pardo-Igúzquiza, E., Pezard, P., Rodríguez-Tovar, F.J. and Williams, T., 2015. Quaternary chronostratigraphic framework and sedimentary processes for the gulf of Cadiz and Portuguese contourite depositional systems derived from natural gamma ray records. Marine Geology.

Loget, N. and Van Den Driessche, J., 2006. On the origin of the Strait of Gibraltar. Sedimentary Geology, 188, 341-356.

Lonergan, L. and White, N., 1997. Origin of the Betic-Rif mountain belt. Tectonics, 16(3), 504-522.

López-Garrido, A. and Sanz de Galdeano, C., 1999. Neogene sedimentation and tectonic-eustatic control of the Malaga Basin, south Spain. Journal of Petroleum Geology, 22(1), 81-96.

Lourens, L.J., Hilgen, F.J., Laskar, J., Shackleton, N.J. and Wilson, D., 2004. The Neogene Period. In: F.M. Gradstein, J.G. Ogg and A.G. Smith (Eds.), A Geologic Time Scale 2004. Cambridge University Press, Cambridge, pp. 409-440.

Loutit, T.S., 1988. Condensed sections: the key to age determination and correlation of continental margin sequences.

Lozano, F.S., 1979. Los foraminíferos planctónicos del Mioceno superior de la cuenca de Ronda y su comparación con los de otras áreas de las Cordilleras Béticas. Departamento de Geología, Facultad de Ciencias, Universidad de Málaga.

Lozar, F., Violanti, D., Dela Pierre, F., Bernardi, E., Cavagna, S., Clari, P., Irace, A., Martinetto, E. and Trenkwalder, S., 2010. Calcareous nannofossils and foraminifers herald the Messinian Salinity Crisis: The Pollenzo section (Alba, Cuneo; NW Italy). Geobios, 43(1), 21-32.

Lozier, M.S. and Stewart, N.M., 2008. On the temporally varying northward penetration of Mediterranean Overflow Water and eastward penetration of Labrador Sea water. Journal of Physical Oceanography, 38(9), 2097-2103.

Lozier, M.S. and Sindlinger, L., 2009. On the Source of Mediterranean Overflow Water Property Changes. Journal of Physical Oceanography, 39(8), 1800-1817.

Lugli, S., Schreiber, B.C. and Triberti, B., 1999. Giant polygons in the Realmonte mine (Agrigento, Sicily): Evidence for the desiccation of a Messinian halite basin. Journal of Sedimentary Research, 69(3), 764-771.

Lugli, S., Manzi, V., Roveri, M. and Schreiber, B.C., 2010. The Primary Lower Gypsum in the Mediterranean: A new fades interpretation for the first stage of the Messinian salinity crisis. Palaeogeography Palaeoclimatology Palaeoecology, 297(1), 83-99.

Lunt, D.J., Valdes, P.J., Haywood, A. and Rutt, I.C., 2008. Closure of the Panama Seaway during the Pliocene: implications for climate and Northern Hemisphere glaciation. Climate Dynamics, 30(1), 1-18.

Maillard, A. and Mauffret, A., 2011. Valencia through. Atlas of the Messinian Salinity Crisis markers in the Mediterranean and Black Seas. Mém. Soc. Géol. Fr. ns, 179.

Maillard, A. and Mauffret, A., 2013. Structure and present-day compression in the offshore area between Alicante and Ibiza Island (Eastern Iberian Margin). Tectonophysics, 591, 116-130.

Major, C.O., Goldstein, S.L., Ryan, W.B.F., Lericolais, G., Piotrowski, A.M. and Hajdas, I., 2006. The co-evolution of Black Sea level and composition through the last deglaciation and its paleoclimatic significance. Quaternary Science Reviews, 25(17-18), 2031-2047.
Maldonado, A., Somoza, L. and Pallares, L., 1999. The Betic orogen and the Iberian-African boundary in the Gulf of Cadiz: geological evolution (central North Atlantic). Marine Geology, 155(1-2), 9-43.
Manzi, V., Lugli, S., Lucchi, F.R. and Roveri, M., 2005. Deep-water clastic evaporites deposition in the Messinian Adriatic foredeep (northern Apennines, Italy): did the Mediterranean ever dry out? Sedimentology, 52(4), 875-902.
Manzi, V., Roveri, M., Gennari, R., Bertini, A., Biffi, U., Giunta, S., Iaccarino, S.M., Lanci, L., Lugli, S., Negri, A., Riva, A., Rossi, M.E. and Taviani, M., 2007. The deep-water counterpart of the Messinian lower evaporites in the Apennine foredeep: The fanantello section (Northern Apennines, Italy). Palaeogeography Palaeoclimatology Palaeoecology, 251(3-4), 470-499.
Manzi, V., Lugli, S., Roveri, M. and Schreiber, B.C., 2009. A new facies model for the Upper Gypsum of Sicily (Italy): chronological and palaeoenvironmental constraints for the Messinian salinity crisis in the Mediterranean. Sedimentology, 56(7), 1937-1960.
Manzi, V., Gennari, R., Hilgen, F., Krijgsman, W., Lugli, S., Roveri, M. and Sierro, F.J., 2013. Age refinement of the Messinian salinity crisis onset in the Mediterranean. Terra Nova, 25(4), 315-322.
Martin, J.M., Ortega-Huertas, M. and Torres-Ruiz, J., 1984. Genesis and evolution of strontium deposits of the Granada Basin (southeastern Spain): evidence of diagenetic replacement of a stromatolite belt. Sedimentary Geology, 39(3), 281-298.
Martín, J.M., Braga, J.C. and Betzler, C., 2001. The Messinian Guadalhorce corridor: the last northern, Atlantic-Mediterranean gateway. Terra Nova, 13(6), 418-424.
Martín, J.M., Braga, J.C., Aguirre, J. and Puga-Bernabéu, Á., 2009. History and evolution of the North-Betic Strait (Prebetic Zone, Betic Cordillera): a narrow, early Tortonian, tidal-dominated, Atlantic-Mediterranean marine passage. Sedimentary Geology, 216(3), 80-90.
Martín, J.M., Puga-Bernabéu, Á., Aguirre, J. and Braga, J.C., 2014. Miocene Atlantic-Mediterranean seaways in the Betic Cordillera (southern Spain). Revista de la Sociedad Geológica de España, 27, 1.
Martínez-García, P., Comas, M., Soto, J., Lonergan, L. and Watts, A., 2013. Strike-slip tectonics and basin inversion in the Western Mediterranean: the Post-Messinian evolution of the Alboran Sea. Basin Research, 25(4), 361-387.
Martin-Suarez, E., Freudenthal, M., Krijgsman, W. and Fortuin, A.R., 2000. On the age of the continental deposits of the Zorreras Member (Sorbas Basin, SE Spain). Geobios, 33(4), 505-512.
Marzocchi, A., Lunt, D., Flecker, R., Bradshaw, C., Farnsworth, A. and Hilgen, F., 2015. Orbital control on late Miocene climate and the North African monsoon: insight from an ensemble of sub-precessional simulations. Climate of the Past, 11(10), 1271-1295.
Mauffret, A., de Lamotte, D.F., Lallemant, S., Gorini, C. and Maillard, A., 2004. E-W opening of the Algerian Basin (Western Mediterranean). Terra Nova, 16(5), 257-264.
Mauritzen, C., Morel, Y. and Paillet, J., 2001. On the influence of Mediterranean Water on the Central waters of the North Atlantic Ocean. Deep-Sea Research Part I-Oceanographic Research Papers, 48(2), 347-381.
Mayer-Eymar, K., 1868. Catalogue systematique et descriptif des fossiles des terrains tertiaires, qui se trouvent au Musée fédéral de Zurich, 3. Schabelitz.
McArthur, J.M., Howarth, R.J. and Bailey, T.R., 2001. Strontium isotope stratigraphy: LOWESS version 3: Best fit to the marine Sr-isotope curve for 0-509 Ma and accompanying look-up table for deriving numerical age. Journal of Geology, 109(2), 155-170.
McArthur, J., Howarth, R. and Shields, G., 2012. Strontium isotope stratigraphy. The geologic time scale, 1, 127-144.
McCartney, M.S. and Mauritzen, C., 2001. On the origin of the warm inflow to the Nordic Seas. Progress in Oceanography, 51(1), 125-214.

McCave, I., Manighetti, B. and Robinson, S., 1995. Sortable silt and fine sediment size/composition slicing: Parameters for palaeocurrent speed and palaeoceanography. Paleoceanography, 10(3), 593-610.
McCave, I. and Hall, I., 2006. Size sorting in marine muds: Processes, pitfalls, and prospects for paleoflow-speed proxies. Geochemistry, Geophysics, Geosystems, 7(10).
McKenzie, J., Jenkyns, H. and Bennet, G., 1979. Stable isotope study of the cyclic diatomite—claystones from the Tripoli formation, Sicily: a prelude to the Messenian salinity crisis. Palaeogeography, Palaeoclimatology, Palaeoecology, 29, 125-141.
McKenzie, J.A., 1999. From desert to deluge in the Mediterranean. Nature, 400(6745), 613-614.
Medialdea, T., Vegas, R., Somoza, L., Vazquez, J.T., Maldonado, A., Diaz-Del-Rio, V., Maestro, A., Cordoba, D. and Fernandez-Puga, M.C., 2004. Structure and evolution of the "Olistostrome" complex of the Gibraltar Arc in the Gulf of Cadiz (eastern Central Atlantic): evidence from two long seismic cross-sections. Marine Geology, 209(1-4), 173-+.
Meijer, P.T. and Krijgsman, W., 2005. A quantitative analysis of the desiccation and re-filling of the Mediterranean during the Messinian Salinity Crisis. Earth and Planetary Science Letters, 240(2), 510-520.
Meijer, P.T., 2006. A box model of the blocked-outflow scenario for the Messinian Salinity Crisis. Earth and Planetary Science Letters, 248(1–2), 486-494.
Meijer, P.T. and Tuenter, E., 2007. The effect of precession-induced changes in the Mediterranean freshwater budget on circulation at shallow and intermediate depth. Journal of Marine Systems, 68(3-4), 349-365.
Meijer, P.T., 2012. Hydraulic theory of sea straits applied to the onset of the Messinian Salinity Crisis. Marine Geology, 326, 131-139.
Michard, A., 1976. Eléments de géologie marocaine, 252. Éditions du Service géologique du Maroc.
Milankovitch, M., 1941. History of radiation on the Earth and its use for the problem of the ice ages. K. Serb. Akad. Beogr.
Minwer-Barakat, R., García-Alix, A., Martín-Suárez, E. and Freudenthal, M., 2012. The late Miocene continentalization of the Guadix Basin (southern Spain) reconsidered: A comment on Hüsing et al. (2010). Geobios, 45(6), 611-615.
Molnar, P., 2008. Closing of the Central American Seaway and the Ice Age: A critical review. Paleoceanography, 23(2).
Montadert, L., Letouzey, J. and Mauffret, A., 1978. Messinian event: seismic evidence. Initial reports of the deep sea drilling project, 42(Part 1), 1037-1050.
Montanari, A., Beaudoin, B., Chan, L., Coccioni, R., Deino, A., De Paolo, D., Emmanuel, L., Fornaciari, E., Kruge, M. and Lundblad, S., 1997. Integrated stratigraphy of the Middle and Upper Miocene pelagic sequence of the Cònero Riviera (Marche region, Italy). Miocene stratigraphy: An integrated approach. Devel. Palaeontol. Stratigr, 15, 409-450.
Moran, K., Backman, J., Brinkhuis, H., Clemens, S.C., Cronin, T., Dickens, G.R., Eynaud, F., Gattacceca, J., Jakobsson, M., Jordan, R.W., Kaminski, M., King, J., Koc, N., Krylov, A., Martinez, N., Matthiessen, J., McInroy, D., Moore, T.C., Onodera, J., O'Regan, M., Palike, H., Rea, B., Rio, D., Sakamoto, T., Smith, D.C., Stein, R., St John, K., Suto, I., Suzuki, N., Takahashi, K., Watanabe, M., Yamamoto, M., Farrell, J., Frank, M., Kubik, P., Jokat, W. and Kristoffersen, Y., 2006. The Cenozoic palaeoenvironment of the Arctic Ocean. Nature, 441(7093), 601-605.
Moreno, A., Targarona, J., Henderiks, J., Canals, M., Freudenthal, T. and Meggers, H., 2001. Orbital forcing of dust supply to the North Canary Basin over the last 250kyr. Quaternary Science Reviews, 20(12), 1327-1339.
Muinos, S.B., Frank, M., Maden, C., Hein, J.R., van de Flierdt, T., Lebreiro, S.M., Gaspar, L., Monteiro, J.H. and Halliday, A.N., 2008. New constraints on the Pb and Nd isotopic evolution of NE Atlantic water masses. Geochemistry Geophysics Geosystems, 9.
Muller, D.W., Mueller, P.A. and McKenzie, J.A., 1990. Strontium isotopic ratios as fluid tracers in Messinian evaporites of the Tyrrhenian sea (western Mediterranean sea). KASTENS, KA,

MASCLE, J., et al., 1990, Proceedings of The Ocean Drilling Program, Scientific Results, 107, 603-614.
Müller, D.W. and Hsü, K.J., 1987. Event stratigraphy and paleoceanography in the Fortuna basin (Southeast Spain): a scenario for the Messinian salinity crisis. Paleoceanography, 2(6), 679-696.
Munch, P., Roger, S., Cornee, J.J., Saint Martin, J.P., Feraud, G. and Ben Moussa, A., 2001. Restriction of the seawater exchanges between the Atlantic and the Mediterranean during the Messinian: contribution of the tephrochronology of the Melilla-Nador area (northeastern Rif, Morocco). Comptes Rendus De L Academie Des Sciences Serie Ii Fascicule a-Sciences De La Terre Et Des Planetes, 332(9), 569-576.
Munch, P., Cornee, J.J., Feraud, G., Saint Martin, J.P., Ferrandini, M., Garcia, F., Conesa, G., Roger, S. and Moullade, M., 2006. Precise Ar-40/Ar-39 dating of volcanic tuffs within the upper Messinian sequences in the Melilla carbonate complex (NE Morocco): implications for the Messinian Salinity Crisis. International Journal of Earth Sciences, 95(3), 491-503.
Murdock, T.Q., Weaver, A.J. and Fanning, A.F., 1997. Paleoclimatic response of the closing of the Isthmus of Panama in a coupled ocean-atmosphere model. Geophysical Research Letters, 24(3), 253-256.
Murphy, L.N., Kirk-Davidoff, D.B., Mahowald, N. and Otto-Bliesner, B.L., 2009. A numerical study of the climate response to lowered Mediterranean Sea level during the Messinian Salinity Crisis. Palaeogeography Palaeoclimatology Palaeoecology, 279(1-2), 41-59.
Naranjo, C., Garcia-Lafuente, J., Sannino, G. and Sanchez-Garrido, J.C., 2014. How much do tides affect the circulation of the Mediterranean Sea? From local processes in the Strait of Gibraltar to basin-scale effects. Progress in Oceanography, 127, 108-116.
Natalicchio, M., Pierre, F.D., Lugli, S., Lowenstein, T.K., Feiner, S.J., Ferrando, S., Manzi, V., Roveri, M. and Clari, P., 2014. Did Late Miocene (Messinian) gypsum precipitate from evaporated marine brines? Insights from the Piedmont Basin (Italy). Geology, G34986. 1.
Omodeo Salé, S., Gennari, R., Lugli, S., Manzi, V. and Roveri, M., 2012. Tectonic and climatic control on the Late Messinian sedimentary evolution of the Nijar Basin (Betic Cordillera, Southern Spain). Basin Research, 24(3), 314-337.
Orszag-Sperber, F., 2006. Changing perspectives in the concept of "Lago-Mare" in Mediterranean Late Miocene evolution. Sedimentary Geology, 188, 259-277.
Orszag-Sperber, F., Caruso, A., Blanc-Valleron, M.-M., Merle, D. and Rouchy, J.M., 2009. The onset of the Messinian salinity crisis: Insights from Cyprus sections. Sedimentary Geology, 217(1-4), 52-64.
Osborne, A.H., Newkirk, D.R., Groeneveld, J., Martin, E.E., Tiedemann, R. and Frank, M., 2014. The seawater neodymium and lead isotope record of the final stages of Central American Seaway closure. Paleoceanography, 29(7), 715-729.
Penaud, A., Eynaud, F., Sanchez-Goni, M., Malaize, B., Turon, J.L. and Rossignol, L., 2011. Contrasting sea-surface responses between the western Mediterranean Sea and eastern subtropical latitudes of the North Atlantic during abrupt climatic events of MIS 3. Marine Micropaleontology, 80(1-2), 1-17.
Perconig, E. and Granados, L., 1973. El estratotipo del Andaluciense. Guidebook. XIII Coloquio Europeo de Micropaleontología, España, Sept. 1973: 225, 246.
Pérez-Asensio, J.N., Aguirre, J., Schmiedl, G. and Civis, J., 2012. Impact of restriction of the Atlantic-Mediterranean gateway on the Mediterranean Outflow Water and eastern Atlantic circulation during the Messinian. Paleoceanography, 27(3).
Pérez-Asensio, J.N., Aguirre, J., Schmiedl, G. and Civis, J., 2012. Messinian paleoenvironmental evolution in the lower Guadalquivir Basin (SW Spain) based on benthic foraminifera. Palaeogeography, Palaeoclimatology, Palaeoecology, 326, 135-151.
Pérez-Asensio, J.N., Aguirre, J., Jiménez-Moreno, G., Schmiedl, G. and Civis, J., 2013. Glacioeustatic control on the origin and cessation of the Messinian salinity crisis. Global and Planetary Change, 111(0), 1-8.
Pérez-Asensio, J.N., Aguirre, J., Schmiedl, G. and Civis, J., 2014. Messinian productivity changes in the northeastern Atlantic and their relationship to the closure of the Atlantic–

Mediterranean gateway: implications for Neogene palaeoclimate and palaeoceanography. Journal of the Geological Society, 171(3), 389-400.
Perez-Folgado, M., Sierro, F.J., Barcena, M.A., Flores, J.A., Vazquez, A., Utrilla, R., Hilgen, F.J., Krijgsman, W. and Filippelli, G.M., 2003. Western versus eastern Mediterranean paleoceano graphic response to astronomical forcing: a high-resolution microplankton study of precession-controlled sedimentary cycles during the Messinian. Palaeogeography Palaeoclimatology Palaeoecology, 190, 317-334.
Pickford, M., Senut, B. and Hadoto, D.P.M., 1993. Geology and Palaeobiology of the Albertine Rift Valley, Uganda-Zaire: Geology, 1. Cifeg.
Piepgras, D. and Wasserburg, G., 1983. Influence of the Mediterranean outflow on the isotopic composition of neodymium in waters of the North Atlantic. Journal of Geophysical Research C, 88(C10), 5997-6006.
Pierre, C., Caruso, A., Blanc-Valleron, M.-M., Rouchy, J.M. and Orzsag-Sperber, F., 2006. Reconstruction of the paleo environmental changes around the Miocene-Pliocene boundary along a West-East transect across the Mediterranean. Sedimentary Geology, 188, 319-340.
Pla-Pueyo, S., Viseras, C., Candy, I., Soria, J.M., García-García, F. and Schreve, D., 2015. Climatic control on palaeohydrology and cyclical sediment distribution in the Plio-Quaternary deposits of the Guadix Basin (Betic Cordillera, Spain). Quaternary International.
Platt, J. and Vissers, R., 1989. Extensional collapse of thickened continental lithosphere: a working hypothesis for the Alboran Sea and Gibraltar Arc. Geology, 17(6), 540-543.
Platt, J.P., Whitehouse, M.J., Kelley, S.P., Carter, A. and Hollick, L., 2003. Simultaneous extensional exhumation across the Alboran Basin: Implications for the causes of late orogenic extension. Geology, 31(3), 251-254.
Platt, J.P., Behr, W.M., Johanesen, K. and Williams, J.R., 2013. The Betic-Rif arc and its orogenic hinterland: A review. Annual Review of Earth and Planetary Sciences, 41, 313-357.
Pound, M.J., Haywood, A.M., Salzmann, U., Riding, J.B., Lunt, D.J. and Hunter, S.J., 2011. A Tortonian (Late Miocene, 11.61-7.25 Ma) global vegetation reconstruction. Palaeogeography Palaeoclimatology Palaeoecology, 300(1-4), 29-45.
Pound, M.J., Haywood, A.M., Salzmann, U. and Riding, J.B., 2012. Global vegetation dynamics and latitudinal temperature gradients during the Mid to Late Miocene (15.97-5.33 Ma). Earth-Science Reviews, 112(1-2), 1-22.
Prange, M. and Schulz, M., 2004. A coastal upwelling seesaw in the Atlantic Ocean as a result of the closure of the Central American Seaway. Geophysical Research Letters, 31(17).
Pratsch, J.C., 1996. Oil and gas potential of the PreRif foreland basin, onshore northern Morocco. Journal of Petroleum Geology, 19(2), 199-214.
Price, J.F., Baringer, M.O.N., Lueck, R.G., Johnson, G.C., Ambar, I., Parrilla, G., Cantos, A., Kennelly, M.A. and Sanford, T.B., 1993. Mediterranean outflow mixing and dynamics. Science, 259(5099), 1277-1282.
Price, J.F. and Baringer, M.O.N., 1994. Outflows and deep water production by marginal seas. Progress in Oceanography, 33(3), 161-200.
Puga-Bernabéu, Á., Martín, J.M., Braga, J.C. and Sánchez-Almazo, I.M., 2010. Downslope-migrating sandwaves and platform-margin clinoforms in a current-dominated, distally steepened temperate-carbonate ramp (Guadix Basin, Southern Spain). Sedimentology, 57(2), 293-311.
Raffi, I., Mozzato, C., Fornaciari, E., Hilgen, F.J. and Rio, D., 2003. Late Miocene calcareous nannofossil biostratigraphy and astrobiochronology for the Mediterranean region. Micropaleontology, 49(1), 1-26.
Rahmstorf, S., 1998. Influence of Mediterranean outflow on climate. Eos, Transactions American Geophysical Union, 79(24), 281-282.
Raymo, M.E., Lisiecki, L.E. and Nisancioglu, K.H., 2006. Plio-pleistocene ice volume, Antarctic climate, and the global delta O-18 record. Science, 313(5786), 492-495.
Reid, J.L., 1978. MIDDEPTH CIRCULATION AND SALINITY FIELD IN NORTH-ATLANTIC OCEAN. Journal of Geophysical Research-Oceans and Atmospheres, 83(NC10), 5063-5067.

Reid, J.L., 1979. On the contribution of the Mediterranean Sea outflow to the Norwegian-Greenland Sea. Deep Sea Research Part A. Oceanographic Research Papers, 26(11), 1199-1223.
Riaza, C. and Martinez del Olmo, W., 1996. S3 depositional model of the Guadalquivir–Gulf of Cadiz Tertiary basin. In: P.F. Friend and C.J. Dabrio (Eds.), Tertiary Basins of Spain: The Stratigraphic Record of Crustal Kinematics, Cambridge University Press, Cambridge, pp. 330-338.
Richter, T.O., Van der Gaast, S., Koster, B., Vaars, A., Gieles, R., de Stigter, H.C., De Haas, H. and van Weering, T.C., 2006. The Avaatech XRF Core Scanner: technical description and applications to NE Atlantic sediments. Geological Society, London, Special Publications, 267(1), 39-50.
Riding, R., Braga, J.C., Martı´n, J.M. and Sánchez-Almazo, I.M., 1998. Mediterranean Messinian Salinity Crisis: constraints from a coeval marginal basin, Sorbas, southeastern Spain. Marine Geology, 146(1), 1-20.
Riding, R., Braga, J.C., Martı´n, J.M. and Sánchez-Almazo, I.M., 1998. Mediterranean Messinian Salinity Crisis: constraints from a coeval marginal basin, Sorbas, southeastern Spain. Marine Geology, 146(1), 1-20.
Robinson, S.A., Murphy, D.P., Vance, D. and Thomas, D.J., 2010. Formation of "Southern Component Water" in the Late Cretaceous: Evidence from Nd-isotopes. Geology, 38(10), 871-874.
Roca, E. and Guimerà, J., 1992. The Neogene structure of the eastern Iberian margin: structural constraints on the crustal evolution of the Valencia trough (western Mediterranean). Tectonophysics, 203(1), 203-218.
Rodero, J., Pallares, L. and Maldonado, A., 1999. Late Quaternary seismic facies of the Gulf of Cadiz Spanish margin: depositional processes influenced by sea-level change and tectonic controls. Marine Geology, 155(1-2), 131-156.
Rodríguez Fernández, J., 1982. El Mioceno del sector central de las Cordilleras Béticas.
Roger, S., Munch, P., Cornee, J.J., Saint Martin, J.P., Feraud, G., Pestrea, S., Conesa, G. and Ben Moussa, A., 2000. Ar-40/Ar-39 dating of the pre-evaporitic Messinian marine sequences of the Melilla basin (Morocco): a proposal for some biosedimentary events as isochrons around the Alboran Sea. Earth and Planetary Science Letters, 179(1), 101-113.
Rogerson, M., Rohling, E.J., Weaver, P.P.E. and Murray, J.W., 2005. Glacial to interglacial changes in the settling depth of the Mediterranean Outflow plume. Paleoceanography, 20(3).
Rogerson, M., Colmenero-Hidalgo, E., Levine, R., Rohling, E., Voelker, A., Bigg, G.R., Schönfeld, J., Cacho, I., Sierro, F. and Löwemark, L., 2010. Enhanced Mediterranean-Atlantic exchange during Atlantic freshening phases. Geochemistry, Geophysics, Geosystems, 11(8).
Rogerson, M., Rohling, E., Bigg, G.R. and Ramirez, J., 2012. Paleoceanography of the Atlantic-Mediterranean exchange: Overview and first quantitative assessment of climatic forcing. Reviews of Geophysics, 50(2).
Rogl, F., 1999. Mediterranean and Paratethys. Facts and hypotheses of an Oligocene to Miocene paleogeography (short overview). Geologica Carpathica, 50(4), 339-349.
Rohling, E.J., 1999. Environmental control on Mediterranean salinity and delta O-18. Paleoceanography, 14(6), 706-715.
Rohling, E., Schiebel, R. and Siddall, M., 2008. Controls on Messinian lower evaporite cycles in the Mediterranean. Earth and Planetary Science Letters, 275(1), 165-171.
Rohling, E.J., Marino, G. and Grant, K.M., 2015. Mediterranean climate and oceanography, and the periodic development of anoxic events (sapropels). Earth-Science Reviews, 143, 62-97.
Rorabacher, D.B., 1991. Statistical treatment for rejection of deviant values: critical values of Dixon's" Q" parameter and related subrange ratios at the 95% confidence level. Analytical Chemistry, 63(2), 139-146.
Rosenbaum, G., Lister, G.S. and Duboz, C., 2002. Relative motions of Africa, Iberia and Europe during Alpine orogeny. Tectonophysics, 359(1–2), 117-129.

Rouchy, J.M. and Caruso, A., 2006. The Messinian salinity crisis in the Mediterranean basin: A reassessment of the data and an integrated scenario. Sedimentary Geology, 188, 35-67.
Rouchy, J.M., Caruso, A., Pierre, C., Blanc-Valleron, M.-M. and Bassetti, M.A., 2007. The end of the Messinian salinity crisis: Evidences from the Chelif Basin (Algeria). Palaeogeography Palaeoclimatology Palaeoecology, 254(3-4), 386-417.
Roveri, M. and Manzi, V., 2006. The Messinian salinity crisis: Looking for a new paradigm? Palaeogeography, Palaeoclimatology, Palaeoecology, 238(1–4), 386-398.
Roveri, M., Bertini, A., Cosentino, D., Di Stefano, A., Gennari, R., Gliozzi, E., Grossi, F., Iaccarino, S.M., Lugli, S. and Manzi, V., 2008. A high-resolution stratigraphic framework for the latest Messinian events in the Mediterranean area. Stratigraphy, 5(3-4), 323-342.
Roveri, M., Lugli, S., Manzi, V. and Schreiber, B.C., 2008. The Messinian Sicilian stratigraphy revisited: new insights for the Messinian salinity crisis. Terra Nova, 20(6), 483-488.
Roveri, M., Flecker, R., Krijgsman, W., Lofi, J., Lugli, S., Manzi, V., Sierro, F.J., Bertini, A., Camerlenghi, A. and De Lange, G., 2014. The Messinian Salinity Crisis: Past and future of a great challenge for marine sciences. Marine Geology, 352, 25-58.
Roveri, M., Lugli, S., Manzi, V., Gennari, R. and Schreiber, B.C., 2014. High-resolution strontium isotope stratigraphy of the Messinian deep Mediterranean basins: Implications for marginal to central basins correlation. Marine Geology, 349, 113-125.
Rowe, H., Hughes, N. and Robinson, K., 2012. The quantification and application of handheld energy-dispersive x-ray fluorescence (ED-XRF) in mudrock chemostratigraphy and geochemistry. Chemical Geology, 324, 122-131.
Ruiz-Constán, A., Galindo-Zaldívar, J., Pedrera, A. and de Galdeano, C.S., 2009. Gravity anomalies and orthogonal box fold development on heterogeneous basement in the Neogene Ronda Depression (Western Betic Cordillera). Journal of Geodynamics, 47(4), 210-217.
Ryan, W.B. and Cita, M.B., 1978. The nature and distribution of Messinian erosional surfaces—Indicators of a several-kilometer-deep Mediterranean in the Miocene. Marine Geology, 27(3), 193-230.
Ryan, W.B., 2009. Decoding the Mediterranean salinity crisis. Sedimentology, 56(1), 95-136.
Saint Martin, J.-P., Cornée, J.-J., Muller, J., Camoin, G., André, J.-P., Rouchy, J.-M. and Benmoussa, A., 1991. Contrôles globaux et locaux dans l'édification d'une plate-forme carbonatée messinienne (bassin de Melilla, Maroc): apport de la stratigraphie séquentielle et de l'analyse tectonique. CR Acad. Sci. Paris, 315, 1573-1579.
Saint Martin, J.-P., 1996. The Messinian reef complex of Melilla, northeastern Rif, Morocco.
Sale, S.O., Gennari, R., Lugli, S., Manzi, V. and Roveri, M., 2012. Tectonic and climatic control on the Late Messinian sedimentary evolution of the Nijar Basin (Betic Cordillera, Southern Spain). Basin Research, 24(3), 314-337.
Salvany, J.M., Larrasoaña, J.C., Mediavilla, C. and Rebollo, A., 2011. Chronology and tectono-sedimentary evolution of the Upper Pliocene to Quaternary deposits of the lower Guadalquivir foreland basin, SW Spain. Sedimentary Geology, 241(1), 22-39.
Santarelli, A., Brinkhuis, H., Hilgen, F.J., Lourens, L.J., Versteegh, G.J.M. and Visscher, H., 1998. Orbital signatures in a Late Miocene dinoflagellate record from Crete (Greece). Marine Micropaleontology, 33(3-4), 273-297.
Santisteban, C. and Taberner, C., 1983. Shallow marine and continental conglomerates derived from coral reef complexes after desiccation of a deep marine basin: the Tortonian-Messinian deposits of the Fortuna Basin, SE Spain. Journal of the Geological Society, 140(3), 401-411.
Sanz de Galdeano, C.M. and Vera, J.A., 1992. Stratigraphic record and palaeogeographical context of the Neogene basins in the Betic Cordillera, Spain. Basin Research, 4(1), 21-36.
Sanz de Galdeano, C. and Alfaro, P., 2004. Tectonic significance of the present relief of the Betic Cordillera. Geomorphology, 63(3–4), 175-190.
Scher, H.D. and Martin, E.E., 2006. Timing and climatic consequences of the opening of Drake Passage. Science, 312(5772), 428-430.
Schildgen, T.F., Cosentino, D., Frijia, G., Castorina, F., Dudas, F.O., Iadanza, A., Sampalmieri, G., Cipollari, P., Caruso, A., Bowring, S.A. and Strecker, M.R., 2014. Sea level and climate

forcing of the Sr isotope composition of late Miocene Mediterranean marine basins. Geochemistry Geophysics Geosystems, 15(7), 2964-2983.
Schneck, R., Micheels, A. and Mosbrugger, V., 2010. Climate modelling sensitivity experiments for the Messinian Salinity Crisis. Palaeogeography Palaeoclimatology Palaeoecology, 286(3-4), 149-163.
Schneider, B. and Schmittner, A., 2006. Simulating the impact of the Panamanian seaway closure on ocean circulation, marine productivity and nutrient cycling. Earth and Planetary Science Letters, 246(3-4), 367-380.
Schroeder, K., Garcìa-Lafuente, J., Josey, S.A., Artale, V., Buongiorno Nardelli, B., Carrillo, A., Gacic, M., Gasparini, G.P., Herrmann, M. and Lionello, P., 2012. Circulation of the Mediterranean Sea and its variability.
Seidenkrantz, M.S., Kouwenhoven, T.J., Jorissen, F.J., Shackleton, N.J. and van der Zwaan, G.J., 2000. Benthic foraminifera as indicators of changing Mediterranean–Atlantic water exchange in the late Miocene. Marine Geology, 163(1–4), 387-407.
Sepulchre, P., Arsouze, T., Donnadieu, Y., Dutay, J.C., Jaramillo, C., Le Bras, J., Martin, E., Montes, C. and Waite, A.J., 2014. Consequences of shoaling of the Central American Seaway determined from modeling Nd isotopes. Paleoceanography, 29(3), 176-189.
Sgarrella, F., Sprovieri, R., DiStefano, E. and Caruso, A., 1997. Paleoceanographic conditions at the base of the Pliocene in the southern Mediterranean basin. Rivista Italiana Di Paleontologia E Stratigrafia, 103(2), 207-220.
Sgarrella, F., Sprovieri, R., Di Stefano, E., Caruso, A., Sprovieri, M. and Bonaduce, G., 1999. The Capo Rossello bore-hole (Agrigento, Sicily): Cyclostratigraphic and paleoceanographic reconstructions from quantitative analyses of the Zanclean foraminiferal assemblages. Rivista Italiana Di Paleontologia E Stratigrafia, 105(2), 303-322.
Shackleton, N., 1974. Attainment of isotopic equilibrium between ocean water and the benthonic foraminifera genus Uvigerina: isotopic changes in the ocean during the last glacial.
Shackleton, N.J. and Kennett, J.P., 1975. Paleotemperature history of the Cenozoic and the initiation of Antarctic glaciation: oxygen and carbon isotope analyses in DSDP Sites 277, 279, and 281. Initial reports of the deep sea drilling project, 29, 743-755.
Shackleton, N., Crowhurst, S., Hagelberg, T., Pisias, N. and Schneider, D., 1995. 6. A new late Neogene time scale: application to Leg 138 sites, Proceedings of the Ocean Drilling Program, Scientific Results, pp. 73-101.
Shackleton, N., Hall, M. and Pate, D., 1995. 15. Pliocene stable isotope stratigraphy of Site 846, Proc. Ocean Drill. Program Sci. Results, pp. 337-355.
Sholkovitz, E. and Szymczak, R., 2000. The estuarine chemistry of rare earth elements: comparison of the Amazon, Fly, Sepik and the Gulf of Papua systems. Earth and Planetary Science Letters, 179(2), 299-309.
Sierro, F.J., 1985. Estudio de los foraminíferos planctónicos, bioestratigrafía y cronoestratigrafía del Mio-Plioceno del borde occidental de la Cuenca del Guadalquivir (SO de España). Studia geologica salmanticensia(21), 7-85.
Sierro, F.J., Gonzalez-Delgado, J.A., Dabrio, C.J., Flores, J.A. and Civis, J., 1990. The Neogene of the Guadalquivir Basin (SW Spain).
Sierro, F.J., Flores, J.A. and Civis, J., 1993. Late Miocene globorotaliid event-stratigraphy and biogeography in the NE-Atlantic and Mediterranean. Marine Micropaleontology, 21(1), 143-167.
Sierro, F.J., Delgado, J.A.G., Flores, J.A., Dabrio, C.J. and Civis, J., 1996. S4 Late Neogene depositional sequences in the foreland basin of Guadalquivir (SW Spain). In: P.F. Friend and C.J. Dabrio (Eds.), Tertiary Basins of Spain: The stratigraphic record of crustal kinematics, pp. 339.
Sierro, F.J., Flores, J.A., Zamarreno, I., Vazquez, A., Utrilla, R., Frances, G., Hilgen, F.J. and Krijgsman, W., 1999. Messinian pre-evaporite sapropels and procession-induced oscillations in western Mediterranean climate. Marine Geology, 153(1-4), 137-146.
Sierro, F.J., Ledesma, S., Flores, J.A., Torrescusa, S. and Martinez del Olmo, W., 2000. Sonic and gamma-ray astrochronology: Cycle to cycle calibration of Atlantic climatic records to Mediterranean sapropels and astronomical oscillations. Geology, 28(8), 695-698.

Sierro, F.J., Hilgen, F.J., Krijgsman, W. and Flores, J.A., 2001. The Abad composite (SE Spain): a Messinian reference section for the Mediterranean and the APTS. Palaeogeography, Palaeoclimatology, Palaeoecology, 168(1), 141-169.
Sierro, F.J., Flores, J.A., Francés, G., Vazquez, A., Utrilla, R., Zamarreño, I., Erlenkeuser, H. and Barcena, M.A., 2003. Orbitally-controlled oscillations in planktic communities and cyclic changes in western Mediterranean hydrography during the Messinian. Palaeogeography, Palaeoclimatology, Palaeoecology, 190(0), 289-316.
Sierro, F., Ledesma, S. and Flores, J., 2008. Astrobiochronology of Late Neogene deposits near the Strait of Gibraltar (SW Spain). Implications for the tectonic control of the Messinian Salinity Crisis, CIESM Workshop Monogr, pp. 45-49.
Simon, D. and Meijer, P., 2015. Dimensions of the Atlantic-Mediterranean connection that caused the Messinian Salinity Crisis. Marine Geology, 364, 53-64.
Sonnenfeld, P. and Finetti, I., 1985. Messinian evaporites in the Mediterranean: a model of continuous inflow and outflow, Geological evolution of the Mediterranean Basin. Springer, pp. 347-353.
Spivack, A.J. and Wasserburg, G., 1988. Neodymium isotopic composition of the Mediterranean outflow and the eastern North Atlantic. Geochimica et Cosmochimica Acta, 52(12), 2767-2773.
Sprovieri, R. and Hasegawa, S., 1990. Plio-Pleistocene benthic foraminifer stratigraphic distribution in the deep-sea record of the Tyrrhenian Sea (ODP Leg 107), Proceedings of the Ocean Drilling Program, Scientific Results, pp. 429-459.
Sprovieri, R., Di stefano, E. and Sprovieri, M., 1996. High resolution chronology for Late Miocene Mediterranean stratigraphic events. Rivista Italiana di Paleontologia e Stratigrafia (Research In Paleontology and Stratigraphy), 102(1).
Sprovieri, M., Barbieri, M., Bellanca, A. and Neri, R., 2003. Astronomical tuning of the Tortonian Sr-87/Sr-86 curve in the Mediterranean basin. Terra Nova, 15(1), 29-35.
Stich, D., Serpelloni, E., Mancilla, F.d.L. and Morales, J., 2006. Kinematics of the Iberia-Maghreb plate contact from seismic moment tensors and GPS observations. Tectonophysics, 426(3-4), 295-317.
Strasser, A., Hilgen, F.J. and Heckel, P.H., 2006. Cyclostratigraphy–concepts, definitions, and applications. Newsletters on Stratigraphy, 42(2), 75-114.
SUC, J. and Bessais, E., 1990. Continuous thermo-xeric climate in Sicily before, during and after the Messinian salinity crisis. COMPTES RENDUS DE L ACADEMIE DES SCIENCES SERIE II, 310(12), 1701-1707.
Suc, J.-P., Violanti, D., Londeix, L., Poumot, C., Robert, C., Clauzon, G., Gautier, F., Turon, J.-L., Ferrier, J. and Chikhi, H., 1995. Evolution of the Messinian Mediterranean environments: the Tripoli Formation at Capodarso (Sicily, Italy). Review of Palaeobotany and Palynology, 87(1), 51-79.
Suc, J., Clauzon, G. and Gautier, F., 1997. The Miocene/Pliocene boundary: present and future. Miocene stratigraphy: an integrated approach. Amsterdam: Elsevier Science BV, 149-154.
Tachikawa, K., Roy-Barman, M., Michard, A., Thouron, D., Yeghicheyan, D. and Jeandel, C., 2004. Neodymium isotopes in the Mediterranean Sea: Comparison between seawater and sediment signals. Geochimica Et Cosmochimica Acta, 68(14), 3095-3106.
Thierstein, H.R. and Berger, W.H., 1978. Injection events in ocean history. Nature, 276, 461-466.
Thomas, D.J., Bralower, T.J. and Jones, C.E., 2003. Neodymium isotopic reconstruction of late Paleocene-early Eocene thermohaline circulation. Earth and Planetary Science Letters, 209(3-4), 309-322.
Thunell, R.C., Locke, S.M. and Williams, D.F., 1988. Glacio-eustatic sea-level control on Red Sea salinity.
Thunell, R., Rio, D., Sprovieri, R. and Vergnaud-Grazzini, C., 1991. An overview of the post-Messinian paleoenvironmental history of the western Mediterranean. Paleoceanography, 6(1), 143-164.
Thurner, S., Palomeras, I., Levander, A., Carbonell, R. and Lee, C.T., 2014. Ongoing lithospheric removal in the western Mediterranean: evidence from Ps receiver functions and

thermobarometry of Neogene basalts (PICASSO project). Geochemistry, Geophysics, Geosystems, 15(4), 1113-1127.
Tjallingii, R., Röhl, U., Kölling, M. and Bickert, T., 2007. Influence of the water content on X-ray fluorescence core-scanning measurements in soft marine sediments. Geochemistry, Geophysics, Geosystems, 8(2).
Topper, R., Flecker, R., Meijer, P.T. and Wortel, M., 2011. A box model of the Late Miocene Mediterranean Sea: Implications from combined 87Sr/86Sr and salinity data. Paleoceanography, 26(3).
Topper, R.P.M. and Meijer, P.T., 2013. A modeling perspective on spatial and temporal variations in Messinian evaporite deposits. Marine Geology, 336, 44-60.
Topper, R., Lugli, S., Manzi, V., Roveri, M. and Meijer, P.T., 2014. Precessional control of Sr ratios in marginal basins during the Messinian Salinity Crisis? Geochemistry, Geophysics, Geosystems, 15(5), 1926-1944.
Topper, R.P.M. and Meijer, P.T., 2015. Changes in Mediterranean circulation and water characteristics due to restriction of the Atlantic connection: a high-resolution ocean model. Climate of the Past, 11(2), 233-251.
Toto, E.A., El Miloudi, A., El Basri, M., Hafid, M., Zouhri, L., El Mouraouah, S., Benammi, M., El Mouraouah, A., Iben Brahim, A., Birouk, A. and Kasmi, M., 2012. New geophysical and geological evidence for the present day southernmost active deformational front of the Rif thrust-and-fold belt and the oceanic accretionary prism of Cadiz: the Dhar Doum-Lalla Zahra fault, Northwestern Atlantic Coastal Morocco. Environmental Earth Sciences, 67(8), 2411-2422.
Tzedakis, P.C., 2007. Seven ambiguities in the Mediterranean palaeoenvironmental narrative. Quaternary Science Reviews, 26(17-18), 2042-2066.
USEPA, 2006. XRF technologies for measuring trace elements in soil and sediment: Oxford X-Met 3000TX XRF Analyzer. Innovative Technology Verification Report.
Utescher, T., Boehme, M. and Mosbrugger, V., 2011. The Neogene of Eurasia: Spatial gradients and temporal trends - The second synthesis of NECLIME. Palaeogeography Palaeoclimatology Palaeoecology, 304(3-4), 196-201.
Vai, G., 1997. Cyclostratigraphic estimate of the Messinian stage duration. Miocene stratigraphy: an integrated approach, 463-476.
Van Assen, E., Kuiper, K., Barhoun, N., Krijgsman, W. and Sierro, F., 2006. Messinian astrochronology of the Melilla Basin: stepwise restriction of the Mediterranean–Atlantic connection through Morocco. Palaeogeography, Palaeoclimatology, Palaeoecology, 238(1), 15-31.
Van Couvering, J.A., Castradori, D., Cita, M.B., Hilgen, F.J. and Rio, D., 2000. The base of the Zanclean Stage and of the Pliocene Series. Episodes, 23(3), 179-187.
van Dam, J.A., Abdul Aziz, H., Sierra, M.A.A., Hilgen, F.J., Ostende, L.W.v.d.H., Lourens, L.J., Mein, P., van der Meulen, A.J. and Pelaez-Campomanes, P., 2006. Long-period astronomical forcing of mammal turnover. Nature, 443(7112), 687-691.
van de Poel, H.M., 1991. Messinian stratigraphy of the Nijar Basin (SE Spain) and the origin of its gypsum-ghost limestones. Geologie en Mijnbouw, 70(3), 215-234.
van den Berg, B.C.J., Sierro, F.J., Hilgen, F.J., Flecker, R., Larrasoaña, J.C., Krijgsman, W., Flores, J.A., Mata, M.P., Martín, E.B. and Civis, J., 2015. Astronomical tuning for the upper Messinian Spanish Atlantic margin: Disentangling basin evolution, climate cyclicity and MOW. Global and Planetary Change, 135, 89-103.
Van der Laan, E., Gaboardi, S., Hilgen, F. and Lourens, L., 2005. Regional climate and glacial control on high-resolution oxygen isotope records from Ain el Beida (latest Miocene, northwest Morocco): A cyclostratigraphic analysis in the depth and time domain. Paleoceanography, 20(1).
Van der Laan, E., Snel, E., De Kaenel, E., Hilgen, F. and Krijgsman, W., 2006. No major deglaciation across the Miocene-Pliocene boundary: Integrated stratigraphy and astronomical tuning of the Loulja sections (Bou Regreg area, NW Morocco). Paleoceanography, 21(3).

Van der Laan, E., Hilgen, F., Lourens, L., De Kaenel, E., Gaboardi, S. and Iaccarino, S., 2012. Astronomical forcing of Northwest African climate and glacial history during the late Messinian (6.5–5.5 Ma). Palaeogeography, Palaeoclimatology, Palaeoecology, 313, 107-126.

van der Made, J., Morales, J. and Montoya, P., 2006. Late Miocene turnover in the Spanish mammal record in relation to palaeoclimate and the Messinian Salinity Crisis. Palaeogeography Palaeoclimatology Palaeoecology, 238(1-4), 228-246.

van der Schee, M., Sierro, F.J., Jiménez-Espejo, F.J., Hernández-Molina, F.J., Flecker, R., Flores, J.A., Acton, G., Gutjahr, M., Grunert, P., García-Gallardo, Á. and Andersen, N., 2016. Evidence of early bottom water current flow after the Messinian Salinity Crisis in the Gulf of Cadiz. Marine Geology.

Van der Zwaan, G., Jorissen, F. and De Stigter, H., 1990. The depth dependency of planktonic/benthic foraminiferal ratios: constraints and applications. Marine Geology, 95(1), 1-16.

Van Hinsbergen, D., Kouwenhoven, T. and Van der Zwaan, G., 2005. Paleobathymetry in the backstripping procedure: Correction for oxygenation effects on depth estimates. Palaeogeography, Palaeoclimatology, Palaeoecology, 221(3), 245-265.

Vautravers, M.J., 2014. Insight into the latest Messinian (5.7–5.2 Ma) palaeoclimatic events from two deep-sea Atlantic Ocean ODP Sites. Palaeogeography, Palaeoclimatology, Palaeoecology, 407, 14-24.

Vegas, R., 1992. The Valencia trough and the origin of the western Mediterranean basins. Tectonophysics, 203(1), 249-261.

Vidal, L., Bickert, T., Wefer, G. and Röhl, U., 2002. Late Miocene stable isotope stratigraphy of SE Atlantic ODP Site 1085: Relation to Messinian events. Marine Geology, 180(1–4), 71-85.

Violanti, D., 1996. Paleoautecological analysis of Bulimina echinata (Messinian, Mediterranean area). Autecology of Selected Fossil OrganismsBolletino della Societa Paleontologica Italiana, 3, 243-253.

Vissers, R.L.M. and Meijer, P.T., 2012. Iberian plate kinematics and Alpine collision in the Pyrenees. Earth-Science Reviews, 114(1-2), 61-83.

Voelker, A.H.L., Lebreiro, S.M., Schoenfeld, J., Cacho, I., Erlenkeuser, H. and Abrantes, F., 2006. Mediterranean outflow strengthening during northern hemisphere coolings: A salt source for the glacial Atlantic? Earth and Planetary Science Letters, 245(1-2), 39-55.

von Suchodoletz, H., Fuchs, M. and Zöller, L., 2008. Dating Saharan dust deposits on Lanzarote (Canary Islands) by luminescence dating techniques and their implication for palaeoclimate reconstruction of NW Africa. Geochemistry, Geophysics, Geosystems, 9(2).

von Suchodoletz, H., Oberhänsli, H., Hambach, U., Zöller, L., Fuchs, M. and Faust, D., 2010. Soil moisture fluctuations recorded in Saharan dust deposits on Lanzarote (Canary Islands) over the last 180ka. Quaternary Science Reviews, 29(17), 2173-2184.

Warren, J.K., 2010. Evaporites through time: Tectonic, climatic and eustatic controls in marine and nonmarine deposits. Earth-Science Reviews, 98(3-4), 217-268.

Wernli, R., 1988. Micropaléontologie du Néogène post-nappes du Maroc septentrional et description systématique des foraminifères planctoniques. Editions du Service géologique du Maroc.

Woodruff, F. and Savin, S.M., 1989. Miocene deepwater oceanography. Paleoceanography, 4(1), 87-140.

Wright, R., 1980. Benthic foraminiferal repopulation of the Mediterranean after the Messinian (Late Miocene) event. Palaeogeography, Palaeoclimatology, Palaeoecology, 29, 189-214.

Wu, W., Danabasoglu, G. and Large, W.G., 2007. On the effects of parameterized Mediterranean overflow on North Atlantic ocean circulation and climate. Ocean Modelling, 19(1-2), 31-52.

Zachos, J.C., Shackleton, N.J., Revenaugh, J.S., Palike, H. and Flower, B.P., 2001. Climate response to orbital forcing across the Oligocene-Miocene boundary. Science, 292(5515), 274-278.

Zhang, J.J. and Scott, D.B., 1996. Integrated stratigraphy and paleoceanography of the Messinian (latest Miocene) across the North Atlantic Ocean. Marine Micropaleontology, 29(1), 1-36.

Zhang, X., Prange, M., Steph, S., Butzin, M., Krebs, U., Lunt, D.J., Nisancioglu, K.H., Park, W., Schmittner, A., Schneider, B. and Schulz, M., 2012. Changes in equatorial Pacific thermocline depth in response to Panamanian seaway closure: Insights from a multi-model study. Earth and Planetary Science Letters, 317, 76-84.

Zitellini, N., Gracia, E., Matias, L., Terrinha, P., Abreu, M.A., DeAlteriis, G., Henriet, J.P., Danobeitia, J.J., Masson, D.G., Mulder, T., Ramella, R., Somoza, L. and Diez, S., 2009. The quest for the Africa-Eurasia plate boundary west of the Strait of Gibraltar. Earth and Planetary Science Letters, 280(1-4), 13-50.

Zouhri, L., Lamouroux, C., Vachard, D. and Pique, A., 2002. Evidence of flexural extension of the Rif foreland: The Rharb-Mamora basin (northern Morocco). Bulletin De La Societe Geologique De France, 173(6), 509-513.